

25
17

NASA TECHNICAL MEMORANDUM

NASA TM X-52876
Volume VI

TECH LIBRARY KAFB, NM



0152455

NASA TM X-52876
Volume VI



SPACE TRANSPORTATION SYSTEM TECHNOLOGY SYMPOSIUM

VI - Integrated Electronics (Including Electric Power)

NASA Lewis Research Center
Cleveland, Ohio
July 15-17, 1970

FACILITY FORM 60	N70-40951	N70-40975
	(ACCESSION NUMBER)	(THRU) ..
	376	1
	(PAGES)	(CODE)
✓	31	
(NASA CR OR TMX OR AD NUMBER)	(CATEGORY)	

N70-40951

1. Report No. TM X-52876 - Volume VI		2. Government Accession No.		3. Recipient's Catalog No.	
4. Title and Subtitle SPACE TRANSPORTATION SYSTEM TECHNOLOGY SYMPOSIUM VI - Integrated Electronics				5. Report Date July 1970	
				6. Performing Organization Code	
7. Author(s)				8. Performing Organization Report No. E-5866	
				10. Work Unit No.	
9. Performing Organization Name and Address				11. Contract or Grant No.	
				13. Type of Report and Period Covered Technical Memorandum	
				14. Sponsoring Agency Code	
12. Sponsoring Agency Name and Address National Aeronautics and Space Administration Washington, D. C. 20546					
15. Supplementary Notes Held at the NASA-Lewis Research Center, July 15-17, 1970					
16. Abstract The Symposium encompassed seven technical areas, each published in a separate volume of NASA Technical Memorandum X-52876: Volume I - Aerothermodynamics and Configurations (includes aerodynamics; atmospheric operations; and aerodynamic heating) II - Dynamics and Aeroelasticity (includes dynamic loads and response; aeroelasticity; and flight dynamics and environment) III - Structures and Materials (includes structural design technology; thermal protection systems; and materials technology) IV - Propulsion (includes main propulsion; auxiliary propulsion; and airbreathing propulsion) V - Operations, Maintenance, and Safety (Including Cryogenic Systems) (includes general and cryogenics) VI - Integrated Electronics (Including Electric Power) (includes system integration; data management, systems monitoring, and checkout; navigation, guidance, and control; communication, instrumentation, and display; and power subsystems) VII - Biotechnology					
17. Key Words (Suggested by Author(s)) <i>1. Conference</i> <i>2. Space Systems</i> <i>3. Space Propulsion</i>			18. Distribution Statement Unclassified - unlimited		
19. Security Classif. (of this report) Unclassified		20. Security Classif. (of this page) Unclassified		21. No. of Pages 371	22. Price* <i>6.00</i> \$3.00

*For sale by the Clearinghouse for Federal Scientific and Technical Information
Springfield, Virginia 22151; also as microfiche
at \$.65 per copy.

FOREWORD

The prospect of undertaking a reusable launch vehicle development led the NASA Office of Manned Space Flight (OMSF) to request the Office of Advanced Research and Technology (OART) to organize and direct a program to develop the technology that would aid in selecting the best system alternatives and that would support the ultimate development of an earth-to-orbit shuttle. Such a Space Transportation System Technology Program has been initiated. OART, OMSF, and NASA Flight and Research Centers with the considerable inputs of Department of Defense personnel have generated the program through the efforts of several Technology Working Groups and a Technology Steering Group. Funding and management of the recommended efforts is being accomplished through the normal OART and OMSF line management channels. The work is being done in government laboratories and under contract with industry and universities. Foreign nations have been invited to participate in this work as well. Substantial funding, from both OART and OMSF, was applied during the second half of fiscal year 1970.

The Space Transportation System Technology Symposium held at the NASA Lewis Research Center, Cleveland, Ohio, July 15-17, 1970, was the first public report on that program. The Symposium goals were to consider the technology problems, their status, and the prospective program outlook for the benefit of the industry, government, university, and foreign participants considered to be contributors to the program. In addition, it offered an opportunity to identify the responsible individuals already engaged in the program. The Symposium sessions were intended to confront each presenter with his technical peers as listeners, and this, I believe, was substantially accomplished.

Because of the high interest in the material presented, and also because the people who could edit the output are already deeply involved in other important tasks, we have elected to publish the material essentially as it was presented, utilizing mainly the illustrations used by the presenters along with brief words of explanation. Those who heard the presentations, and those who are technically astute in specialty areas, can probably put this story together again. We hope that more will be gained by compiling the information in this form now than by spending the time and effort to publish a more finished compendium later.

PRECEDING PAGE BLANK NOT FILMED.

A. O. Tischler
Chairman,
Space Transportation System
Technology Steering Group

CONTENTS

	Page
FOREWORD	iii
INTRODUCTION AND OVERVIEW	
Theodore S. Michaels, NASA Headquarters	1
SYSTEM INTEGRATION	
INTEGRATED AVIONICS ARCHITECTURE	
D. M. Petrie, The Boeing Company	71 ✓
SIMULATION OF THE SHUTTLE SUBSYSTEMS MANAGEMENT AND CONTROL FUNCTION	
Michael A. Cowan and David J. Freeman, McDonnell Douglas Corporation	29 ✓
SOFTWARE INTEGRATION FOR INTEGRATED ELECTRONICS	
R. F. Klawa, General Dynamics/Convair	51 ✓
INTEGRATED CONTROL AND AIRFRAME DEVELOPMENT CONSIDERATIONS	
Donald L. Martin, The Boeing Company	67 ✓
DATA MANAGEMENT, SYSTEMS MONITORING, AND CHECKOUT	
ONBOARD DATA MANAGEMENT	
R. E. Poupard, IBM Corporation	85 ✓
MULTIPLEX DATA BUS TECHNIQUES	
Walter O. Frost, NASA-Marshall Space Flight Center	91 ✓
DATA BUS DESIGN TECHNIQUES	
Donald J. Spencer, TRW Systems Group	95 ✓
CHECKOUT OF REDUNDANT SYSTEMS	
H. L. Newman, General Dynamics/Convair	115 ✓
NAVIGATION, GUIDANCE, AND CONTROL	
EXPERIENCE WITH UNPOWERED TERMINAL-AREA INSTRUMENT APPROACHES	
B. Lyle Schofield, Air Force Flight Test Center, Harold G. Gaidstick and Shu W. Gee, NASA Flight Research Center	133 ✓
AUTOMATIC AND MANUAL TERMINAL GUIDANCE AND CONTROL STUDIES IN SUPPORT OF THE SPACE SHUTTLE PROGRAM	
D. W. Smith, NASA-Ames Research Center	149 ✓
TERMINAL CONTROL AND AUTOMATIC LANDING OF UNPOWERED SPACE SHUTTLE VEHICLES	
Stephen S. Osder, Sperry-Rand	155 ✓

STABILIZATION AND CONTROL OF THE SPACE SHUTTLE ORBITER DURING ENTRY/PITCHDOWN MANEUVERS	
D. Engels, E. Estrine, P. Shipley, North American Rockwell	177 ✓
GUST ALLEVIATION AND MODAL SUPPRESSION CONTROL TECHNOLOGY	
Mario H. Rheinfurth, NASA-Marshall Space Flight Center	193 ✓
ACTIVE FLEXURE CONTROL TODAY	
G. B. Skelton, Honeywell Inc.	209 ✓
FLY-BY-WIRE	
E. Bumby, Grumman	227 ✓
SCANNING LASER RADAR FOR RENDEZVOUS AND DOCKING	
Terry Flom, IIT Aerospace/Optical Division	237 ✓
 <u>COMMUNICATION, INSTRUMENTATION, AND DISPLAY</u>	
A LASER SYSTEM SUITABLE FOR SPACE APPLICATIONS	
P. Schuddeboom, M. Teare, and D. Bennett, RCA Research Laboratories	279 ✓
AN ALL-SOLID-STATE, S-BAND PARAMP UTILIZING MICROWAVE INTEGRATED CIRCUITS	
P. H. Dalle Mura, NASA-Goddard Space Flight Center	289 ✓
INSTRUMENT LANDING SYSTEMS FOR THE SPACE SHUTTLE	
Herbert P. Raabe, IBM Corporation	295 ✓
COMPUTER GENERATED IMAGERY AS APPLIED TO SPACE SHUTTLE DESIGN EVALUATION AND SYSTEM SIMULATION	
W. Marvin Bunker, General Electric Co.	313 ✓
 <u>POWER SUBSYSTEMS</u>	
SOLID-STATE POWER MANAGEMENT	
I. Rakofsky, Grumman	323 ✓
POWER PROCESSING AND DISTRIBUTION FOR THE SPACE SHUTTLE CRAFT	
Francisc C. Schwarz, NASA-Lewis Research Center	339 ✓
FUEL CELL TECHNOLOGY PROGRAM	
David Bell, NASA-Manned Spacecraft Center	349 ✓
SPACE SHUTTLE AUXILIARY POWER UNIT (APU)	
Donald G. Beremand and Harry M. Cameron, NASA-Lewis Research Center	361 ✓

INTRODUCTION AND OVERVIEW

Theodore S. Michaels

National Aeronautics and Space Administration

Washington, D.C.

The purpose of this session is to present a forum for the dissemination and discussion of the latest thoughts and developments in the electronics area which could be applied to the Space Shuttle.

Before we begin I would like to take a few minutes to give you a brief overview of the scope of the electronic R&D efforts applicable to the Space Shuttle. In order to help identify the Shuttle R&D within NASA the Office of Advanced Research and Technology adopted an overlaying organization which is responsible for the correlation of this effort. It might be helpful to review this operating mode. Figure I shows the overall NASA organization. The offices which are primarily concerned with the Space Shuttle research and development are the Office of Advanced Research and Technology (OART) and the Office of Manned Space Flight (OMSF). Figure 2 shows a simplified picture of the in-line organization of OART and OMSF. For the sake of clarity only three of the ten OART Divisions are shown. Each OART Division is responsible for discipline oriented research and development which is applicable to many mission goals. In order to identify the Space Shuttle technology a technical steering group was formed which consists of seven technology working groups as illustrated. It is the responsibility of these working groups to assure that a balanced program in its area is maintained by identifying necessary R&D as well as avoiding duplication of effort. Their responsibilities also include monitoring the program of approved efforts. The composition of the working groups encompass OART and OMSF Centers, as well as Headquarters and the Air Force. R&D efforts which are under cognizance

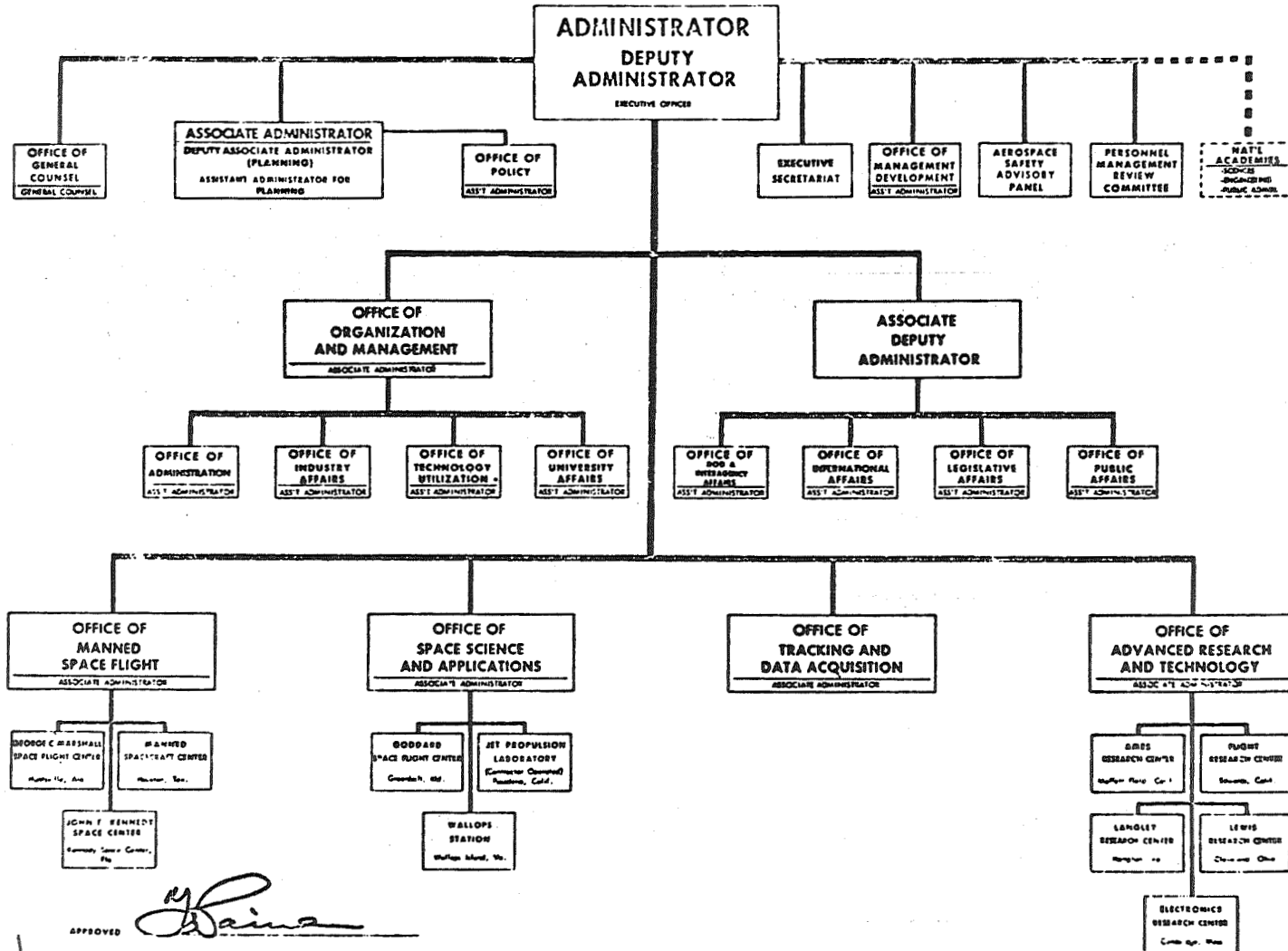
of the integrated electronics working group are primarily in the Electronics and Control Division, Power and Electric Propulsion Division, and the Advanced Manned Missions Program.

In addition to these efforts there are the Phase B Shuttle contracts which have been funded by the Space Shuttle Program Office in OMSF. The NASA-Industry relationship for the management of this effort is shown in Figure 3.

The estimated FY 71 funding for integrated electronics under present cognizance of the integrated technology working group is 8.6 million dollars. Funding which will be applied to this area by the Phase B contractors will also be reviewed by this working group.

The requirements imposed on the Space Shuttle present a new and challenging task to the electronics system development engineer. Specifications such as landing at existing airports under Category II conditions, complete reusability, maximum turnaround time of 2 weeks and safety equivalent to that of a commercial airline have never been imposed on a space vehicle. Additionally a further requirement for a checkout and control system which provides autonomous operation by the crew without major support from the ground is also a new space vehicle refinement. The experiences on our past space flights point to the desirability of eliminating as much of the mechanical monitoring instrumentation as possible, and essentially substituting cathode ray tube displays driven by computers to help simplify the pilot's monitoring tasks. These and other needs we are here to address our attention to, and so since we have an interesting and full program ahead of us let us begin with the first paper.

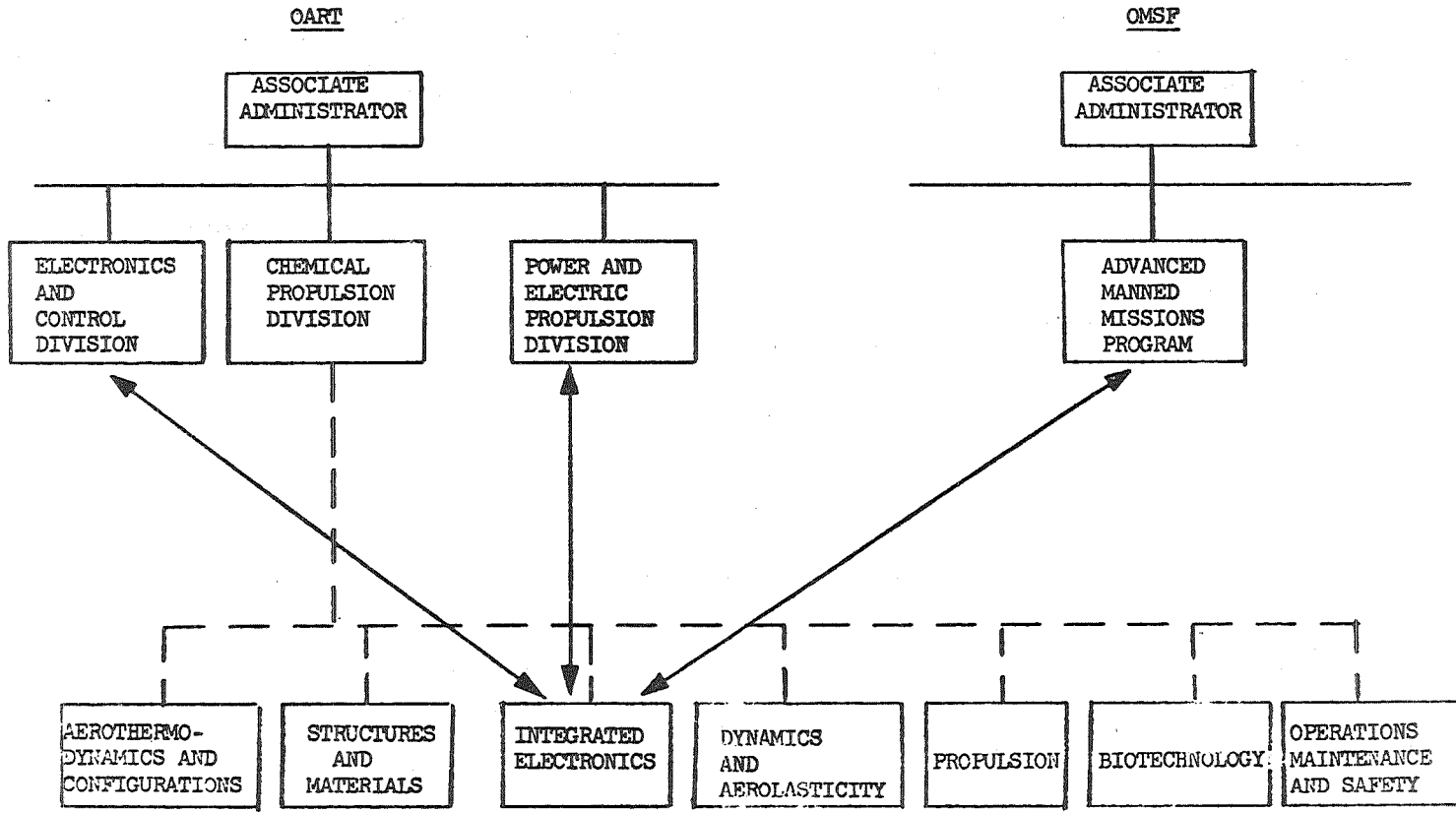
NATIONAL AERONAUTICS AND SPACE ADMINISTRATION



APPROVED *[Signature]*
EFFECTIVE 1 MAY 1970

Figure 1

PARTIAL OART-OMSF ORGANIZATION
 AND
 SPACE SHUTTLE TECHNICAL STEERING GROUP JUXTAPOSITION
 INTEGRATED ELECTRONIC SYSTEMS HIGHLIGHTED



4

Figure 2

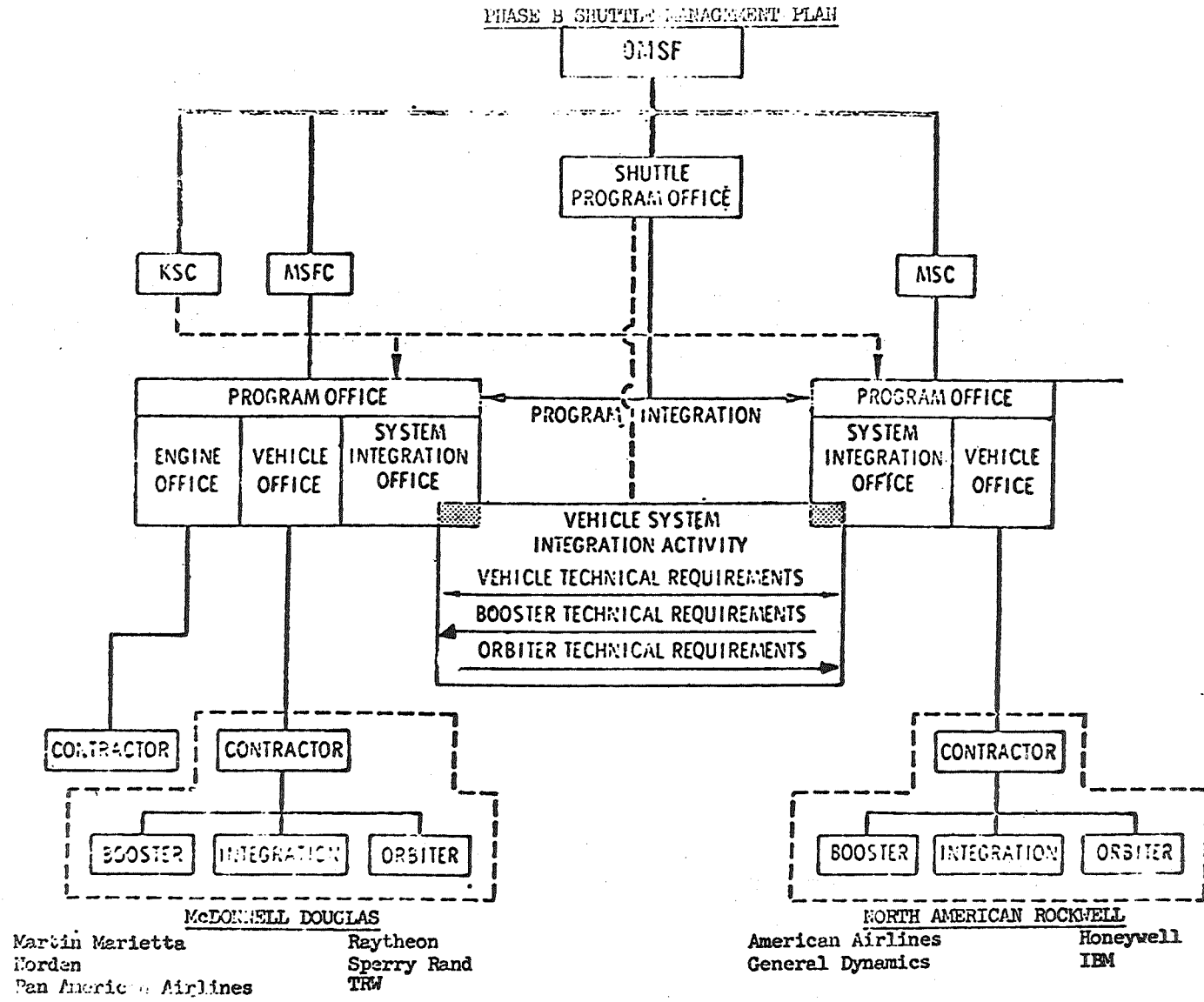
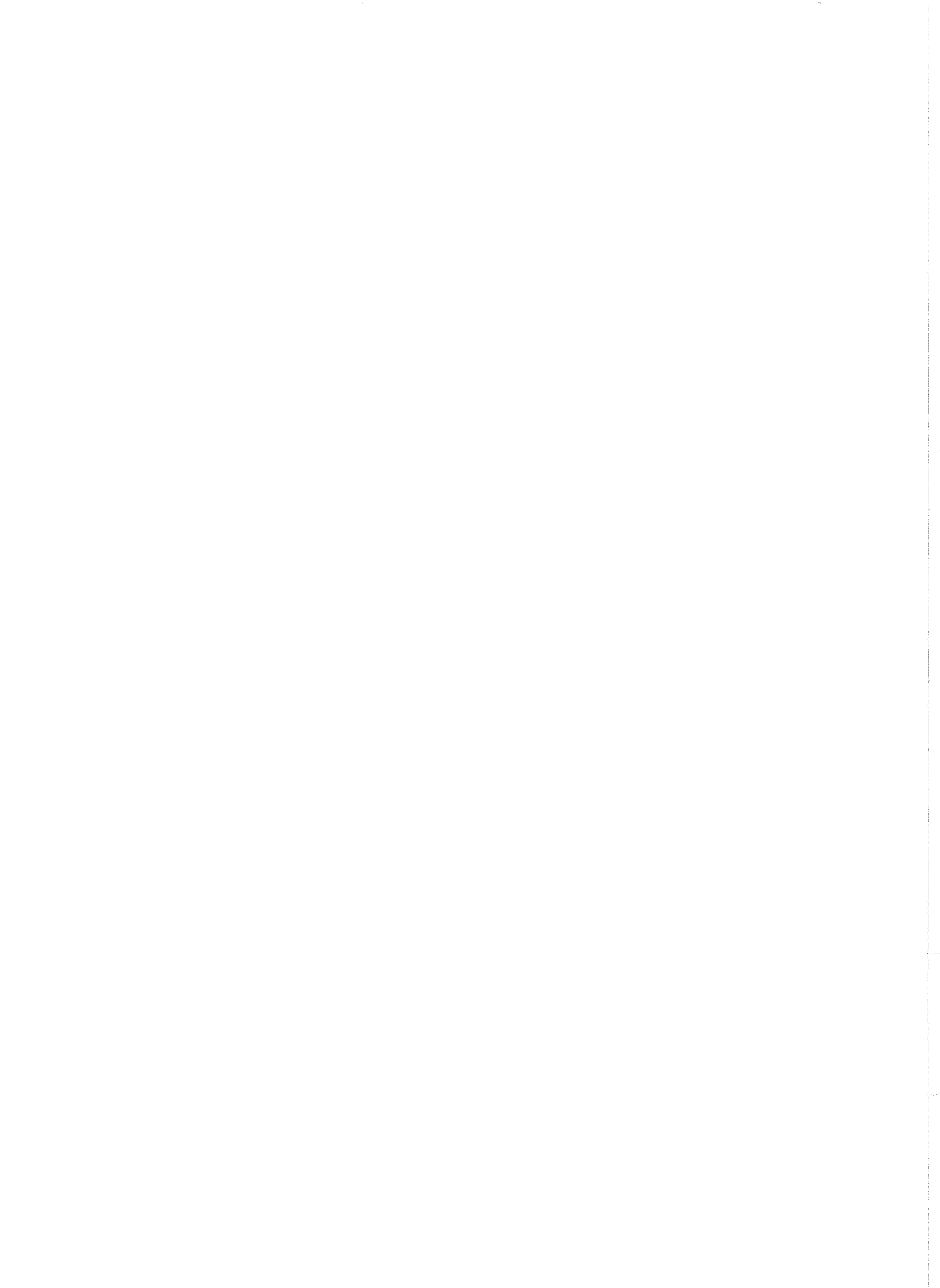


Figure 3



N70-40952

INTEGRATED AVIONICS ARCHITECTURE

D. M. Petrie

The Boeing Company
Seattle, Washington

SUMMARY

An integrated avionics system is described that is characteristic of that which will be found in future aircraft and manned space vehicles. Design rules have been developed, beginning with conceptual studies on the SST in 1966, that have matured to produce a design that is considered to be a saddle point in overall cost and weight, that is also consistent with safety requirements in man-rated vehicles. The design approach points out the need to avoid generalities in use of design rules; rather, that the details of the question at hand should be used to reach configuration decisions. The system design represents a mix of centralized/decentralized concepts and covers the high-leverage redundancy question. Subsystem elements that are described include central "data management" computer, data bus, CRT displays, manual interface, navigation sensors, flight control, rocket engine control, and telecommunications. Traditional approaches to system organization and subsystem design practice must be altered in order for this new approach to be successful. Development program requirements should include a breadboard demonstrator connected to peripheral electromechanical equipment; and a test bed airplane.

7

PRECEDING PAGE CONTAINS INFORMATION

INTRODUCTION

The integrated avionics conceptual evolution is currently being characterized by a convergence of aircraft electronics and space electronics. The impetus for the development of integrated avionic systems is to increase the operational payload weight fraction, minimize program costs, and improve flight safety. Increased payload weight results from equipment items that can be made multi-purpose, thus reducing the inert weight of the prime vehicle. Costs are reduced by placing on-board the vehicle the checkout and mission control functions, thus providing a much greater degree of vehicle autonomy, relative to current launch and flight operations that utilize ground-based facilities. Reliability is increased because integration of certain functions facilitate a more practical redundancy design and relieves the flight crew of error-susceptible routine activity.

Centralization of Functions

Airplanes and spacecraft have, in the past, employed special-purpose electronics for such functions as navigation, fuel management, and checkout; that is, one computer (analog or digital) per function. The advent of the high-speed, reprogrammable digital computer makes it practical to time-share certain of these functions in a single computer. The benefit is a lighter weight, more simple avionics complex. This alone does not justify pursuit of this new technique; however, the additional SSV requirement of on-board checkout and autonomy from the Apollo-like mission control function makes integrated (simplified) computing mandatory.

cc

Typically, there are some 4,000 pounds of inert wiring weight in a large aerospace vehicle, assuming the usual one pair of wires per remotely controlled or sensed function. The use of a multiplex data bus, employing only a few pairs of wires strung throughout the vehicle, shows promise of reducing this weight by approximately 3,300 pounds. A standardized interface technique between the bus and subsystem is also desired to couple a wide range of data points and controls; and to facilitate subsystem design modifications without requiring time-consuming redevelopment for each change.

The use of an inertial measurement unit for all functions requiring measurement of vehicle motion, rather than use of dedicated sensors, is an economy measure that is gaining acceptance.

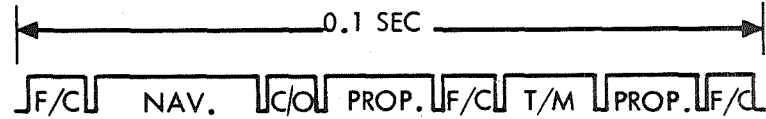
Replacement of virtually all needle and dial type displays by the reprogrammable CRT is most useful as a means to present more information to the flight crew and thus better utilize the judgment skills of man.

Reduction of the number of modulators, R.F. transmitters/receivers, and antennas required is availed through multiplexing and a digital up/down link.

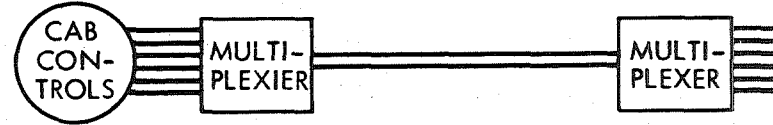
The potentially lower weight of centralized power conditioning must be weighed against the adverse cross-coupling problems generally inherent in such an approach.

CENTRALIZATION OF FUNCTIONS

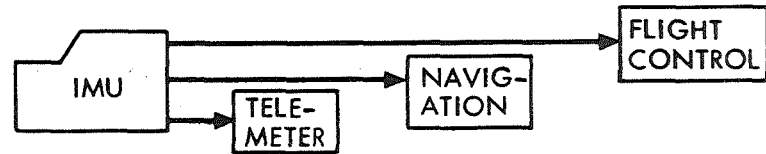
- TIME-SHARED COMPUTING



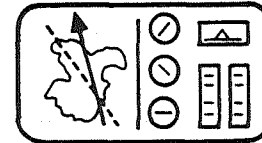
- MULTIPLEX WIRING



- COMMON INERTIAL SENSORS



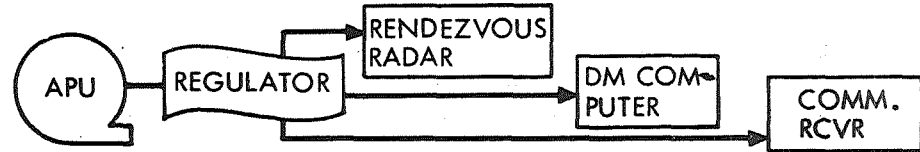
- CRT DISPLAYS



- COMMON RF LINKS



- POWER CONDITIONING



Why Integrated Avionics?

The gross objective of the space shuttle is to reduce the total cost of transporting payload between earth and earth orbit. The facing chart shows, in qualitative terms, how this economy will be effected. Recovery of the launching vehicle components is a dramatically obvious way to reduce costs; however, minimization of operational costs, by placing on-board the shuttle the equipment required for essentially autonomous checkout and mission control, is a more subtle and less glamorous aspect of the current program. Accordingly, it is more difficult to gain funding support and emphasis for this segment of the shuttle program, relative to engine and airframe preliminary design studies. This problem is compounded by the dramatic success of the Apollo 12 mission, in which the lunar module was guided to the touchdown target with vernier precision. Furthermore, existence of avionics complexes found in such modern airplanes as the 747 and C-5A adds more fuel to the question: Why integrated avionics?

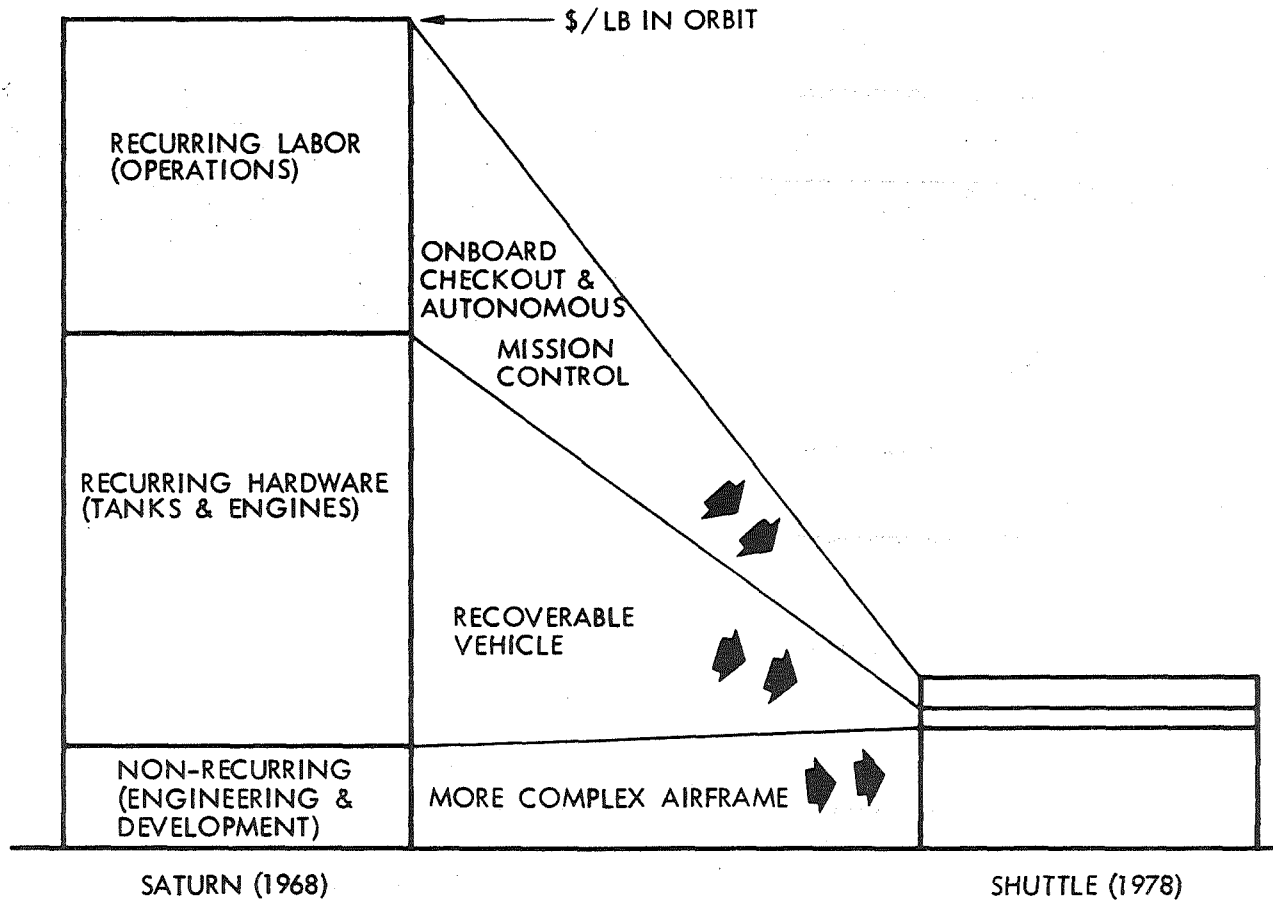
The difference between these forementioned programs and shuttle must be considered in gaging the early requirement for system-level (contrasted with subsystem level) development programs; such as breadboard demonstrators and test bed airplanes.

Prelaunch checkout of a space vehicle is vastly more complex than that required in airplanes, due largely to the cryogenic propellants required and the developmental nature of relatively low traffic space transportation operations. The payload for shuttle is approximately 1% of the launch weight, as compared to 25% for a large aircraft. This difference places new demands on use of multi-purpose (integrated) equipments to reduce avionics weight. The major difference between Apollo and shuttle avionics requirements is the aforementioned autonomy issue.

In summary, a new approach to avionics architecture for shuttle is required for two basic reasons; operational autonomy and minimum inert weight.

These factors place new demands on the shared use of displays, computers, data buses, sensors, and R.F. links. This, in turn, threatens the status quo of organizational structures and traditional demarcations of equipment. Because of this, demands on managerial skills may exceed the technical challenges. Specifically, the tenets of system engineering must be made to pervade the avionics and related organizations; or an avionics systems engineering group must be established with broad powers that transcend special interest groups. Avionics equipment manufacturers will be faced with the dilemma to either specialize in certain components or to attempt encroachment into technologically adjacent market areas. Similarly, the airlines, the military, the NASA, and the so-called "systems houses" must assess their capability to survey technology, write detailed and highly interrelated specifications, and develop the integrated system so that the components play together.

WHY INTEGRATED AVIONICS?



Integrated Avionics Design Rules

The rationale for synthesis of an integrated avionics system was developed for general applicability to any control process involving men and machines. Use of these design rules results in complementary roles for manual and automatic functions, with the gross objectives being to simultaneously achieve highly reliable operation at minimum overall cost.

A complex process that must be precisely controlled in response to a given set of input data should be handled by machines. An example in an aerospace vehicle is boost trajectory guidance. Automation of routine manual tasks relieves workload pressures. This enhances man's adaptive ability to generate a decision from an array of data that he has never seen before. An example of this is landing go-around at a busy air terminal.

Man's ability to intervene in emergency situations, either to override a normally automatic function or to take over a tedious control task, can be exploited to reduce equipment redundancy requirements. Examples of this are cabin temperature control and reentry flightpath guidance.

Experience in manned aircraft and spacecraft operations has shown that backup (off-line) functions should employ differing principles of operation: the phenomenon that caused failure of the primary thread may be characteristic rather than statistical. An example is R.F. NAV AIDS (VOR/DME) as backup to an inertial navigation system.

On-line (active) redundancy is a relatively infant technology that has reached its highest level of development in flight control systems. Experience to date has shown that voting and switching techniques can introduce branches in the fault tree that were first discovered by an incident investigative board. Accordingly, the design rule that results is that on-line redundancy should be used only on absolute flight-safety items where manual judgement and switching is too slow; and should be then exhaustively tested in simulators using flight-rated hardware. In contrast to the design rule for off-line redundancy, on-line redundancy should use identical principles of operation. This derives from the difficulty of fine-scale voting on the rapidly varying output signals that are produced by equipments operating on differing principles.

The time-sharing capability of the digital computer makes it a prime candidate for centralization. However, the extent to which this is cost-effective is restrained by data transfer rate requirements throughout the vehicle and, most of all, by flight-safety considerations. In particular, on-line and isolable redundant computing functions tend to propagate this burdensome requirement to functions that are not absolute safety-critical and/or can utilize manual backup. Examples are short-period flight control versus long-period guidance and energy management. Also, functions that are basically central in nature (onboard checkout) cannot be dedicated and hardened against programming errors or maintenance malpractice as readily as functions that are amenable to LSI micro-processor technology (air data computer).

Integration design rules should avoid casual abrogation of traditional interfaces.

INTEGRATED AVIONICS DESIGN RULES

- ROUTINE FUNCTIONS SHOULD BE AUTOMATED; JUDGMENT FUNCTIONS SHOULD BE EFFECTED BY THE FLIGHT CREW.
- MANUAL INTERVENTION SHOULD BE USED AS BACKUP TO AUTOMATIC MODES WHERE SUCH MANUAL, OFF-LINE REDUNDANCY IS NOT TIME CRITICAL WITH REGARD TO HUMAN RESPONSIVENESS.
- OFF-LINE BACKUP FUNCTIONS SHOULD CONSIDER DIFFERING PRINCIPLES OF OPERATION, WHERE POSSIBLE.
- ON-LINE (PARALLEL OPERATION) REDUNDANCY OF EQUIPMENT SHOULD BE LIMITED TO THOSE FUNCTIONS WHICH ARE TIME-CRITICAL AND SHOULD USE IDENTICAL PRINCIPLES OF OPERATION.
- COMPUTING FUNCTIONS THAT ARE NOT UNIQUE TO A GIVEN SUBSYSTEM, AND/OR ARE TAILORED TO EACH MISSION, SHOULD BE CENTRALIZED IN A REPROGRAMMABLE COMPUTING COMPLEX. COMPUTING FUNCTIONS THAT DO NOT VARY MISSION-TO-MISSION, ARE UNIQUE TO A GIVEN SUBSYSTEM, AND/OR ARE SAFETY-CRITICAL SHOULD EMPLOY DEDICATED COMPUTING.
- IN THOSE CASES WHERE THE TECHNICAL TRADES OF COST, WEIGHT AND RELIABILITY ARE NOT DECISIVE, THE DEDICATED EQUIPMENT APPROACH SHOULD BE FAVORED AS A MEANS TO MINIMIZE DEVELOPMENT AND FUNCTIONAL INTERDEPENDENCE.

Integrated Avionics System

The Executive Processor generates guidance and master control commands, and effects subsystem monitoring, checkout, and display management.

Manual inputs to the executive processor are made using a keyboard which interfaces with the display/control processor. In the unmanned mode, inputs to the executive processor are made via the digital data link in the Communications subsystem.

The Manual/Automatic Mode Switches are mixing points for safety-critical commands normally issued by the executive processor(s) or for manual override by the crew, when mandatory. Safety-critical functions employ dedicated, non-multiplexed data buses between the cab and the critical subsystems.

A dual, off-line redundant, multiplexed data bus is used for checkout, monitoring, and non safety-critical sequencing and control of all subsystems. An on-line redundant mode is available for unmanned missions.

The Standard Interface Units (SIU) are elements which provide access to the data bus, and data acquisition and processing capability, as required. The SIU can be modularly expanded to provide the data bus interface backed up by signal multiplexing, parallel-to-serial/serial-to-parallel conversion, analog to digital conversion, signal buffering, and specialized local data processing (such as built-in test functions that are not amenable to integration with the subsystem itself).

The Fixed Displays contain dedicated displays (attitude indicator, Mach/indicated airspeed, altimeter, compass) to manually operate the vehicle in a safe-return mode, - not necessarily a mission-complete mode.

The Navigation subsystem consists of all non-RF sensors (inertial, star or optical trackers). High data-rate computations (coordinate transformation) are done in a dedicated, hard-wired navigation computer.

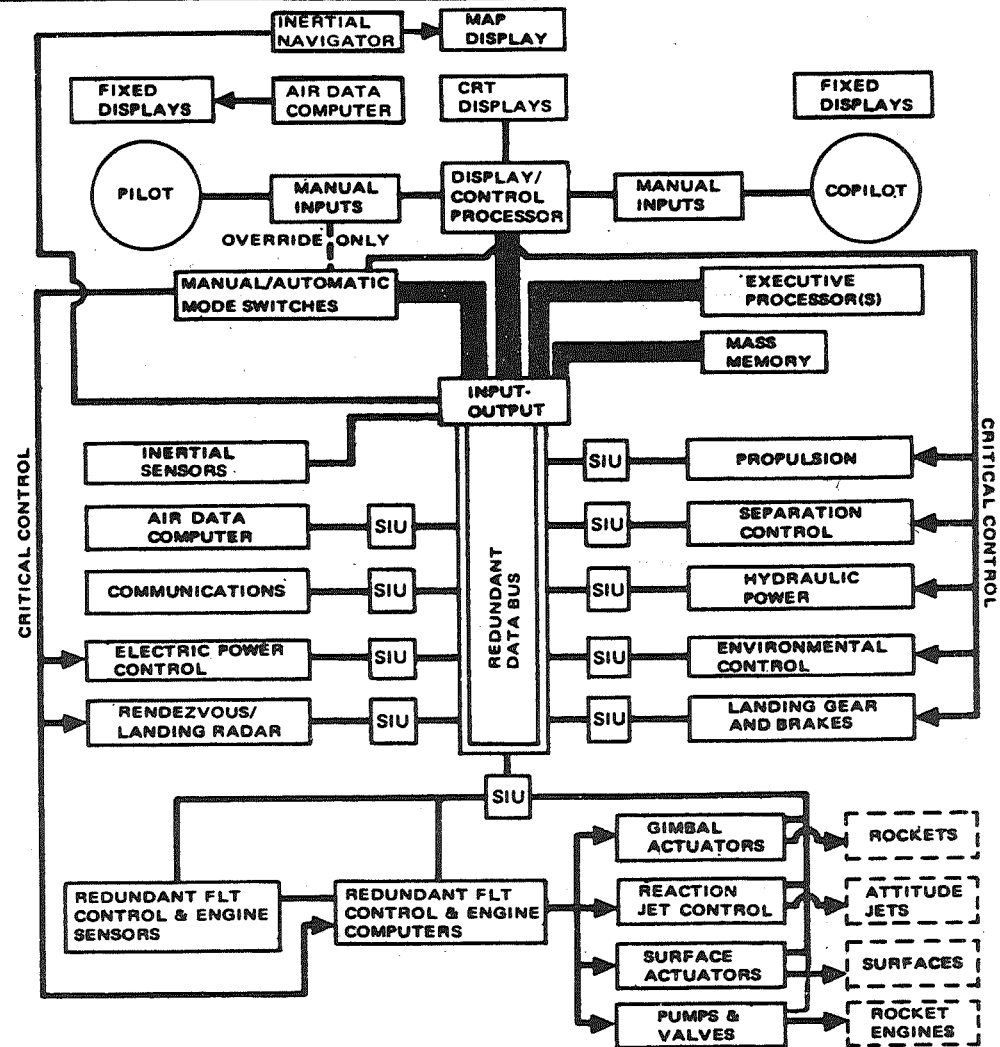
The Communications subsystem includes all R.F. NAV-AIDS (rendezvous radar, transponders, VOR/DME) and digital or voice data links.

The Flight Control and composite boost Engine Control subsystems are individually dedicated and hardwired. These subsystems employ triply on-line redundant sensors (rate gyros, linear accelerometers, pressure and flow-rate transducers), time-shared computers, and dedicated wires from the cab controls to the aft avionics bay, thence to the actuators.

The Air Data Computer, used for automatic operation, is dedicated and is not required for operation of the flight control subsystem, which is self-adaptive.

The Propulsion subsystem includes the necessary fuel and reactant tankage, valves and distribution lines for the total requirement of the vehicle systems as well as airbreather jet engines.

INTEGRATED AVIONICS SYSTEM



Data Management

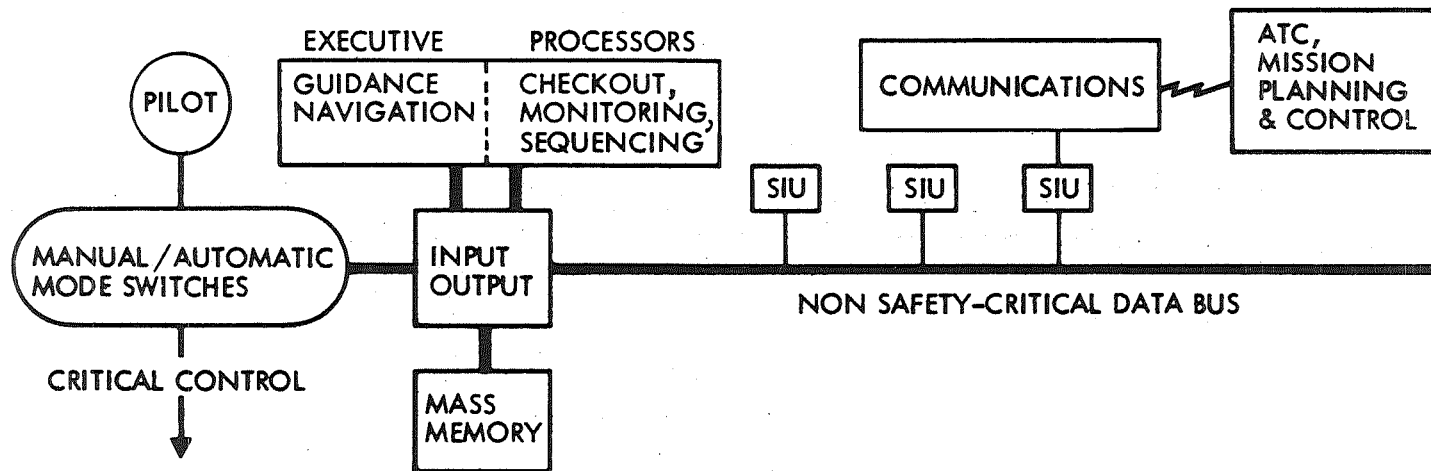
The computing complex system is designed to minimize developmental cost and risk and yet provide application flexibility and growth potential. The configuration consists of dual central processors operating out of multiport main memory modules and provides sufficient central processor, memory, and input/output capability to maintain full operation in the event of single unit failures. The operational software processing load is distributed between the asynchronously operating executive processors in a dedicated fashion, and is modular in construction to permit reconfiguration and growth. Recovery techniques are employed to help circumvent failures and reduce hardware and software redundancy requirements. Growth to a multiprocessing system is possible through the addition of executive software.

The data collection and distribution system consists of a single-thread dual redundant data bus for transferring non-safety-critical data, and a set of redundant hardwires for handling safety-critical functions. Data is transmitted on the bus using time-division multiplexing and employs a self-clocking manchester modulation scheme. The transmission medium is a shielded twisted pair coupled to a receiver transmitter (R/T) operating in a balanced mode. Each R/T has a unique address and provides a standard interface between the data bus and the standard interface units. Information is transferred serially at a 2 megahertz rate.

The standard interface unit (SIU) provides a method of electrically interfacing the data bus with the vehicle subsystems. These units are modular devices partitioned so as to be functional in nature. Each unit performs any or all of the following functions: converts analog signals to digital words, performs limit checking between programmed limits, accepts discrete and digital inputs, and converts pulse trains into digital words. It also is capable of taking digital words from the bus and converting this information into the appropriate discrettes, digital words, pulse trains, or analog signals. Each SIU has a built-in test feature that is capable of identifying internal system failures.

The mass storage system is a mixture of fast random access mass storage (e.g. drums) and low cost transportable storage (e.g. tape cassettes). The fast random access storage is used for mission data entry storage (via an R.F. link from a ground-based computing complex), and operational storage backup. The low cost transportable storage is used for mission history data recording, checkout and diagnosis, and as backup to the fast random access storage. All mass storage is controlled by the executive central processors through the input/output processors and has direct flow access to the main memory modules.

DATA MANAGEMENT



- TWO IDENTICAL EXECUTIVE PROCESSORS, OPERATING ASYNCHRONOUSLY IN A DEDICATED MANNER. CONFIGURATION IS SINGLE FAILURE, FAULT-TOLERANT.
- DATA COLLECTION AND DISTRIBUTION SYSTEMS EMPLOYS A DUAL REDUNDANT DATA BUS FOR NONCRITICAL DATA AND A REDUNDANT HARDWIRED SYSTEM FOR CRITICAL FUNCTIONS
- STANDARD INTERFACE UNITS PROVIDE LOCAL SPECIALIZED PROCESSING AND A MEANS OF COUPLING THE SUBSYSTEMS TO THE DATA BUS
- MASS STORAGE IS A MIXTURE OF FAST RANDOM ACCESS AND LOW COST TRANSPORTABLE STORAGE. PRIME ENTRY MECHANISM IS VIA A RF DATA LINK FROM GROUND BASED COMPUTING COMPLEX.

Displays and Controls

The displays and controls subsystem places emphasis on the concept of programmable displays, and a high degree of automation with a manual override mode for every function. Utilization of this concept relies on the fact that the need for particular display and control parameters is not continuous but can be programmed, to a large extent, well in advance of a mission.

The basic layout of each crew station includes four cathode ray tubes (CRT) with each assigned the following specific functional task: 1) vehicle attitude display presents actual, command, or error values of attitude, velocity and altitude parameters, with a background of a TV picture looking forward; 2) horizontal situation display contains present position geographically along with prediction and command values; 3) mission events display presents a moving scroll of system events, used by the crew to monitor automatic sequencing and controls; 4) system status display presents subsystem status and monitoring of changes to the configuration, as affected by either automatic or manual control commands. Two swiveled periscopic vidicons, one above the cab and one below, supplant the requirement for windscreens. An optical viewing screen, requiring a 5 inch port, is used for backup.

The switch logic portion of the subsystem allows crew or automatic initiation of functional interchange of displays between the four available indicators at each crew station. This feature allows performance degradation in the event of either indicator or generation logic failures.

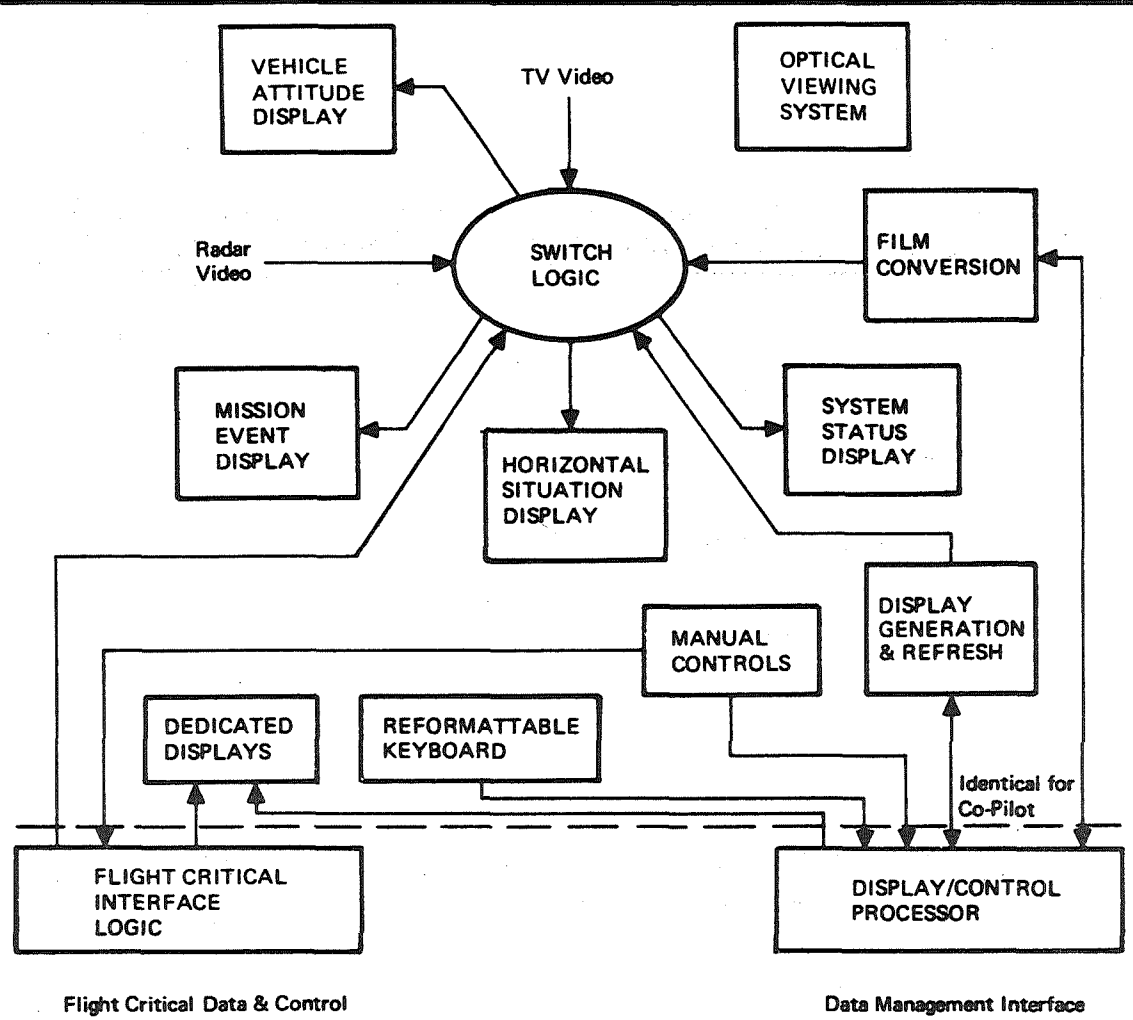
Certain dedicated displays and manual controls provide the interface of the crew with those parameters which are flight-safety critical, for operation in the event the data management subsystem fails.

Certain types of data such as maps, checklists, tech manuals and procedures are rarely revised and represent either high resolution or density demands for the storage and dissemination of such data. These types of data will be stored in film cassettes with reproduction provided by conversion to an electronic format allowing presentation on the CRT indicators.

The reformattable keyboard concept, in conjunction with a set of control devices (both linear and discrete) associated with the system status display, provide the entry means for crew-initiated responses and controls via the interface with the data management subsystem. The theory of operation of these devices assumes a discrete set of reactions or responses for any set of displayed parameters.

The display/control processor is responsible for the collection of data, conversion of this data into the appropriate electronic signals to drive the CRT indicators, and definition of the multifunction input devices as the configuration of displayed information and control is selected by either the automatic sequencing or manual crew selection. Computation and data storage requirements of the display/control subsystem will be handled by the data management equipment.

DISPLAY AND CONTROLS



Guidance/Navigation

The guidance and navigation functions are distributed differently from that found in previous aircraft and space vehicles: angular and linear acceleration data in vehicle coordinates are sensed by a strapdown inertial sensor block, with navigation and guidance computations being effected by the executive processors of the data management sub-system. In the primary navigation mode, raw data from the sensor block is fed directly into the input/output section of executive processor "A". In the back-up mode, a conventional gimballed platform feeds latitude and longitude, in addition to angular data in inertial coordinates, into executive processor "B". The navigation software for processor "B" is obviously different than that of processor "A"; this, along with the contrasting inertial sensing technique, illustrates one application of the "differing principles" design rule previously mentioned. Additional back-up for ferry operations is provided by VOR/DME.

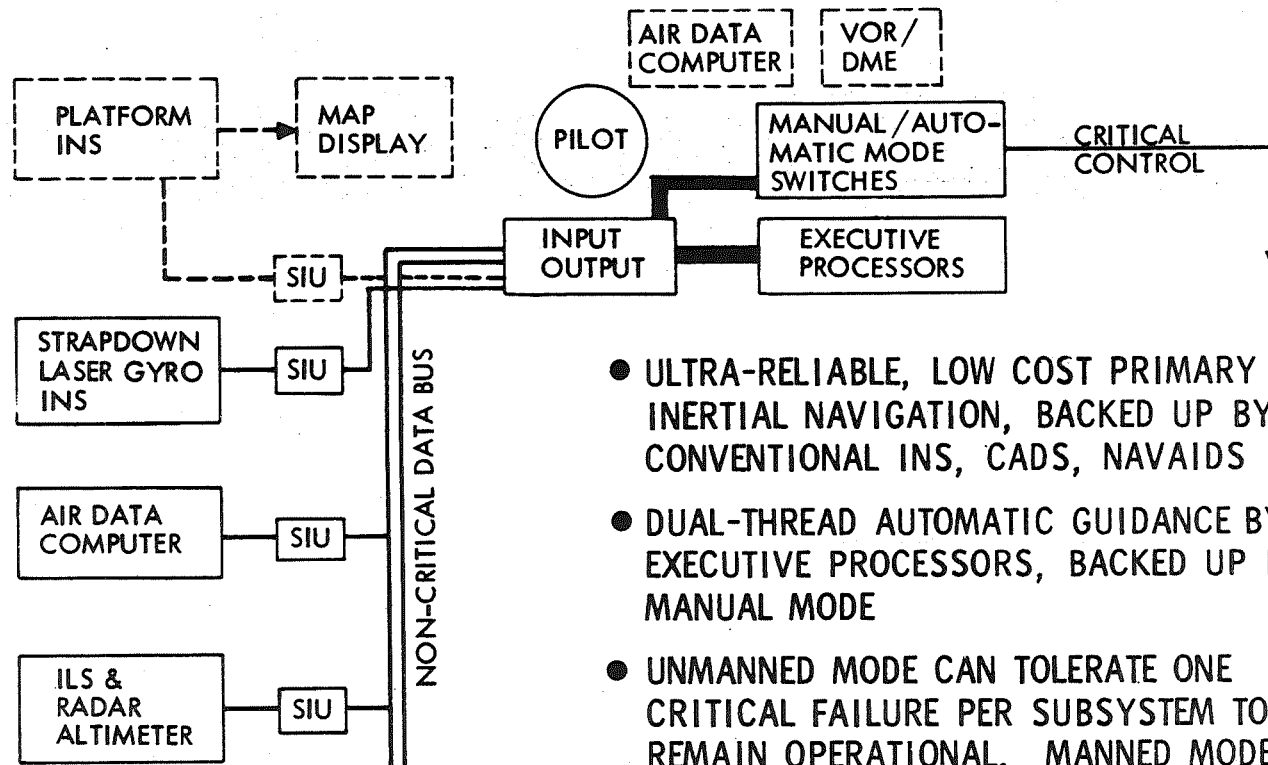
20

Simulation studies of reentry from earth orbit, and flight test experiments of the let-down phase, have shown the feasibility of a safe-return mode, using rudimentary data in combination with manual guidance. This point, carefully qualified, permits guidance/navigation, data management, and portions of other sub-systems to be configured to a lower level of redundancy than that required for absolute safety-critical functions, like flight control. A safe-return mode is thus available in the event both threads of the data management sub-system and the primary navigation sensors should fail. Off-line redundancy is also permissible, thus de-sensitizing these portions of the avionics system to hidden branches of the voter and switching fault tree.

Both air data sub-systems are available to the executive processors: one through data bus "A", the other through data bus "B". One unit is always hardwired to a dedicated display for manual guidance modes.

The type selection of rendezvous, docking, and autoland sensors is not critical to the basic system architecture. However, automation of the related guidance functions should be a design goal because these functions are error-susceptible in the manual mode and are amenable to automation.

GUIDANCE/NAVIGATION



- ULTRA-RELIABLE, LOW COST PRIMARY INERTIAL NAVIGATION, BACKED UP BY CONVENTIONAL INS, CADS, NAVAIDS
- DUAL-THREAD AUTOMATIC GUIDANCE BY EXECUTIVE PROCESSORS, BACKED UP BY MANUAL MODE
- UNMANNED MODE CAN TOLERATE ONE CRITICAL FAILURE PER SUBSYSTEM TO REMAIN OPERATIONAL. MANNED MODE CAN TOLERATE TWO FAILURES FOR SAFE-RETURN MODE

Flight Control

The flight control system is dedicated primarily because it is absolute flight-safety critical, requiring special protection against maintenance errors and physical or electrical damage. It is on-line redundant because a statically unstable vehicle, flying through a fluid medium, will experience structural breakup (within 2 - 5 seconds) in the event of loss of active control. The equipment is located in an aft avionics bay because of the large number of safety critical wires that radiate from the controller to the effectors (thrust vector and aero surface actuators, and reaction control jets), most of which are located near the aft end of the vehicle. Six dedicated command lines are required to transfer signals (roll, pitch, yaw and translation) from the sidarm controllers in the cab to the flight control electronics. Guidance commands from the data management system are injected into the flight control system at the sidarm controller, the latter serving as either a manual bias of the normal automatic commands or as an override of the automatic mode of operation.

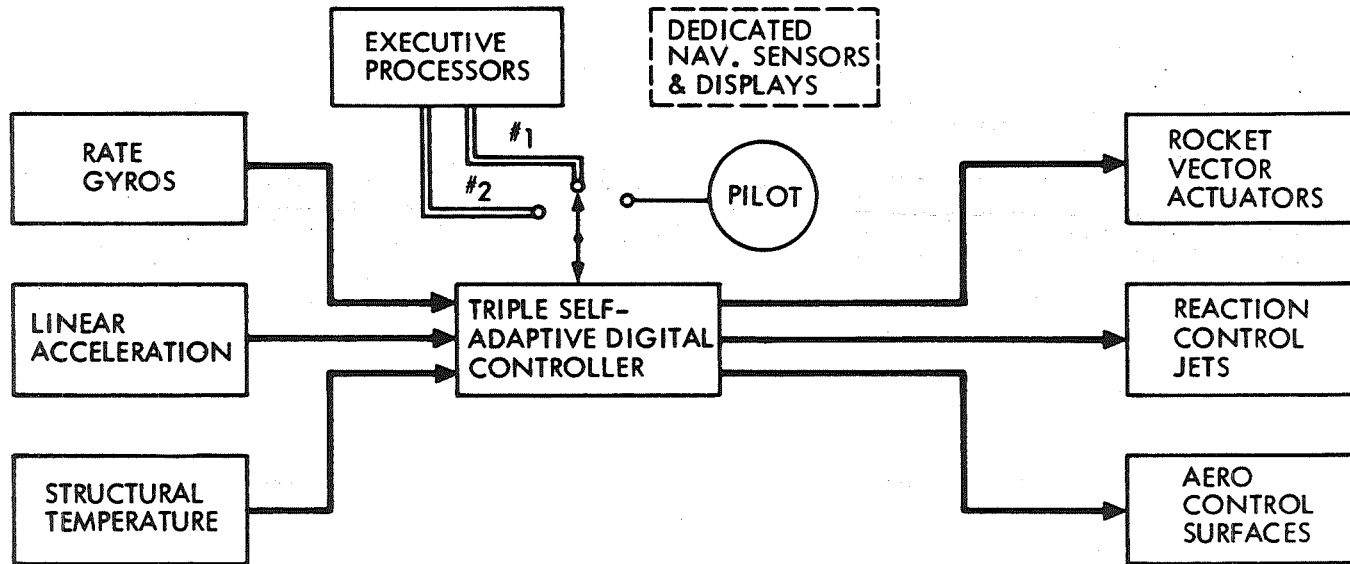
22

The basic control law within the atmosphere is pitch or yaw rate, at speeds below 250 knots, shifting to a pitch linear acceleration and roll-to-steer mode at speeds above 250 knots. Blending of control authority between thrust vector, aerodynamic, and reaction control is done automatically by the self-adaptive gain adjustment feature. Automatic gain compensation is effected by constantly measuring vehicle response to a sub-liminal test signal. The self-adaptive gain control technique was chosen over direct air data measurement or navigation-derived data so as to preserve the integrity of the flight control function by minimizing susceptibility to failure of subsystems that have been configured with lesser redundancy.

The rate gyros provide data necessary to effect the proper value of stiffness and damping to the aerodynamic weathercock of the airframe. The linear accelerometers are required for proportional and limit control while in the acceleration mode of aerodynamic and reaction control. Airframe temperature at key points is measured to prevent inadvertent structural overheat when under manual flightpath control. Stalling is prevented by inferred measurement of angle-of-attack, then comparing this computed result with conditional data on stall onset that has been derived from wind-tunnel tests.

The computing requirements for the flight and engine controllers are mutually similar and somewhat unique, relative to the computers used in the data management computer complex; both employ digital frequency-selective filters with time-varying coefficients, and require high sampling rates to effect stable, active control. The multiple axes and multiple engine control requirements also make time-shared centralized computing a significant weight economy. A single processor configuration, specially designed for this class of function, is postulated as a means to reduce development and maintenance costs.

FLIGHT CONTROLLER



- PERMITS PILOT OVERRIDE FOR SAFE RETURN
- PROVIDES AUTOMATIC G-LIMIT STRUCTURAL PROTECTION
- PROVIDES AUTOMATIC STALL PREVENTION & DEEP-STALL LOCK-OUT
- PROVIDES INNER-LOOP PROTECTIVE CONTROL AGAINST STRUCTURAL OVERHEAT
- LOCATED IN AFT AVIONICS BAY WITH DEDICATED, CENTRALIZED, ENGINE CONTROL COMPUTERS OF IDENTICAL HARDWARE DESIGN

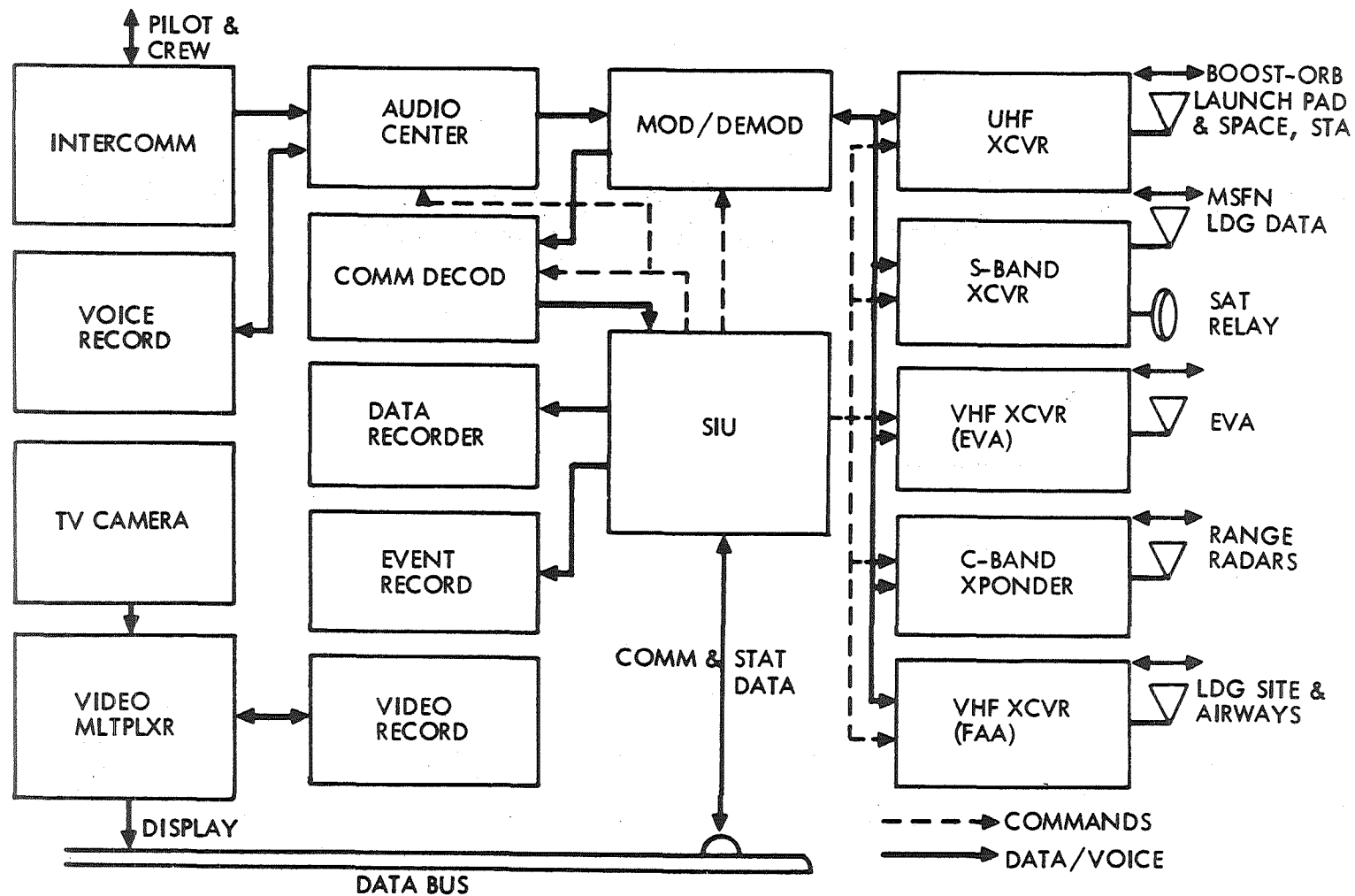
Telecommunications

The communications subsystem is designed for simultaneous handling of digital command, telemetry data, and voice on any single R.F. carrier in contact with the ground, the space base, or a communication satellite. The automatic landing aid employs swept beam microwave radar: The current instrument landing system (ILS), requiring 3° glide slopes, is not practical for orbiter configurations that use turbo-jets that are installed only for ferry missions.

Specialized encoding and decoding is done by a special processor within the standard interface unit (SIU).

TELECOMMUNICATIONS

25



Avionics Equipment Location

The avionics equipment is concentrated in two major locations in the vehicle; the rocket engine control and flight control computers in the empennage and the vast majority of the equipment forward in the avionics equipment bay and the cab. The location of each item of equipment which is not in the equipment bay is dictated by the function which it performs and its interfaces with other equipment, the data management subsystem (DMS), or the crew.

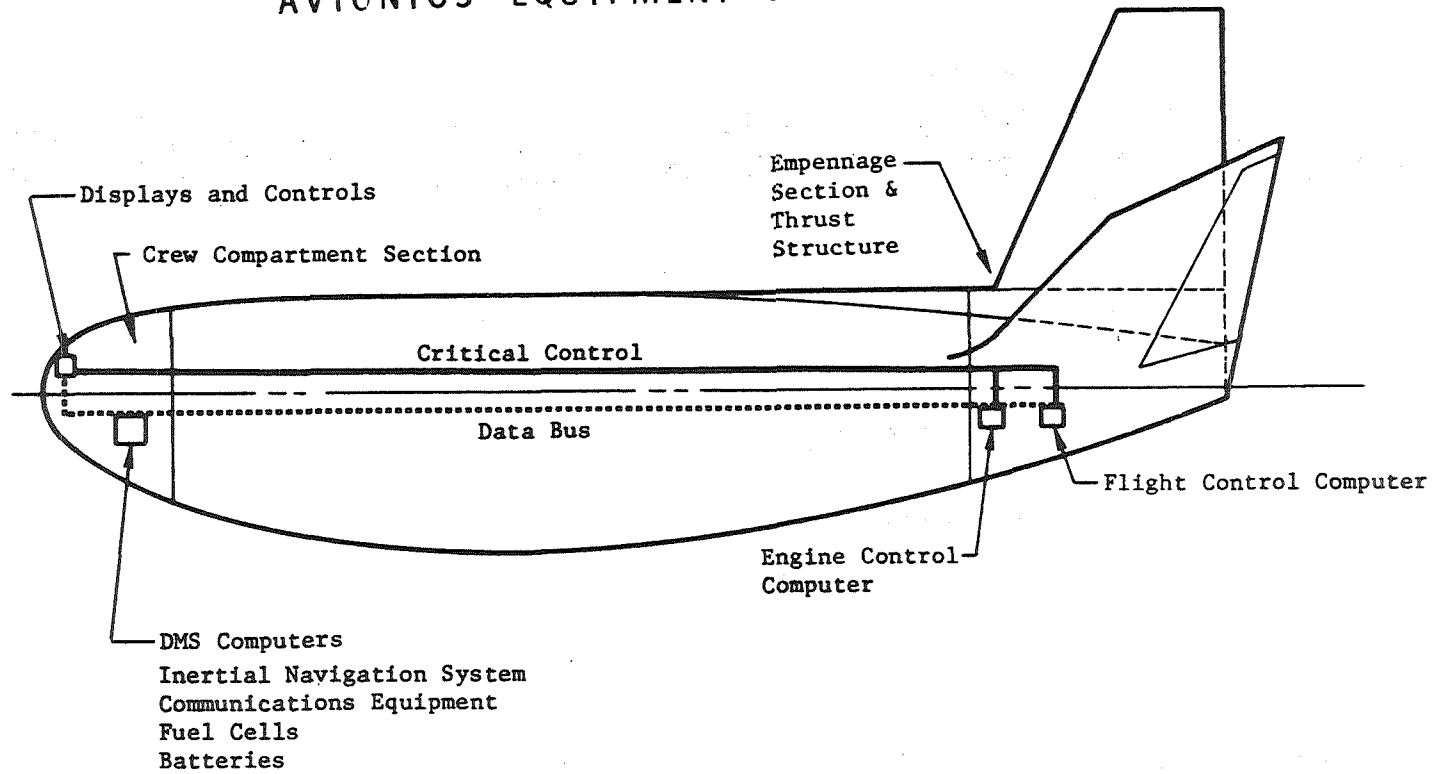
26 The DMS will be centralized with two separate computers and the principal data bus terminal located in the forward equipment bay. This will locate the guidance and navigation computing function close to its principal data interface, the Inertial Measurement Unit (or strap-down sensor block), minimizing the data transfer problem. The highest data rate and density for the checkout and monitoring functions will involve the remainder of the contiguous avionics located forward and the displays and controls in the cab. There is also an interface with the flight control and engine control computers but at a much lower data rate. In addition to the above equipment, the forward equipment bay contains the communication equipment, fuel cells, batteries and power conversion and switching equipment.

The dedicated flight control and engine control computers are located aft in order to be close to their sensors and actuators. This results in two subsystems which have a high data rate between their dedicated computers and their sensors and actuators, and a much lower data rate to the DMS computers in the forward equipment bay.

The data bus and its associated Standard Interface Units (SIUs) are distributed throughout the vehicle, thus tying all the units of the integrated avionics together. The SIUs are the DMS interface with all other equipment. They provide all conversion and conditioning of signals.

Antennas and power loss-related elements of the communication subsystem have their location dictated by required antenna coverage.

AVIONICS EQUIPMENT LOCATION



CONCLUSIONS

The integrated avionics required for shuttle employs a degree of functional centralization that has not, heretofore, been attempted on a large program. Gaining the confidence of technology interests at large, who normally have a parochial approach to equipment functions, may well be the most formidable hurdle. An integrated avionics breadboard demonstrator, connected to peripheral electromechanical equipment, is one way to gain this support and mutual cooperation. An avionics test bed airplane would also be persuasive. Another managerial tool is the so-called "systems engineering directorate," whose task is to adjudicate configuration options.

In conclusion, integrated avionics shows promise of achieving a breakthrough in lowering operational costs and launch weight requirements for shuttle. Organizing the equipment beginning with the system requirements, rather than with classical subsystems developed for non-integrated avionics, is the name of the game. Technological breakthroughs, as such, are not required: A better organization of existing components will do the job.

SALIENT FEATURES OF INTEGRATED DESIGN

28

	EXPERIENCE
● "MISSION CONTROL" AND ONBOARD CHECKOUT IS COMPATIBLE WITH COMMERCIAL AIRLINE OPERATIONS OF 1980	AIRLINES, CURRENT SPACE OPERATIONS
● EMPLOYS MIX OF CENTRALIZATION, DECENTRALIZATION, AND REDUNDANCY CONCEPTS TO MINIMIZE WEIGHT, COST, AND PROGRAM RISK	APOLLO GN & C, AIRCRAFT, TITAN III
● AVOIDS ERROR-SUSCEPTIBLE CREW FUNCTIONS	AIRCRAFT, MANNED SPACE PROGRAM
● UTILIZES MAN	AIRCRAFT, MANNED SPACE PROGRAM
● AVOIDS MARGINAL TECHNOLOGY e.g. MULTIPROCESSING AND FAIL-OP MULTIPLEXED DATA BUS	LACK OF SATISFACTORY INDUSTRIAL EXPERIENCE
● EMPLOYS DIFFERING PRINCIPLES OF OPERATION FOR MANUAL BACK-UP MODES	AIRCRAFT NAVIGATION

N70-40953

SIMULATION OF THE SHUTTLE SUBSYSTEMS MANAGEMENT AND CONTROL-FUNCTION

Michael A. Cowan and David J. Freeman

McDonnell Douglas Corporation
St. Louis, Missouri

INTRODUCTION

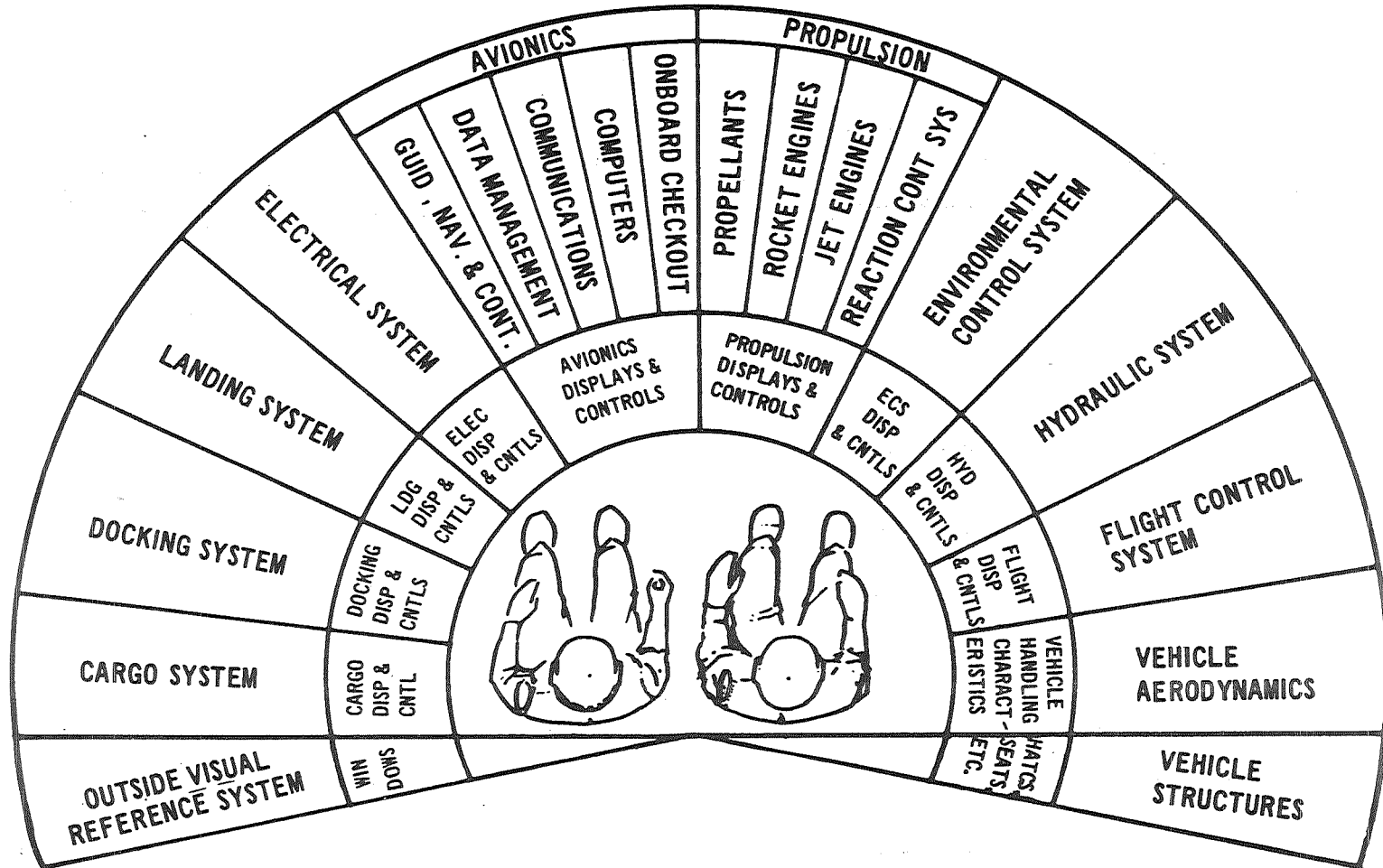
In many areas the true scope of the Space Shuttle has not been roughed out. Like an iceberg, what we see now is a small part of the total. This is certainly true in the integrated avionics area. I would like to focus attention on one aspect of the shuttle integrated avionics system, its controls and displays, and outline what I believe to be a significant technology requirement in this area. Specifically, I want to discuss simulation of a part of the crew/control and display interface which I have called the subsystem management interface.

Admittedly, involvement with the man machine relationship touches the human factors technology. Dr. Jones of MDAC-East addresses the human factors aspects more directly in a related paper being presented at this symposium. Electronic designers and human factors specialists will be working together to investigate subsystem management and control functions on the Space Shuttle.

The crew/shuttle control and display interface (Figure 1) includes the flight control subsystems, and the controls and displays to manage and operate shuttle subsystems. The largest subsystems, in terms of potential crew workload are the flight control, propulsion, and avionics subsystems.

Workload imposed by the propulsion subsystem will be higher than in past spacecraft due to the incorporation of main boost rocket engines, reaction control jets, and air breathing engines, all within the same vehicle. Avionics management workload will increase not only because of an increase in scope of avionics requirements, but also because of a high level of equipment redundancy which will multiply the number of electronic units carried onboard.

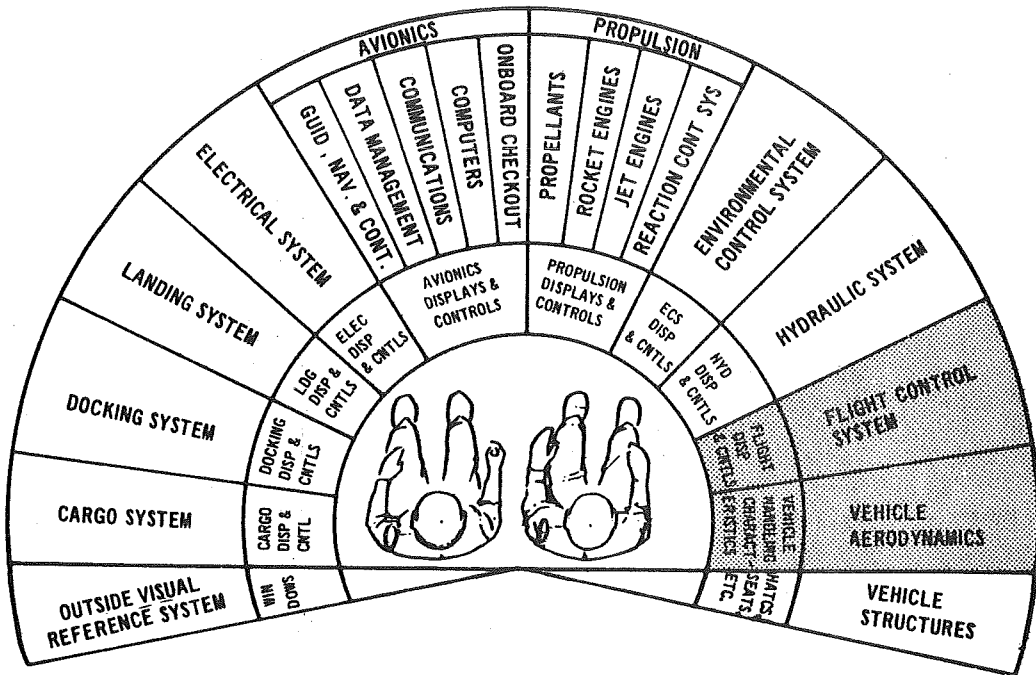
CREW SUBSYSTEM



The term flight control subsystem is reasonably explicit, and well understood to include those displays, controls, actuators and autopilot elements used to direct the flight of the vehicle along a desired path. (Figure 2A) Vehicle aerodynamics directly influence the design and usage of the flight controls and are shown here as a part of the total flight control subsystem.

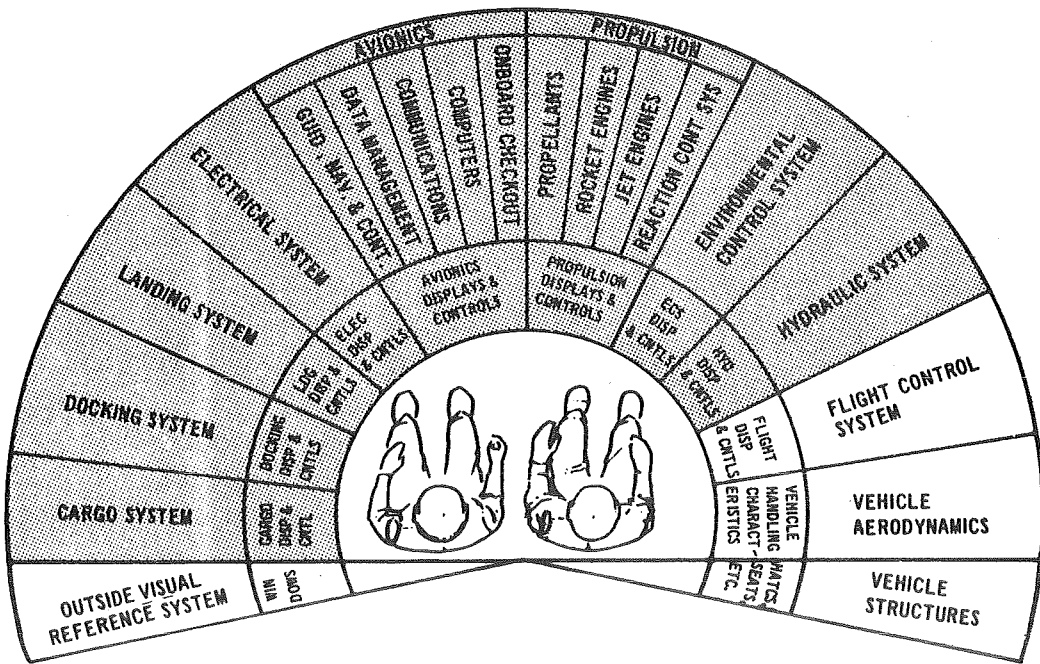
There is a notable lack of an equally common term which encompasses crew interaction with the remainder of the shuttle subsystem, (Figure 2B). We propose the use of the expression "subsystem management" to describe these other subsystem control and display functions.

CREW SUBSYSTEM FLIGHT CONTROL MANAGEMENT



CREW SUBSYSTEM SUBSYSTEM MANAGEMENT

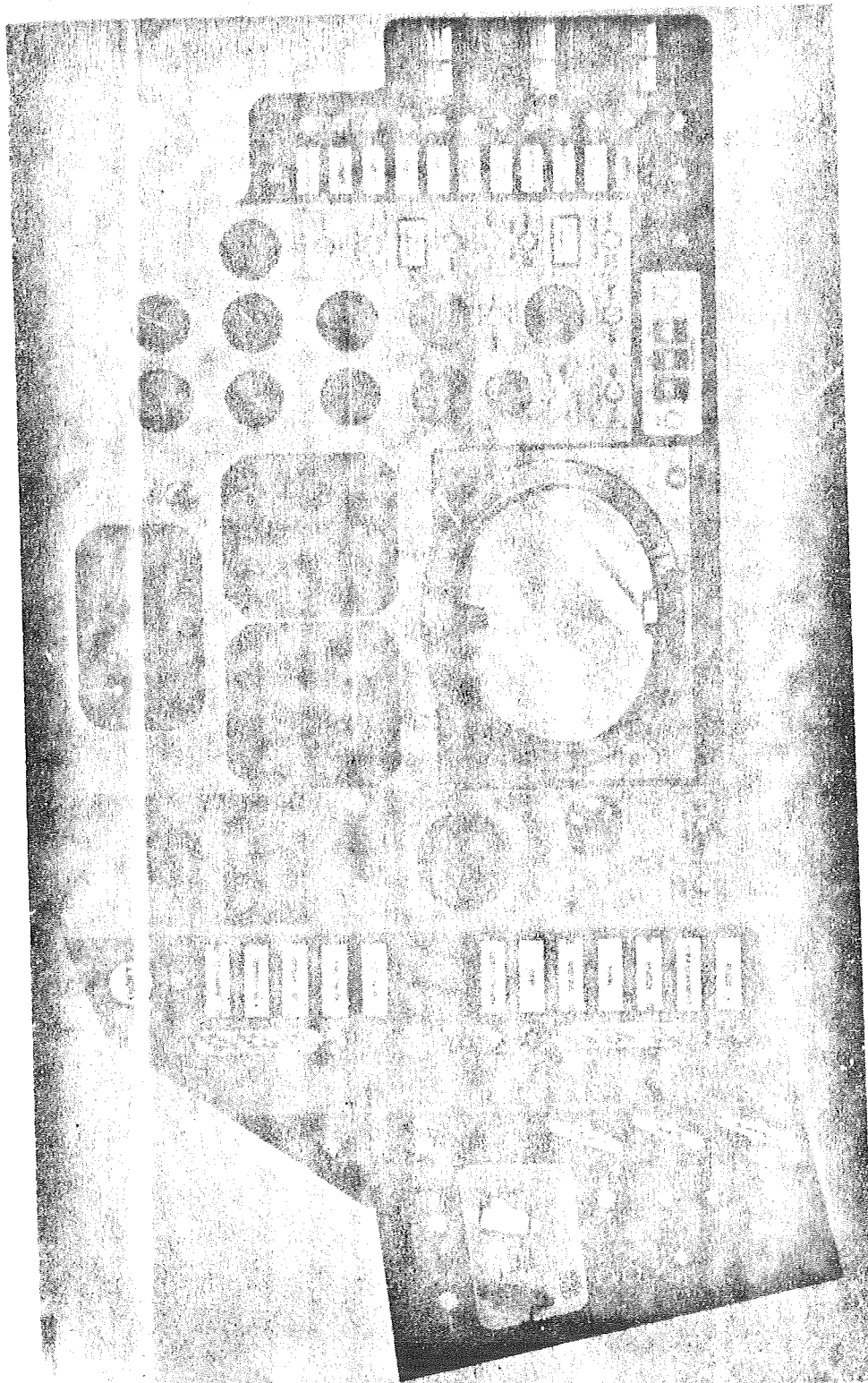
1041
23011278



One way to project the scope of the shuttle display and controls is to extrapolate from past manned space programs. The Mercury control panel (Figure 3) was a simple grouping of a few basic instruments. Flight displays are in the upper center panel. Subsystem management controls and indicators are at right, and sequencing and configuration controls are at left. Mercury, while simple in concept and design, was highly automated, and made a long series of unmanned flights.

Gemini controls and displays became more extensive as more subsystems were placed onboard. Flight control displays were placed in front of each crew member and subsystem management controls occupied central and side panels. At this point in spacecraft evolution, subsystem management controls began to occupy the major portion of panel area, yet the absolute number was still small enough to pose no major problem to a well trained crew.

The ambitious and difficult objectives of the Apollo program created a demand for more subsystems, both to increase reliability, and to satisfy new requirements. In Apollo, the large majority of the panel area is given over to subsystem management functions.

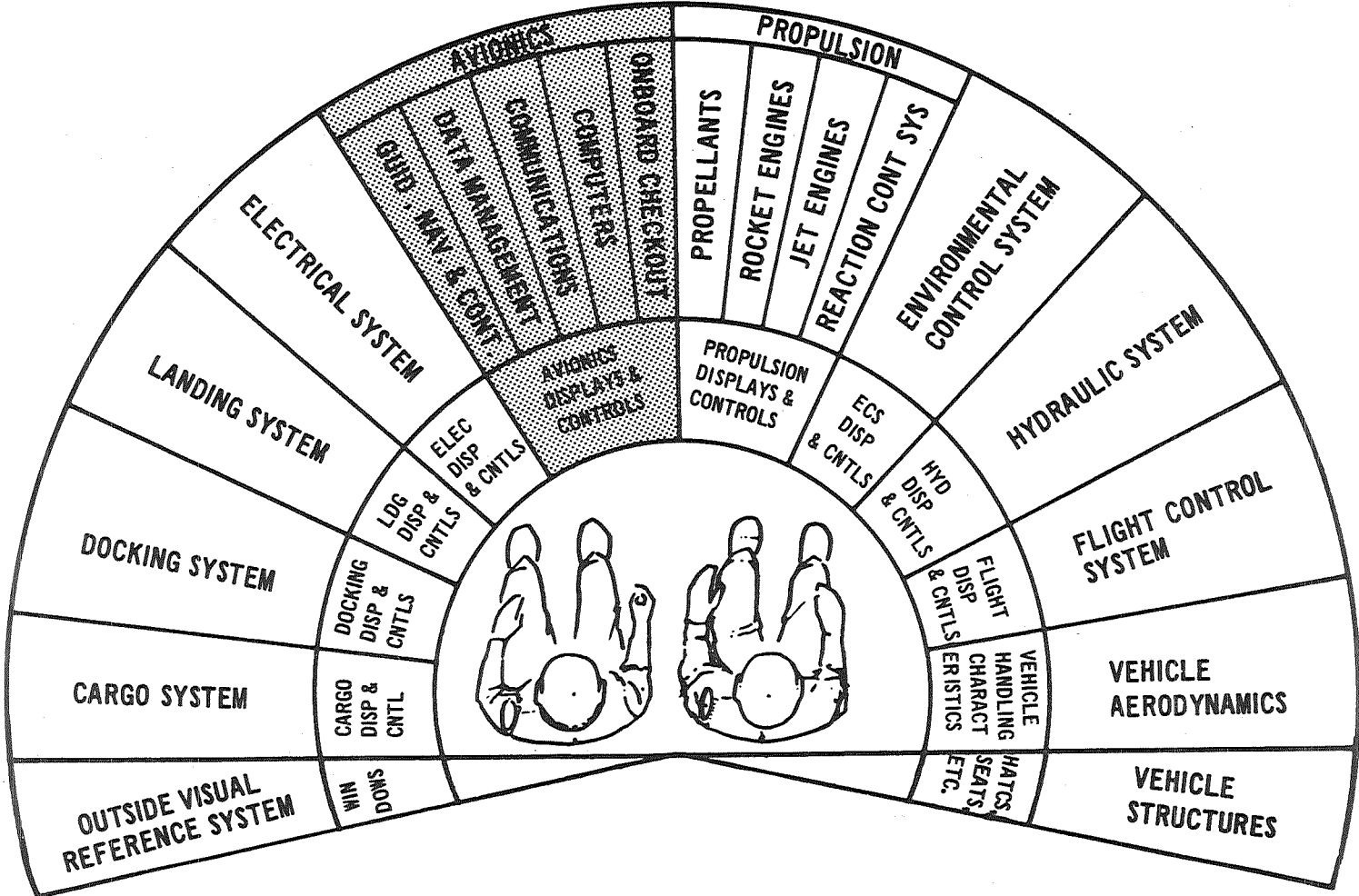


Subsystem management in Apollo involves a lot of detailed subsystem control. The crew must make configuration decisions within a mode as well as select the operational mode itself. For example, either one of 2 sets of redundant body mounted attitude gyros may be selected, or alternatively, platform derived attitude, before the crew makes the final "management decision" of placing the spacecraft in an attitude hold mode. While this design is flexible to mission changes, the burden on the crew of safely making a multitude of similar second level configuration changes is large, as can be estimated from the size of the checklists carried onboard, and the amount of consultation that takes place with subsystem specialists in Mission Control. For the shuttle program, the desire for autonomous mission operations will place the complete burden of submode configuration on the crew. It is anticipated that computer aided configuration control will be used to restore a more realistic level of mode control activities to the crew so that they are free to act as true system managers.

The shuttle will have an aircraft mode of operation and thus share many functional requirements with large transport aircraft such as the DC-10.

Adding onboard checkout to the spacecraft, aircraft, and mission control functional requirements (Figure 4) we can begin to appreciate the true size of the shuttle display and control iceberg.

CREW SUBSYSTEM AVIONICS MANAGEMENT

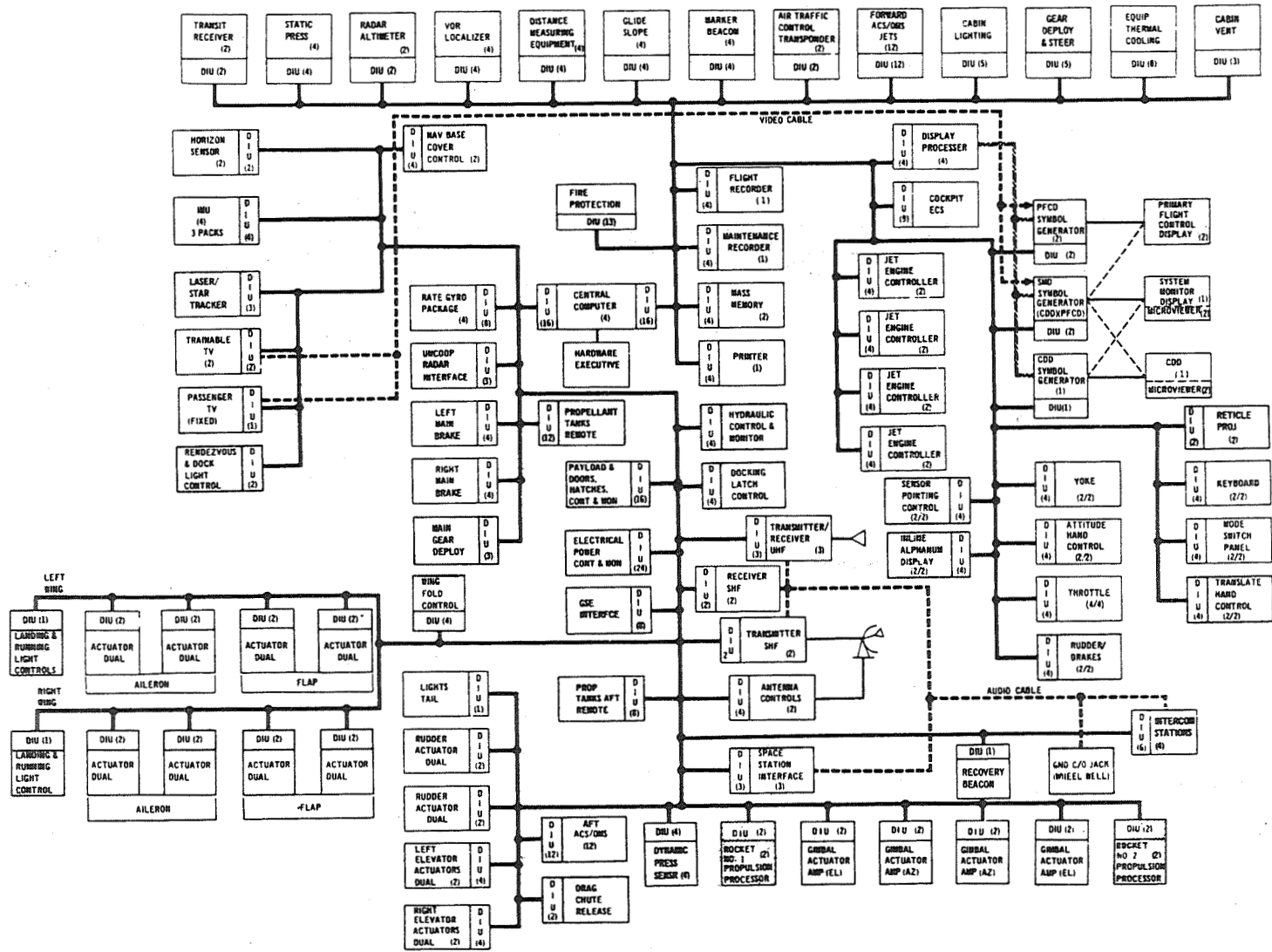


Consider merely the avionics subsystem (Figure 5). This subsystem contains 350 line replaceable units, joined by a quadruply redundant data bus. These units will carry on 6000 conversations at a combined rate of 10^6 bits/sec. The total avionics weight will be 2600 lbs. and the equipment is expected to consume 5000 watts of power.

Interfacing this subsystem with the crew, and making it easy and safe to manage is indeed a formidable design objective.

SPACE SHUTTLE LCR ORBITER AVIONICS SYSTEM (Configuration 2)

POSS
600-670



68

To date, the program guidelines (Figure 6) have been to reduce the number of displays and controls through integration of common functions.

The aim of integration is to reduce crew workload by using computer aided controls to carry out detailed, low level control tasks, while displaying sufficient data to the crew to ensure absolute, safe control over the total shuttle system.

One promising candidate for an integrated display is the CRT. This device can display alphanumeric data, pictorial flight displays, and graphic information with equal facility, and is truly a multipurpose display. Digital computers will be used to drive CRT displays and, can also be expected to preprocess much raw data before presentation to the crew.

Switching functions can be integrated by using them to control the logical state of a computer program which itself will carry out the detailed connection of circuit networks.

PROGRAM APPROACH TO SUBSYSTEM MANAGEMENT

INTEGRATION OF CONTROLS AND DISPLAYS

- MULTIPURPOSE DISPLAYS
- PREPROCESSED DISPLAY DATA
- REPROGRAMMABLE SWITCHES
- COMPUTER AIDED CONTROL

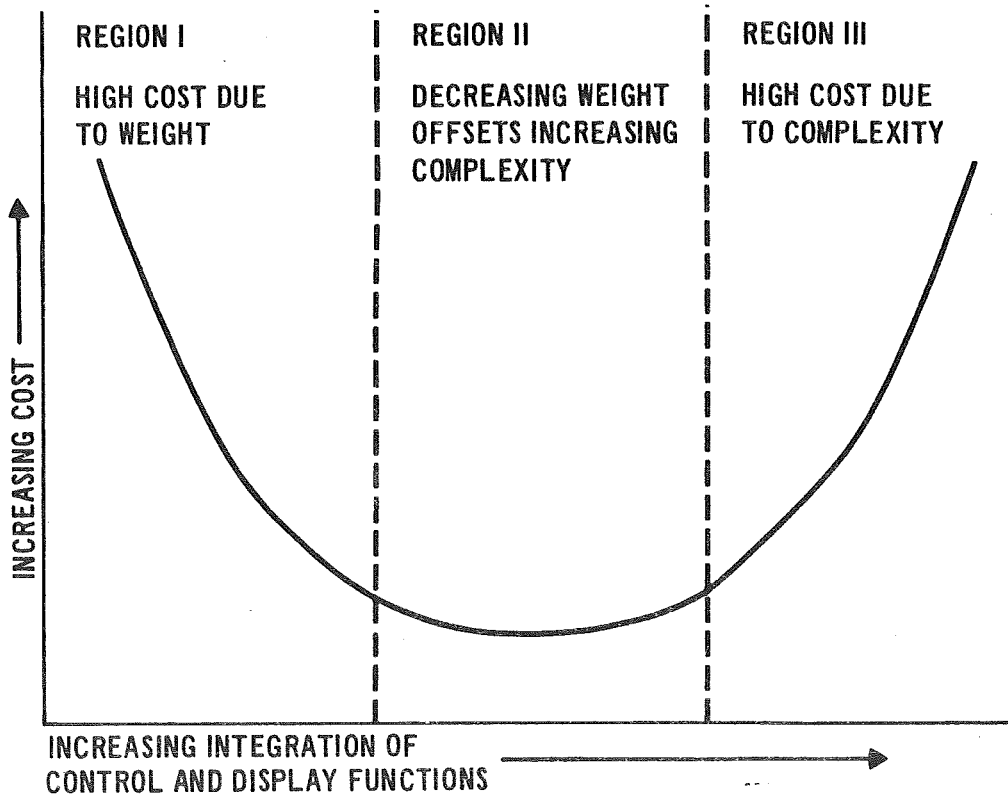
Two questions immediately become apparent, (Figure 7) how far should integration be carried, and how much should the design be automated?

KEY ISSUES

- DEGREE OF INTEGRATION
- DEGREE OF AUTOMATION

The answers to both questions will influence the program cost (Figure 8), and will determine how much flexibility of choice the crew will be able to retain in their role as system managers. Since the crew is of prime importance in manned space flight, we consider flexibility of the man/machine interface to be the driving variable, and cost to be the dependent variable in control and display trade studies. The chart illustrates that extreme flexibility (no integration) increases costs because of weight robbed from payload capability, and extreme integration incurs costs in design and development effort.

COST VS. DEGREE OF INTEGRATION



After initial trade study groundwork and workload analyses, a baseline configuration (Figure 9) can be proposed that embodies a trial answer to the question of "how integrated?" and "how automated?"

A CANDIDATE WELL INTEGRATED CONTROL AND DISPLAY BASELINE

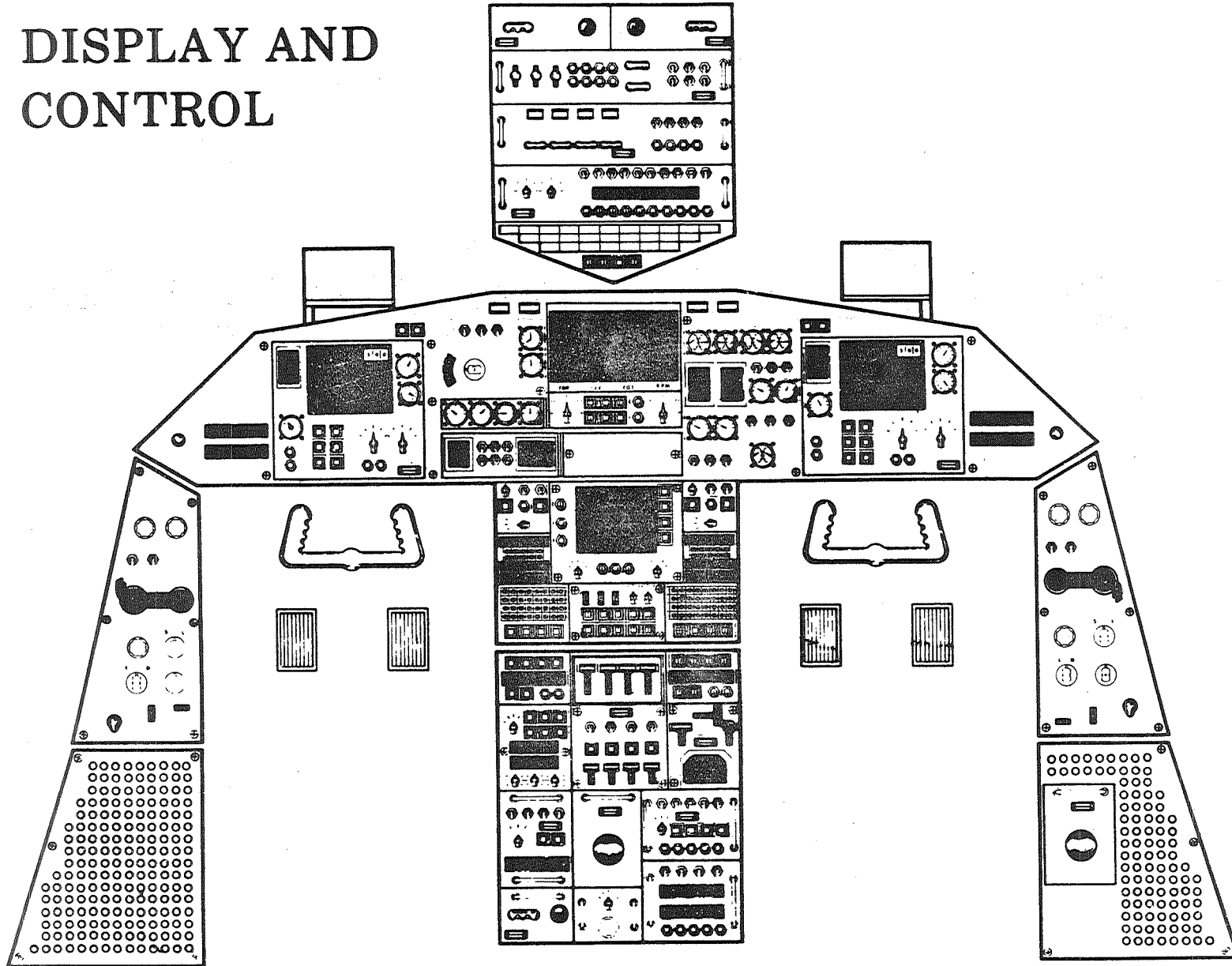
- FOUR MULTIPURPOSE CRT CONTROLS/DISPLAYS
 - FLIGHT CONTROL
 - SUBSYSTEM STATUS
 - COMPUTER INPUT/OUTPUT
- SOME DEDICATED CONTROLS/DISPLAYS
 - ELECTRICAL SUBSYSTEM FAILURE INDICATION
 - ECLS AND PROPULSION MONITOR
- MANUAL MODE SELECTION AND OVERRIDE
 - AUTO-SELECT WITHIN MODE

This baseline (currently based on pre-Phase B trade offs) is then developed into a panel design (Figure 10). Now we can study the question "does this integrated design provide the desired flexibility at a reasonable cost?"

Dynamic simulation technology should play an important role in these studies. Flight control simulation techniques and equipment are in common use in all major aerospace companies. Consequently, a shuttle flight control simulation can be quickly assembled at a reasonable incremental cost (on the order of 10^5 dollars). A complete system simulation is considerably more expensive, (on the order of 10^6 dollars), but more importantly, is difficult to achieve in the early phases of a program because of the small amount of design detail that is available in these phases. Thus by a vicious circle of events, the tool that should be used to help design the details of integrated subsystem management displays and controls is not available because of the lack of design details.

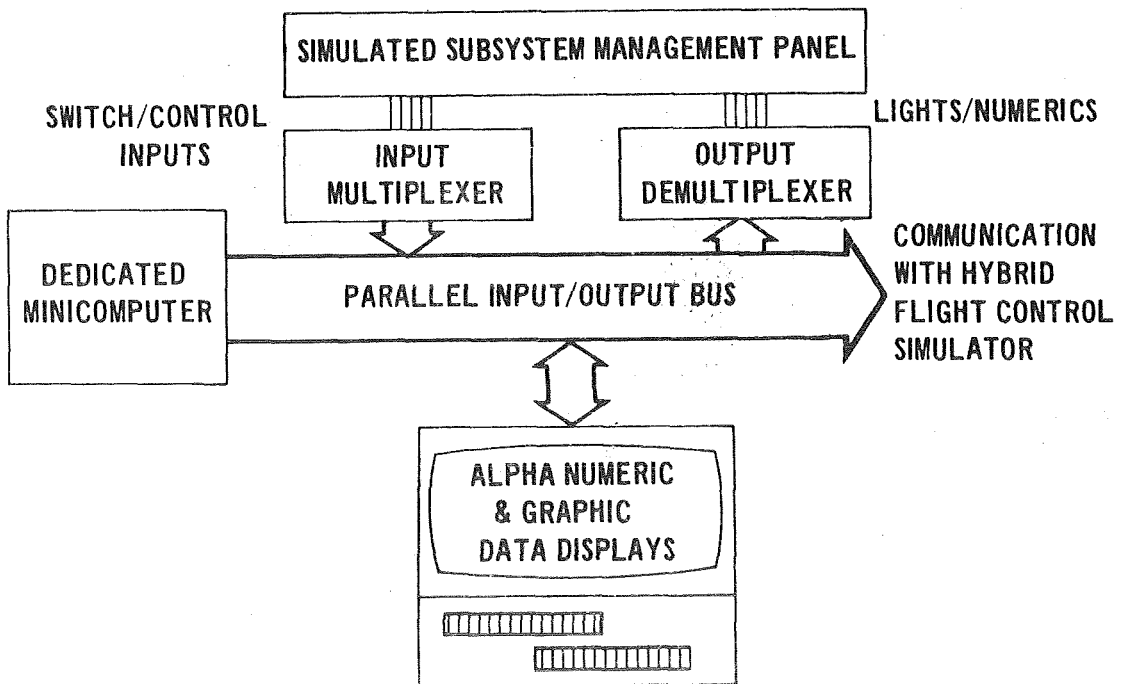
Therefore, a need exists for a tool, or technology, to fill this "simulation gap." This tool, for studying subsystem management panels should be flexible, inexpensive and available for use early in the design cycle. One MDC attempt at subsystem management simulation was to build a self-contained functional simulator of the desired panel, in this case, a total integration of all fighter avionics into one 18 in. by 18 in. control and display panel. For lesser degrees of integration, involving several panels this approach becomes less practicable.

DISPLAY AND CONTROL



Building on this experience, we have looked at the possibility of using small inexpensive dedicated computers (Figure 11) operating in conjunction with standard telemetry equipment to make completely functional subsystem management panels. Representative lights, switches, numerics, etc. are made available to the designer as basic building blocks with which to make a soft, but functional, mockup of his panel design. These building blocks are made up to plug into the multiplexer/demultiplexer equipment and thereby communicate with a dedicated minicomputer. Random access slide projectors can act the part of displays or alternatively, low cost remote computer terminal CRT displays can be used to display alphanumeric/graphic data. Such display equipment can handle problems where page update times of one second or greater are allowable. (The faster flight control displays require updating every 1/60 to 1/40 second and rightly belong in the province of special purpose flight simulation equipment.)

SIMULATION OF SUBSYSTEM CONTROLS AND DISPLAYS



Our effort to implement the complete simulation of the man/machine interface for the Space Shuttle (Figure 12) began early this year with parallel efforts in both flight control systems and subsystems management simulations. We have completed feasibility demonstration of the subsystems management functional simulation using a time shared computer facility operating at slower than real time rates. In a related effort, the flight control simulation has progressed normally using an existing hybrid computer facility, and CRT type flight director displays. By January 1971, we expect to have the subsystem management simulator converted to real time capability using a small dedicated computer.

IMPLEMENTATION PLAN

ACTIVITY	1970	1971	1972
SLOW TIME PROTOTYPE	■		
REAL TIME SIMULATOR	■		
SUBSYSTEM MANAGEMENT CONTROL PANEL STUDIES		■	
FLIGHT CONTROL SIMULATION	■	■	
TOTAL MAN/MACHINE SIMULATION		■	
HIGH FIDELITY SHUTTLE SIMULATION			■

After six months of separate use in support of the Space Shuttle Phase B studies, we plan to combine the two simulations. This will provide a simulation capability for studying the total man/machine interface.

TOTAL SHUTTLE SIMULATION

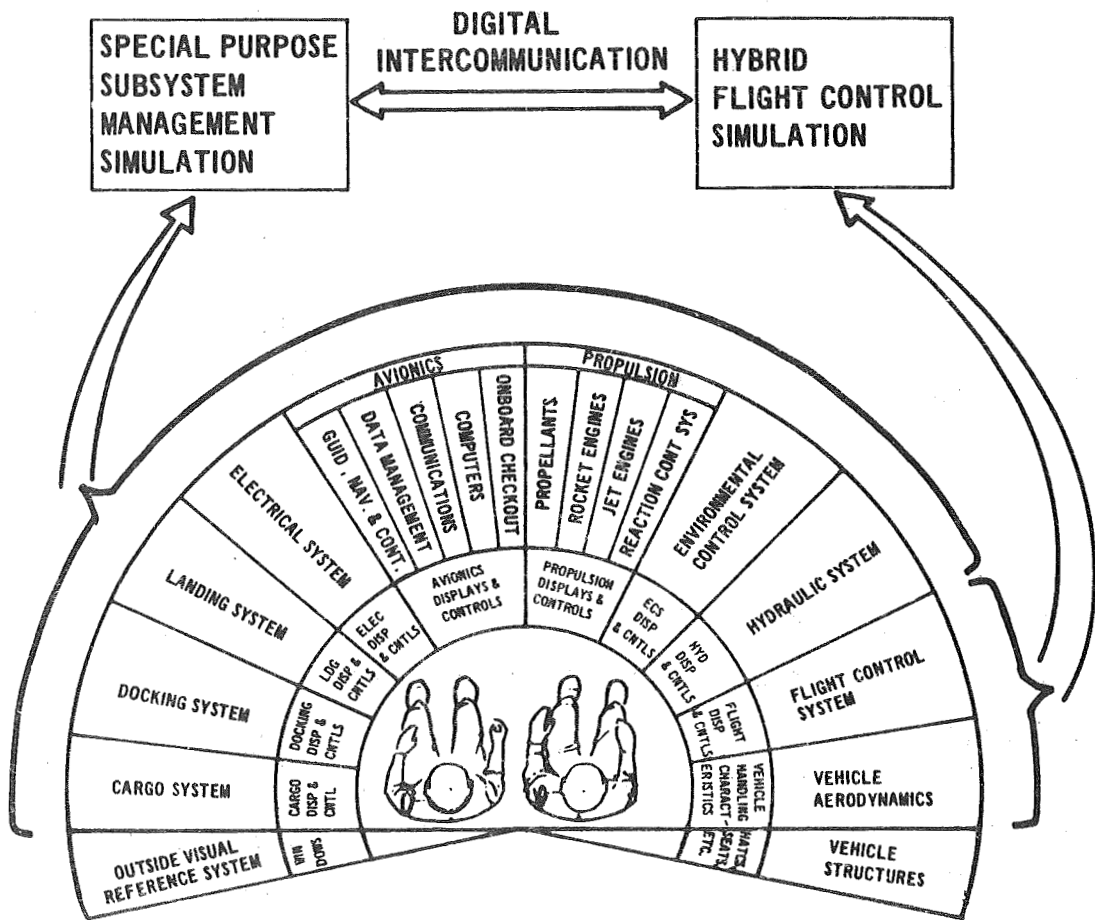


(Figure 14) Our technology objective may be summarized by saying that we must provide the means to an end; the means is a flexible, economical, subsystems management simulation capability, and the end is early human factors and equipment validation of the best degree of integration to be used in the shuttle subsystems management displays and controls.

TECHNOLOGY OBJECTIVES

- SUBSYSTEM MANAGEMENT CONTROL AND DISPLAY SIMULATION
 - FLEXIBLE
 - ECONOMICAL
 - DESIGN TOOL
- EARLY HUMAN FACTORS VALIDATION OF THE DEGREE OF INTEGRATION TO BE USED IN THE SHUTTLE SUBSYSTEM MANAGEMENT CONTROLS AND DISPLAYS
- FUNCTIONAL SIMULATION OF THE COMPLETE MAN/MACHINE INTERFACE FOR THE SPACE SHUTTLE

SOFTWARE INTEGRATION FOR INTEGRATED ELECTRONICS

R. F. Klawe

General Dynamics/Convair
San Diego, California

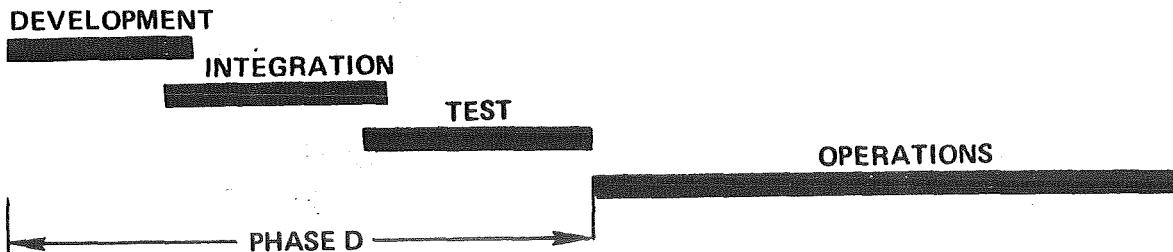
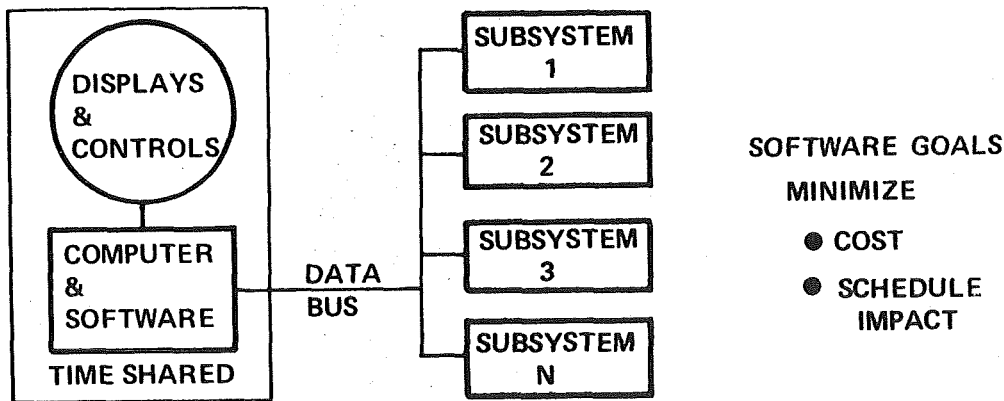
Today's genesis of integrated avionics has greater flexibility to changes and, therefore, resists technical obsolescence. Key hardware items that integrate the avionics system and allow these qualities and economics are:

- (1) Computers
- (2) Multipurpose Displays and Controls
- (3) Data Bus

These hardware subsystems have the common characteristics of being time shared and software controlled.

The development, integration and test of a flexible system of software to support not only the operational vehicles, but the necessary hardware development program provides a major challenge.

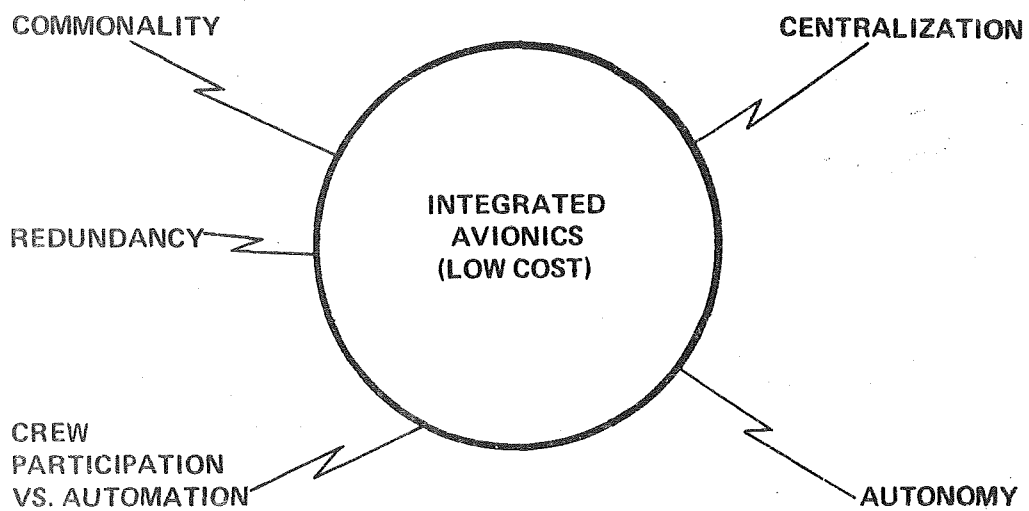
An approach is discussed which will minimize problems associated with current techniques. The software goals are therefore to minimize cost and schedule impacts through the understanding, awareness, and responsive action to long-lead time software requirements.



During phases B and C Basic Avionic/Vehicle Decisions affecting software are the degrees of:

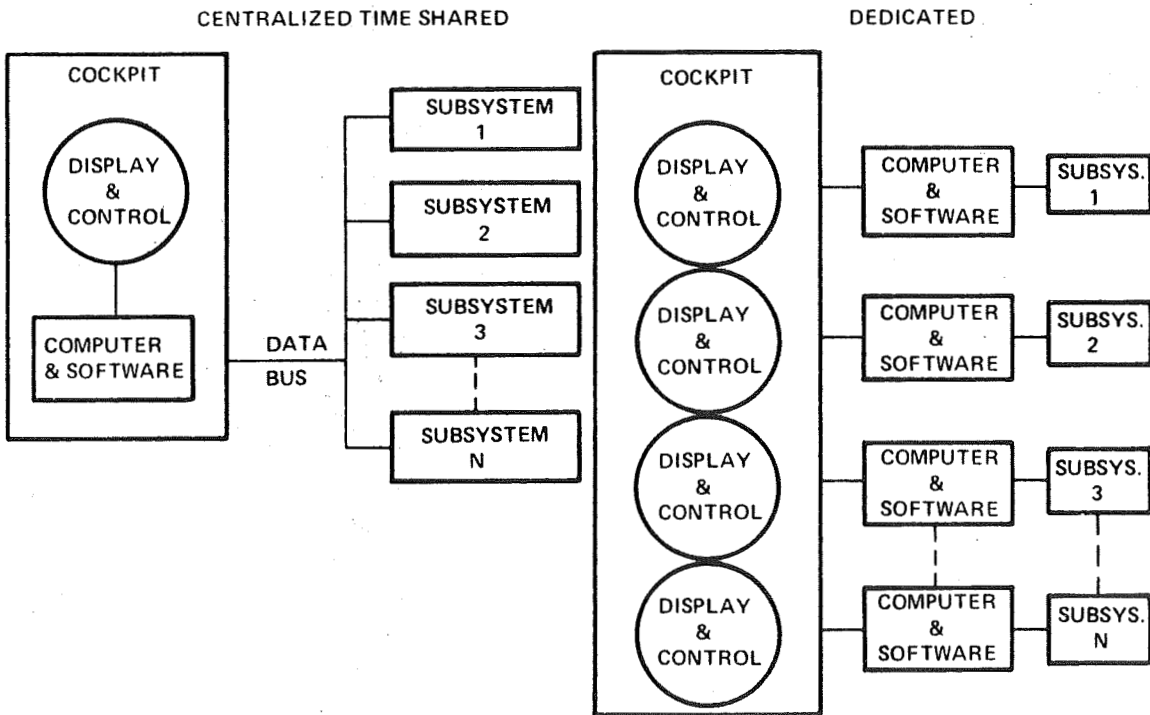
- (1) Centralization
- (2) Autonomy
- (3) Crew Participation versus Automation
- (4) Redundancy
- (5) Commonality

which are targeted at low cost integrated avionics.



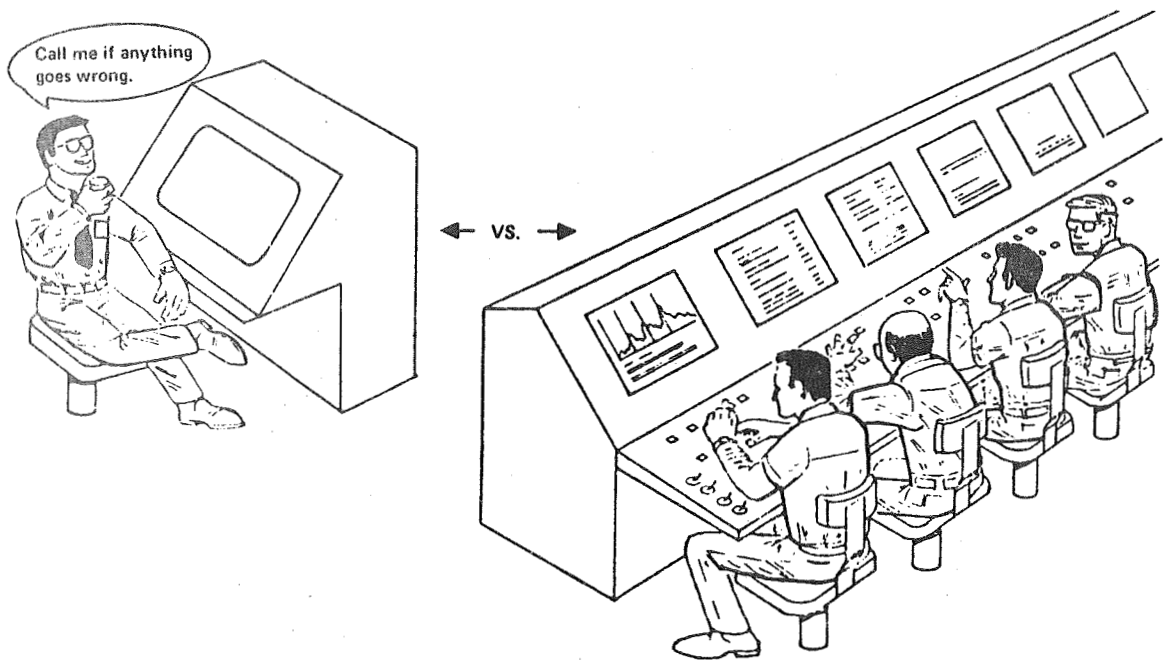
Software is evident in the degree of centralization question whether we talk of a centralized time shared system on one hand, a dedicated subsystem concept on the other, or somewhere between these extremes.

DEGREE OF CENTRALIZATION



The degree of automation to be determined during Phase B can impose a significant software impact during the subsequent Space Shuttle development, integration, test and operational project phases.

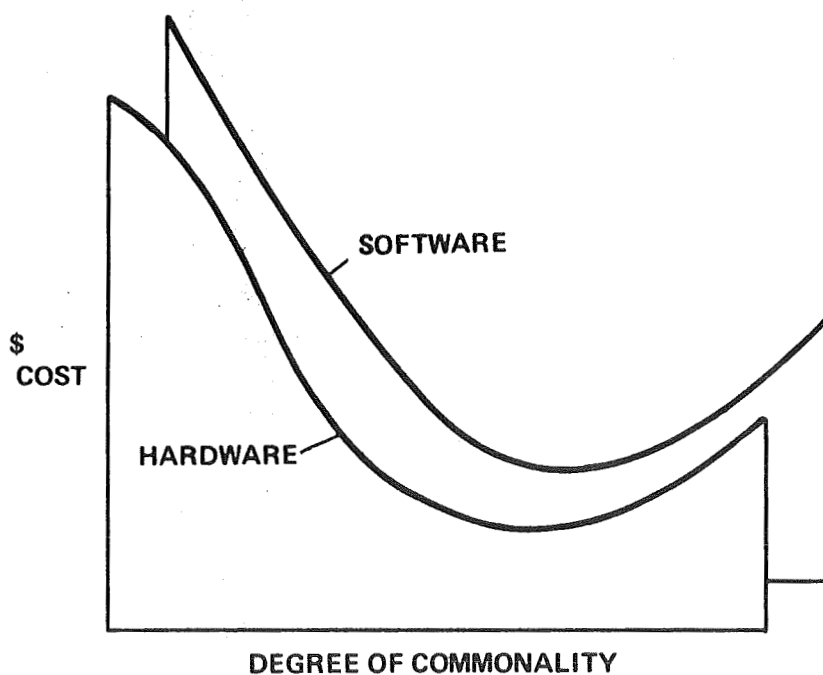
DEGREE OF AUTOMATION VS. CREW PARTICIPATION



The extent of avionic hardware and software commonality will show some optimum point relative to Space Shuttle's:

- (1) Booster
- (2) Orbiter
- (3) Ground Turnaround
- (4) Launch
- (5) Contingency Mission Support Facilities
- (6) Crew Training

EXTENT OF COMMONALITY OF HARDWARE & SOFTWARE



Since we've briefly covered Space Shuttle's Phase B and C objectives, let's concentrate on Phase D.

Anticipated Phase D go-ahead is third quarter of calendar 1972. At that point in time we could foresee the beginning of Engineering release which will continue up to the start of calendar 1974. The first two avionics ship sets for booster and orbiter are required by the first quarter of 1975 to support the first horizontal flights in the third quarter of that same year 1975. Although, subsequent ship's sets of avionics are required in pairs at 6-month intervals, let's focus our attention on the first avionic ship sets required in the first quarter of 1975.

One of the identified critical paths to producing the first avionics ship sets by first quarter 1975 shows the inter-relationship of:

- (1) Development of the on-board computer(s)
- (2) Code generator to interconnect the computer operation codes with that of a higher order programming language
- (3) Integration, testing and validation of the first avionics ships set

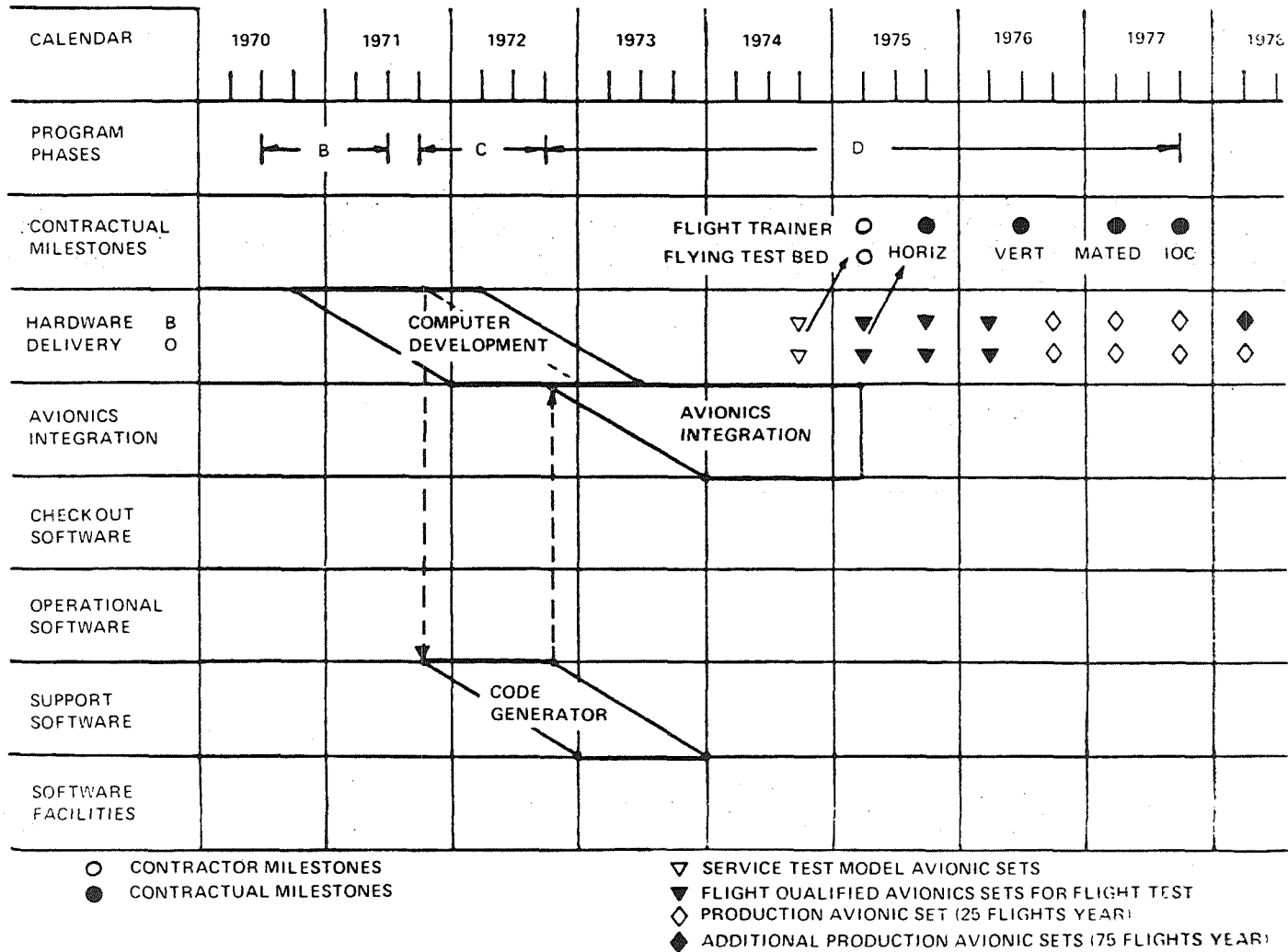
This is a parametric schedule presentation. The following minimums were derived from recent launch vehicle, manned spacecraft and military programs with similar requirements, although some requirements were greater than those for Space Shuttle.

- (1) Computer Development — 18 months
Design freeze on operational code and timing — 12 months
- (2) Code Generator — 12 months
- (3) Avionics Integration — 15 to 30 months

(The longer duration exemplifies avionics dependent manned vehicles.)

The longest duration path starts at the top left of computer development block to the right until the dashed diagonal of the computer op-code and timing design freeze. The downward vertical arrow takes us to the initiation of development of the code generator (12 months), then up to the initiation of the long path (30 months) of avionics integration. The shortest duration commences computer development first quarter '72, code generator first quarter '73, and avionics integration first quarter '74 for 15 months.

AVIONICS INTEGRATION CRITICAL PATH



Visualization of the avionics integration consists of establishing the interdependency between hardware systems and operational systems to determine what items are order dependent. It is easily seen that (1) computer hardware, (2) data bus, and (3) display and control are common dependencies for all operational systems and therefore are critically needed to initiate the avionics integration.

SYSTEM/SUBSYSTEM DEPENDANCY MATRIX

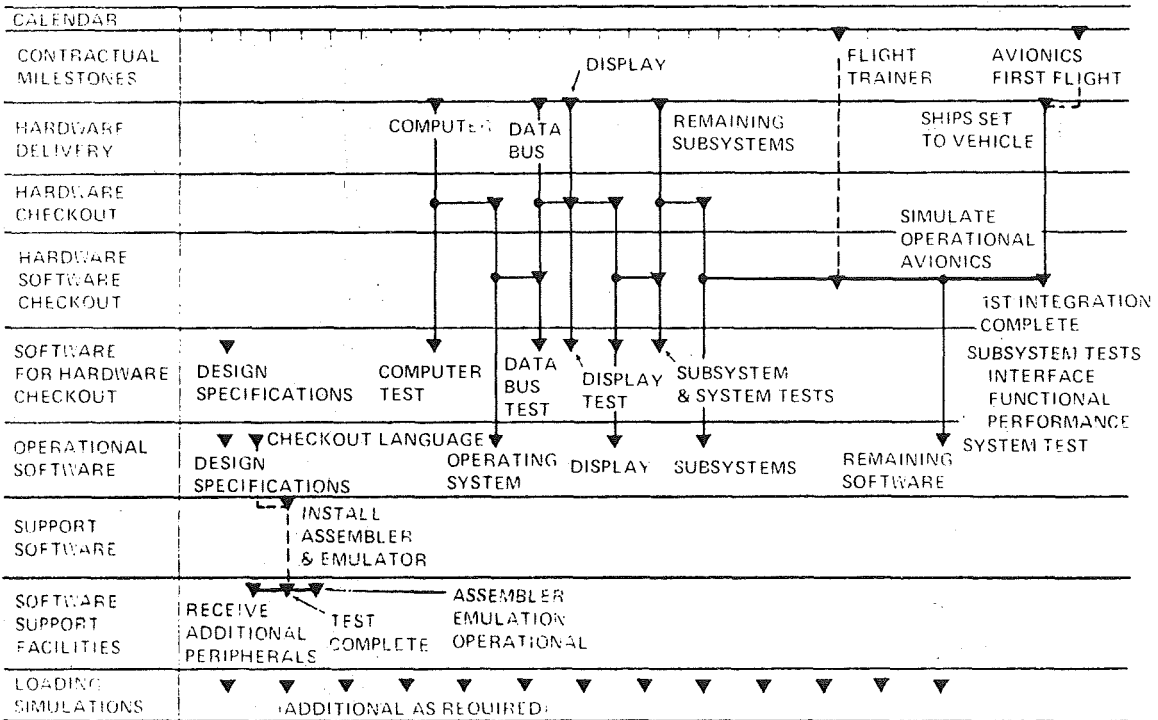
OPERATIONAL SYSTEMS	HARDWARE SYSTEMS														
	COMPUTER	DATA BUS	DISPLAY & CONTROL	RENDEZVOUS & DOCKING	AUTO LANDING	FLIGHT CONTROL	PROPULSION	POWER SYSTEMS	THERMAL PROTECTION	LANDING GEAR	PAYLOAD TRANSFER	COMMUNICATION	GUIDANCE & NAVIGATION	ENVIRONMENTAL LIFE SUPPORT	REACTION CONTROL
COMPUTER	X	O	O	O	O	O	O	O	O	O	O	O	O	O	O
DATA BUS	X	X	O	O	O	O	O	O	O	O	O	O	O	O	O
DISPLAY & CONTROL	X	X	X	O	O	O	O	O	O	O	O	O	O	O	O
RENDEZVOUS & DOCKING	X	X	X	X	O	O	O	O	O	O	O	O	O	O	O
AUTO LANDING	X	X	X	X	X	O	O	O	O	O	O	O	O	O	O
FLIGHT CONTROL	X	X	X	X	X	X	O	O	O	O	O	O	O	O	O
PROPULSION	X	X	X	X	X	X	X	O	O	O	O	O	O	O	O
POWER SYSTEMS	X	X	X	X	X	X	X	X	O	O	O	O	O	O	O
THERMAL PROTECTION	X	X	X	X	X	X	X	X	X	O	O	O	O	O	O
LANDING GEAR	X	X	X	X	X	X	X	X	X	X	O	O	O	O	O
PAYLOAD TRANSFER	X	X	X	X	X	X	X	X	X	X	X	O	O	O	O
COMMUNICATION	X	X	X	X	X	X	X	X	X	X	X	X	O	O	O
GUIDANCE & NAVIGATION	X	X	X	X	X	X	X	X	X	X	X	X	X	O	O
ENVIRONMENTAL LIFE SUPPORT	X	X	X	X	X	X	X	X	X	X	X	X	X	X	X
REACTION CONTROL	X	X	X	X	X	X	X	X	X	X	X	X	X	X	X
INFLIGHT TRAINING	X	X	X	X	X	X	X	X	X	X	X	X	X	X	X
ONBOARD CHECKOUT	X	X	X	X	X	X	X	X	X	X	X	X	X	X	X

MAJOR
COMMON
DEPENDENCIES

LEGEND
X PRIMARY
O SECONDARY

Keeping the critical order in mind, intervals of time are shown as the sub-avionics integration periods to substantiate the integrity of operation of the various classes of software for hardware checkout, and operational software with the hardware.

AVIONICS INTEGRATION SCHEDULE

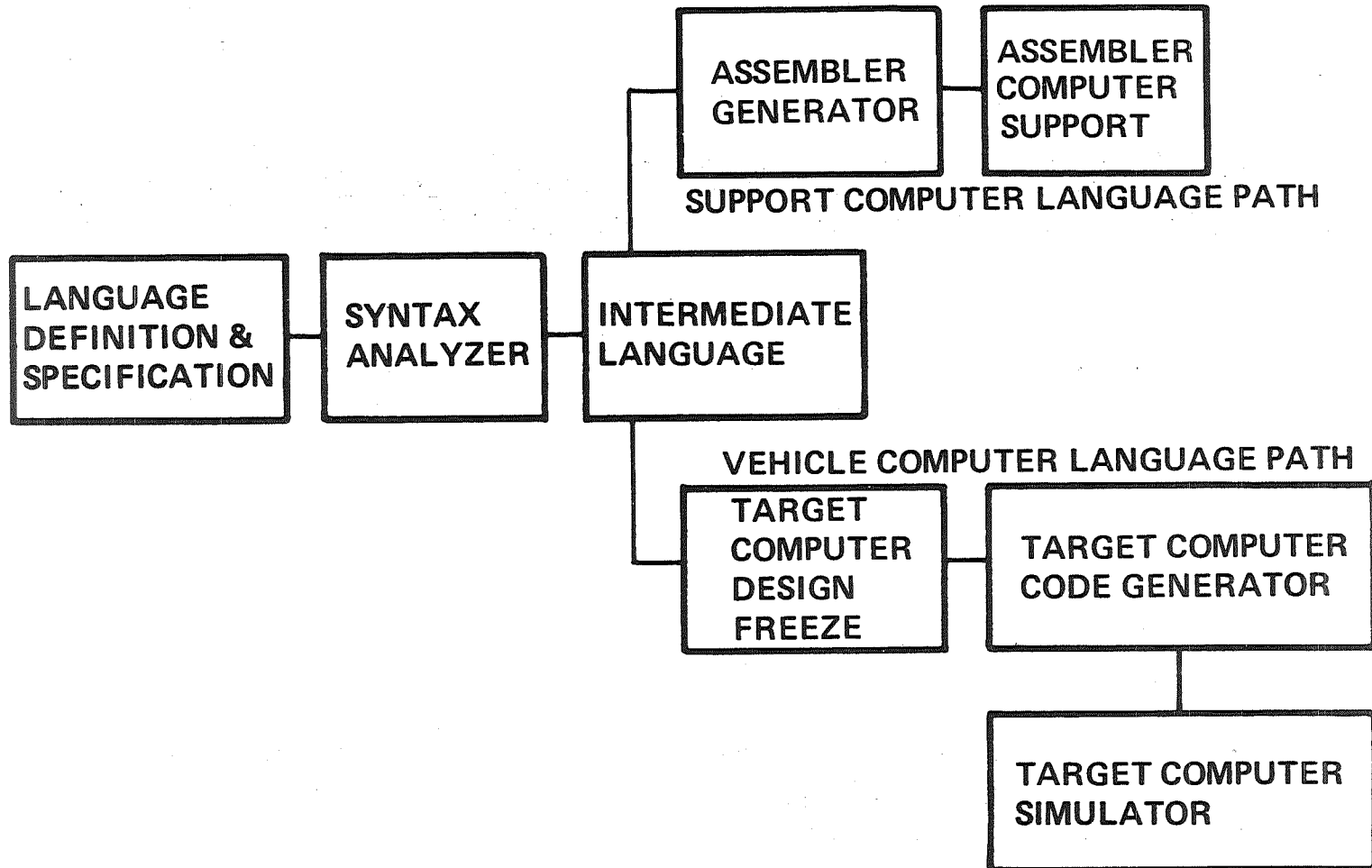


The Code Generator, previously shown as the middleman in the avionic's critical path, is shown at the lower right in the Vehicle Computer Language Path of the Computer Language Development process.

The left hand portion depicts the higher level language design and development through the intermediate language. At this junction the language can be operative on an existing support computer via the support computer language path. The lower vehicle computer language path requires the vehicle computer design freeze, development of vehicle computer code generator and the development of the vehicle computer simulator on an existing computer.

If the execution timing on the support computer is nearly the same as the vehicle computers, much of the software validation and representative timing can be accomplished on the support computer prior to vehicle computer design freeze. The vehicle computer simulator will enable the final software validation prior to integration with the flight hardware in the avionics integration cycle.

COMPUTER LANGUAGE DEVELOPMENT

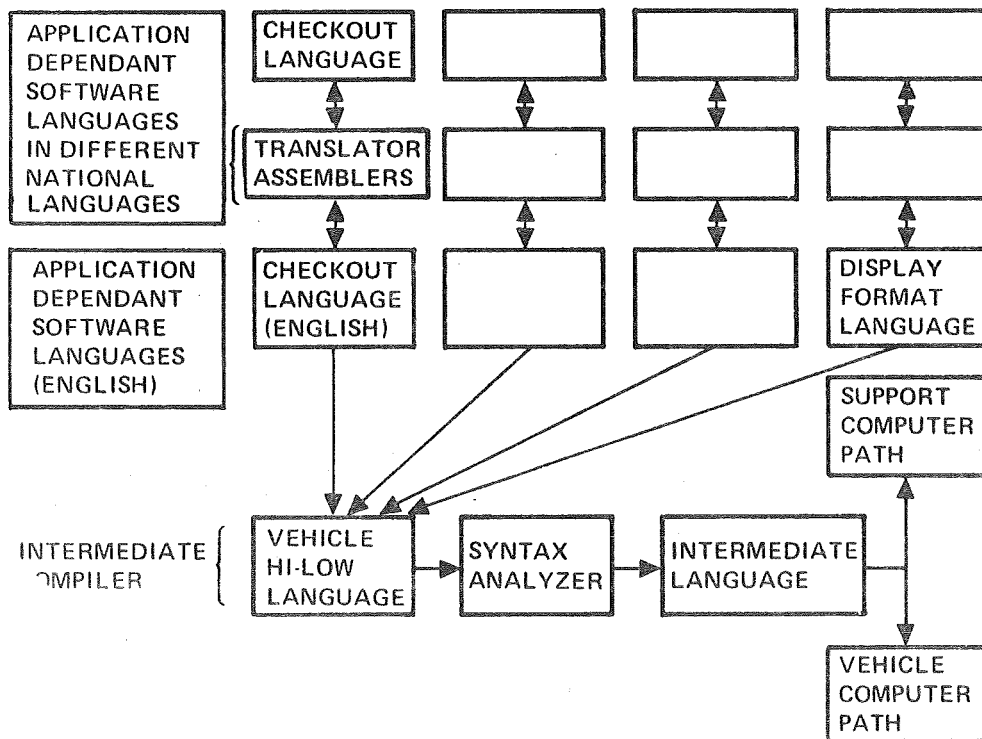


The intermediate compiler language developed in the previous slide could well serve as the base for many peculiar application dependent computer languages such as for checkout and display formatting.

These limited application dependent languages could well serve as a limited language bridge to other national languages using bilateral assembly translators to and from English. This could help solicit and promote foreign participation.

Application languages could well serve to bridge the communications gap within the aerospace and electronics industry and eliminate the multi-language problems now existing in the United States working on different facets of the same project.

POSSIBLE LANGUAGE HIERARCHY



SUMMARY

- **SOFTWARE IS A PRIME AVIONICS INTEGRATOR.**
- **SOFTWARE COMMONALITY IS NECESSARY FOR LOW COST & SCHEDULE IMPACT.**
- **SCHEDULE IMPACTS SEEM LIKELY DUE TO COMPUTER DEVELOPMENT AND SOFTWARE LANGUAGES IF WE WAIT UNTIL PHASE D.**
- **INTERNATIONAL PARTICIPATION VIA SOFTWARE APPLICATIONS LANGUAGES WOULD SOLICIT INVOLVEMENT OF OTHER NATIONS.**
- **AVIONICS INTEGRATION TAKES CALENDAR TIME**

CONCLUSIONS

- **TAKE BOLD GUESS FOR GROWTH ETC. AND START THE VEHICLE COMPUTER DEVELOPMENT NOW.**
- **START INTERMEDIATE COMPILER DEVELOPMENT NOW, OR ADOPT AN EXISTING HI-LOW LANGUAGE.**
- **START DEVELOPMENT OF APPLICATIONS LANGUAGES AS SOON AS INTERMEDIATE COMPILER IS FIRM.**

INTEGRATED CONTROL AND AIRFRAME DEVELOPMENT CONSIDERATIONS

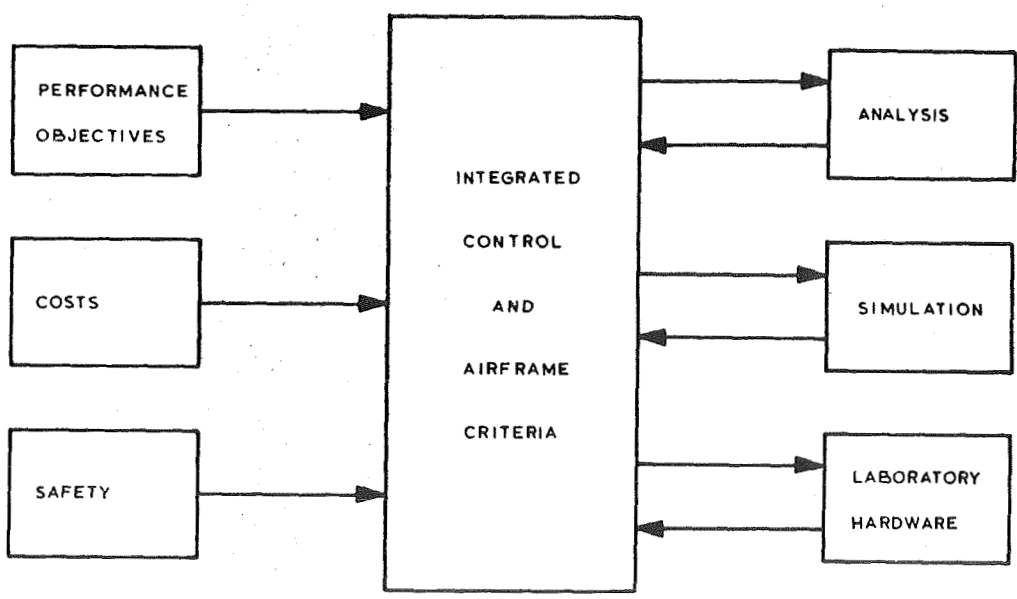
Donald L. Martin

The Boeing Company
Seattle, Washington

INTRODUCTION

Integration of the guidance and control systems with the airframe requires close association of all technologies during design and development of the airframe. To most effectively manage the development of these systems it is necessary to maintain a flexible organization which allows a continual refinement of the system requirements as the airframe configuration is evolving. Mission performance, system costs and safety are some of the parameters used to develop the overall requirements. Analytical models, simulation and laboratory hardware are the tools used to obtain the necessary trade data and to refine the detailed system requirements as shown in Figure 1.

Examples taken from the SST prototype development program will be used to illustrate those cross technology considerations.



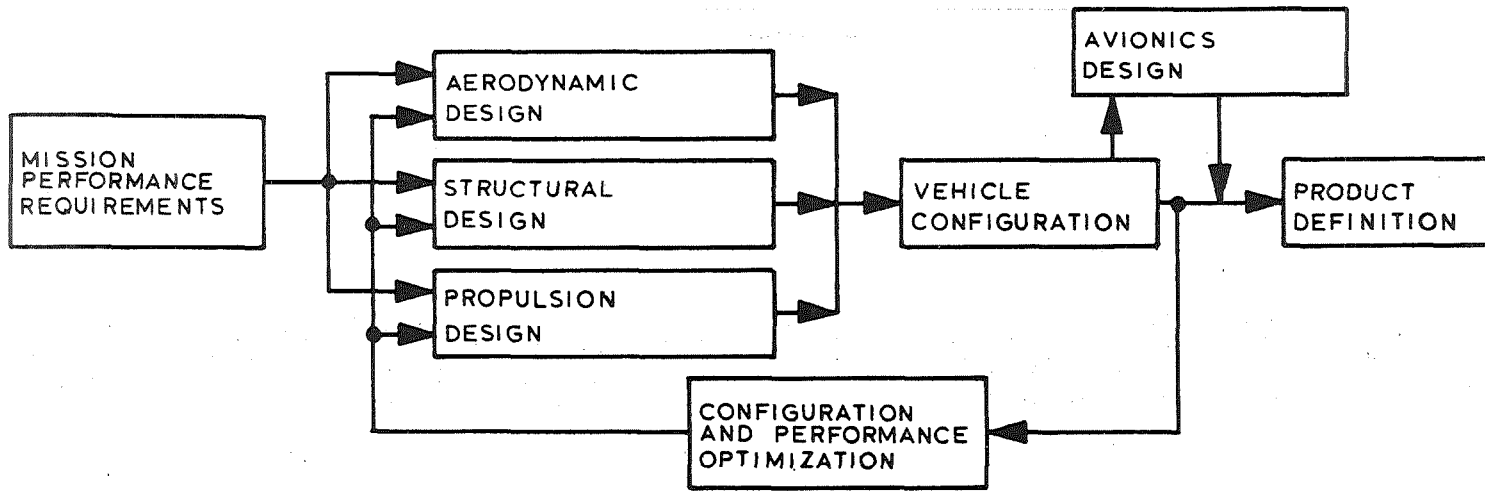
PRELIMINARY DESIGN APPROACH

The early Boeing SST configuration development began with the ground rule that the handling qualities of the basic airframe should be equal or better than that of the existing subsonic jets. This allowed a conventional design approach (see figure 2) in which a configuration was to be established from propulsion, aerodynamic, and structural design trades. The avionics design was not considered in the configuration optimization loop. With this approach it was found that the optimization process did not converge to a configuration which met the payload range requirements required for economic success.

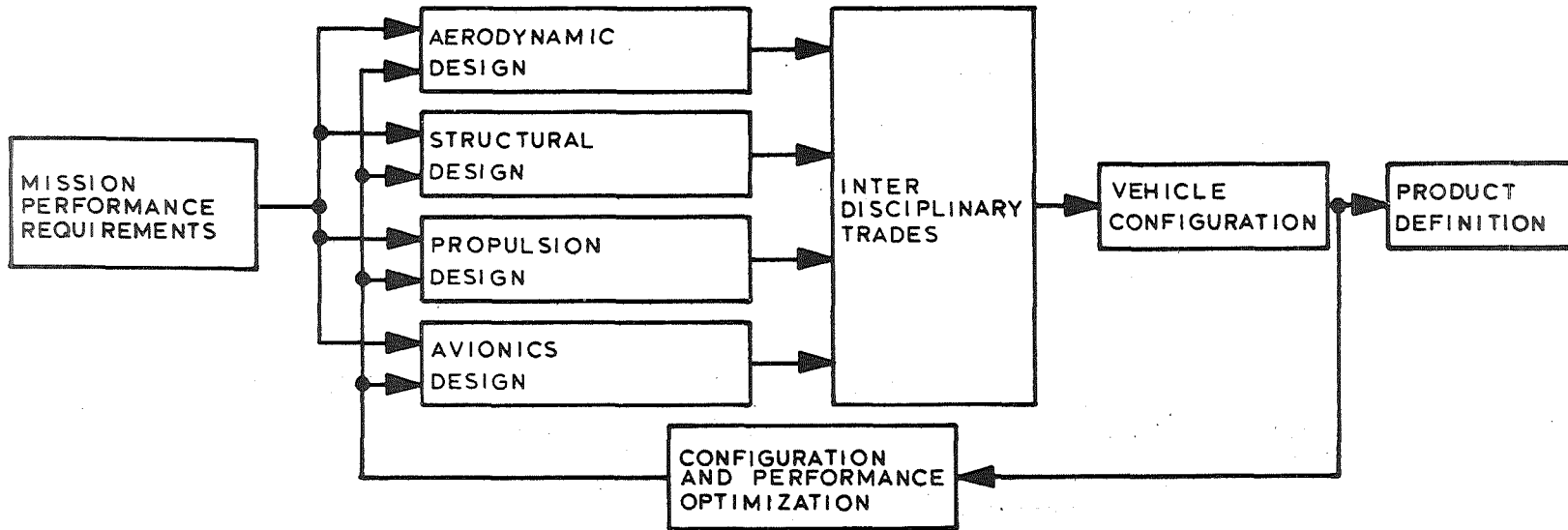
When it was realized that the necessary improvement in performance could be obtained through added dependence on the avionics, the control oriented design approach was evolved. This brought the avionics design into the configuration design loop and included avionics technology in the interdisciplinary trades.

This was a departure from past experience and a number of rules existed which no longer applied. A new set of rules had to be written and made available to all groups involved in the design. Specific criteria which establish these rules play an important part in allowing the avionics to be used to enhance vehicle performance and operational characteristics.

(A) CONVENTIONAL DESIGN



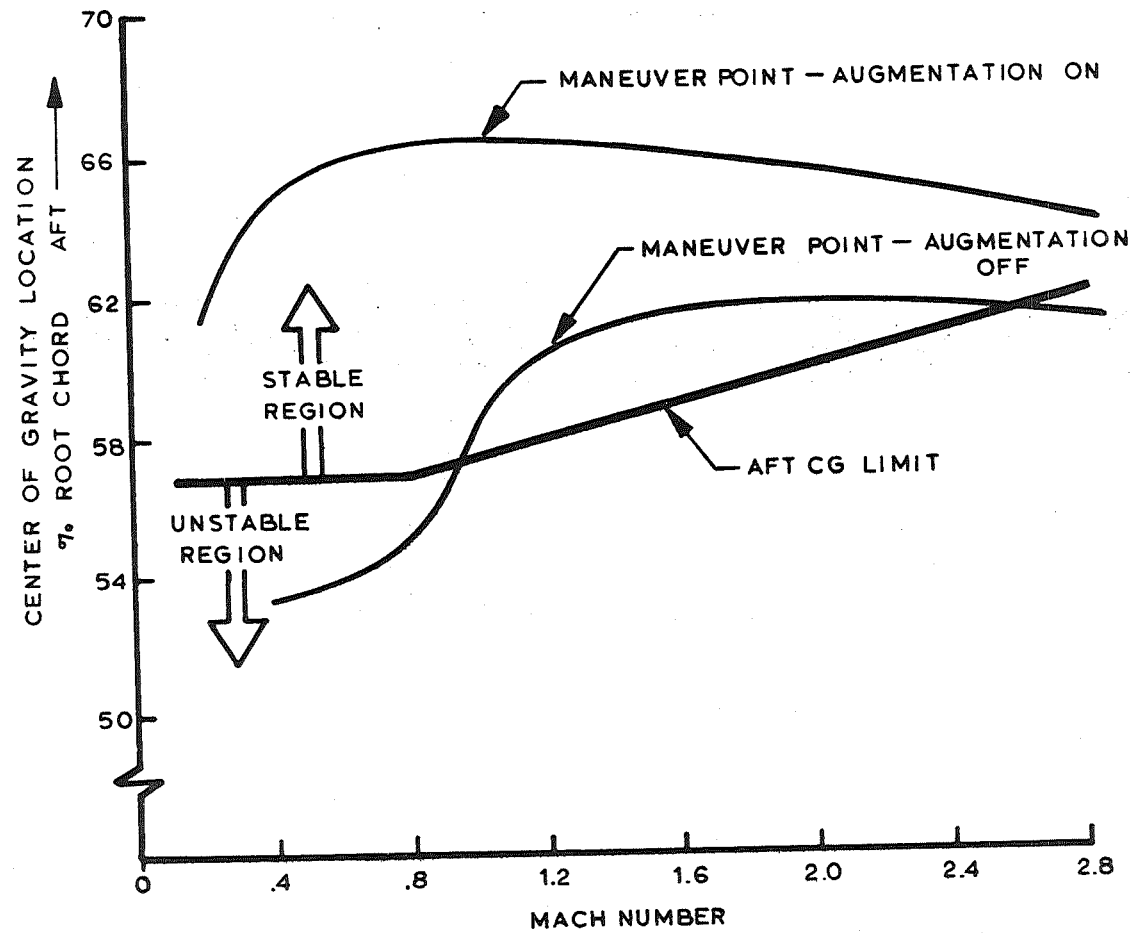
(B) CONTROL ORIENTED DESIGN



CONVENTIONAL AND CONTROL ORIENTED DESIGN

APPLICATION OF CONTROL TECHNOLOGY TO
SST LONGITUDINAL AXIS DESIGN

A significant performance benefit was obtained on the SST by balancing the airframe so that the trim drag at supersonic cruise was minimized. Figure 3 indicates that the maneuver point, with augmentation off, moves aft as the airplane goes from subsonic to supersonic speeds. When the airframe is balanced for optimum cruise performance the maneuver point is ahead of the center of gravity position for some flight conditions if the airplane is loaded to its aft limit. This results in unstable characteristics for subsonic flight unless a pitch axis augmentation system is provided. With the augmentation on, the airplane is dynamically stable at all flight conditions and all allowable c.g. conditions. Notice that, with the airplane loaded at the forward limit the airplane is dynamically stable at all flight conditions without augmentation.



EFFECT OF STABILITY AUGMENTATION ON MANEUVER POINT

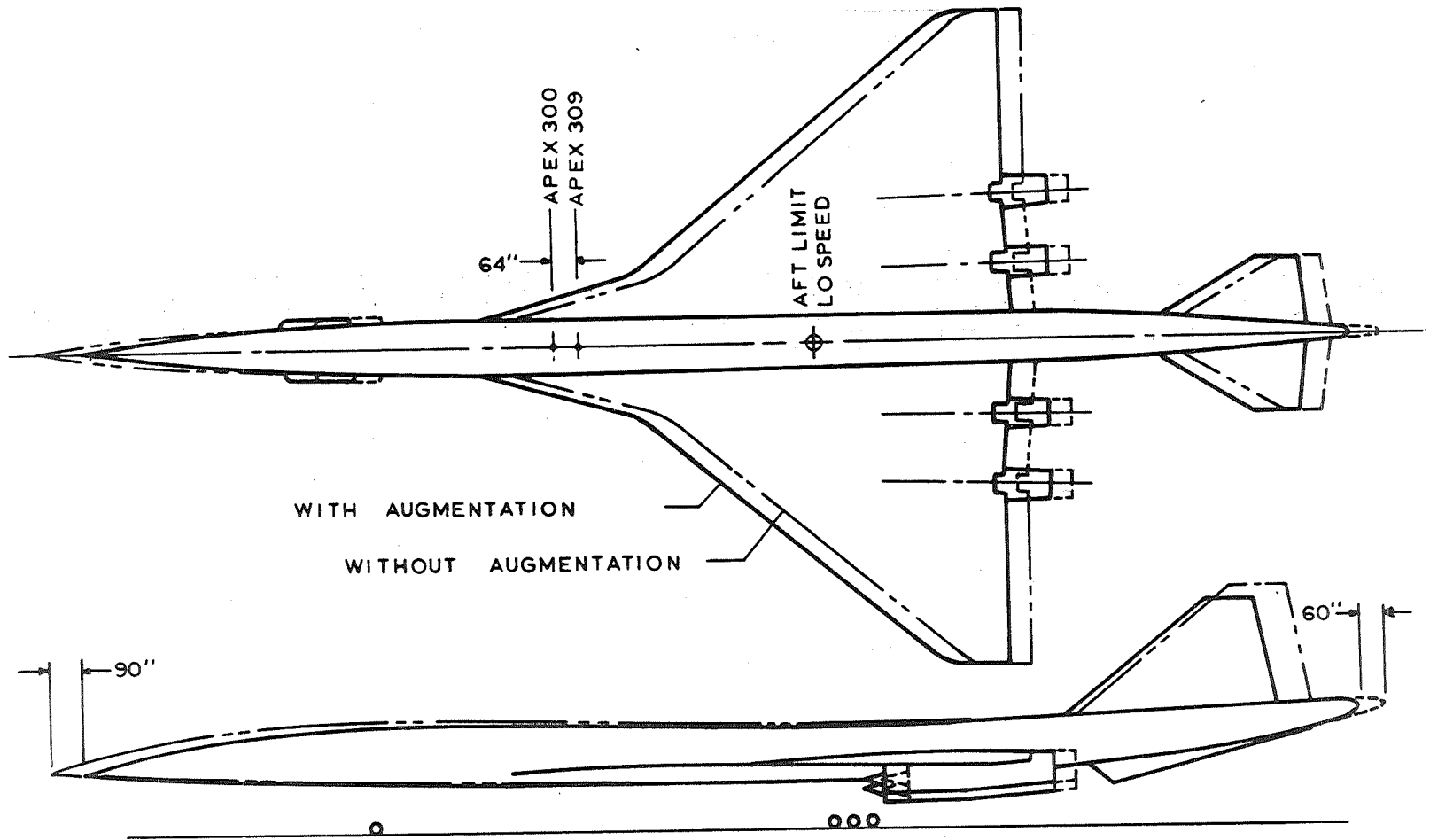
INCREASED SST PERFORMANCE

The result of this dependence on avionics for pitch axis stability is shown in figure 4. The configuration resulting from the conventional design approach is shown by the dashed lines and is superimposed on the configuration resulting from the control-oriented design shown by the heavy line. Both drawings are positioned so that the aft center of gravity locations are identical.

This change in configuration resulted in the ability to carry an additional 4800 pounds of payload; an increased range of 190 nautical miles; a reduction in takeoff noise of two PNdb.

A similar use of avionics to enhance performance has been made in the lateral directional axis. In this case the stability augmentation system is employed to help control the effects of an engine failure at supersonic cruise speeds. Without augmentation, the vertical tail size would need to be almost doubled. This would reduce the payload by approximately 7000 pounds without any allowances being made for the additional forward ballast that would be required, or for the effect of the additional drag. Iteration of this configuration cycle becomes divergent and a major configuration change would be required.

73



EFFECT OF AVIONICS ON SST CONFIGURATION

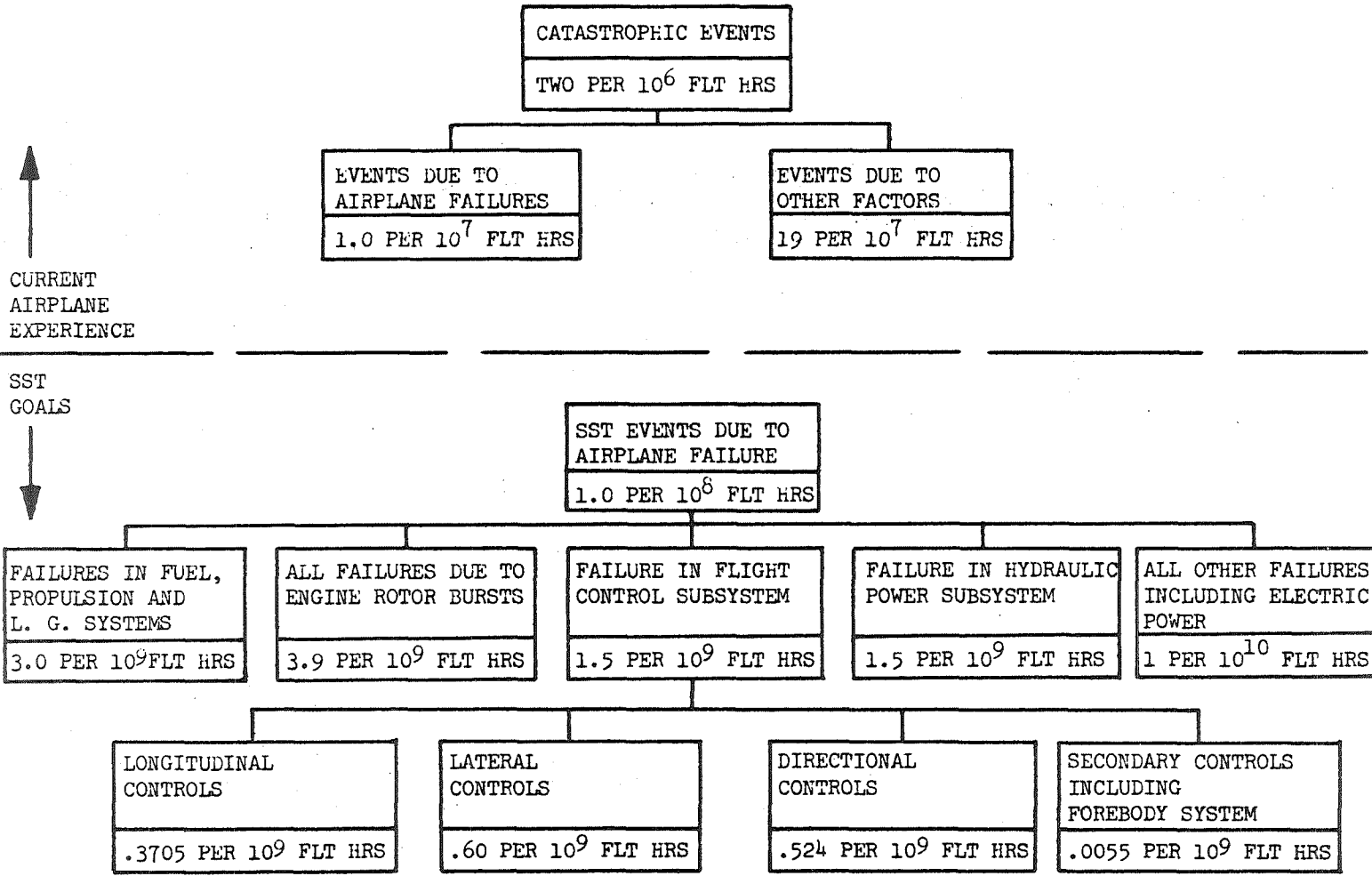
SAFETY

These performance advantages have not been required in previous programs. However, experience from less critical applications has provided confidence that the state-of-the art is now ready for a more demanding application. The dual yaw damper on the 727 airplane is necessary to provide positive directional stability over a small portion of the flight envelope. After a single channel failure the airplane is flown at a Mach number and altitude outside of the critical region.

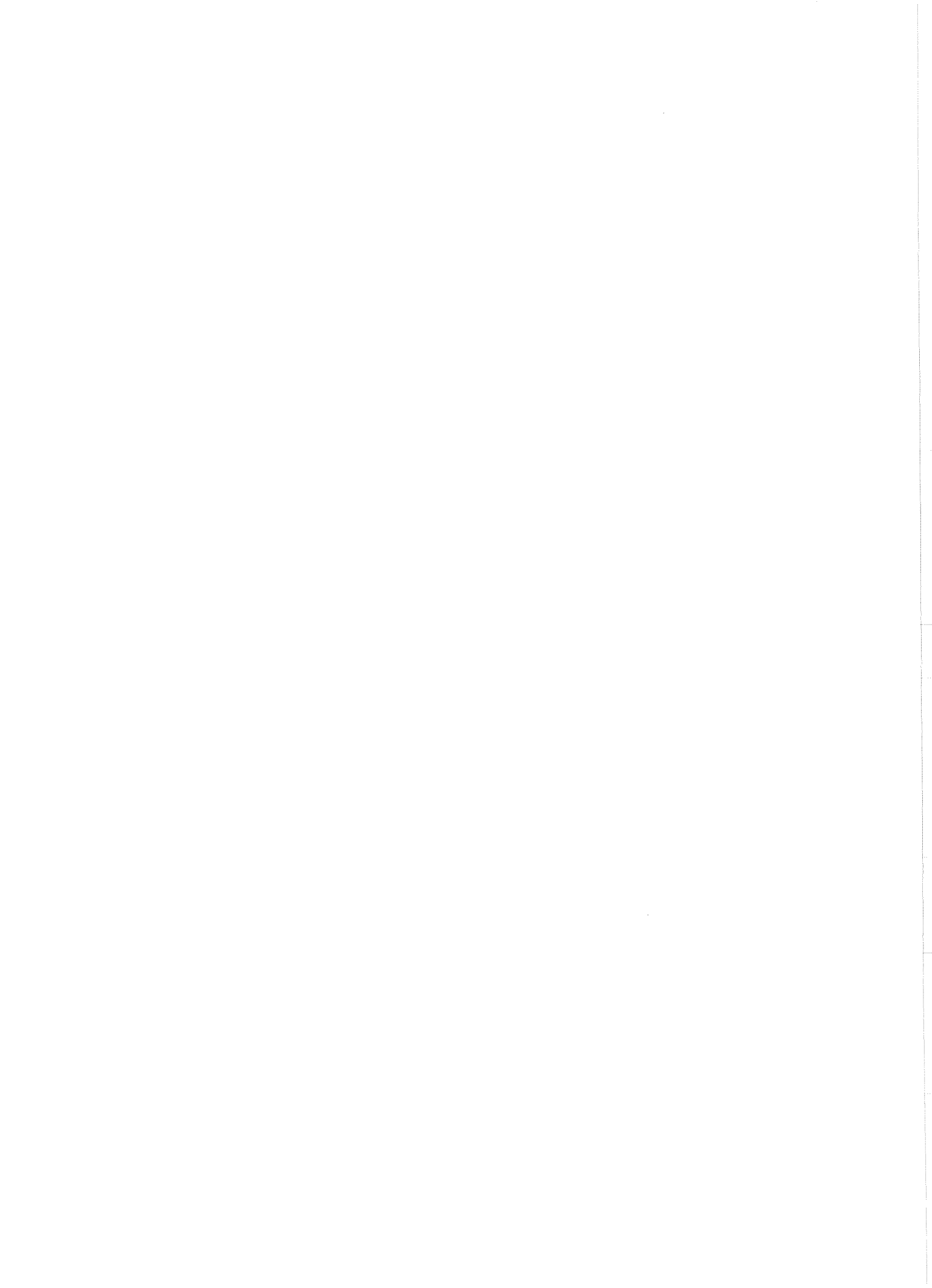
Where an alternate operational procedure did not exist, as with the pitch axis for the SST, a rationale was required to establish the level of redundancy required for the flight critical avionics. This was achieved by means of safety reliability allocations as shown in figure 5. Airline fleet experience shows that there are two catastrophic events (airplane accidents) per million flight hours. Of these one in twenty is due to airplane failures while the other nineteen are due to other factors. For the SST the design goal was set at providing an order of magnitude improvement in the catastrophic event due to airplane failures, i.e., one catastrophic failure per hundred million flight hours. This allocation was then shared between the major systems which could contribute to failures, with the flight control subsystem receiving a 15 percent share.

Using failure rate estimates for separate channels of the pitch axis augmentation, four channels were required and the probability of loss of three or more channels was extremely remote. This is also true of the hydraulic and electrical systems.

SAFETY RELIABILITY ALLOCATIONS

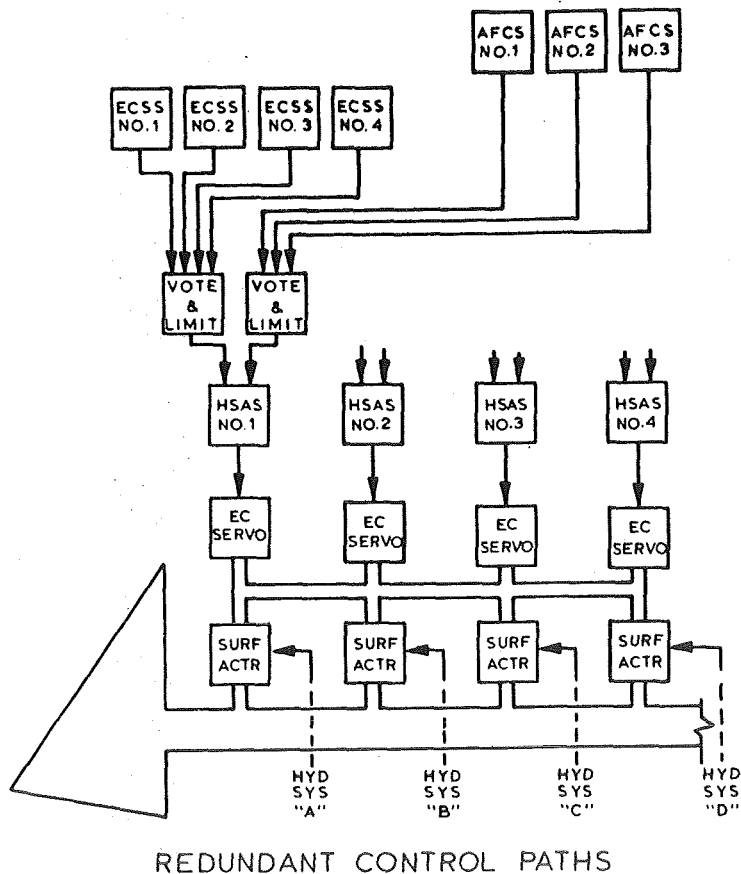


75



This system is used in conjunction with a more sophisticated control and augmentation system, the Electrical Command and Stability System (ECSS), which raises the level of handling qualities to the normal, good, category. When operating together, the Hard SAS and the ECSS provide the handling qualities which are considered necessary and desirable based on conventional subsonic transport standards. That is, such requirements as stick force per normal load factor, response and damping characteristics are provided by these systems.

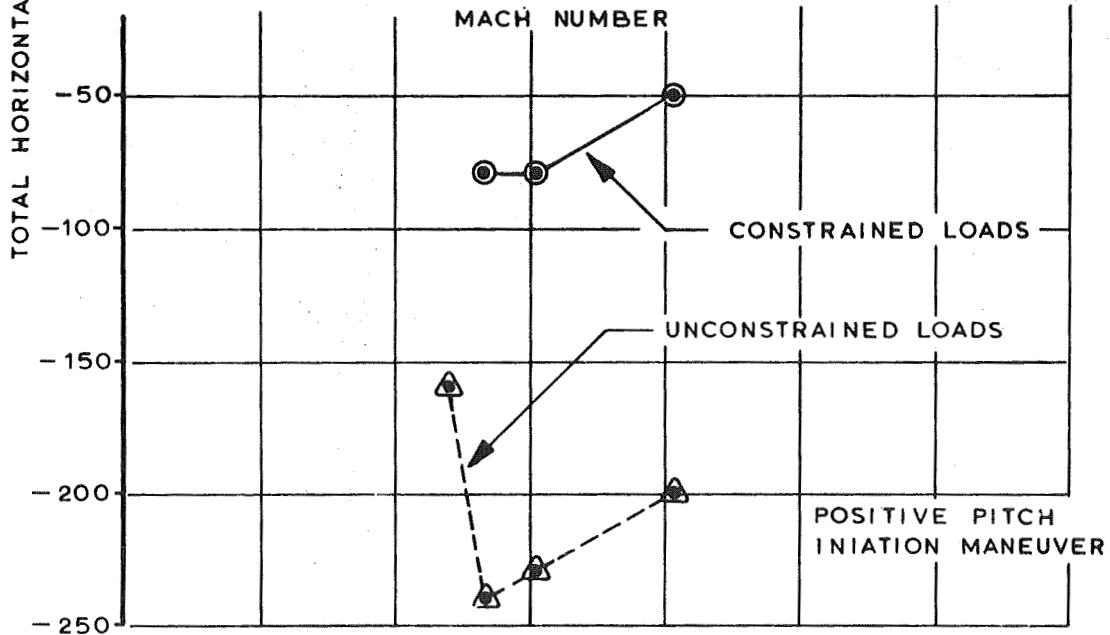
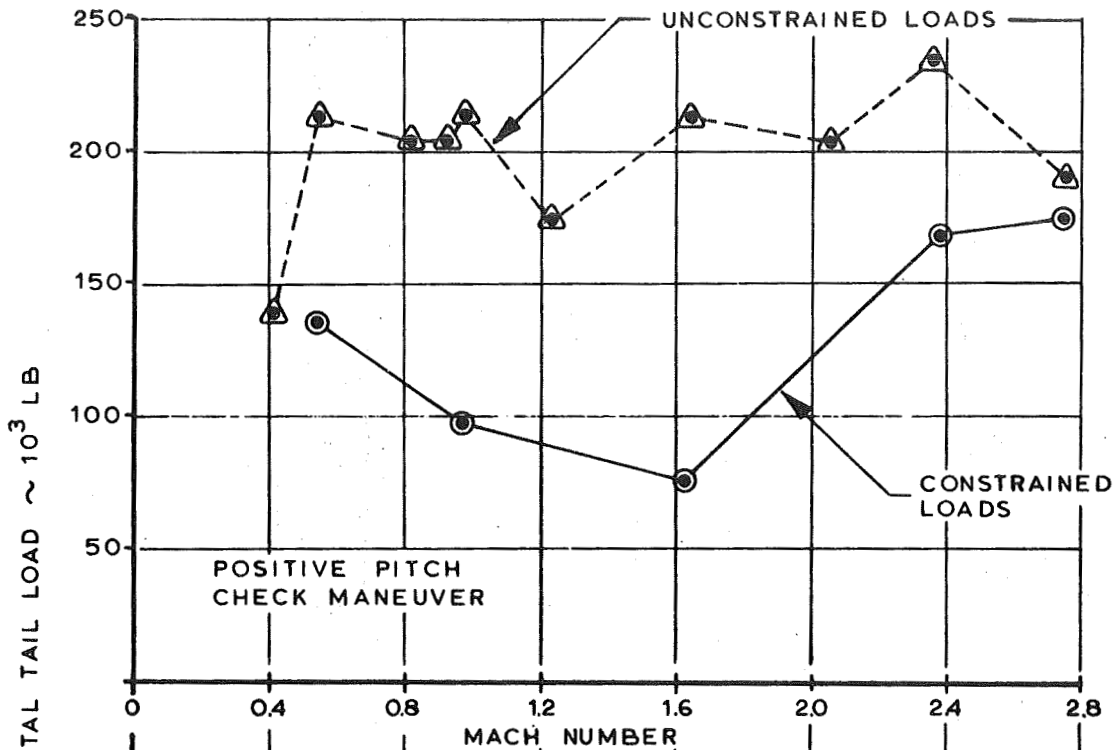
Both the ECSS and the Hard SAS are fail operational following the first and second failures, and fail passive after the third failure. A three channel, digital, Automatic Flight Control System (AFCS) which is fail operational after the first failure and fail passive after the second failure provides control wheel steering, automatic landing and navigation control modes. Limiting and voting of the commands from the ECSS and the AFCS are used to isolate failures of these less critical functions from the Hard SAS.



ANALYSIS

Because of the large authority of the electronic control inputs, a number of the past practices and regulations for structural design were not applicable to the SST. Close coordination between the augmentation system designers and the structural engineers is required to make sure that the structure is safe for the maneuvering demands expected. Dynamic loads must be computed by use of simulations which include the total flight control system. This presents a problem during the initial design cycle since it forces the stability augmentation and flight control system designers to establish preliminary configurations which can be evaluated during the dynamic loads analysis. This forces an iteration procedure because the stability augmentation system design is based upon the aerodynamic characteristics, which are a function of the stiffness of the structure and which are in turn dependent upon the loads -- the first thing we started out to check.

One advantage of this influence of the avionics design on the loads is that there is a greater flexibility to tailor the avionics system to minimize loads than when the control inputs were provided directly by the pilot. The horizontal tail loads will be used as an example, see figure 7. The surface actuator is sized such that it can deflect the slab tail to the required deflection and at the required rate to meet handling qualities requirements. The case where two hydraulic systems have failed and the airplane is at the most demanding flight condition represents the design case. For the major part of the time, when all four hydraulic systems are operating and the airplane is in a less demanding flight condition, the control authority is several times that required for adequate airplane control. This excessive control authority, which could be inadvertently commanded by the pilot, could create excess loads on the structure. These unconstrained loads can be limited by placing position and rate limits in the pilot's control path through the electronics. The result on the loads of applying these constraints can be seen by reference to figure 7.

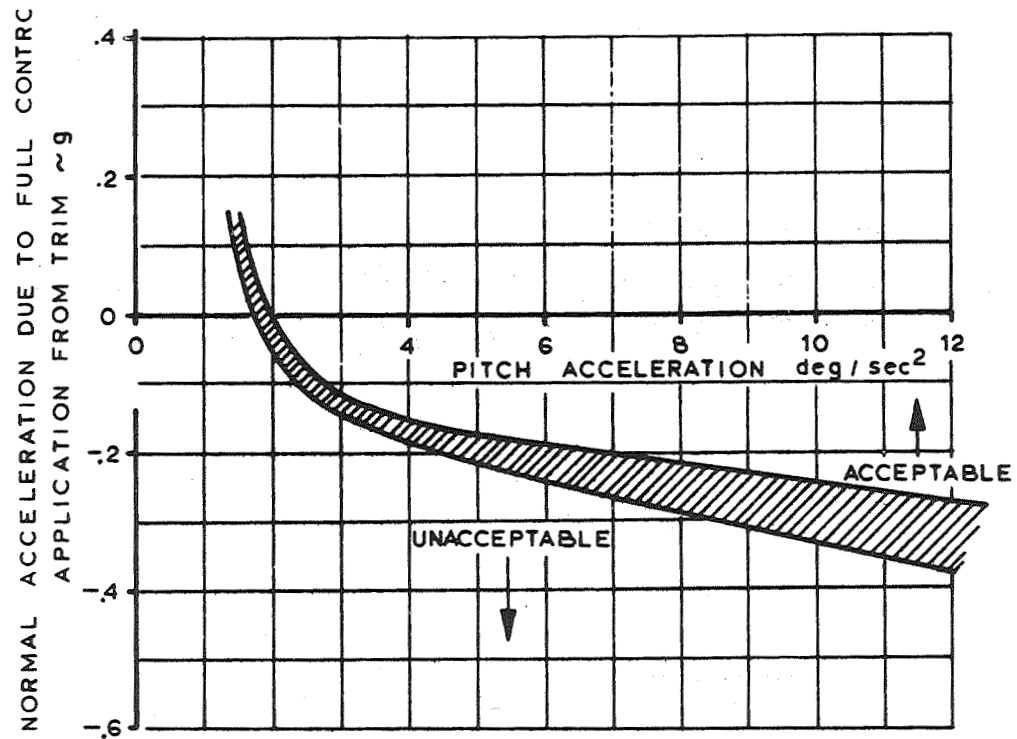


HORIZONTAL TAIL LOADS DURING PITCH MANEUVERS

PILOTED SIMULATION

The SST program has made extensive use of simulators to determine suitable criteria where these were not existing and where past experience could not be used as a satisfactory guide. It has been essential to have a sophisticated simulation operating early enough in the design cycle to provide an excellent means for synthesizing and evaluating systems found in the controls and avionics areas. As a result of these simulator programs a new set of design requirements has evolved for the SST. These requirements apply to static and dynamic stability, response to control inputs, maneuver limits, effects of turbulence, emergency conditions and procedures, and recovery from upsets.

Because the size of the horizontal tail and the actuation rate requirements are determined by the final approach and flare before landing, a considerable time was spent simulating piloted landings to determine these requirements. The large inertia of the SST, the relatively short tail arm and the large authority augmentation system presented a range of new conditions which needed to be analyzed. Results of this study are shown in figure 8. The flight simulator used in this study has a sophisticated visual display to provide a realistic view out of the window. A servoed TV camera is driven over a terrain model and the image is projected on a thirty-foot diameter hemispherical screen in front of the pilot.

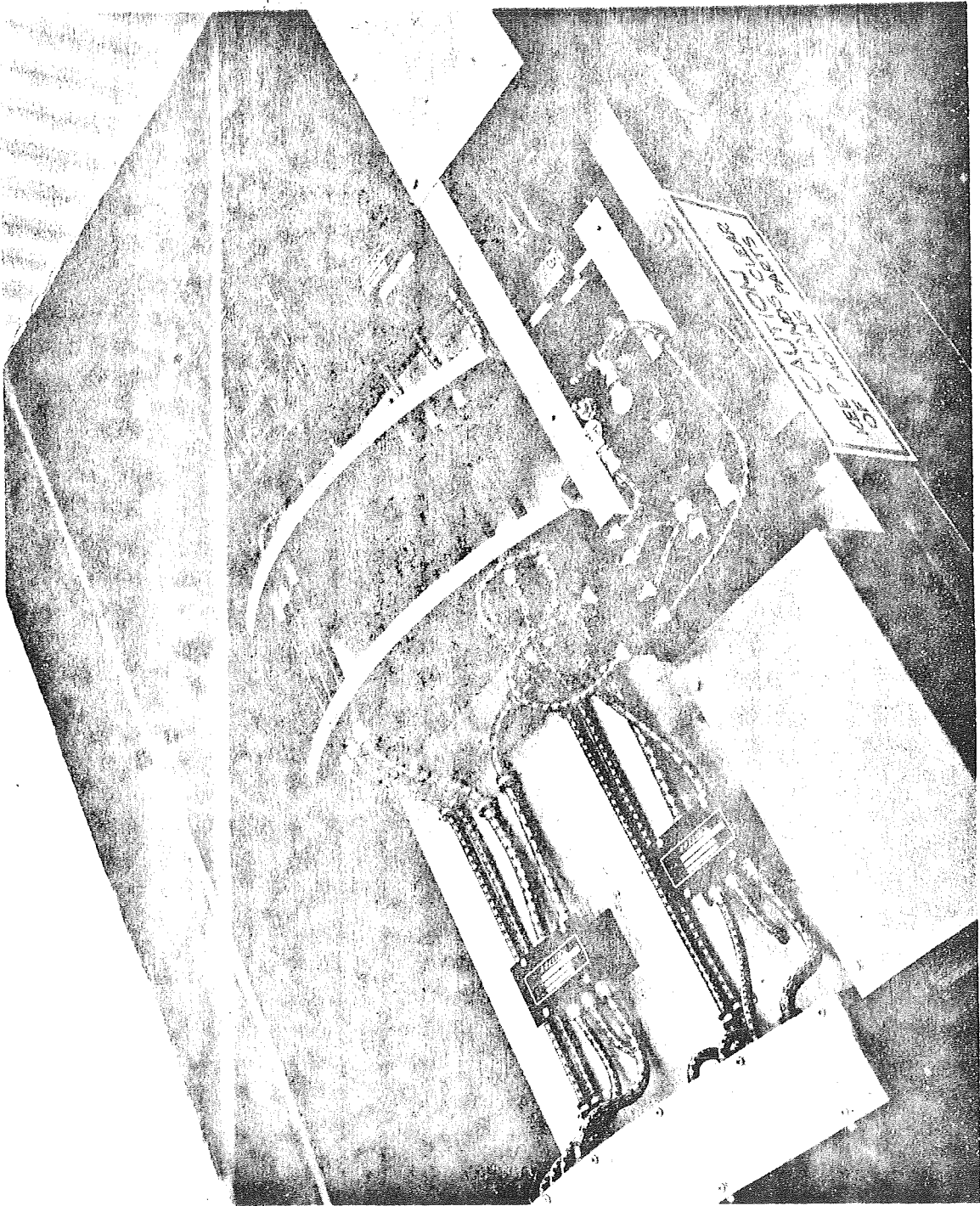


APPROACH AND LANDING CONTROL POWER REQUIREMENT

HARDWARE DEVELOPMENT

Our experience has been that it is difficult to gain acceptance of a new concept unless it is presented at a timely point in the program, usually during the preliminary design phase. These proposals must be accompanied by some lab, and preferably flight test experience, which gives proof that the concept is feasible.

Figure 9 shows a test rig which was established to prove the Hard SAS concept, early in the program. Two channels of the Hard SAS electronics were built as flightworthy, highly reliable sets of equipment. The system was set up to drive a dual servo and a modeled surface actuator. The use of armored cables and the physical and electrical isolation of the channels was demonstrated. An airplane simulation and a control cab were used to close the control loop. This is representative of the initial stages of a hardware development program which finally uses a full scale mockup of the control system including the electronics.



CONCLUSIONS

During the development of an advanced vehicle it is necessary to develop a new set of design rules. These criteria have to be prepared early in the design cycle and distributed to all design disciplines concerned as a means of obtaining an integrated design.

It must then be remembered that the function of these criteria is to provide information. As the vehicle configuration becomes better defined and as new knowledge is gained the criteria have to be changed accordingly.

To assist in establishing a criteria set as a working tool an attentive management organization is required. SST management has a Technical Council consisting of the Chief of Technical Staff, Chief Project Engineer, and the Program Manager established for this purpose. They meet with the various design groups on a regular basis to consider problems which need management attention.

The Space Shuttle Vehicle has a greater range of flight phases than the SST, the performance objectives are even more difficult, and the problems are further complicated by the three vehicle configurations -- composite, booster and orbiter. It is apparent that it will be necessary to specify avionics applications to enhance the performance of the vehicle systems and to make up for deficiencies and control problems as they occur.

The extent of this application of avionics will have an even greater influence on the configuration than it did for the SST. The avionics will become the means for coordinating the operation of all systems at their peak efficiency, and will permit any degree of automatic operation.

N70-40956

ONBOARD DATA MANAGEMENT

R. E. Poupard

**IBM Corporation
Huntsville, Alabama**

INTRODUCTION

ELEMENTS

**DATA PROCESSORS
SUBSYSTEM INTERFACE UNITS
DATA TRANSMISSION MEDIUM
SOFTWARE**

FUNCTIONS

**DATA PROCESSING
DATA CONTROL
VEHICLE SEQUENCING AND CONTROL
CHECKOUT AND FAULT ISOLATION
DISPLAY GENERATION AND FORMATTING
VPS SUBSYSTEM MANAGEMENT**

CENTRAL INTEGRATING ELEMENT OF ELECTRONICS SYSTEM

SIGNIFICANT PROBLEM AREAS

- CHECKOUT/FAULT ISOLATION/REDUNDANCY MANAGEMENT
- SOFTWARE
- DISPLAYS AND CONTROLS

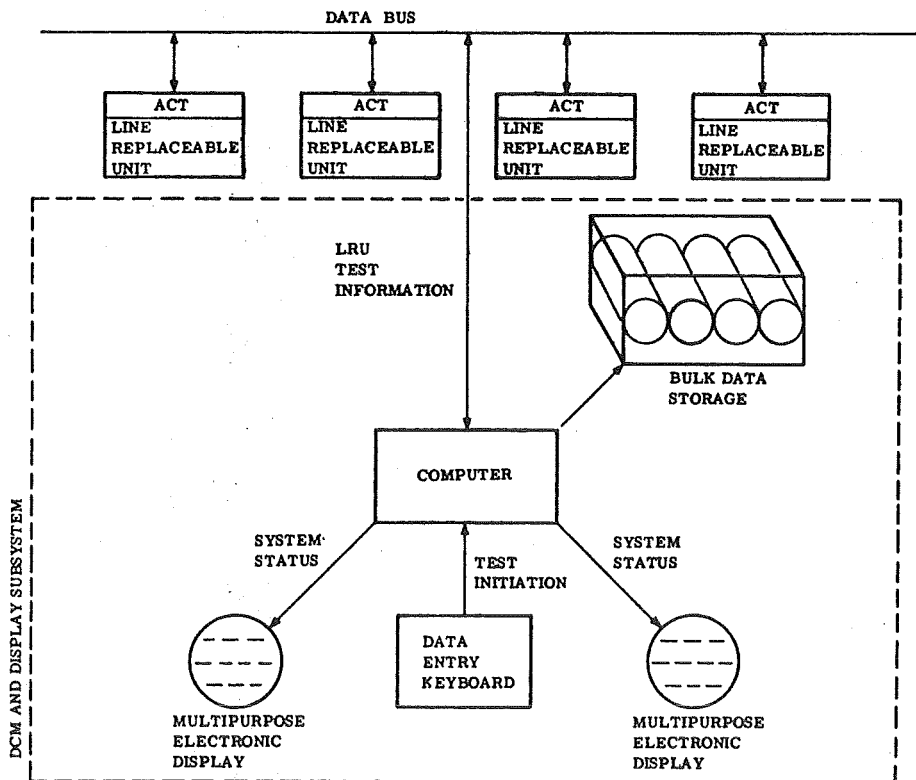
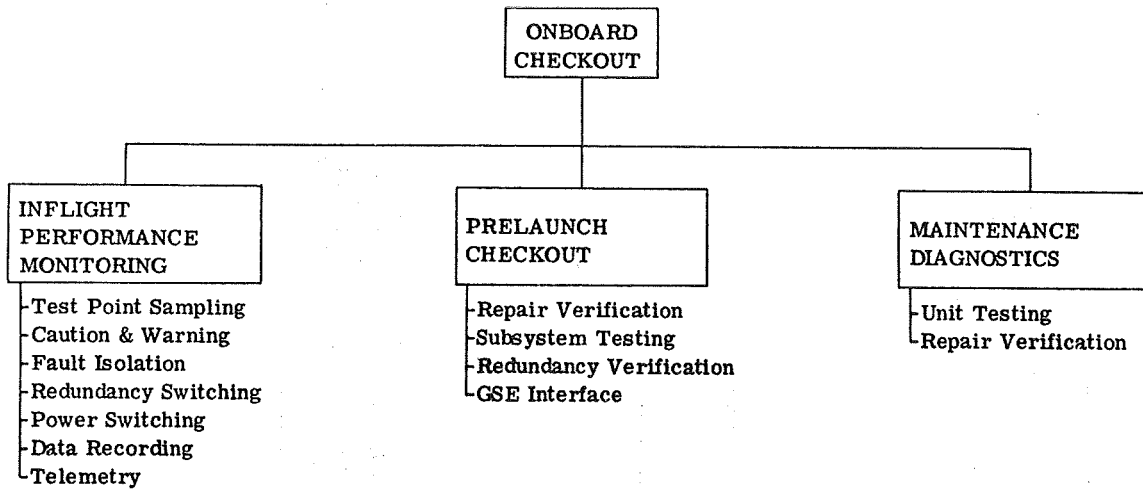
CHECKOUT/FAULT ISOLATION/REDUNDANCY MANAGEMENT

- NASA DESIRES/REQUIREMENTS
 - FAIL OPERATIONAL/FAIL OPERATIONAL/FAIL SAFE
 - SINGLE POINT FAILURE ELIMINATION
- REQUIRES REDUNDANT SYSTEM/ELEMENTS
- REQUIRES 100% FAILURE DETECTION/ISOLATION
- HOW?
 - DEVELOP NEW CHECKOUT TECHNIQUES
 - ASSESS DESIRABILITY OF
 - CHECKOUT LANGUAGE
 - ONBOARD DIAGNOSTIC "PROGRAMMING"
- MOST DIFFICULT TECHNICAL PROBLEM
- IMPORTANT FACTOR IN SIZING DATA MANAGEMENT SUBSYSTEM

CHECKOUT APPROACH

- FUNCTIONAL DATA WHERE POSSIBLE
- MINIMIZE DEDICATED CHECKOUT HARDWARE
- LIMIT CHECKING IN INTERFACE UNIT

SCOPE OF ONBOARD CHECKOUT



CHECKOUT SYSTEM FUNCTIONAL BLOCK DIAGRAM

SOFTWARE

- PROBLEM IS TO RECOGNIZE THAT SOFTWARE CAN AND MUST BE MANAGED AND CONTROLLED USING HARDWARE TECHNIQUES
- REQUIRES CAREFUL ATTENTION TO AVOID PITFALLS OF PREVIOUS PROGRAMS
- MUST BE SPECIFIED/DESIGNED/BUILT/VERIFIED USING HARDWARE MANAGEMENT AND CONTROL TECHNIQUES
- MUST BE CONSIDERED AS SYSTEM ELEMENT IN SYSTEM/SUBSYSTEM DESIGN

SOFTWARE REQUIREMENTS

STORAGE

64,000 WORDS MAIN STORE
300,000 WORDS BULK STORE

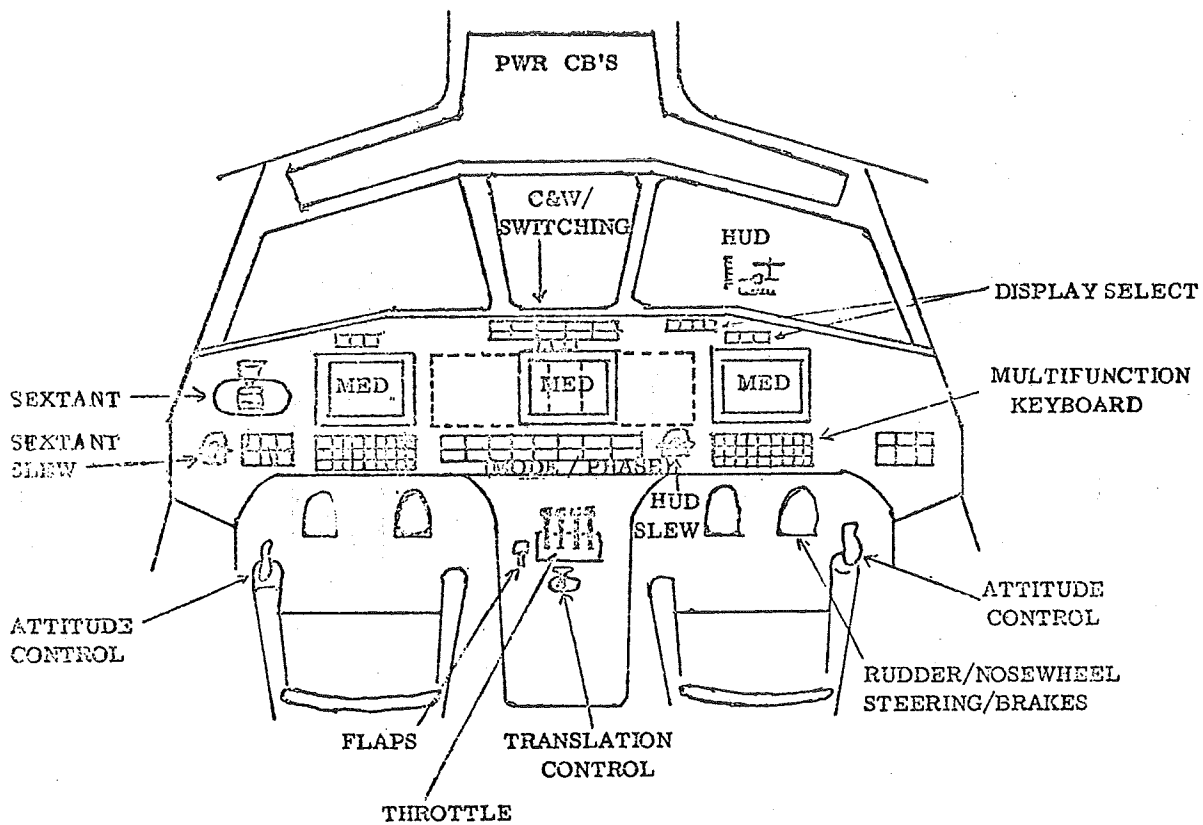
SPEED

350K EQUIVALENT ADDS PER SECOND

- OPERATIONAL REQUIREMENTS WITHIN TODAY'S STATE OF THE ART
- MAIN STORE FOUR TIMES SATURN MAIN STORE
- DEVELOPMENT TECHNIQUES PROVEN ON SATURN PROGRAM

DISPLAYS AND CONTROLS

- AUTONOMY REQUIRES SIGNIFICANT INCREASE IN DATA DISPLAYED
- CREW PARTICIPATION IN CHECKOUT/MONITORING REQUIRES SEVERAL LEVELS OF STATUS DATA
- CRT STATE OF ART ALLOWS GREATER DEGREE OF INTEGRATION
- MEANINGFUL COMBINATION OF SPACECRAFT/AIRCRAFT DATA



COMPUTER CONFIGURATION

DATA MANAGEMENT

- 4 CENTRAL PROCESSOR UNITS
- 4 BUS CONTROL UNITS
- 9 MAIN STORAGE UNITS
- 4 MASS MEMORY UNITS
- 4 MASS MEMORY CONTROL UNITS

FLIGHT CONTROL

- 4 CENTRAL PROCESSOR UNITS
- 4 MAIN STORAGE UNITS

COMPUTER ALTERNATES

- CENTRALIZED
- CENTRALIZED WITH SELECTED DEDICATED
- DISTRIBUTED/PREPROCESSORS

BASELINE

CENTRALIZED WITH SELECTED DEDICATED/PREPROCESSING

- DEDICATED FLIGHT CONTROL COMPUTER
- IMU PRE-PROCESSOR
- LIMITED "PROCESSING" IN INTERFACE UNIT

N70-40957

MULTIPLEX DATA BUS TECHNIQUES

Walter O. Frost

NASA-Marshall Space Flight Center
Huntsville, Alabama

Summary

The application of data bus techniques in the Space Shuttle provides potential improvements in size and weight, flexibility, and reliability. The general requirements for a Space Shuttle Data Bus are described, and critical technology considerations are discussed. Some design alternatives for transmission media, signal design, synchronization and control, input/output interfaces, and operational reliability are described.

Introduction

Astounding reductions in the size, weight, and volume of a complex Avionics system such as that required for the space shuttle will result from MSI/LSI Technology. However, past experience indicates that a significant fraction of the weight of such a system is attributable to the wires, connectors, and associated mounting hardware required to interconnect the various physically separated elements of the system. To prevent such interconnections from becoming a disproportionately large fraction of the system size and weight, the merits of using multiplexing techniques for the transfer of data and command signals between the system elements is under consideration.

The use of multiplex techniques for acquiring signals necessary to monitor system operation has been used by telemetry engineers for many years. However, point-to-point wiring has generally been used for the critical commands and operational signals flowing within an Avionics system. The extension of multiplexing techniques to form an internal communication system for transfer of commands and operational signals, as well as monitoring signals, has by popular usage gained the designation data bus techniques.

The following definition describes a data bus subsystem: A multiplexed signal collection and distribution arrangement with multiple input and/or output terminals interconnected by a shared transmission medium. The key words associated with such a subsystem are multiplexed data flow, multiple inputs and outputs, and shared transmission media. A data bus subsystem has three essential elements. The bus controller supervises the flow of signals so that the multiple users do not interfere with one another. The transmission media provides a shared path (or paths) for multiplexed supervisory and data signals, and data terminals process and route the signals to and from user subsystems and produce signals appropriate for the transmission media.

In addition to possible savings in size and weight resulting from the elimination of wires, connectors, and associated hardware, two other potential advantages accrue from use of multiplexed data bus techniques. First, it should simplify the initial installation of equipment because of reduction in cabling requirements and reduce the cost of later modifications

because system changes can be made entirely within line replaceable units without impacting vehicle cabling. Second, gains in reliability may become possible, because with a marked decrease in interconnections it becomes practical to use redundancy in the data bus subsystem. Thus eliminating the single point failures inherent in conventional point-to-point wiring.

General Requirements

To properly consider a data bus subsystem design for a specific application, the design engineer needs a definition of data flow requirements. It is convenient to express this information in terms of a data flow model. This model provides a detailed description of each message path between physically separated elements of the avionics system. It includes information such as: point of origin, destination(s), signal function, type of signal (analog, discrete, digital word, etc.) resolution, accuracy, occurrence statistics, and any special characteristics or requirements pertinent to data bus design and operation.

The data and command signals handled by the multiplex data bus include discrete and proportional commands from the computational subsystem to various subsystems as well as sensor and subsystem inputs to the computers. It is important to notice that many signal paths may not involve the computers. Monitor signals from various sensors and subsystems to telemetry and onboard recorders, signals for updating of status indications, and signal flow between elements of distributed subsystems are examples of message paths which may be independent of the computers.

The design engineer also needs a description of those physical and environmental characteristics of the application which are pertinent to design of the data bus subsystem. These include location of user-subsystems, cable lengths between locations, expected temperature variations and vibration levels at specific locations, and EMI characteristics. In addition he needs descriptions of input/output characteristics of the various user subsystems pertinent to signal transfer operations to and from the data terminals.

Design Technology

Given the general requirements described above, plus specific system requirements such as weight limitations, power constraints, and reliability or failure criteria, the design engineer is prepared to consider the merits of numerous design alternatives for a multiplexed data bus subsystem. It is convenient to discuss the technology for such a design under the following categories: (1) transmission media (2) Signal design and detection (3) synchronization, timing, and control (4) user-subsystem interfaces, and (5) operational reliability.

Transmission Media

Numerous forms of transmission media have been suggested for use in data bus subsystems. Among these are twisted-shielded pairs, coaxial cable, twinaxial cable, and triaxial cable. For transfer of digital signals at rates less than about two megabits, twisted shielded pairs and twinaxial cable have received most prominent mention. These two are balanced

arrangements which potentially can provide greater resistance to sources of low frequency interference.

The media properties and parameters significant to a data bus design, in addition to interference susceptibility, include propagation delay and signal transfer characteristics such as amplitude, time, frequency and phase characteristics. These properties typically vary as a function of loading, line terminations, signal form, and length of path as well as media form. Hence it is necessary to acquire test results under a variety of conditions to properly assess the potential of specific forms of media.

Signal Design and Detection

A second important technology category which requires careful consideration in the multiplex data bus design is the selection, generation, and detection of transmission signals. Three types of information must be transmitted: data/command information between various user subsystems, bus supervisory information, and the timing and synchronization information required for proper bus operation. Some of the considerations covered by this category are:

- (a) Type of multiplexing
- (b) Form of modulation
- (c) Spectral characteristics and bandwidth requirements of candidate signals.
- (d) Signal generation, demodulation, and detection methods
- (e) Coding techniques
- (f) Message format arrangements

Both time division and frequency division multiplexing have merits for specific data bus applications. However, in applications such as the space shuttle a digital time division arrangement is mentioned most often. Carrier modulation techniques which have been proposed for bus applications include phase shift keying (PSK), amplitude shift keying (ASK), and frequency shift keying (FSK). Baseband modulation forms prominently mentioned include NRZ-L, polar RZ, bipolar NRZ, and Bi- \emptyset .

Synchronization, Timing, and Control

A third technology category critical to the multiplexed data bus design is the synchronization and control of bus operation. Considerations which fall into this category include:

- (a) Bus access control - methods for supervision of multiplex operation so that the transmission media can be shared without interference between user subsystems
- (b) Message routing control - Methods for directing the routing of messages from the point of origin to their proper destinations.
- (c) Timing and synchronization - Methods for the timing and synchronization of transmission and message transfer operations such as modulation/demodulation, bit identification/detection, word or group identification, and bus/user subsystem transfers.
- (d) Programming - Methods and problems relating to the programming of data acquisition and distribution operations including both software and hardware techniques.

Studies of synchronization, timing, and control methods and problems should emphasize the capability of the data bus subsystem to flexibly adapt to changing requirements of the user subsystems. Careful consideration also should be given to the interaction with and impact on design and programming of user subsystems.

User-Subsystem Interfaces

Because of the variety of subsystems which must interface with the data bus subsystem, extensive study of bus/user subsystem interface and integration problems is appropriate. A myriad of electronic operations are required at each interface location. These may include modulation, demodulation, bit and word synchronization, detection, error checking, multiplexing, demultiplexing, data sampling and conversion, and buffering. Various subsystems may require different methods for information transfer such as synchronous or non-synchronous and parallel or serial. Together with these diverse requirements one must consider the merits of standardization of interface terminals or elements thereof. Standardization may reduce design costs and logistic requirements, but introduce limitations and constraints into the design. Physical considerations such as the packaging of interface elements and the electrical interconnections with user subsystems must also be considered at this point.

Operational Reliability

A final technology category of critical importance to the multiplexed data bus design is operational reliability. Typically the designer is given specific failure and reliability criteria, along with test and maintenance requirements. A variety of alternatives are available to enhance these aspects of the design. These include parallel redundant arrangements such as circuit redundancy, triple modular redundancy with voting, and switchable redundant blocks. The designer may also include self-checking features such as error-detection (or correction) coding, return verification of messages, periodic test message transfers, and time-dependent coding checks. He must give appropriate consideration to potential sources of interference such as EMI, common-mode signals, and power supply perturbations.

Test and checkout is an operational problem inherent in avionics system. Hence, suitable methods and techniques must be derived for monitoring the operational readiness of the data bus subsystem including the status of redundant subsystem elements. A closely related consideration is problems and alternatives relating to the maintainability of the data bus subsystem.

Conclusions

Although multiplexed data bus techniques have been used for several years in the instrumentation and telemetry area, these applications have not approached the degree of complexity involved in proposed programs such as the space shuttle. In these applications, the data bus subsystem must interface with and function intimately with all elements of the avionics system. A commitment to a preferred design configuration must be made only after intensive studies and analyses.

DATA BUS DESIGN TECHNIQUES

Donald J. Spencer
TRW Systems Group
One Space Park, Redondo Beach, California

Introduction

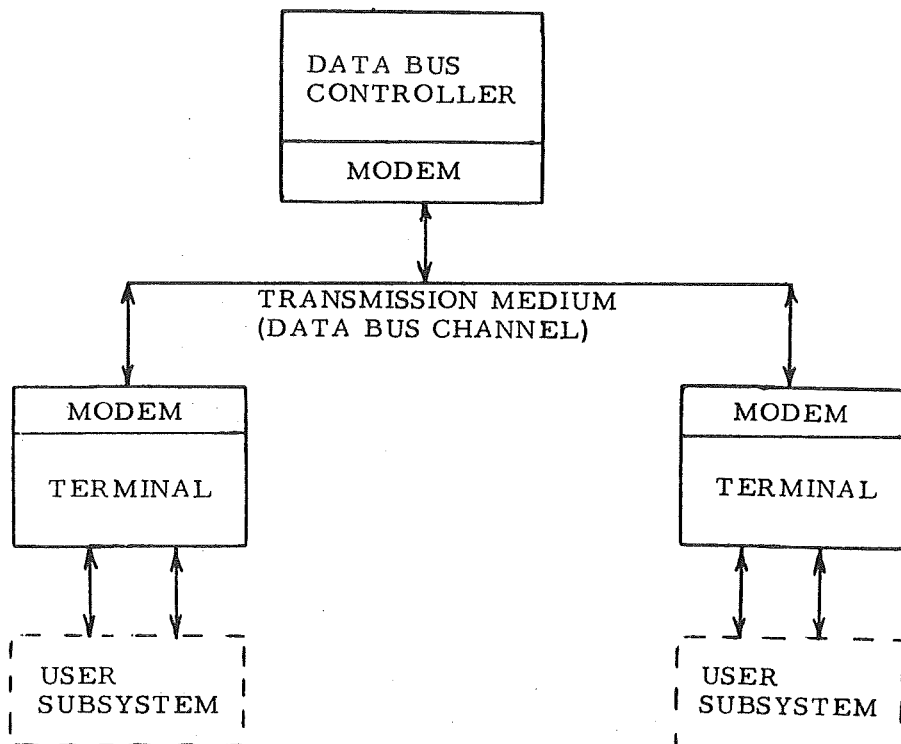
The need has been well recognized for a multiplexed data system to meet the internal communication requirements of a Space Shuttle Vehicle. Not only significant weight savings are achievable but concomitant reliability and maintainability improvements are easily demonstrable. These lead to operating cost savings over the usual point-to-point wiring systems employed in avionic systems. Because of the common carrier nature of such a multiplexed interior communications system, it is called a data bus. Recent progress in microcircuitry has brought the data bus to the threshold of widespread use by solving the weight and cost penalties inherent in the complex modems and interface circuitry.

In this paper, we discuss some of the basic considerations leading to a data bus design. As there is such a variety of techniques available for a Space Shuttle data bus, particular care must be taken in the design process. Basic steps to be taken begin with an analysis of the requirements, design of the data bus communication system and finally generation of the functional use of the data bus. Our emphasis shall be on the steps required to reach a satisfactory data bus system design thus answering the questions, "How to get those bits between the users?" It should be mentioned here that only digital data bus techniques will be considered. This restriction itself is a step in the design process and is made here because:

- 1) There are many communication advantages to digital techniques
- 2) Uniform digital interfaces are becoming prevalent in avionics systems
- 3) Most Shuttle concepts employ digital computers putting digital data into the majority.

The primary functional parts of a data bus are shown in the Figure. A bus controller may not, in some designs, exist as an entity, its function being dispersed among the various terminals. No indication is given of the complexity of an actual data bus layout that could involve highly asymmetric geometries. We shall be concerned below in the choice of the modem and transmission medium rather than with the controller or terminals.

The results and examples described in this paper are derived in large part from the first phase of an on going TRW Data Bus Study.*



FUNCTIONAL DATA BUS

* Data Bus Technology Studies; Phase 1. Analytical Aspects.
TRW Report No. 7331.3-39, June 1970.

Transmission Media

A fundamental choice in the data bus design is the interconnecting medium whose function is to provide a communicating path between the large variety of user subsystems. It is essential that the data bus be flexible to meet changing requirements such as data distribution constraints as the Shuttle program matures. The transmission media must

- o Provide adequate bandwidth margin
- o Be amenable to configuration changes
- o Allow simple coupling to modems
- o Provide noise immunity
- o Meet manned spacecraft environmental and reliability constraints.

Light beams, radio waves, and other techniques can be used for data bus channels but we shall consider only wire (cable) lines in the data rate range of 50 Kbps to 5 Mbps as this is the media of most immediate interest to Shuttle. As far as geometry is concerned, only a general constraint of 350-ft line length and a maximum of 50 terminals will be imposed.

Line Transfer Characteristics

From the transmission standpoint, wire lines are four-terminal networks and as such have frequency dependent transfer characteristics. Unlike more conventional networks, however, the constants of a wire line are uniformly distributed along its length instead of being lumped into discrete units of inductance, capacitance, and resistance. These effects are typically measured as attenuation, α , and phase β which describe the propagation function and by the characteristic impedance $Z_0 = R_0 + j X_0$. For analytic purposes, experience has shown that these parameters may be modeled in three frequency zones, low, intermediate and high. Their dependence on frequency for the two higher zones is shown in Table 1.

Quantity	Intermediate Frequency Zone 100 Hz-500 KHz	High Frequency Zone > 500 KHz
α	$\sqrt{\omega}$	$\sqrt{\omega}$
β	$\sqrt{\omega}$	ω
R_0	$1/\sqrt{\omega}$	Constant
$-X_0$	$1/\sqrt{\omega}$	$1/\sqrt{\omega}$

Table 1.
Frequency Dependence On Line Parameters

Laboratory tests of cables reveal characteristics as shown in the Figure, which apply to a particular twisted shielded pair. For the cable shown, the frequency breakpoint was chosen at 500 KHz. Thus for a 100-ft length line

$$\beta(\omega) = \begin{array}{ll} 2.9 \times 10^{-4} \times \sqrt{\omega} & \omega < \omega_0 \\ 1.60 \times 10^{-7} \times \omega & \omega > \omega_0 \end{array}$$

$$\alpha(\omega) = 0.6 \times 10^{-3} \sqrt{\omega/2\pi} \quad \text{dB/100 ft.}$$

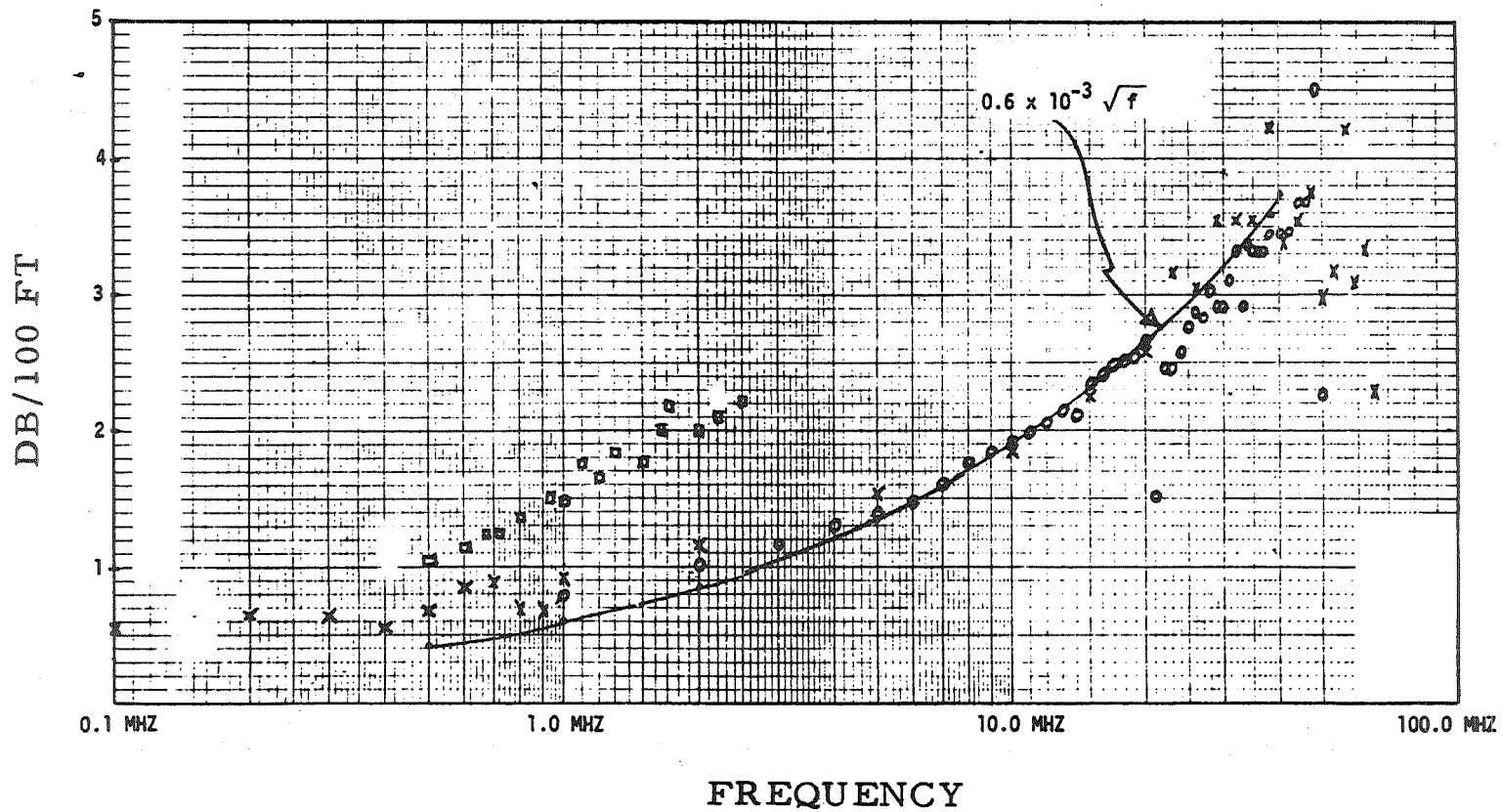
Loading, Matching and Branching Effects

A typical data bus will be composed of several branches. The loads, their spacing, the branch points and the terminations on the branch ends all lead to reflections in the signal wavetrain, thereby increasing the bit probability of error. A single branch of the line appears as a multiply loaded transmission line. For large number of loads, such lines are difficult to analyze. However, the reflection coefficient, ρ , may be used in determining the percentage of incident voltage at a load which is reflected rather than transmitted. The voltage at any load is the sum of all the incident and reflected voltages associated with that load after n reflections.

Equations were developed to study the variations of reflection coefficient with frequency, loads and terminating impedances. The numerical

ATTENUATION VS FREQUENCY (D-210-1 CABLE)

66



examples were based on the transmission line model above with a total of 35 loads on a 360 ft line at fixed spacing. Graphs, typified by the Figure were plotted to study the effects of variations. General conclusions when the line is terminated in its characteristic impedance are:

- o As the load impedance increases, the reflection coefficients decrease
- o The reflection coefficients decrease with frequency
- o The greatest reflections appear at the source end of the line and decrease as the load number increases. At a frequency of approximately 5 MHz, this effect is reversed.

In using the transmission medium, consideration must be given to simplex or duplex operation requirements. Duplex may be shown to lead to lower cable and modem weights for the data rates and configurations given. However, duplex operation implies complexity in the branch points as they must allow two-way signalling. Three approaches have been considered:

- o Four-port resistance coupling
- o Three and four port hybrid couplers
- o Multiple repeater modems.

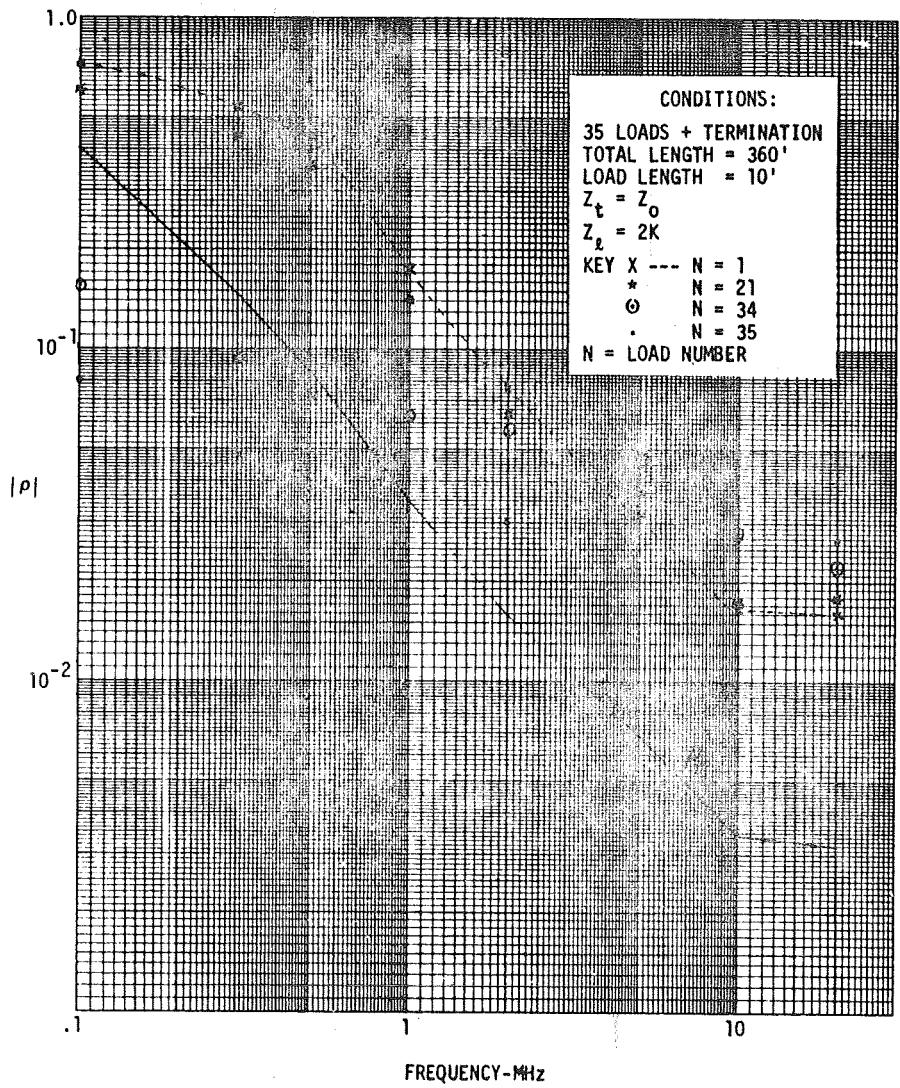
The simplest approach, resistive coupling, is found to meet the requirement of assuring proper matching with tolerable reflections through the junction. With terminating impedance equal to Z_0 and load impedance equal to 10 K, the reflection coefficient above 0.3 MHz is negligible and the line appears unloaded. With terminating impedance equal to R_0 and load impedance equal to 10 K, the reflection coefficient above 0.4 MHz is low and the line appears unloaded with characteristic impedance Z_0 .

Noise Environment

The effects of noise on the data bus may vary greatly with location in the vehicle. It is thus important to have an accurate model of the noise environment in the vehicle reflecting the effects of:

- o Cross-talk from nearby cables
- o Coupled noise from noisy subsystems such as motors and relays

REFLECTION COEFFICIENT VS FREQUENCY



- o Atmospheric static (lightning)
- o Radio transmitters
- o Possible electrostatic discharges

The primary effect of such sources will be through inductive or capacitive coupling on the transmission medium due to its length. However, noise will also exist at the modems and terminals in the form of thermal noise, power supply transients and ground loops.

Choice of a transmission medium depends heavily on its noise immunity. Optical systems, such as optical fibers, have nearly ideal noise insensitivity. Common mode rejection of 100 dB is easily obtainable and ground loops may be eliminated since there is no shield. In some very noisy locations, sub-busing by optical systems may be desirable. For cable transmission media, however, care must be taken to minimize noise sensitivity.

Shielding effects of different cables are compared in the Figure*. It has been found that load variations have little effect on the noise immunity. As can be seen, the shielded twisted pair is better than coaxial cable at all frequencies with the greatest improvement at the lower frequencies. The low frequency rejection in the twisted pair is due to twisting while the high frequency rejection is primarily due to the shielding.

All of the cables shown had the cable shields grounded at both ends. If single end grounding is used with twisted shielded pair there is a degradation in noise attenuation of as much as 30 dB.

Where data bus cables run adjacent to each other over extended distances, special consideration must be taken. Again careful grounding is required, and pickup is low between coax and TSP. However, two or more TSP's running together require different pitch to avoid inductive coupling.

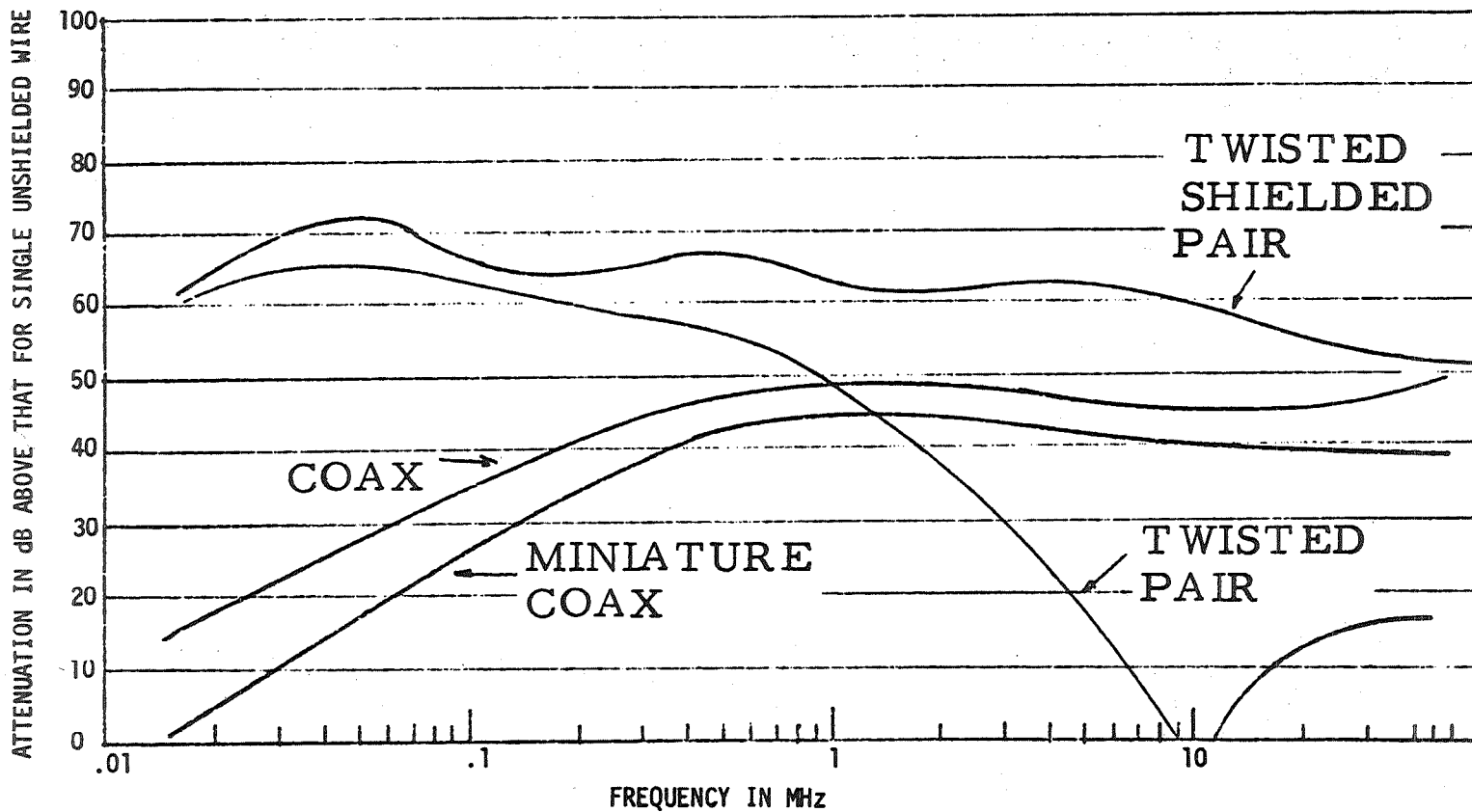
Transmission Line Choices

The technique of coupling to the line is of great effect in the overall transmission medium characteristics. Primarily considered are balanced,

* R. Loveland and J. Goodwin, "Addressable Time Division Multiplexer System (Cable and Connector Study)," Martin Marietta Corp., Denver Division, March 1968.

NOISE ATTENUATION OF CABLES TERMINATED IN CHARACTERISTIC IMPEDANCE

108



transformer coupled and non-balanced or single-ended. There is a complexity weight and volume penalty in transformer coupling but its superior noise rejection make it more desirable than direct coupling for noisy environments.

Taking into account the expected interference environment and cable characteristics, recommended cables are shown in the Table below. TSP seems clearly indicated for low level data and signalling requiring high accuracy due to its superior noise rejection. Shielded twisted pair should be driven from balanced circuitry to achieve optimum advantage. At very high data rates (in excess of 10 watts) the attenuation in shielded pairs is insurmountable and coax must be used.

	Moderate Data Rate	Very High Data Rate
High SNR	<u>Shielded Twisted Pair</u> Single-Ended	<u>Coaxial Cable</u> Single-Ended
Low SNR	<u>Shielded Twisted Pair</u> Balanced Line	<u>Coaxial Cable</u> Balanced Line- With Double Shield

Table 2.

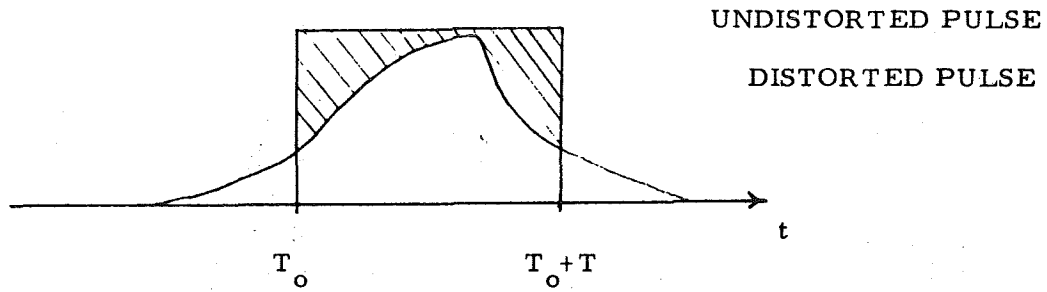
Recommended Data Bus for
Different Operating Conditions

Modulation and Detection

Line Induced Distortion

Associated with any communication channel is a channel impulse response $h(t)$. The effect of non ideal line characteristics lead to distortion of each transmitted signal as indicated in the Figure. There is an energy loss during the period, indicated by cross-hatching, and intersymbol interference due to received energy in other bit periods. These, combined with additive noise

LINE INDUCED DISTORTION



DISTORTED AND UNDISTORTED RECEIVED PULSES

CRITERIA FOR MODULATION/DETECTION SCHEMES

- NOISE IMMUNITY
- INTERSYMBOL INTERFERENCE
- BANDWIDTH EFFICIENCY
- BIT SYNCHRONIZATION
- COST COMPLEXITY

tend to increase the bit probability of error. A modulation and detection scheme must be chosen which minimizes the effects of such distortion and meets the criteria stated. Intersymbol interference is caused by overlapping of the positive and negative overshoots of the past pulses into the current time slot. It is most significant at the sampling and transition instants. Equalization may be used to decrease the intersymbol interference in the form of transversal filters or pre-emphasis techniques. These compensating filter techniques have not been found necessary in the Shuttle data bus due to modest data rates and line length.

Modulation techniques may be generally divided into carrier and non-carrier where the former refers to mixing a carrier frequency with the data. Typical non-carrier (baseband) modulation schemes, their advantages and disadvantages are shown in the first Figure. Similar lists may be studied for carrier systems. Carrier systems are found to be most applicable to higher data rates where their higher complexity is offset by increased communication efficiency due to lower percentage bandwidths. Any hybrid time division/frequency division multiplexing scheme also requires carrier type signalling. In the summary below a recommended carrier system for higher data rates is described.

The bit error performance of the several baseband modulation schemes may be analytically predicted as shown in the second Figure. However, including the effects of the channel distortion becomes a complex task and can be done properly only with lengthy computer calculations or simulation. One interesting comparison is offered in the third Figure. The Manchester (biphase) modulation results antipodal signalling while bipolar requires only half as much bandwidth. For a fixed error rate in the presence of noise, a lower data rate/low pass bandwidth ratio favors bipolar signalling. However for the chosen typical twisted shielded pair, Manchester is best for reasonable operating values.

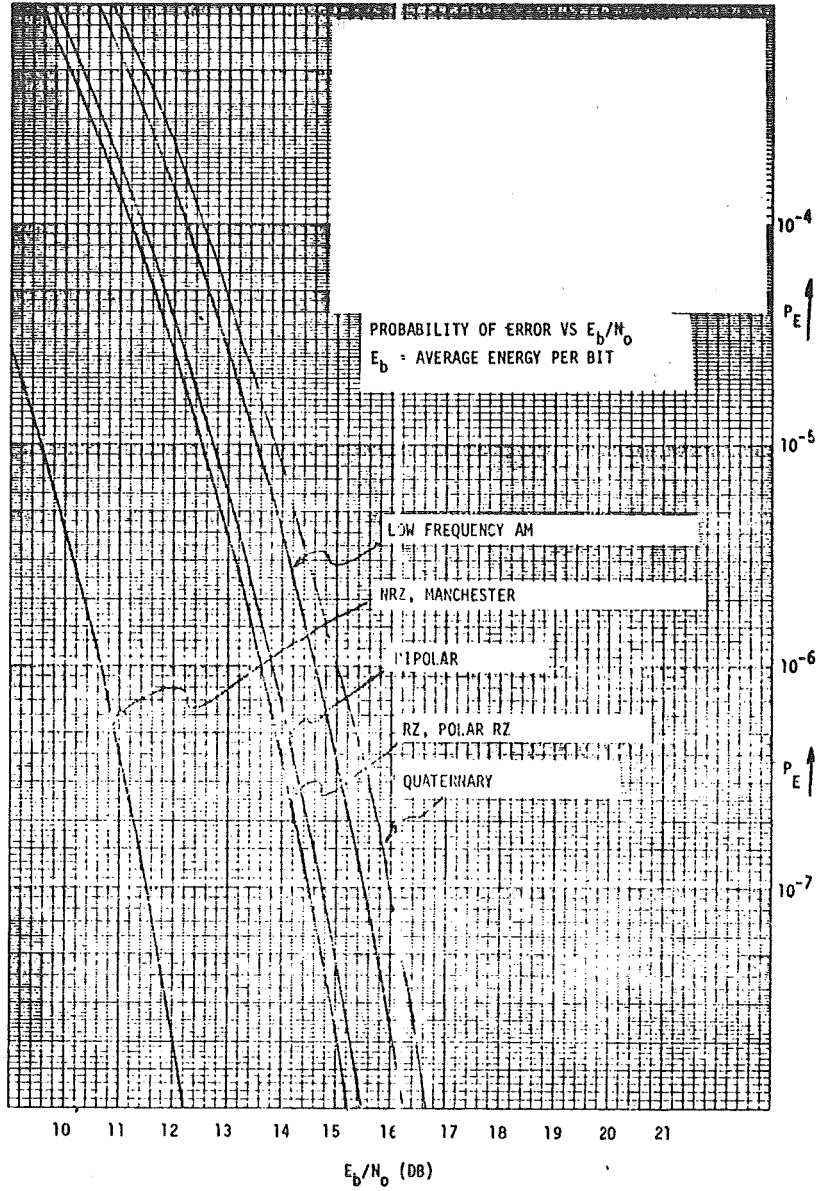
There are three general ways to provide bit synchronization for detection:

- 1) Provide a separate clock line
- 2) Reconstruct the clock from the data
- 3) Frequency multiplex the clock with the data.

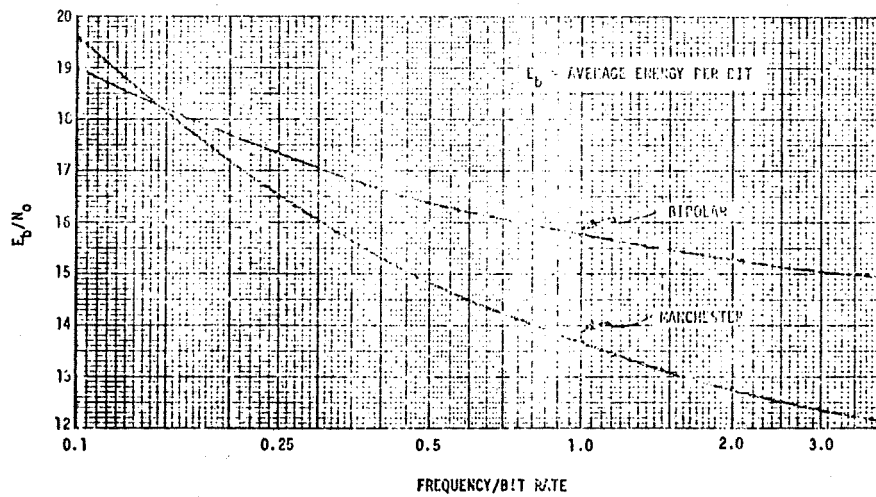
Comparisons of Baseband Signalling Techniques

Modulation Scheme	Application	Advantages	Disadvantages
NRZ	DC coupled system	<ol style="list-style-type: none"> 1. Best performance in gaussian noise 2. Bandwidth equal to data rate 	<ol style="list-style-type: none"> 1. Sync obtainable from data but relatively complex
RZ	DC coupled system	<ol style="list-style-type: none"> 1. Easy to generate 	<ol style="list-style-type: none"> 1. Inferior in performance to NRZ 2. Same sync difficulties as NRZ
Polar RZ	DC coupled system	<ol style="list-style-type: none"> 1. Sync easily derived from the data stream 	<ol style="list-style-type: none"> 1. Inefficient in its use of bandwidth as compared to RZ 2. Requires that a positive and negative polarity pulse be generated
Manchester	AC coupled system	<ol style="list-style-type: none"> 1. Performance in gaussian noise equal to that of NRZ 2. Sync easily derived from the data stream 	<ol style="list-style-type: none"> 1. Requires approximately twice the bandwidth of NRZ
Low frequency AM	AC coupled system	<ol style="list-style-type: none"> 1. Sync readily derived from the data 	<ol style="list-style-type: none"> 1. Wasteful of signal energy 2. Optimal receiver difficult to implement
Bipolar	AC coupled system	<ol style="list-style-type: none"> 1. Bandwidth equal to data rate 	<ol style="list-style-type: none"> 1. Subject to dc wander 2. Requires an encoder 3. Same sync problems as NRZ
Pair selected ternary	AC coupled system	<ol style="list-style-type: none"> 1. Bandwidth equal to the data rate 2. No dc wander 3. Sync easily derived from the data 4. Inherent error performance monitoring 	<ol style="list-style-type: none"> 1. Framing required -- adds to circuit complexity -- but lends itself to digital implementation
Duobinary	AC coupled systems	<ol style="list-style-type: none"> 1. Achieves 2 to 1 bandwidth compression, i.e., bandwidth equals half the data rate 2. Sync obtainable from the data 3. Insensitive to sync filter 	<ol style="list-style-type: none"> 1. 6 dB worse than NRZ in performance 2. Requires signal shaping
Multilevel signalling	AC or dc coupled systems	<ol style="list-style-type: none"> 1. Achieves bandwidth compression 	<ol style="list-style-type: none"> 1. Harder to implement than simpler binary signalling

PERFORMANCE OF VARIOUS SIGNALLING SCHEMES
 ASSUMING A DISTORTIONLESS CHANNEL



E_b/N_0 REQUIRED TO OBTAIN PROBABILITY OF ERROR = 1×10^{-6}
 AS A FUNCTION OF CHANNEL 3-DB POINT, RECTANGULAR PULSES



Each of these techniques have been used often in telemetry and data systems and are well understood. Numerous implementation have been worked out for each modulation scheme. Just as with modulation, different synchronization schemes have penalties in bit error performance due to synchronization noise. A number of sync schemes were analyzed in detail. The conclusion was that near optimal performance in the sense of obtaining the error rate predicted with ideal synchronization can be obtained with the use of an external line or certain analog self synchronizers. Performance to within 1 dB of theory is possible with a simple digital bit synchronizer.

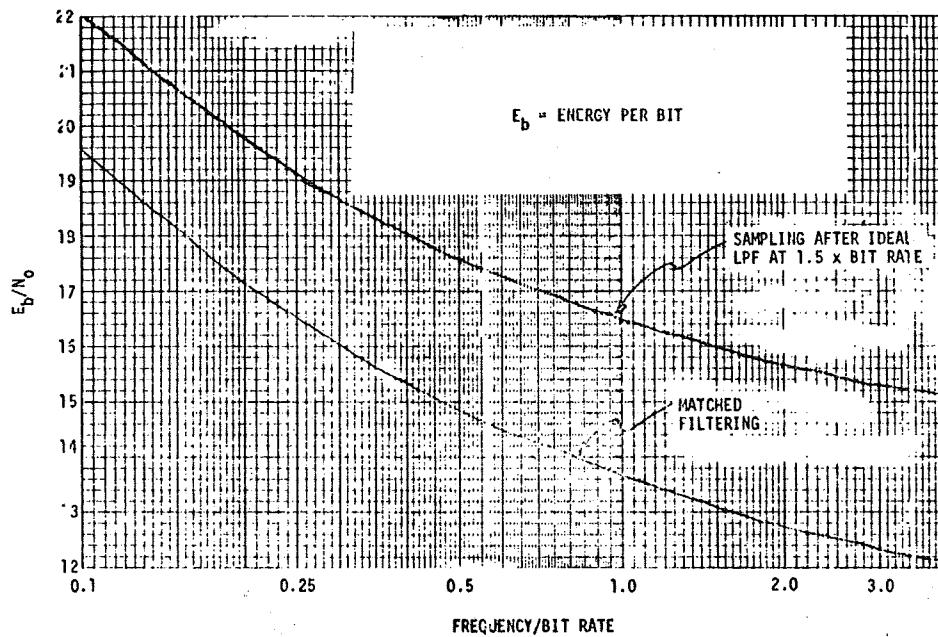
For detection of the modulated signal, optimum (energy detection), sub-optimum (low-pass filtering and sampling), and simple level detection can be employed. The Figure shows the penalty in sub-optimum detection for Manchester coded data. Trade-offs are required to determine the optimum combination of modulation, synchronization and detection for a given operating environment including the effects of the transmission line. Relative costs of implementation for combinations of synchronization and detection schemes in the data bus modem are given in Table 3. LSI analog and digital units are used where applicable.

Type	No. of LSI Packages	No. of Discretes	Power In Watts	Normalized Costs*
Manchester code				
Single line, optimum	2.5	4	2.0	10
Two line, non-optimum	0.6	2	0.3	6
Two line, optimum	1.5	2	0.6	7
Single line, non-optimum	0.7	1	0.5	6
NRZ code				
Single line, optimum	2.0	3	1.4	10
Single line, non-optimum	0.8	1	0.4	6
Sync tone, non-optimum	1.6	0	0.8	8
Bipolar code				
Non-optimum	1.1	1	0.4	7

* Assuming a subassembly production run of 4000

Table 3.
Detection Schemes and Bit Synchronization Comparisons

E_b/N_0 REQUIRED TO OBTAIN PROBABILITY OF ERROR
 $= 1 \times 10^{-6}$ VS CHANNEL 3-DB POINT



Recommended Data Bus Modulation Techniques

The previous sections have described the applicable considerations for communication performance in the presence of noise, intersymbol interference and transmission line induced distortion. We now produce modulation, detection and synchronization schemes for several sets of operating conditions. Implicit in the findings will be the transmission line model for twisted shielded pair. One type of calculation leading to the recommended approaches is the communications power budget. A simplified calculation for a 1 Mbps, low signal-to-noise ratio case is now shown. Let the transmission line be the previous twisted shielded pair model, length 350 ft and 35 equally spaced 10 K loads. Assume a desired bit error probability of 10^{-6} at the last load and the use of matched filter (optimum) detection with a separate synchronization line. Then the following values are found:

Transmission Line Degradation	1.4 dB
Noise and Distortion Requirements	12.7 dB
Noisy Synchronization Degradation	.5 dB
<hr/>	
Required E_b/N_0	14.6 dB

The sample systems are now summarized.

Low SNR (< 20 dB), Data Rate < 5 Mbps

- o AC coupled, balanced configuration to minimize noise
- o Manchester (biphase) modulation, energy detection
- o Separate clock line. Cheaper than phase lock loop required to obtain sync from noisy data.

High SNR (> 40 dB), Data Rate < 5 Mbps, AC coupled

- o Manchester signalling, sampling (simple) detection
- o Clock extracted from data. Less expensive than two-line system in high SNR case.
- o Manchester more easily synchronized, less expensive than bipolar modulation

Low SNR, High Data Rate, Carrier System

- o Coherent binary PSK. Better noise tolerance than FSK or ASK.
- o Pilot tone outside signalling band for sync phase locking assumed for non-time varying channel
- o PSK superior to differential PSK for linear differential delay distortion across signalling band.

Acknowledgment

The data bus study, from which the results reported here were derived, was performed by F. P. Kaiser, Thelma Rodriguez, J. H. Stevens, M. S. Stone, H. M. Trachtenberg, B. S. Yolken, and others at TRW Systems.

N70-40959

CHECKOUT OF REDUNDANT SYSTEMS

H. L. Newman

General Dynamics/Convair
San Diego, California

Present analytical tools, such as Failure Mode and Effect Analysis (FMEA), used in the design process are of limited usefulness for integrated checkout systems in a redundant environment.

Space Shuttle demands careful consideration of the new factors introduced by onboard checkout and redundant hardware/software systems which are configured to be fail operational, fail operational, fail safe.

A rational approach is discussed with focus on the problems of utilizing the classical methods. Some of the inadequacies are explained and several possible approaches outlined.

- PHASES OF CHECKOUT
- SHUTTLE AVIONICS CHARACTERISTICS
- POSSIBLE PROBLEM AREAS
- POTENTIAL SOLUTIONS

PRECEDING PAGE BLANK NOT FILMED.

PHASES OF SHUTTLE CHECKOUT

Shuttle checkout is divided into three major phases.

Pre-flight checkout, used to determine if the systems will perform properly, will be accomplished utilizing on-board equipment and if necessary, some ground support equipment.

In flight checkout, performance monitoring, and fault isolation is performed with only on-board equipment. The crew is limited in size, and are not maintenance experts. The checkout function is critical to flight safety as it is used not only to inform the crew of vehicle status, but also to provide the information necessary to manage subsystem redundancy.

The post flight checkout phase is concerned principally with maintenance assistance.

- **PREFLIGHT CHECKOUT**

 - **CONVENTIONAL USING ONBOARD EQUIPMENT AND NECESSARY GROUND SUPPORT EQUIPMENT**

- **INFLIGHT PERFORMANCE MONITORING AND FAULT ISOLATION**

 - **ONBOARD EQUIPMENT ONLY**

 - **LIMITED CREW**

 - **SAFETY CRITICAL**

 - **MANAGES REDUNDANCY**

- **POSTFLIGHT CHECKOUT AND MAINTENANCE ASSIST**

SHUTTLE AVIONICS

The avionics systems on shuttle will be fail-operational fail-operation fail-safe, with this failure tolerance achieved by the use of multiple redundancy.

The shuttle launch rate of 25 to 75 launches per year and a program life in excess of 10 years means that between 250 and 750 launches will occur. If we assume a typical mission to require 5 days in orbit, we will have at the end of 10 years accumulated somewhere between 45,000 and 130,000 hours in orbit.

The equipment used for shuttle will have to be reliable, but over the life of this program, multiple failures, though rare, will probably occur.

The onboard systems should have the capability of coping with multiple failures.

- SUBSYSTEMS DESIGNED FAIL-OPERATIONAL FAIL-OPERATIONAL FAIL-SAFE
- 250 TO 750 FLIGHTS OVER 10-YEAR PERIOD
- ABOUT 100,000 HOURS OF ORBITAL FLIGHT
- EQUIPMENT WILL BE RELIABLE
- MULTIPLE FAILURES RARE
- MULTIPLE FAILURES WILL OCCUR
- ONBOARD SYSTEM MUST CONSIDER MULTIPLE FAILURE

SELECTION OF EXAMPLES

One of the best ways to determine what type of problems might occur in the checkout of space shuttles redundant systems, is to examine other vehicles with similar applications.

The inflight performance monitoring function is an extrapolation of present day airline operating practice, and situations where airlines have had difficulty should be considered.

The airlines utilize multiple redundancy for two reasons; to provide safety, and to increase the probability of on-time dispatch. This quite frequently leads to triple and quadruple redundancy in critical areas, such as engines, hydraulic systems and electrical power.

The electrical power systems, have evolved over many years of experience, and a large effort has been expended in their design, to insure that total power failures will not occur.

SELECTION OF EXAMPLES

- **AIRLINE PRACTICE**
- **MULTIPLE REDUNDANCY**
- **YEARS OF EXPERIENCE**
- **MAN-MACHINE INTERFACE**
- **INFLIGHT PROBLEMS**

AIR-LINE ELECTRICAL POWER SYSTEMS

The typical electrical system on a commercial airliner derives its prime power from engine-driven A. C. generators mounted one on each engine.

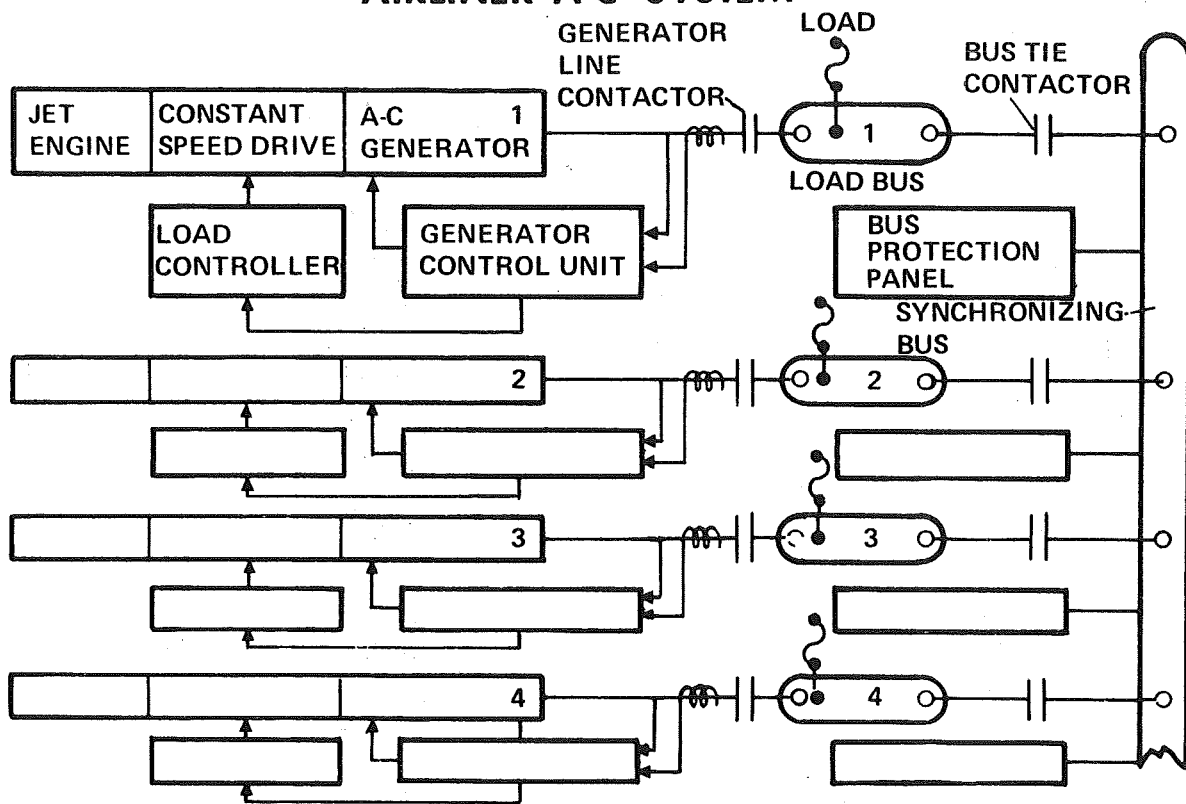
Alternating current power is supplied to using equipments by means of multiple distribution buses, with circuit breakers protecting the buses and generating equipment.

Direct current supply is provided by transformer-rectifiers and batteries with distribution again accomplished by means of multiple distribution buses.

The inflight checkout, monitoring and switching of these systems is semi-automatic with supervision provided by the flight crew.

Two recent airline incidents involving complete loss of electrical power will be examined for information of possible use to shuttle.

AIRLINER A-C SYSTEM



727 ACCIDENT

A 727 aircraft was dispatched with the number 3 A. C. generator known to be inoperative. This was possible because the minimum equipment list for this aircraft only requires two operative generators.

During climbout, a fire warning signal was observed on number one engine and this led to the shutdown of the number one engine and its operable electrical generator.

A short time after this engine shutdown the remaining generator (#2) was lost. The exact reason for this loss was not determined, although it was probably caused by the total A. C. load being imposed on the single generator.

This vehicle carried a standby electrical power supply that could supply the essential bus with power for critical flight instruments and radios. This standby system either was not activated or malfunctioned.

The aircraft was flying under poor visibility conditions, and when the electrical power failure resulted in the loss of attitude reference instruments, the crew was unable to control it, and the aircraft crashed.

727 ACCIDENT

- **DISPATCHED WITH NO. 3 A-C GENERATOR INOPERATIVE**
- **NO. 1 ENGINE SHUTDOWN AFTER FIRE WARNING**
- **NO. 2 A-C GENERATOR LOST**
- **STANDBY POWER NOT UTILIZED**
- **NO. 2 A-C GENERATOR PARTIALLY RESTORED FOR 9-15 SEC.**
- **AIRCRAFT CRASHED INTO OCEAN**

CV 880

An 880 recently lost all electrical power after experiencing multiple failures. The sequence went as follows:

One of the air conditioning system freon compressor motors malfunctioned, throwing an oscillating load on the power system.

The freon motor protection system did not detect the motor malfunction (overcurrent, overtemperature, overpressure, loss of phase), since some protectors had failed. Other generator system protective functions, although operative, did not interpret this type of cycling load as a failure, and thus did not isolate the paralleled system.

The contractors associated with the four paralleled generators did not trip.

The oscillating load caused the hydromechanical constant speed drives to overspeed. This resulted in an automatic protective device in each of the four constant speed drives to cycle to underspeed and lock into this mode. When in underspeed, the jet engine must cease rotation before the constant speed drive can be reset. This of course is impossible with the aircraft in flight, with the fans windmilling. Thus all alternating current generating capability was lost.

The emergency battery failed thirty seconds after loss of the AC system, due to four defective cells, leaving the aircraft with no electrical power.

Unlike the 727 accident however, the 880 was flying in good visibility conditions and was able to land safely.

880 INCIDENT

- FREON MOTOR IN AIR-CONDITIONING SYSTEM FAILED
- FAILURE PUT OSCILLATING LOAD ON SYSTEM
- MOTOR PROTECTOR DID NOT OPERATE
- BUS PROTECTIVE PANEL DID NOT TRIP BUS TIE CONTACTOR
- GENERATORS ALL EXPERIENCED OVERSPEED
- GENERATORS ALL LOCKED INTO UNDERSPEED
- BATTERY FAILED AFTER 30 SECONDS
- AIRCRAFT LANDED SAFELY

PROBLEM AREAS

Looking at the 727 and 880 electrical problems, we find that multiple failures do occur, although of course they are rare.

The failures that do occur are not necessarily related, and can occur in two different subsystems, and still cause an unexpected complete system failure.

The shuttle subsystems should be examined to assess the probability of such multiple failures, and if necessary action should be taken to insure vehicle safety.

PROBLEM AREAS

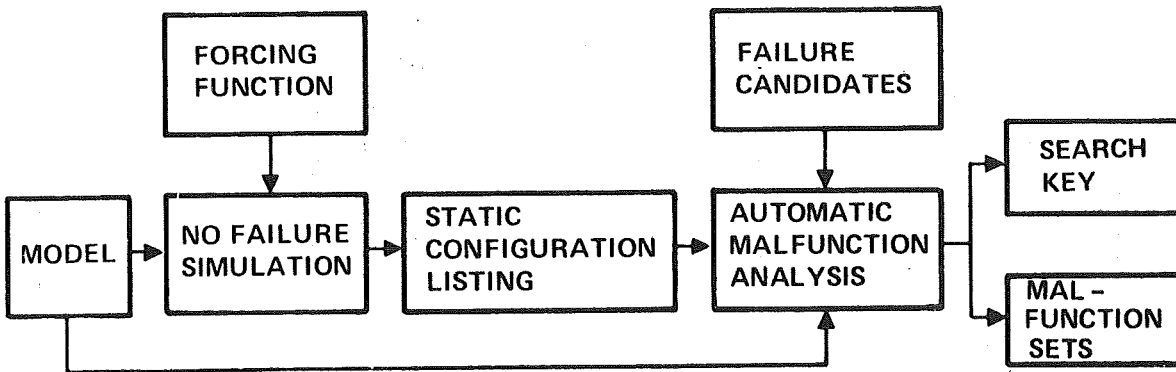
- **MULTIPLE FAILURES**
- **UNRELATED FAILURES**
- **TOTAL SYSTEM FAILURE**
- **SYSTEM FAILURE NOT PREDICTED**

AUTOMATIC MALFUNCTION ANALYSIS

The application of modern computer simulation and analysis techniques to shuttle design and checkout could assist in resolving some of the problem areas.

Typical of techniques available to aid in solution of checkout problems is a group of programs known as Automatic Malfunction Analysis (AMA). AMA was developed for MSFC on NAS8-20016, NAS8-21338 and previous contracts. AMA is designed to simulate and analyze large discrete networks, and to provide for any failure a rapid identification of the malfunctioning component. This analysis, due to its inverse organization is much more efficient than one employing malfunction insertion. For example, an analysis was performed of the Saturn S1C engine cutoff network which consists of approximately 3700 elements with over 200 monitoring points or indicators and which assumes 216 different states as it is cycled through normal operation. AMA took about 12 hours running time on a 7094 to produce the output search key and malfunction set tapes. Similar analysis utilizing fault insertion techniques would have taken over seven years to complete. This output data will then permit identification of any malfunctioning component within approximately 50 ms seconds. While at present structured to analyze only single point failures, inspection of the malfunction set outputs and program organization indicates that an extension of AMA capabilities to analyze multiple failures is possible.

AUTOMATIC MALFUNCTION ANALYSIS



AMA COMPUTER TIME REQUIREMENTS

3,700	ELEMENTS	}	12 HR. ON 7094 TO PRODUCE OUTPUT SEARCH KEY AND MALFUNCTION SETS
200	INDICATORS		
216	STATES		

RECOMMENDATIONS

The problems identified in this paper can best be solved in the design phase of the shuttle program. Due to the large total number of hours in orbit, shuttle will probably experience multiple failures, and systems should be designed to keep multiple component failures from producing unexpected total system failures. An example of this type of design is the hydraulic actuator planned for the SST. This internally redundant actuator, while complex, is simple enough that multiple failure analysis can be performed at the actuator level, without having to consider the remainder of the flight control and hydraulic subsystems.

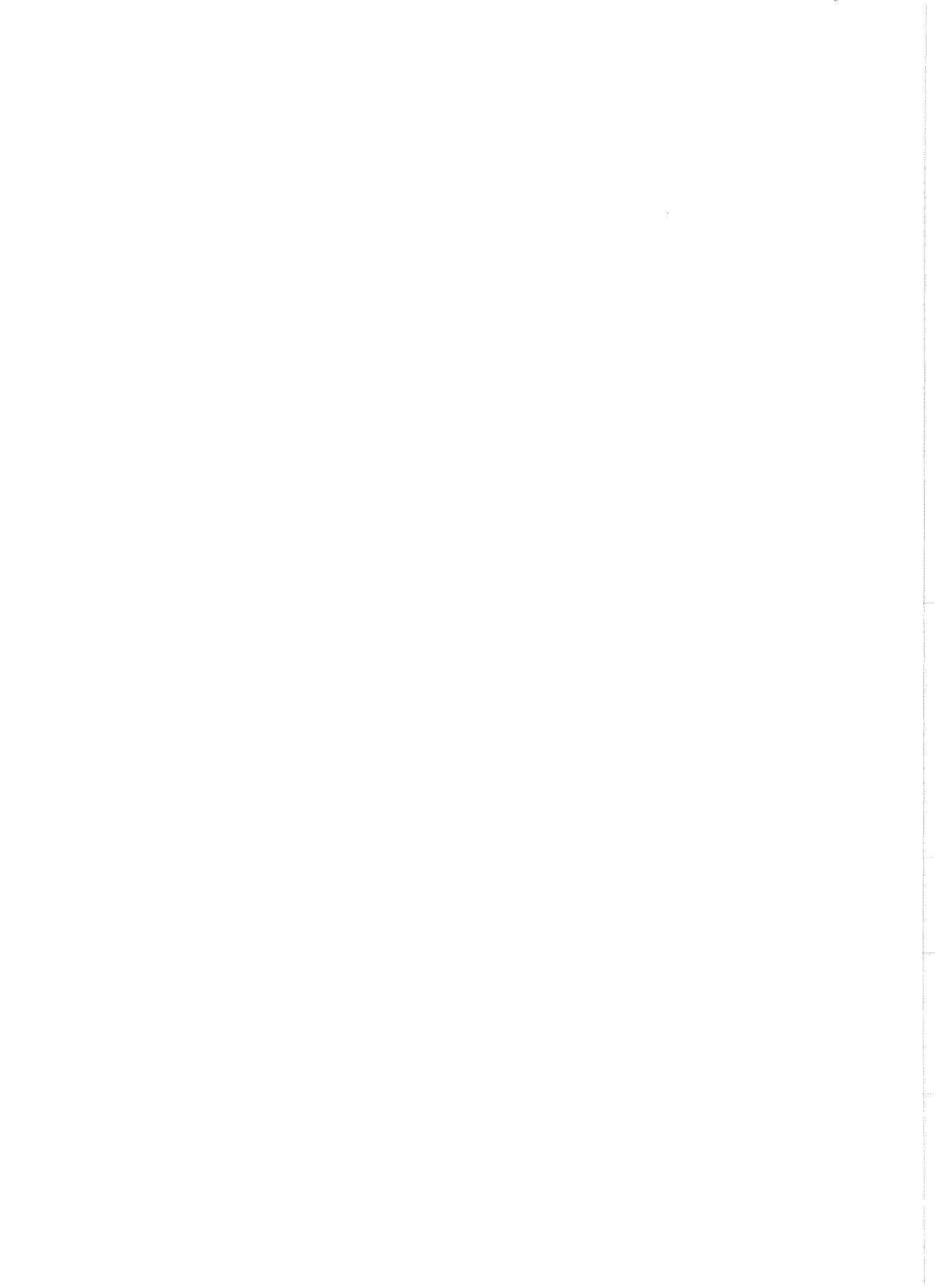
Mere inclusion of multiple redundancy will not achieve shuttle goals and the design process should include a documented analysis that will verify that the system is truly fail operational fail operational fail safe.

The Failure Mode and Effect Analysis (FMEA) process should be extended to analyze failure effects under multiple failure conditions, and to also recognize that the effect of a particular failure is also a function of the system state.

The on-board checkout function, utilized to manage subsystem redundancy, should be designed to recognize multiple failures, and properly assist in any necessary reconfiguration.

RECOMMENDATIONS

- **DESIGN FOR MULTIPLE FAILURE SURVIVABILITY**
- **VERIFY FAIL-OPERATIONAL FAIL-OPERATIONAL FAIL-SAFE BY ANALYSIS IN DESIGN PROCESS**
- **PERFORM FMEA THAT CONSIDER NOT ONLY MULTIPLE FAILURES, BUT STATE OF SYSTEM AT TIME OF FAILURE**
- **ONBOARD CHECKOUT MUST BE ABLE TO COPE WITH MULTIPLE FAILURES**



N70-40960

EXPERIENCE WITH UNPOWERED TERMINAL-
AREA INSTRUMENT APPROACHES

B. Lyle Schofield

Air Force Flight Test Center

and

Harold G. Gadsick and Shu W. Gee

NASA Flight Research Center
Edwards, California

INTRODUCTION

The return of a manned space shuttle to a predetermined runway will require a terminal-area guidance technique for an instrument approach and landing. The technique is dictated by the requirement that the terminal maneuvers be made with power off. This requirement exists when engine start after entry cannot be accomplished and because it would be beneficial from the standpoint of weight saving to eliminate the approach propulsion and fuel requirements. The need for a power-off precision instrument approach had not existed in the past, and, therefore, no guidance system has been developed.

The operational feasibility of conducting power-off approaches after entry into the earth's atmosphere has been demonstrated by the X-15 program, and the feasibility of power-off approaches with low lift-to-drag ratio (L/D) configurations has been further demonstrated by the M-2, HL-10, and X-24A lifting bodies. However, these power-off approaches have all been demonstrated under visual flight rules. Some of the proposed shuttle vehicle configurations are low L/D vehicles that will approach and land much like the X-15 airplane or lifting body vehicles.

The first part of this paper will discuss a terminal-area guidance technique recently developed by the Air Force Flight Test Center around the F-111A inertial navigation system. The results of flying under instrument flight rules using this guidance scheme will be reported as will the results of ground controlled approaches (GCA) using an NB-52B airplane in an unpowered, low L/D configuration. The latter portion of this paper will discuss a circular approach guidance scheme under development at the NASA Flight Research Center.

PRECEDING PAGE BLANK NOT FILMED.

The F-111A airplane with its variable wing sweep and relatively large variation in gross weight made it possible to investigate the flight characteristics for a range of low lift-drag ratios and planform loadings (fig. 1). The 72.5° wing sweep configuration with gear retracted (clean) was representative of a reentry vehicle with a high fineness ratio. The maximum L/D was relatively high (6.0), and the speeds associated with the L/D were also high (288 knots at 45 lb/ft² planform loading and 349 knots at 66 lb/ft², the highest planform loading tested in this configuration).

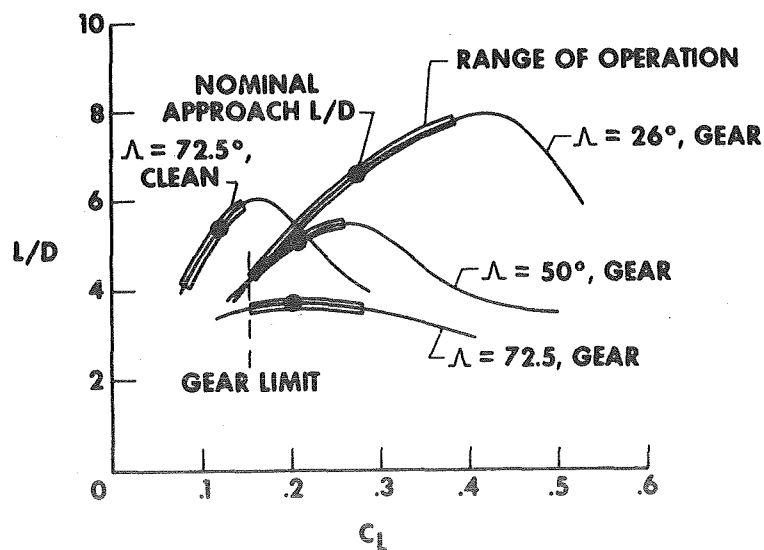
The 72.5° wing sweep and gear-extended configuration provided a maximum L/D of 3.7, which was representative of the lifting bodies now under flight test (HL-10 and X-24A). The F-111A gear limit speed of 295 knots prevented operation on the steep front side of the L/D curve where the lifting bodies operate during their landing approach. As can be seen in the figure, this restricted L/D variation and consequently vehicle ranging.

From the standpoint of maximum L/D, the 50° wing sweep, gear-down configuration was representative of many configurations proposed for the space shuttle except that the peak L/D occurred at a somewhat higher speed (lower lift coefficient) than for the space shuttle configurations. At 45 lb/ft² planform loading, the F-111A maximum L/D speed was 226 knots and the space shuttle speeds are approximately 175 knots.

The F-111A 26° wing sweep, gear-down configuration has an L/D range which covers the maximum performance which might be anticipated for reentry configurations.

Labeled on each curve is a "nominal approach L/D" which was used in defining ILS approach patterns. The nominal L/D was selected to provide a moderately high L/D for the particular configuration as well as to provide for variations in L/D and speed while staying within the constraints imposed by the gear limit speed. Operation on the front side of the L/D curves was found to be important in the control of ILS approaches. The cues to the pilot in correcting to glide slope were in the proper direction; that is, if the aircraft was below the glide slope, he pulled the nose up which increased the angle of attack (and lift coefficient) and provided a higher L/D and a shallower flight-path angle. When the shallower flight path intersected the desired glide slope, the pilot pushed the nose down to maintain the glide slope, and the speed began increasing to the desired value.

SUBSONIC F-111A LOW L/D PERFORMANCE



The onboard F-111A inertial navigation system provided the capability to generate any desired glide slope to any preselected site below 10,000 feet altitude. The pilot was presented with distance, bearing, glide slope, and course deviation information to the preselected site. Additionally, a sensitive radar altimeter provided the pilot with accurate height information for flare initiation. Using this onboard equipment, a navigational and terminal-area energy-management scheme was developed to investigate approaches of the ILS type for unpowered, low L/D configurations. A model of this scheme is shown in figure 2.

The approach technique can be broken down into the following four phases, with a transition maneuver between each phase:

Energy dissipation - deceleration and descent at a constant radius around point A down to the initial approach altitude (similar to traversing the surface of a cylinder)

Initial approach - constant airspeed, straight descent toward point B for the turn to final approach (similar to traversing the surface of a cone)

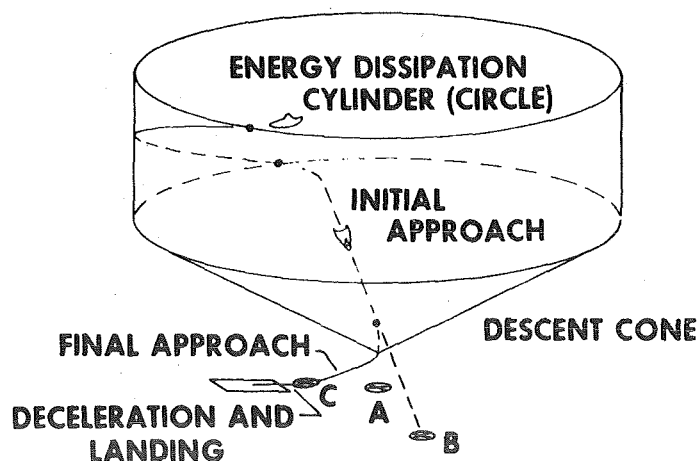
Final approach - constant airspeed descent on the runway heading toward point C down to flare altitude

Deceleration and landing - deceleration on a very shallow glide slope to touchdown

The only assumption made in the implementation of this scheme was that a reentry guidance scheme would be capable of guiding the pilot to intersect the energy dissipation cylinder at speeds greater than Mach 0.85 and less than about Mach 2.0.

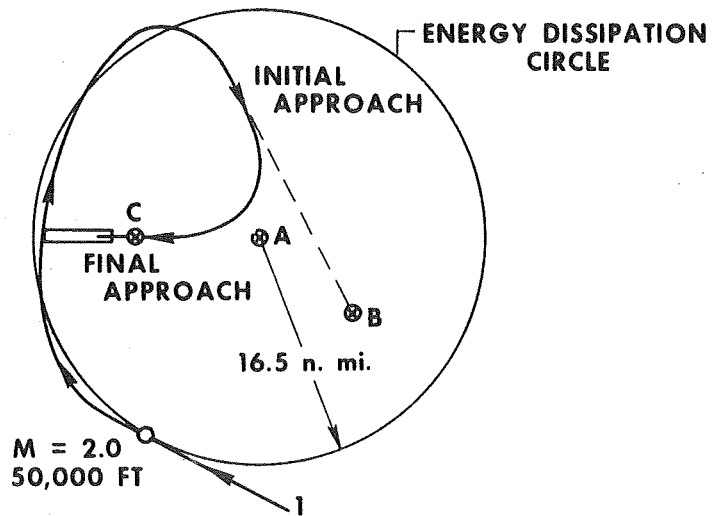
A number of these approach maneuvers were performed starting at Mach 2.0 and 50,000 feet altitude. A supersonic configuration of 72.5° wing sweep, gear retracted (clean) was used down to Mach 0.85 where the airplane was reconfigured to 50° wing sweep, gear down, the configuration most representative of space shuttle configurations.

MODEL OF ILS APPROACH TECHNIQUE



At the start of the approach maneuver, the center coordinates (A, fig. 3) of the energy dissipation circle were selected so that the inertial distance measuring equipment (DME) presented the distance or radius to the center. As the aircraft slowed and descended, the bank angle was reduced and modulated to maintain the 16.5-nautical-mile turn radius. When a predetermined turn-in altitude of 34,000 feet and an indicated airspeed of 285 knots were reached, the gear was lowered and the wings were swept to establish the 50° wing sweep, subsonic L/D configuration. An initial approach radial was determined at that time, and the coordinates and glide slope for the radial aim point (B) were inserted into the inertial system.

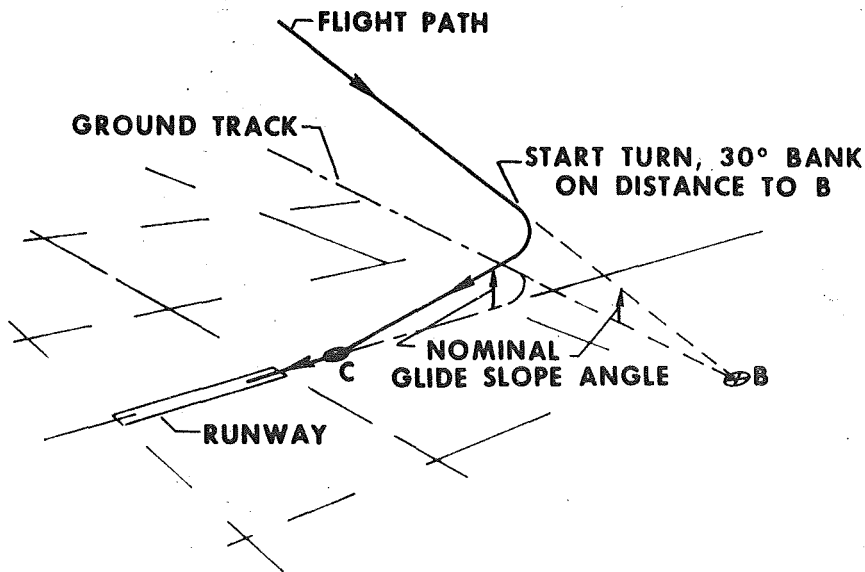
ILS APPROACH TECHNIQUE PLAN VIEW



During the initial approach phase (fig. 4), the pilot modulated airspeed and bank angle to center the glide slope and course deviation displays while monitoring the DME, which presented the distance to the glide slope aim point (B).

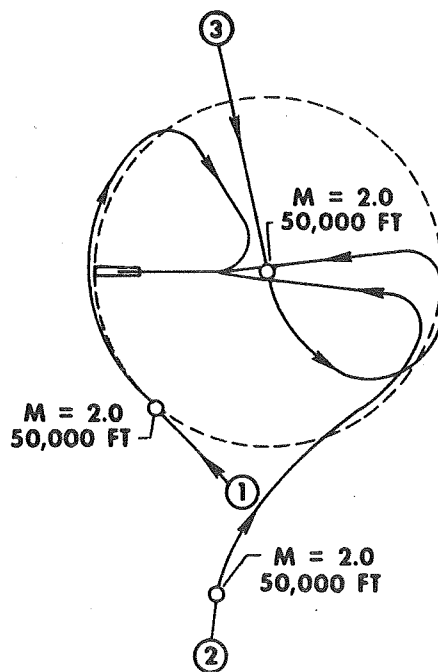
Very little attention to speed and altitude was required. The altitude was determined by the glide slope, and when on glide slope the airspeed tended to stabilize at the proper speed. When the precomputed turn distance appeared in the DME display, the pilot started a 30° bank to final approach while maintaining airspeed. During the turn, the final approach aim-point (C) coordinates were selected. The airplane was rolled out of the turn on the final runway heading, and the pilot's attention was returned to the glide slope and course deviation displays. These displays were centered during the final approach while the pilot monitored the radar altimeter. As the radar altitude reached the proper flare height above the runway, the pilot reverted to visual flight by removing the hood and initiated the flare. Because of ground clearance and tire speed limits of the F-111A airplane, the wings were moved to 26° sweep between start of flare and touchdown.

INITIAL AND FINAL APPROACH PHASES



In addition to the terminal-area energy-management maneuver, two other methods of intersecting the energy dissipation circle were demonstrated (fig. 5). These two methods were based on headings directly toward the center of the circle at the time power was cut (Mach 2.0 and 50,000 feet altitude). In one instance, the power was cut 30 nautical miles from the center and the pilot turned the airplane to intersect the energy dissipation circle tangentially (approach 2). In the other instance (approach 3), the power was cut directly over the center of the circle and the pilot banked the airplane to intersect the energy dissipation circle from the inside. The energy dissipation circle constitutes, in essence, a landing approach window of 33 nautical miles in diameter, because the approach can be made from any direction to intercept the dissipation circle. A Mach range from 0.85 to 2.0 for interception of the landing approach window between 34,000 and 50,000 feet altitude was demonstrated during the program. Approaches 2 and 3 were representative of the kind of positioning that would be available from a very simple reentry guidance system such as the guidance scheme used in the Precision Recovery Including Maneuvering Entry (PRIME-SV-5D configuration) program. It should be pointed out that these two approaches were performed under the hood. All three of these ground tracks are actual test results.

THREE TYPES OF HIGH-ENERGY APPROACHES



Four pilots flew more than 50 approaches (mostly hooded) using the range of lift-drag ratios and the configurations shown in figure 1. Of these, nine were started at about Mach 2.0 and 50,000 feet altitude and five of the nine were performed hooded down to flare initiation.

Of the pilots who participated in the F-111A low L/D evaluation, two were experienced lifting body pilots and the other two were Air Force test pilots assigned to the F-111A Test Force. All pilots performed hooded approaches of the ILS type in the four configurations. The approach conditions flown are summarized in figure 6. The lowest start-flare/hood-removal altitude (200 feet) was with the 26°, gear-down configuration which provided the highest L/D at the start of flare (6.6), the lowest approach glide slope and airspeed, and the largest L/D variation for flare (6.6 to 8.0). The highest start-flare/hood-removal altitude (800 feet) was associated with the 72.5°, gear-down configuration which exhibited the highest approach glide slope (lowest approach L/D) and essentially no L/D variation availability during flare. Hood removal altitudes were selected from tests which showed that the pilot could descend hooded to flare altitude, remove the hood, and perform a comfortable flare.

The major conclusion from the low L/D, simulated IFR test was that it was possible to consistently make hooded approaches from Mach 2.0 and 50,000 feet altitude down to flare initiation. Further, these maneuvers were performed by four different pilots, two of whom attempted and performed the maneuver from Mach 2.0 only once. The pilots considered the flying task for this type of ILS approach to be less demanding than that associated with normal, low speed, powered ILS approaches because:

- (1) The higher approach speed associated with low L/D approaches provided significantly better handling qualities than provided by low-speed powered approaches.
- (2) Approaching at the higher speeds provided sufficiently large stall margins that the pilot was not concerned with speed changes associated with flight-path control.
- (3) Operation on the speed stable (front) side of the L/D curve allowed the pilot to make corrections to glide slope with pitch changes only rather than a combination of power and pitch change which is required for the conventional, low-speed ILS approach.

REPRESENTATIVE F-111A UNPOWERED, L/D APPROACH CONDITIONS

NOMINAL L/D	CONFIGURATION	APPROACH		START FLARE/HOOD REMOVAL ALTITUDE, FT ABOVE GROUND LEVEL
		GLIDE SLOPE ANGLE, DEG	AIRSPED, KNOTS	
6.6	$\Lambda = 26^\circ$, GEAR DOWN	8.1	250	200
5.0	$\Lambda = 50^\circ$, GEAR DOWN	10.1	285	450
3.7	$\Lambda = 72.5^\circ$, GEAR DOWN	13.6	270	800
5.3	$\Lambda = 72.5^\circ$, CLEAN	8.6	410	450

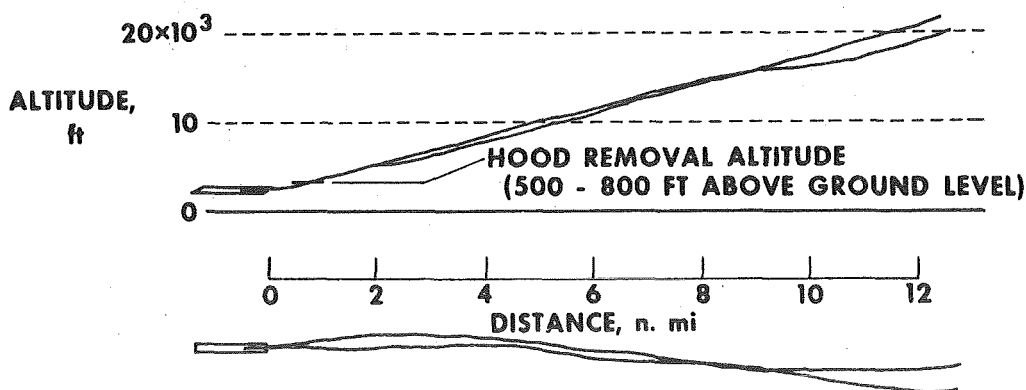
Hooded ground controlled approaches (GCA) were conducted with the NB-52B airplane in a configuration of idle power, landing gear extended, and airbrakes fully deployed. This provided approach lift-drag ratios from 3.2 to 4.4. Straight-in approaches were flown from about 16,000 feet above ground level (AGL) through flare to touchdown (fig. 7). The approach airspeeds for these maneuvers varied from 230 to 250 knots indicated, and the flare initiation altitudes were from 500 to 800 feet AGL.

The Flight Research Center precision radar was used by a flight-test engineer to provide glide slope corrections to the pilot. Course steering information was provided to the hooded pilot by the non-hooded safety pilot through visual contact with the runway.

Three pilots participated in this portion of the evaluation, with the resulting conclusion that the piloting task associated with this maneuver was no more demanding than for normal powered GCA approaches. The piloting task was less demanding because the airplane was being flown in the speed stable region, which required no throttling, and the handling qualities were better at the higher approach speeds. However, because of the lack of vertical speed indications (the rate-of-climb meter was pegged throughout the approach), it was necessary to use pitch attitude alone to make corrections to the glide slope. This was a somewhat more difficult task than using pitch attitude and vertical speed for corrections to glide slope in a normal GCA. As a result, the overall task was about as demanding as a normal, powered GCA approach. The addition of trend indicators such as vertical speed would undoubtedly improve the pilots rating of the unpowered GCA approach.

It should be noted here that ILS approaches as accomplished with the F-111A evaluation were easier than the GCA approaches, because trend information was available to the F-111A pilot through monitoring the glide slope and centerline displays, but only position information with some delayed trend information was available using ground control procedures.

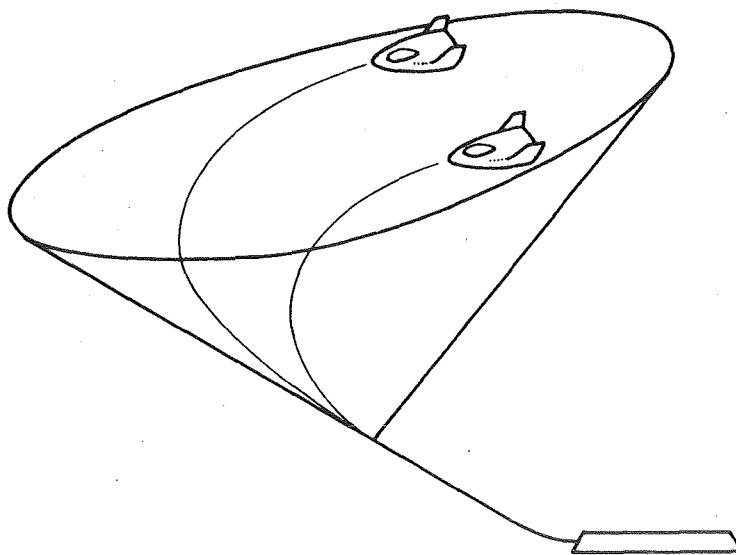
NB-52B GCA APPROACHES



The results of the flight tests with the F-111A and NB-52B airplanes have demonstrated that IFR power-off approaches from high altitudes are feasible. The avionic systems used in these flight studies were not designed for these operations, and therefore a relatively high workload was required of the co-pilot or ground controller. To improve the system, a terminal-area guidance scheme is being investigated to provide the avionics for a power-off, fully IFR, circular approach capability. The guidance scheme is tailored to the aerodynamic characteristics of a lifting body vehicle, because the lifting body is representative of one of the possible manned space shuttle configurations.

Figure 8 is a general representation of the circular approach scheme. A somewhat conic surface, based on the aerodynamic characteristics of a vehicle, is generated for various bank angles and a given approach speed and stored in a computer. The location of the aircraft in space is compared with the location of the conic surface, and the error signal is fed to a flight-director type of display system for the pilot. When the vehicle is on the conic surface, the result is a steady-state flight condition (constant bank and constant airspeed) in a curved path that will arrive at the apex in the direction of the runway. The apex is considered to be at an outer marker or a point that coincides with the ILS localizer and glide slope beams. The conic surface resembles a tilted cone but is a distorted figure to allow for turn radius and true airspeed variations that occur during descending flight on a standard day.

GUIDANCE SCHEME



The conic surface of figure 8 was generated by assembling a number of simulated flight profiles of a lifting body at constant bank and constant speed. Figure 9 shows only four such profiles for a left turn system. Each path represents a flight from 50,000 feet altitude to ground elevation. By positioning these paths to a common end point and direction, a set of nominal solutions was formed. The set contains an infinite number of solutions for bank angles from 0° to 40°. The 220° heading at the end point is arbitrary and was chosen because it is the heading of a runway at Edwards Air Force Base. For a right turn system, a mirror image set of nominal solutions must be generated.

SET OF LEFT TURN SOLUTIONS

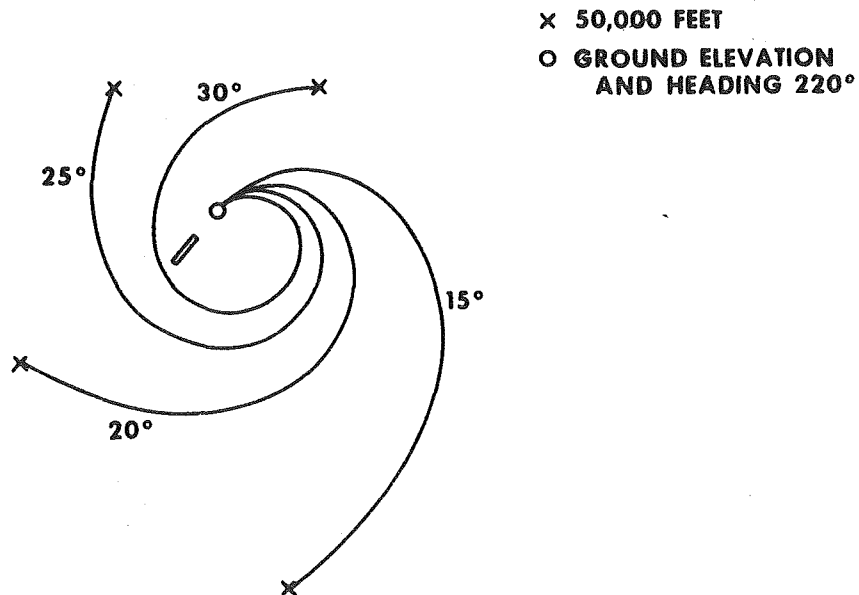


Figure 10 shows the terminal-area circular approach guidance laws that are being investigated; HG_c is heading command and GS_c is glide slope command. In the heading command equation, the actual aircraft heading $HG_{a/c}$ is compared with a desired heading HG_d to form an error signal. The desired heading HG_d is a function generated from the headings of the nominal solutions and is stored in a computer. The energy term contains elevation error ΔEL , which is potential energy, and airspeed error $\Delta A/S$, which is kinetic energy. When the energy level is above a desired level, the error signal causes a heading command away from the apex of the conical surface, thus increasing the flight-path length to dissipate the excess energy. When the command is satisfied, the vehicle will eventually reach a nominal solution. The variable coefficients C_x and C_y are sized to give a desirable convergence to the nominal solutions. The glide slope command GS_c is mechanized in much the same way as the heading command. By displaying heading command and glide slope command on the crosspointers of a flight director display, the pilot has his choice of techniques for satisfying the commands. To limit airspeed variations during flight, the preferred technique would be to satisfy the heading command first and then the glide slope command.

GUIDANCE LAWS

$$HG_c = HG_d - HG_{a/c} + C_x(\Delta EL + 0.001 \Delta A/S)$$

$$GS_c = GS_d - GS_{a/c} + C_y(\Delta EL + 0.0005 \Delta A/S)$$

WHERE

$$\Delta EL = \frac{EL_d - EL_{a/c}}{EL_d}$$

$$\Delta A/S = A/S_d - A/S_{a/c}$$

$HG_d, EL_d =$ STORED CURVES

$A/S_d =$ CONSTANT (260 KNOTS)

$GS_d =$ CONSTANT IN TERMS OF
MODIFIED ALTITUDE $H = f(H_{TRUE})$

$A/S_{a/c} =$ INDICATED AIRSPEED

$$EL_{a/c} = \frac{H}{D}$$

$$GS_{a/c} = \frac{\dot{H}}{V}$$

$HG_{a/c} =$ HEADING

$HG_c, GS_c =$ HEADING AND GLIDE
SLOPE COMMANDS

$C_x, C_y =$ VARIABLE SCALING COEFFICIENTS

A digital program was written to simulate the circular approach guidance system and the flight of a lifting body. The heading and glide slope commands were fed back (through a function that simulates a pilot) to control the vehicle in pitch and roll. Figure 11 shows computed data of the performance of the system. Paths 1, 2, and 3 are nominal solutions starting at 50,000 feet altitude. Paths 4, 5, and 6 are high energy conditions, starting at 60,000 feet altitude. Because of the higher energy in paths 4, 5, and 6, the vehicle turns away from the conical apex to solve the energy problem, which results in a different solution than for paths 1, 2, and 3. The dashed portions of the paths show the convergence to a nominal solution and the path length required to solve the energy problem. The solid portions are when the energy problem is solved. Paths 7, 8, and 9 are low energy conditions which result in shorter paths.

The guidance scheme is designed to provide a minimum of pilot workload, and the commands are compatible with normal visual piloting techniques where the pilot mentally assesses his present situation and applies the best solution from that position. Because the scheme requires the pilot to maintain his position anywhere on the surface, his workload should be less than to maintain his position on a line such as with the ILS system.

STARTS FROM DIFFERENT ALTITUDES

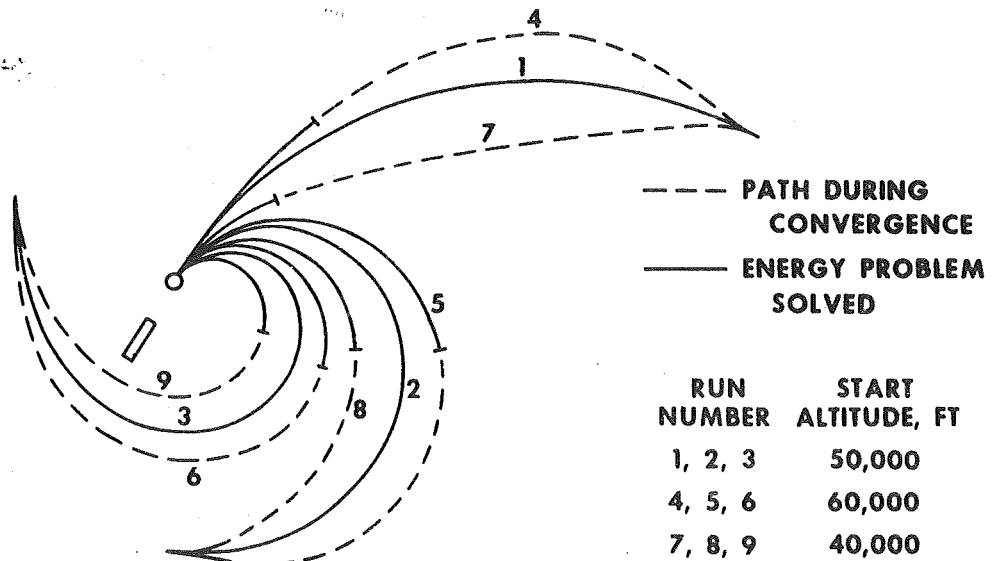
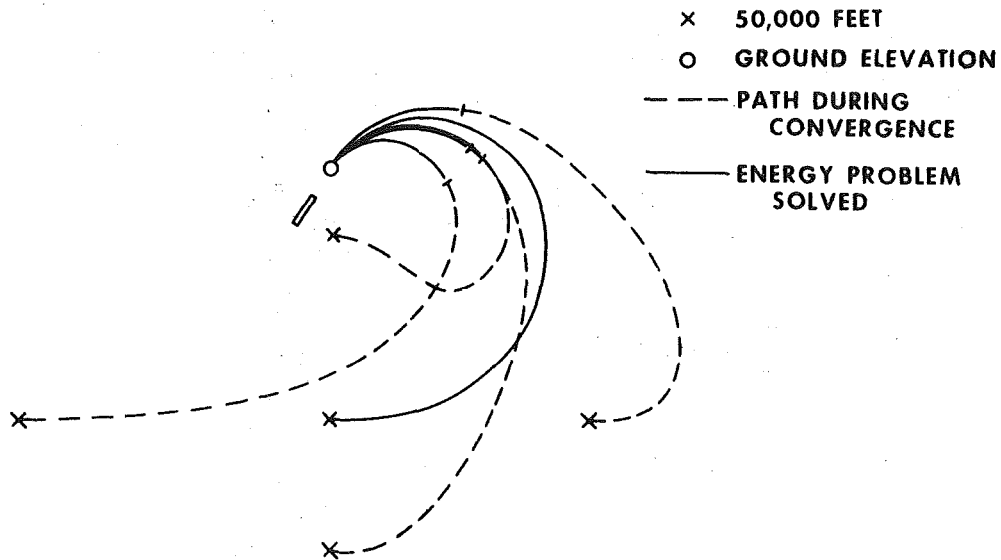


Figure 12 shows another way of looking at the performance of the circular approach guidance system by starting at the same altitude but at different locations with respect to the runway. Although the guidance scheme provides navigation information, it does not determine the operating boundaries of the system. The convergence on a solution is limited by the operating capabilities of the vehicle. For example, at low energy conditions, the vehicle is flown at an angle of attack related to maximum L/D which limits the range of the vehicle when converging to a solution. When a solution is reached simultaneously with reaching the conical apex, the convergence limit is reached. Thus, the operating boundaries for this vehicle are dictated by the practical L/D operating range of the vehicle.

STARTS FROM DIFFERENT LOCATIONS



The circular approach guidance system described is still being studied and requires further simulation with a cockpit and a pilot in the loop. Although this work uses low L/D aerodynamics, it can be applied to high L/D by changing the guidance coefficients. The system may be easier to fly than the conventional ILS because the pilot is required to stay anywhere on the surface as opposed to staying on a line such as the ILS system requires.

The simplicity of the system makes it attractive for a practical application.

The system can be mechanized from VOR, DME, and altitude information for on-board data processing, although the scheme under study uses azimuth and elevation angles from radar inputs.

The guidance scheme is one of many potential solutions for providing a terminal-area, IFR, circular approach guidance system for an unpowered space shuttle vehicle.

GUIDANCE STUDY RESULTS

LOW PILOT WORKLOAD

SIMPLE

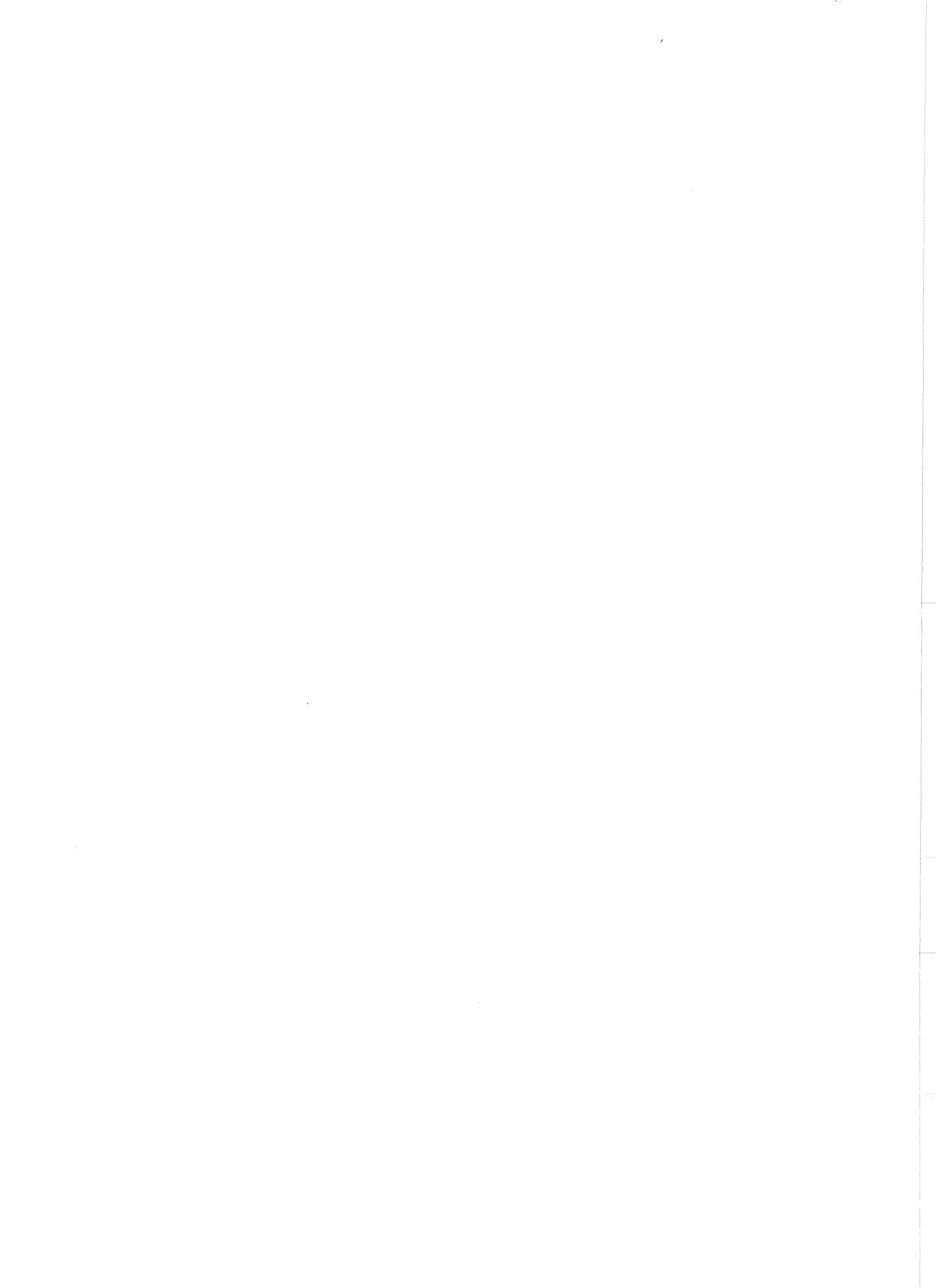
PRACTICAL

POTENTIAL SOLUTION

SUMMARY

Unpowered terminal-area instrument approaches have been the object of recent flight and ground studies at the Air Force Flight Test Center and the NASA Flight Research Center. The results of these studies showed that:

- (1) Power-off IFR approaches were feasible.
- (2) The approaches were conducted on the speed stable side of the L/D curve.
- (3) The pilots considered the flying task to be less demanding than that associated with normal, low speed, powered ILS approaches.
- (4) The higher approach speeds provided significantly better handling qualities than conventional powered approaches.
- (5) A guidance scheme that may provide a power-off, fully IFR, circular approach capability was described.



N70-40961

AUTOMATIC AND MANUAL TERMINAL GUIDANCE AND CONTROL STUDIES

IN SUPPORT OF THE SPACE SHUTTLE PROGRAM

D. W. Smith

NASA-Ames Research Center
Moffett Field, California

INTRODUCTION

Following reentry from orbit, the Space Shuttle Vehicle must be able to perform automatic landings under Category II conditions. In addition, a piloted landing capability is required. Since the SSV will fly and respond much like a large jet transport aircraft during the approach and landing, a significant transfer of jet transport autoland technology is expected. However, the Space Shuttle is in many ways different from large jet transports. For example, the Shuttle will probably have a lower L/D max, may be unpowered in the approach, and may fly subsonically at high angles of attack (up to 60 degrees) for a portion of the approach trajectory. Based on these differences and on results of the recent NASA ILRV studies, it appears that research is necessary to develop a technology base for the design of the terminal guidance and control system for the lifting-entry, horizontal landing Space Shuttle Vehicle. This research should establish the guidance laws and the guidance and control equipment and instrumentation, both airborne and ground-based, necessary to accomplish automatic guidance and control from a "high gate" at 100,000 feet to the ground. The minimum equipment, instrumentation, displays, etc., which are necessary for the pilot to monitor the performance of the automatic system or to assist the pilot to any degree he desires to manually guide and control the vehicle to the landing site should also be defined. To meet the needs of the Space Shuttle project, a supporting research program has been defined, and is being implemented by the Ames Research Center. A brief description of the program objectives, plans, and status follows.

As stated previously, the basic objective of this program is to provide technology for the design of a terminal area navigation, guidance and control system suitable for automatic or piloted landings under Category II conditions. In our studies, we will emphasize an examination of the problems associated with the high cross-range orbiter. However, the low cross-range vehicle will also be examined.

PRECEDING PAGE BLANK NOT FILMED.

An illustration of the problem is presented in figure 1. The Ames' studies will be concerned with that phase of flight which begins at the end of reentry (approximately 100,000 feet and Mach equal 2.5) and extends on through the final approach to flare and touchdown.

The problem initial conditions are set by the "end-of-reentry footprint" which is defined by the accuracy of the reentry navigation guidance and control system. Given a set of initial conditions, the vehicle energy must be managed, and the vehicle precisely controlled so that it is guided to an approach target area from which the final approach is initiated.

The flight control system will include a sophisticated inertial navigator and digital computer. The combination of information from the ground-based navigation aids and the onboard inertial navigation system, using the onboard computer, holds promise of achieving precise navigation and guidance during automatic landings under Cat II conditions. In addition, such a system holds the potential of (1) minimizing the ground-based equipment and, hence, allowing for a wider selection of landing site; and (2) improving system reliability.

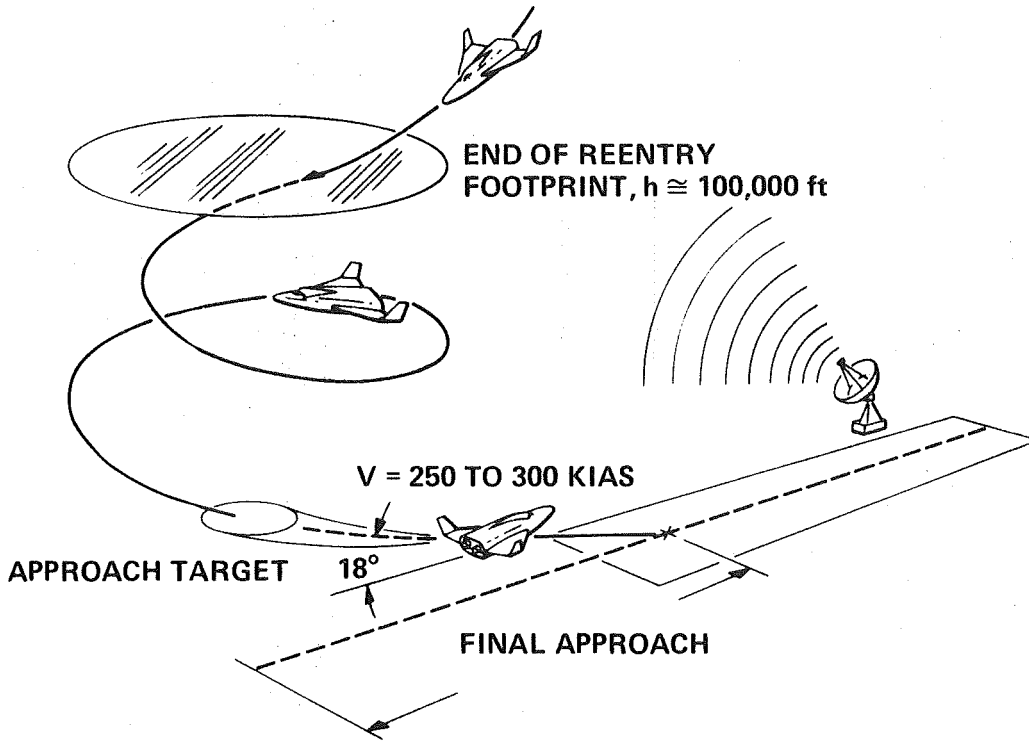
Having achieved the approach target area, the final approach begins. In this flight phase, the vehicle flies along a steep glideslope approaching 18 degrees, with velocities approaching 300 knots.

The landing flare and runway alignment maneuver represents one of the most critical phases in the landing of the Space Shuttle Vehicle (Orbiter). The demands on the automatic flare and runway alignment control system are particularly severe, if the shuttle is an unpowered configuration. The problem is further complicated by gust disturbances, wind shear, instrumentation errors and noise, as well as dispersions in the initial conditions from which the flare is initiated.

An additional point, which should be mentioned, is that even though the Space Shuttle is envisioned to have a highly automated flight control system, a manual control capability is required; therefore, it is necessary for this vehicle to have satisfactory piloted handling qualities. The achievement of satisfactory flying qualities affects vehicle shape, the flight control system, vehicle weight, and flight safety. Thus, the Space Shuttle handling qualities will have a major influence on the Space Shuttle Vehicle program.

The Ames' supporting research and technology effort will be focused on providing practical solutions to these problems and solutions which fit within the guidelines of the Space Shuttle Vehicle program.

LANDING APPROACH • TYPICAL L/D ORBITER



BLENDED INERTIAL/RADIO NAVIGATION. - This task is primarily concerned with the navigation problem, that is, the precise determination of the vehicle state (position, velocity, and attitude). There will be a high-quality inertial navigation system onboard the Space Shuttle Vehicle, as well as an airborne digital computer. On the ground will be various radio navigation aids. The objective of this study is to determine how we can best use navigation measurements from the onboard inertial navigation system combined with signals received from the ground-navigation aids to solve the navigation problem. In other words, we will be concerned with the analysis and simulation of a precision landing system, using a state estimator based on a filter which processes information obtained from the INS and various ground aids. A contract effort for this portion of the program has not been formulated. At the present, the in-house program consists of an experimental flight-test program involving the Ames' Convair 340. A digital computer and certain navigation receivers are in operation onboard the vehicle, and an inertial navigation system is presently being installed. This system will be used to investigate the so-called tri-lateration techniques, and should be flying in approximately a year from the present time.

AUTOMATIC FLARE AND RUNWAY ALIGNMENT SYSTEM STUDIES. - The basic objective of this program is to define automatic flare and runway alignment systems for a candidate Shuttle (Orbiter) configuration. Systems performance for various values of gust disturbance, wind shear, instrumentation errors, and noise assuming various initial conditions will be evaluated. A contract was recently initiated with Bell Aero Space Systems to begin the analysis for the high cross-range orbiter configuration. A parallel program is being initiated at Ames Research Center to investigate this same problem for the low cross-range orbiter configuration.

HANDLING QUALITIES CRITERIA DEFINITION. - The objective of this phase of the program is to analyze and derive generalized handling qualities criteria for the Space Shuttle Vehicle (Orbiter). The first step in this program will be to derive preliminary handling qualities criteria using closed-loop systems analysis techniques and a mathematical model for the pilot. The results from the analytical phase of the investigation will then be refined and validated using fixed-cockpit flight simulation in operation at Ames. A contract was recently initiated with Systems Technology, Inc., Hawthorne, California to begin the investigation of this problem. An in-house study is presently underway at Ames, using a fixed-cockpit simulator to investigate the handling qualities problems associated with the transition from high to low angles of attack during the landing and approach phase of the straight-wing orbiter. As part of this in-house handling qualities program, a study is being initiated to investigate landing and approach performance using various sidarm controllers.

TERMINAL CONTROL AND AUTOMATIC LANDING OF UNPOWERED
SPACE SHUTTLE VEHICLES

Stephen S. Osder

Sperry-Rand
Phoenix, Arizona

SUMMARY

N70-40962

Guidance and control techniques used to accomplish terminal energy management and automatic horizontal landings of unpowered vehicles are described. The concepts discussed were previously used in the X-20 Dynasoar remote recovery system. This system was to acquire the Dynasoar glider at an altitude of about 120,000 feet and provide the guidance and energy management for an automatic landing of an unmanned, single orbit, test flight. The final approach and landing concepts are also similar to the manual techniques used in landing lifting body vehicles in VFR conditions.

The roll of the terminal guidance system is to converge errors associated with reentry guidance and navigation so that the vehicle is brought to a precise position and velocity state at flareout. In the Dynasoar, the convergence capability involved a window of about ± 40 nautical miles cross-range and about ± 20 nautical miles downrange. In candidate shuttlecraft configurations, similar capability is being achieved in simulations. The technique of selecting an equilibrium glide path that permits precise flight path control despite the lack of thrust capability is described. Typical landing trajectories obtained in shuttle vehicle simulations are demonstrated. Finally, the method of achieving the automatically controlled flareout that satisfies terminal vertical velocity, forward velocity, and touchdown position requirements consistent with those of conventional jet transports is described. The flareout technique involves two phases. First, the vehicle is flared to a shallow glide path that allows the

SALIENT VEHICLE CHARACTERISTICS

Two generic classes of vehicles are being studied; the MSC straight wing configuration (optimized for low speed aerodynamic flight) and a high hypersonic L/D, high cross range "delta wing" configuration.

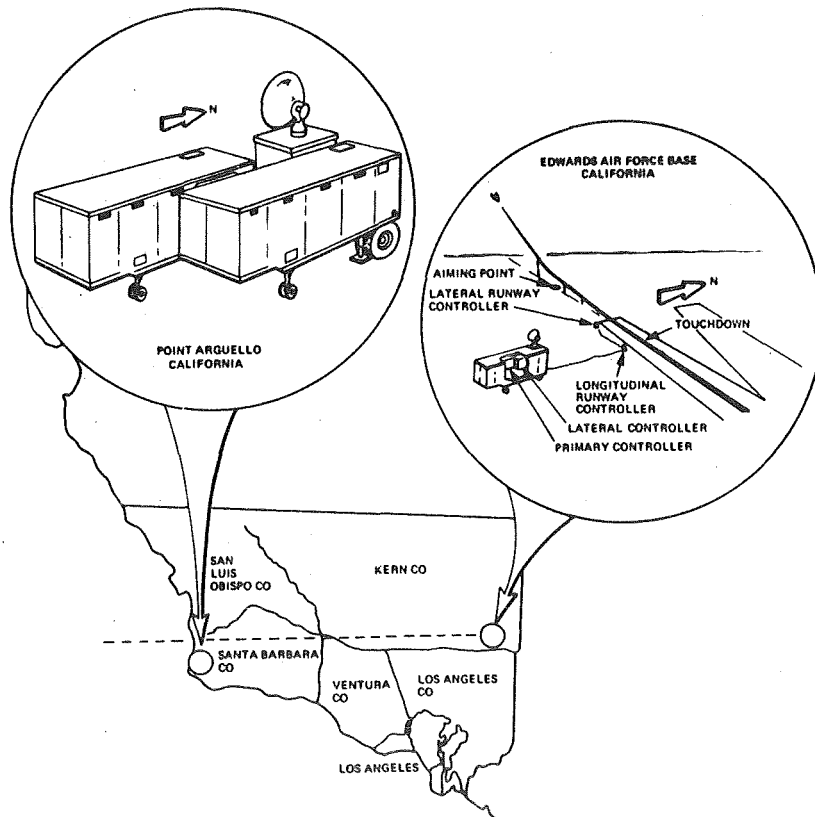
SALIENT VEHICLE CHARACTERISTICS (APPROACH AND LANDING)

VEHICLE CHARACTERISTIC	MSC CONFIGURATION (245 ORBITER)	HIGH CROSS RANGE CONFIGURATION
WEIGHT (POUNDS)	154,000	203,000
LENGTH (FEET)	148	164
I_{xx} (SLUG FT ²)	0.778×10^6	1.6×10^6
I_{yy} (SLUG FT ²)	5.85×10^6	10×10^6
I_{zz} (SLUG FT ²)	5.95×10^6	11.1×10^6
W/S POUNDS/FT ²	83.1	40.0
MAX SUBSONIC L/D	6.83 (NO FLAPS)	4.75 (NO FLAPS)
α FOR MAX L/D	8.5 DEGREES	20 DEGREES

PREVIOUS MECHANIZATIONS OF UNPOWERED LANDING TECHNIQUES

The geographic and functional characteristics of a previous system that performed a similar guidance function are shown. This system, the Remote Control Recovery System (RCRS), was developed to guide an unmanned X-20 (Dynasoar) to an automatic horizontal landing following a "once around" suborbital flight. It employed a steep angle, equilibrium glide path followed by a shallow decelerating glide path which was followed by a final flareout to touchdown. It is essentially an automatic mechanization of the manual techniques used in landing unpowered, low L/D vehicles. In the X-20 system, ground based computations plus a microwave data link were used to generate and transmit steering information. In the shuttlecraft under study all computations are airborne and the reference flight paths are synthesized from combinations of NAVAID, inertial and altimeter information.

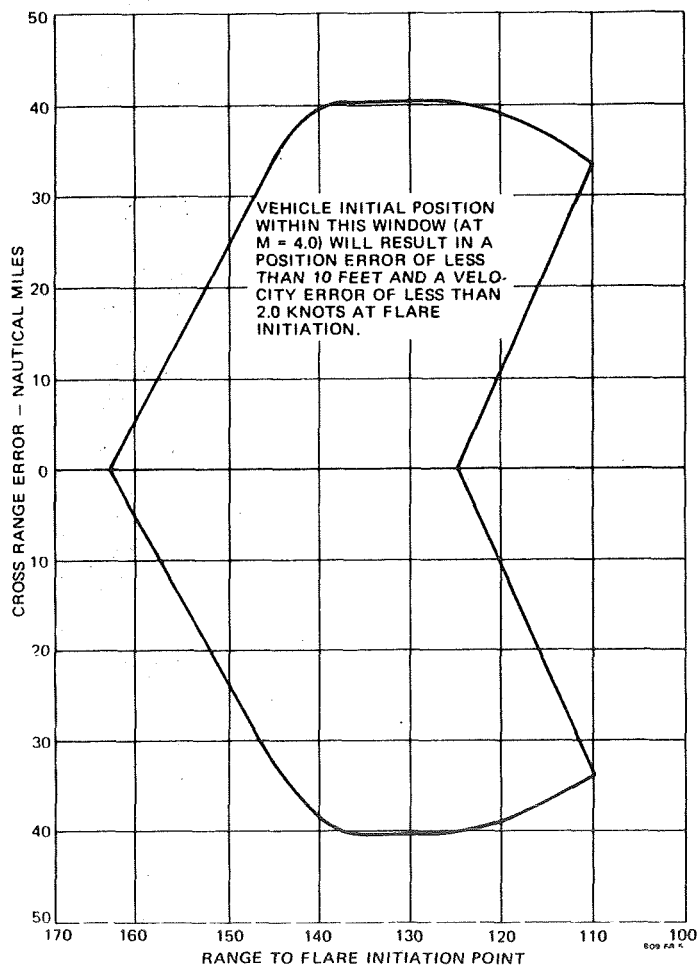
RCRS CONTROL CENTERS GEOGRAPHIC LOCATIONS



TERMINAL AREA RECOVERY WINDOW

The recovery window of the X-20 (Dynasoar) RCRS is shown. If the vehicle reached a velocity of about 4000 ft/sec and fell within this window, the RCRS terminal energy management capability would converge the state vector to within a few feet of the desired lateral and longitudinal alignment at the point of flareout with velocity errors bounded to about ± 2 knots. Similar results are being obtained with the high cross-range shuttle vehicle although the specification of a recovery window is complicated by the need to consider 360 degree approaches to the terminal area.

X-20 DYNASOAR TERMINAL GUIDANCE RECOVERY WINDOW FROM M = 4.0 TERMINAL CONTROL INITIATION

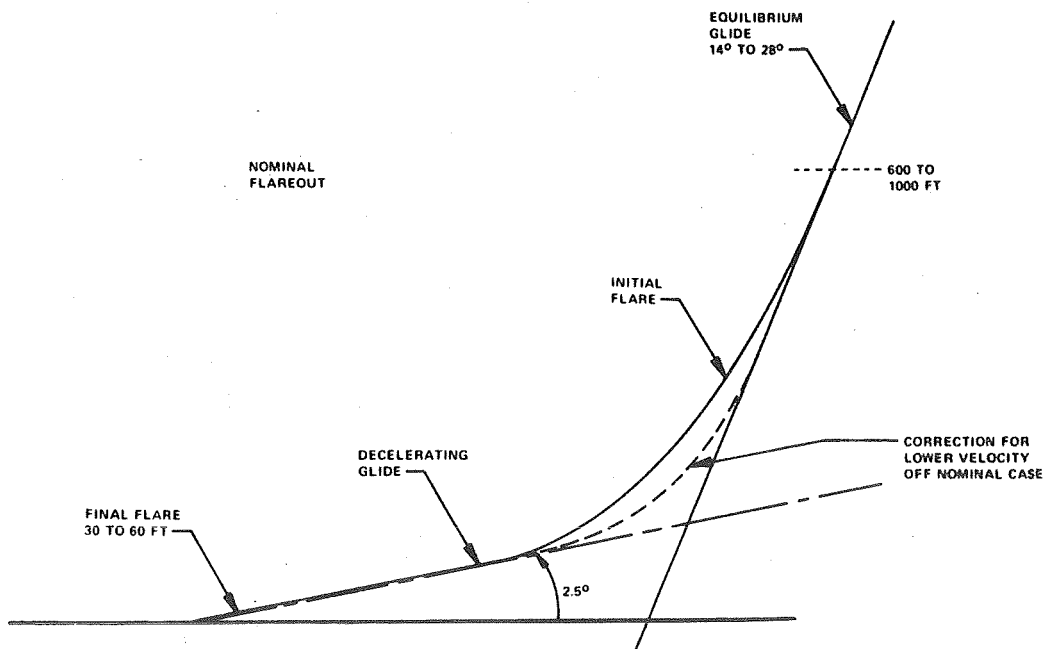


GUIDANCE CONCEPT

The equilibrium glide approach plus the two phase flareout concept is shown. At an altitude between 600 and 1000 feet, the vehicle is flared from the steep equilibrium glide path to the shallow decelerating glide path. When it is constrained to the steep path, its calibrated airspeed converges to a nearly constant value. Flying this path simultaneously satisfies terminal position and velocity constraints. The initiating altitude for the first flare may be made adjustable to cope with off-nominal position and velocity errors.

Flareout to the shallow glide path and holding that path cause a rapid deceleration to more conventional landing speeds. As the final flareout altitude is reached, the vehicle's rate of descent and velocity are compatible with those of a conventional jet transport prior to landing.

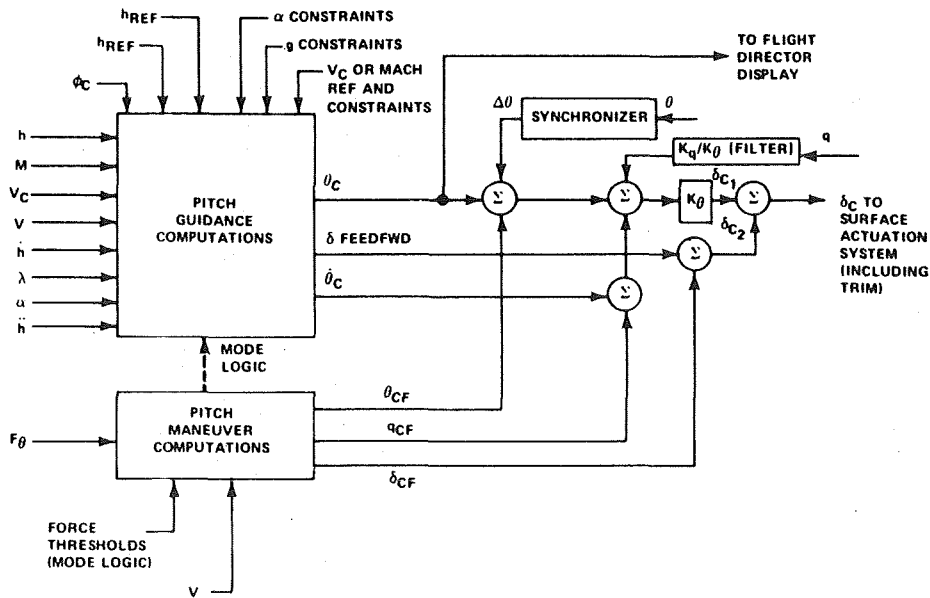
NOMINAL FLAREOUT



GUIDANCE AND CONTROL SYSTEM MECHANIZATION, PITCH

The pitch guidance and control block diagram in general form is shown. A displacement plus integral elevator control law provides pitch attitude stabilization in response to body axis pitch rate and local vertical oriented pitch attitude error. The pitch stabilization system receives both the steering commands based on the guidance computations and the maneuver commands inserted by the pilot for semi-automatic control modes. Guidance inputs are pitch commands with appropriate attitude, attitude rate, and control surface feedforward compensations to minimize errors in the closed loop process. Manual inputs command attitude rate (that is, rate of change of the attitude reference proportional to applied force) with appropriate adjustment of the command sensitivity as a function of velocity.

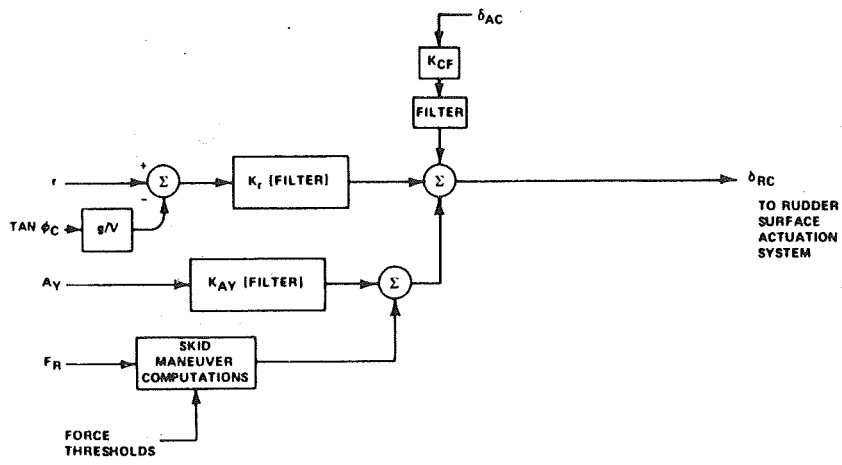
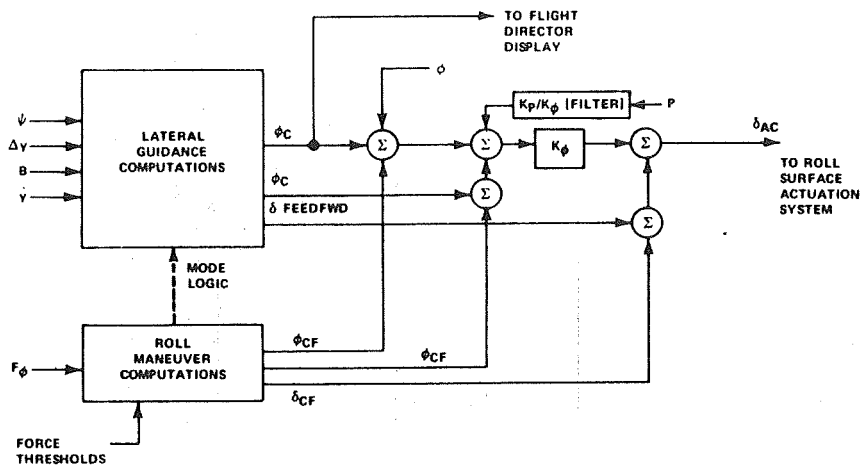
PITCH GUIDANCE AND CONTROL – AUTOMATIC AND AUTO/MANUAL BLOCK DIAGRAM



GUIDANCE AND CONTROL SYSTEM MECHANIZATION, LATERAL-DIRECTIONAL

The lateral-directional guidance and control block diagram is shown in general form. Roll attitude stabilization is provided as a function of body axis roll rate and local vertical oriented roll attitude error. The roll stabilization system receives both the steering commands based on the guidance computations and the maneuver commands inserted by the pilot. As in the case of the pitch system, appropriate feedforward commands are generated to minimize errors in the closed loop process. Manual commands result in roll rates proportional to applied force. The rudder control provides for dutch roll damping (in combination with the roll stabilization system), turn coordinations, and artificial directional stability. Body axis lateral acceleration, roll-yaw crossfeed, and computed turn rate command contribute to the turn coordination capability.

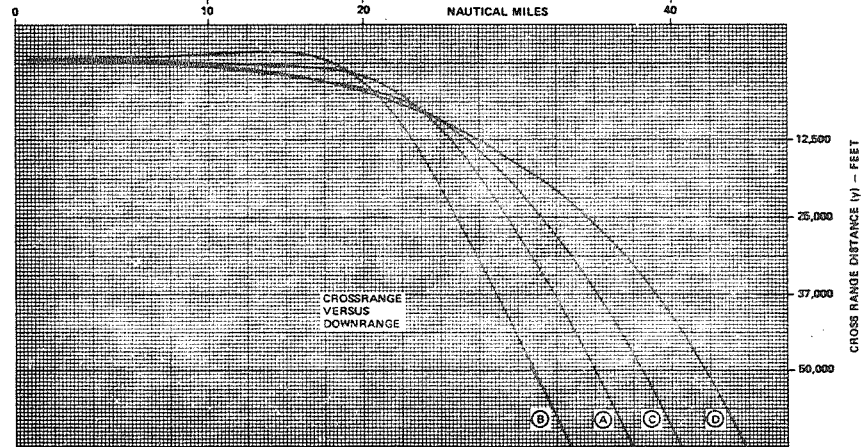
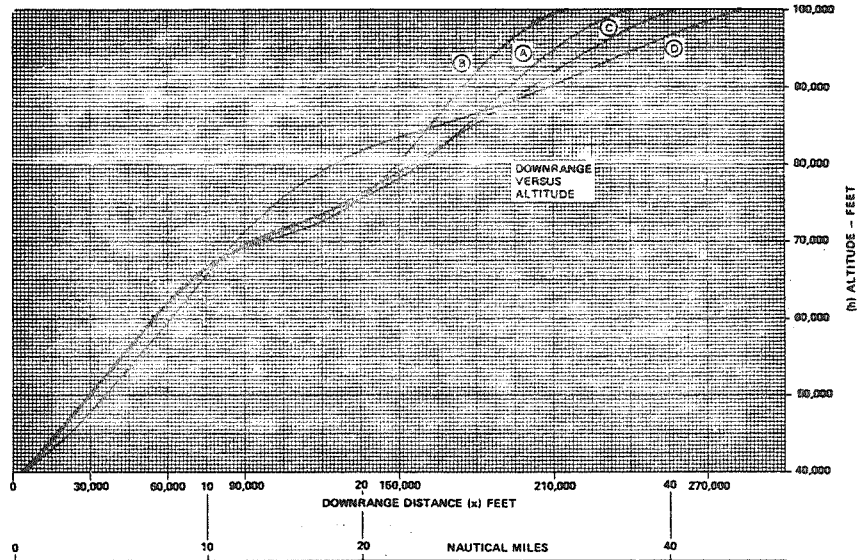
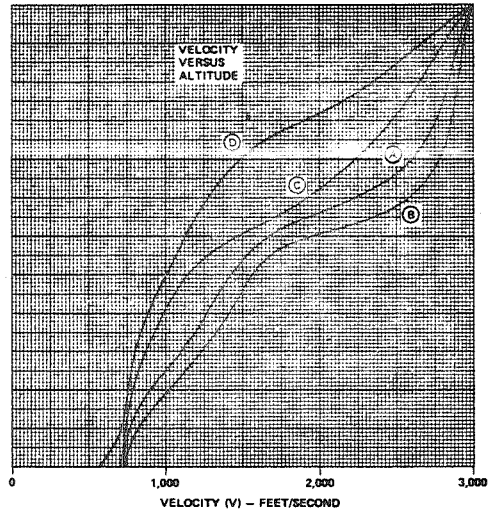
LATERAL-DIRECTIONAL GUIDANCE AND CONTROL AUTO AND AUTO/MANUAL BLOCK DIAGRAM



HIGH ALTITUDE ENERGY MANAGEMENT

Typical trajectories covering the approach to the terminal equilibrium glide path for the high crossrange orbiter are shown. The nominal trajectory (A) starts with a 45 degree intercept angle to the final approach lateral path. It is about 10 NM crossrange from that path and about 40 nautical miles downrange from its desired position at the 40,000 ft altitude. It is at an altitude of about 100,000 feet with a velocity of 3,000 feet/second. The trajectories terminate at an altitude of 40,000 feet where they end with a 20 degree descent angle, ideally aligned with the final approach glide path. Range depletion trajectories and range extension trajectories covering a downrange spread of about 11 nautical miles are shown. Range adjustment is obtained with a guidance law that adjusts angle-of-attack as a function of range error. Maximum Q (dynamic pressure) and α (angle-of-attack) constraints are included in the closed loop guidance law.

TYPICAL TERMINAL AREA ENERGY MANAGEMENT AND GUIDANCE TO FINAL APPROACH PATH - DELTA WING, HIGH CROSSRANGE ORBITER



EQUILIBRIUM GLIDE PATH SELECTION

The equilibrium glide paths for the MSC 245 orbiter are shown for zero flap and full flap cases. For each airspeed one flight path angle exists that permits airspeed to be maintained. Stated in reverse, two quasi-equilibrium airspeeds can result from constraining the flight path angle to a fixed value. If γ is initially below the curve, the vehicle accelerates, moving at constant γ to the right until it intercepts the curve at the equilibrium speed. If γ is initially above the curve, it decelerates until it either intercepts the curve or is no longer capable of aerodynamic flight. The peak of the curve corresponds to the airspeed for maximum L/D. Stable flight path control for unpowered vehicles is possible only for velocities to the right of the peak L/D point.

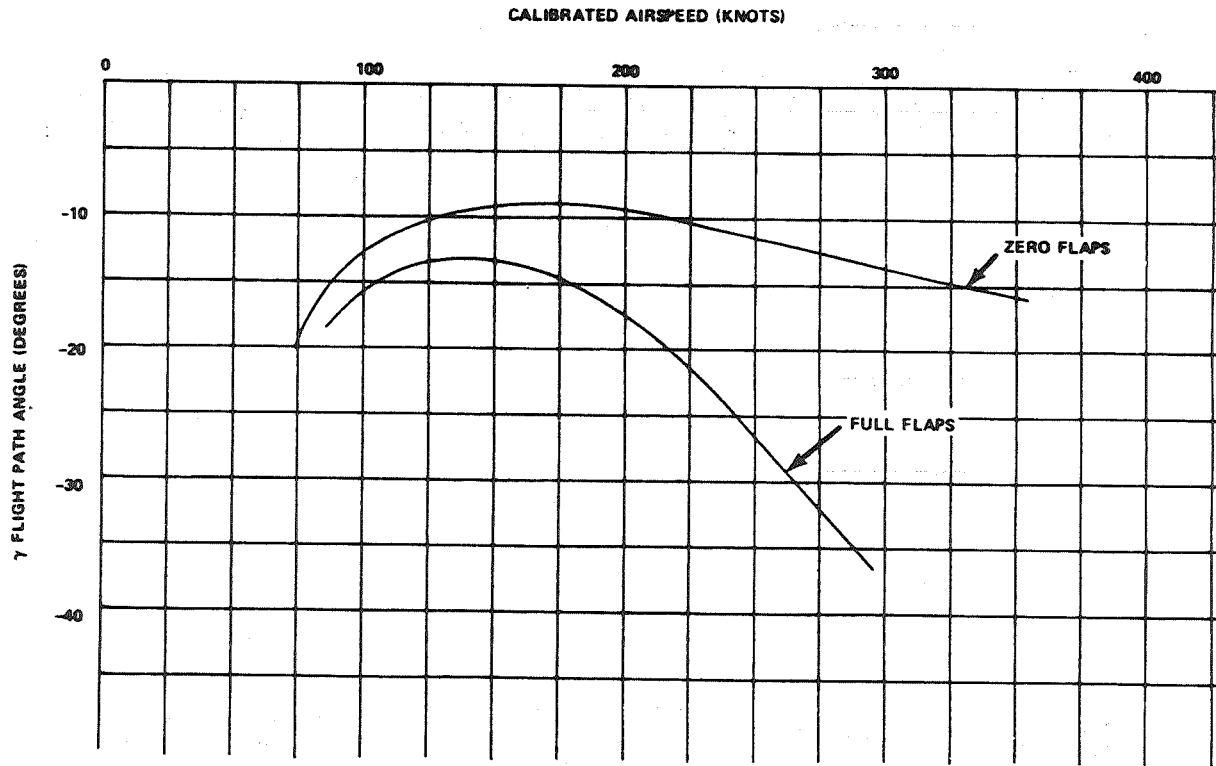
The equilibrium glide equation stated in terms of dynamic pressure, Q and flight path angle γ is

$$\sin^2 \gamma + \frac{Q}{a(W/S)} \sin \gamma - \left(1 + \frac{C_{D_0} Q^2}{a(W/S)^2} \right) = 0$$

where a is the constant of the drag polar

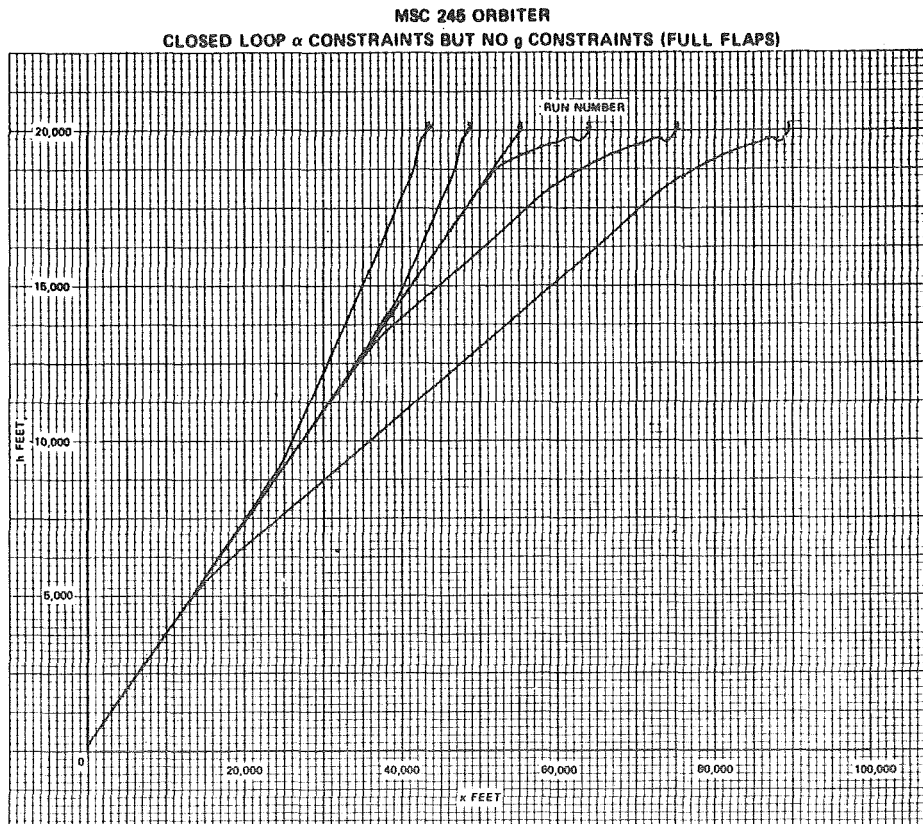
$$C_D = C_{D_0} + aC_L^2$$

CALIBRATED AIRSPEED FOR VARIOUS EQUILIBRIUM GLIDE ANGLES – 245 ORBITER



GLIDE PATH ACQUISITION TRAJECTORIES

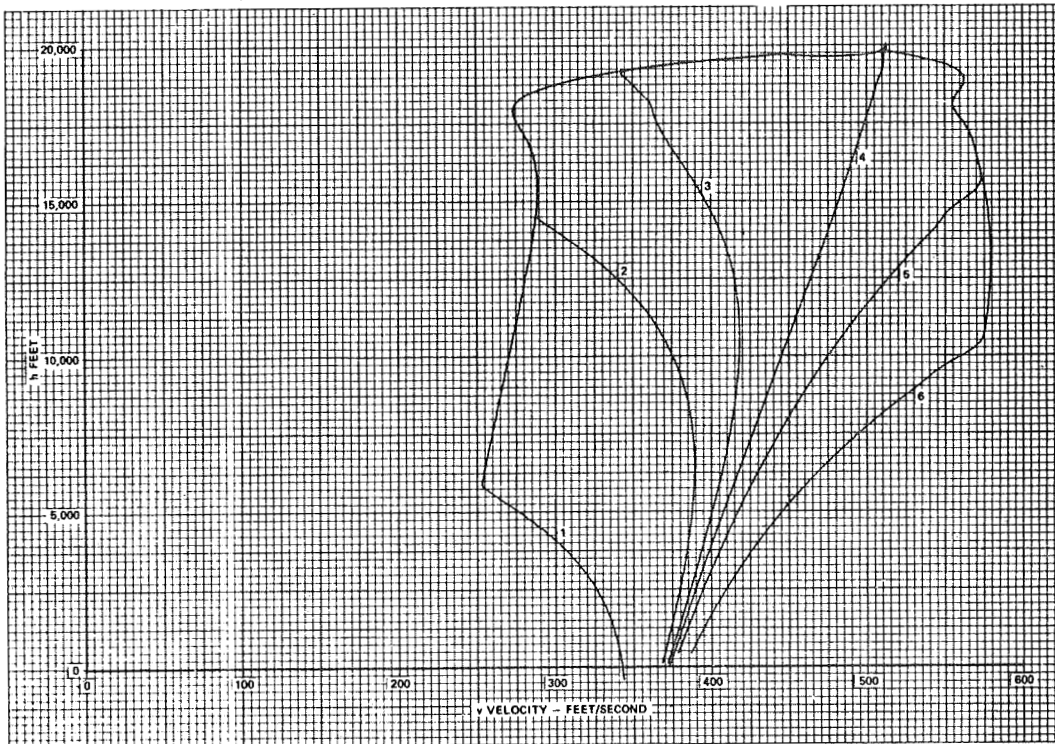
Trajectories for the full flap MSC 245 orbiter configuration acquiring a -20 degree terminal approach glide path are shown. Initial conditions are a 20 degree dive angle and velocities of about 500 feet/second but displacements from the nominal path cover a total spread of about 7.5 nautical miles. The guidance law imposes maximum angle of attack, maximum speed, and maximum and minimum flight path angle constraints through closed loop pitch commands based on the detection of the approach to the constraint boundaries. Acceleration constraints were not imposed; hence, obviously high accelerations (in excess of 3g) occurred during the initial maneuver. Case (1) shows the imposition of an angle of attack constraint that effectively limited the intercept angle to the α corresponding to maximum L/D.



VELOCITY HISTORIES FOR GLIDE PATH ACQUISITIONS

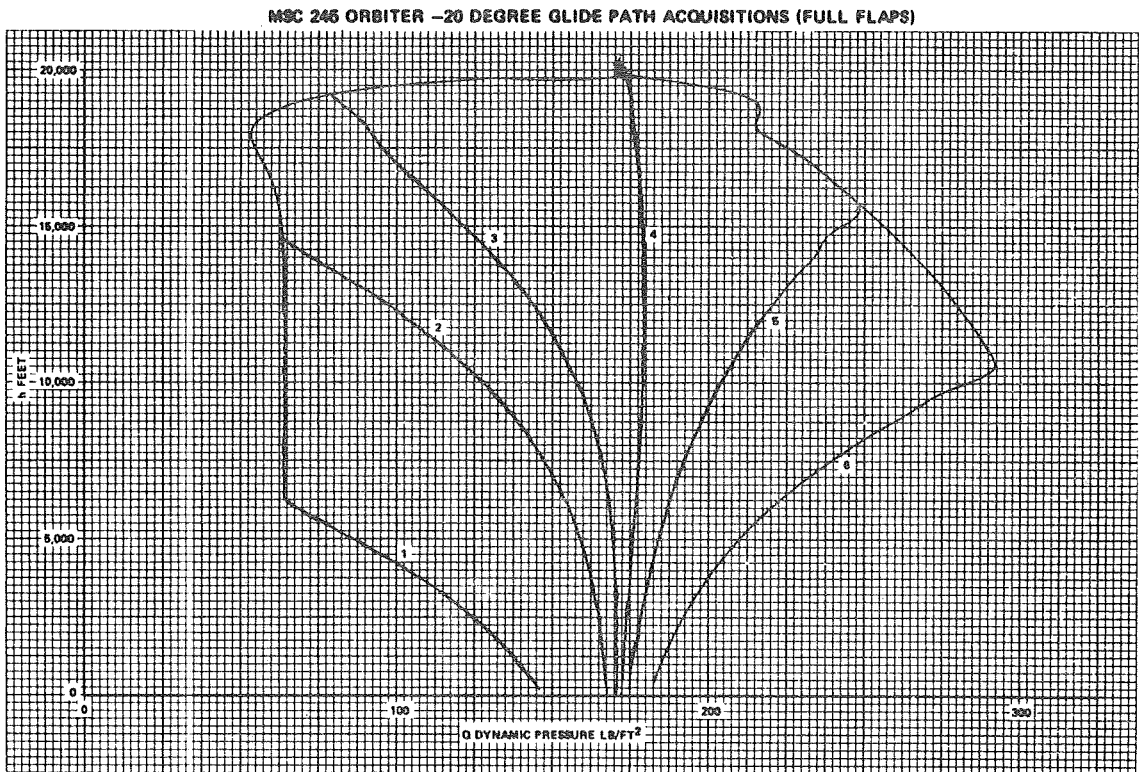
The velocity versus altitude histories for the acquisition trajectories shown previously are also shown here. The nominal velocity is decreasing since calibrated airspeed (or Q) tends to remain constant. After achieving the desired glide path, all trajectories converge toward the nominal case.

MSC 245 ORBITER -20 DEGREE GLIDE PATH ACQUISITIONS (FULL FLAPS)



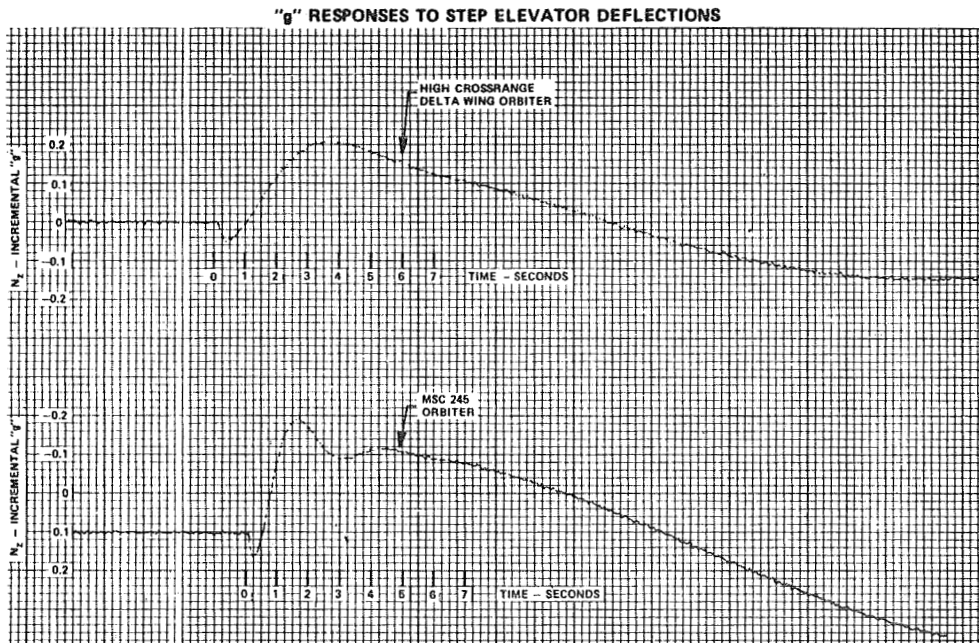
DYNAMIC PRESSURE HISTORIES FOR GLIDE PATH ACQUISITIONS

The large dynamic pressure transients associated with the acquisition trajectories described previously are shown here. The spread of the dynamic pressure variation during these transients is more than 140 percent larger than the nominal dynamic pressure; nevertheless, convergence to the nominal, nearly constant value of Q is rapid following acquisition of the nominal descent path.



VEHICLE NORMAL ACCELERATION RESPONSE CAPABILITY

A tight (or high gain) closed loop flight path control system requires a rapid flight path angle rate capability. Sluggish normal acceleration capability necessitates lower control loop bandwidths and hence lower gain systems. Large shuttlecraft tend to have sluggish acceleration capability primarily because of their size. This problem is also found in large transport aircraft. The g-response at the cg for step elevator deflections in the MSC straight wing configuration and the delta wing high crossrange configuration is shown here. Both responses are for approach and landing conditions with zero flaps. A significant part of the lag in the response results from the initial acceleration reversal caused by the lift of the control surface. In the delta wing vehicle, nearly one second elapses before a positive acceleration occurs. These responses are for the free vehicle and hence the phugoid mode is apparent after several seconds.

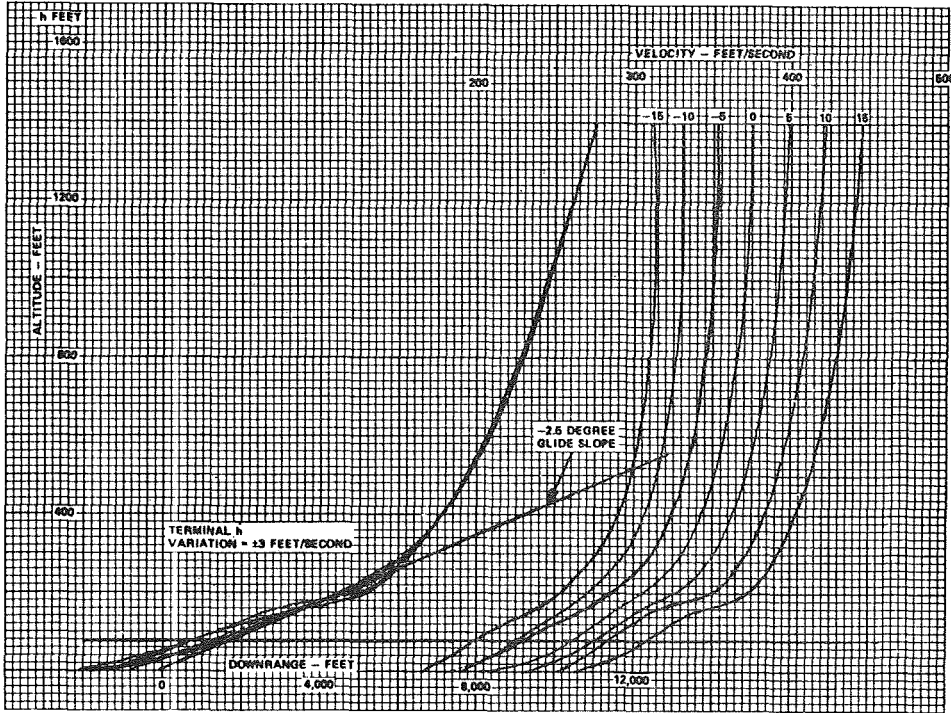


FLAREOUT TRAJECTORIES - STRAIGHT WING CONFIGURATION

WITH FULL FLAPS

Flareout trajectories for the MSC 245 orbiter with full flaps are shown for nominal and ± 15 percent initial velocity errors (in 5 percent increments). These velocity errors could be viewed as the result of a low altitude acquisition of the equilibrium glide path. They are also analogous to large headwinds and tailwinds in their effects on the trajectory. The shallow glide path (2-1/2 degrees) is maintained, in general, for less than a 100 foot altitude duration. The total touchdown dispersion spread was about 1200 feet. The spread of vertical velocities, \dot{h} , at touchdown was about ± 3 feet/second which is considered excessive. A simple h and \dot{h} flareout control law was used for the final flare. A terminal controller that continuously computes accelerations required to satisfy the touchdown \dot{h} constraints should cut this excessive touchdown velocity even for the large range of off nominal errors shown. A modified guidance law that varied the first flare initiating altitude as a function of initial velocity error resulted in a 50 percent reduction in the touchdown \dot{h} dispersion. This law, however, increased runway touchdown dispersion.

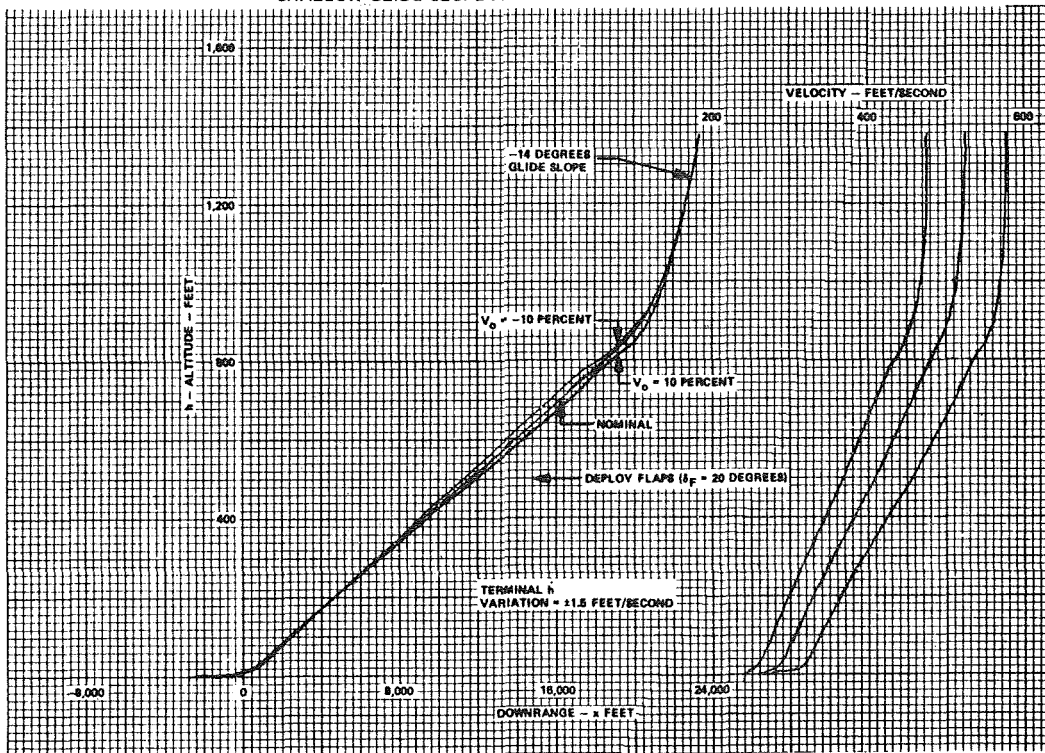
FLAREOUT TRAJECTORIES FOR ±15 PERCENT OFF NOMINAL VELOCITY
INITIAL CONDITIONS
MSC 245 ORBITER
FULL FLAPS
SIMPLE FLAREOUT LAW



FLAREOUT TRAJECTORIES - STRAIGHT WING CONFIGURATION
FLAPS DEPLOYED ON THE SHALLOW GLIDE PATH

Equilibrium glide angles with full flaps are steeper than those with zero flaps. The shallower glide angles with zero flaps require higher velocity. To dissipate the higher velocity, the shallow glide angle can be acquired at higher altitudes and a longer decelerating glide can be maintained on this shallow path. To permit landing at lower velocities, the flaps are deployed while on the shallow glide path. The resultant trajectories for this procedure with nominal and ± 10 percent velocity errors are shown here.

**FLAREOUT TRAJECTORIES, MSC 245 ORBITER
 ZERO FLAP APPROACH WITH 1/2 FLAP DEPLOYMENT DURING EXTENDED
 SHALLOW GLIDE SLOPE PHASE ±10 PERCENT INITIAL VELOCITY ERRORS**



CONCLUSIONS

- The feasibility of performing automatic approaches and successful landings of large, unpowered shuttlecraft can be demonstrated in simulations.
- Despite the fact that the vehicles are unpowered, the final phase of the approach and the final flareout can be made to emulate a conventionally powered jet transport in its final 50 feet of descent to the runway.
- The high cross-range, delta wing (or lifting body) vehicle can readily be brought to a precise position and velocity alignment for flareout if it enters a window at 100,000 feet that is approximately 30 nautical miles cross-range and downrange. The terminal energy management window for the MSC straight-wing configuration is dependent on aerodynamic control capability prior to and during transition. This capability has not yet been determined.

N70-40963

STABILIZATION AND CONTROL OF THE SPACE SHUTTLE ORBITER
DURING ENTRY/PITCHDOWN MANEUVERS

D. Engels, E. Estrine, P. Shipley

North American Rockwell
Downey, California

SUMMARY

Results of recent Shuttle entry flight control studies are discussed with respect to both high and low L/D orbiter vehicles. A pitchdown control system for the low L/D orbiter is synthesized, and typical time histories shown. Effects of variations and uncertainties in aerodynamic parameters on the entry control problem are discussed.

INTRODUCTION

During reentry, a shuttle orbiter vehicle will require a transition from reaction jet control to aerodynamic control surfaces. The exact nature of the blending operation to change from one mode to the other depends on the vehicle configuration and guidance laws.

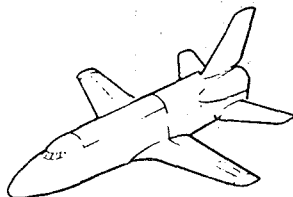
For atmospheric control, attitude control and damping can be performed by either aerodynamic control surfaces or by reaction jets. For some vehicle configurations, aerodynamic control may not be possible because the high angle of attack results in the control surfaces being blanketed by the backwash of the vehicle fuselage. In addition, heating problems must be a consideration. On the other hand, if reaction jet control is used, the vehicle must be trimmed aerodynamically in pitch to the required angle of attack to avoid excessive fuel consumption. Thus, the pitch axis requires only a damper loop, as does the yaw axis if the vehicle also is stable in yaw ($C_{N\dot{\phi}} > 0$). The roll axis requires attitude control to follow the guidance commands, which may be implemented with phase-plane logic. The yaw axis of an unstable vehicle also requires attitude control. If aerodynamic control surfaces are used, attitude control in all three axes is feasible, and the vehicle is capable of accepting commands from a guidance system which modulates both bank angle and L/D for improved performance and reduced heat loading.

If the vehicle has two stable angles of attack (a high angle for entry and a low angle for subsonic cruise and landing), the control mode may be switched from reaction jets to aerodynamic surfaces at the time of the pitchdown maneuver to cruise orientation. On the other hand, if the transition from entry to subsonic cruise is gradual, it may be desirable to blend gradually from reaction jet control to aerodynamic control. For the aerodynamic control loops, conventional linear feedback with gain scheduling appears adequate.

Control systems for two vehicle configurations shown in Slide 2 were studied. The low crossrange orbiter is a winged vehicle with two stable angles of attack; one for entry and the other for low-speed aerodynamic flight. A pitchdown maneuver is required to shift from one stable point to the other. The high crossrange orbiter is a lifting body with only one stable angle of attack.

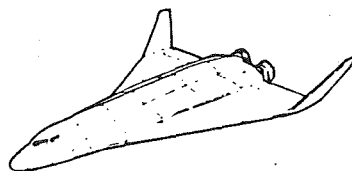
In each case a six-degree-of-freedom digital simulation was performed to verify control system performance.

TPS & STRUCTURE REQUIREMENTS



LOW CROSS RANGE CONFIGURATION

- FACTORS OF SAFETY
 - CREW COMP 2.0
 - STRUCTURE 1.5
 - PROP TANKS 1.5
- HI ANGLE OF ATTACK ENTRY ($\alpha = 60^\circ$)
- HEAT LOAD 15% OF HI CROSS RANGE VALUE
- MAX HEATING ON BOTTOM ONLY



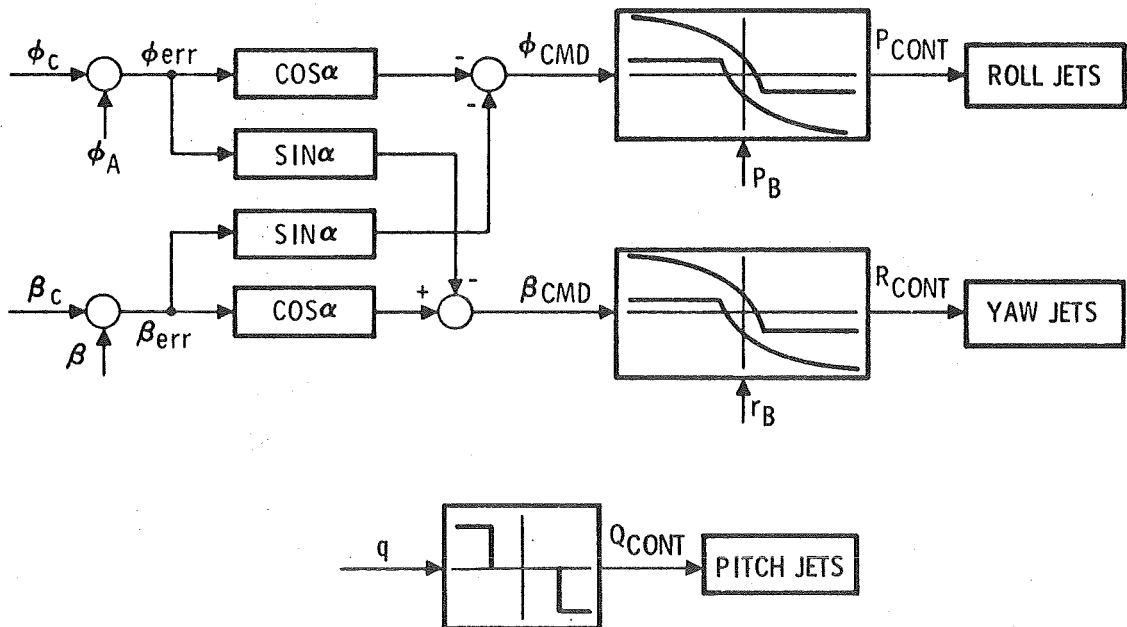
HIGH CROSS RANGE CONFIGURATION

- FACTORS OF SAFETY
 - CREW COMP 2.0
 - STRUCTURE 1.5
 - PROP TANKS 1.5
- VARIABLE ANGLE OF ATTACK ($\alpha = 55^\circ$ TO 10°)
- MAX SURFACE HEATING OVER TOTAL
- THERMAL PROTECTION SYSTEM CRITICAL TO FEASIBILITY
- CAN BE USED FOR HI & LOW ANGLE ENTRY

LOW CROSSRANGE ORBITER CONTROL SYSTEM DESIGN

Regardless of whether reaction jets or aerodynamic surfaces are used to achieve attitude control, some form of turn coordination during roll maneuvers is required to minimize sideslip. Turn coordination is required primarily because the guidance system commands roll maneuvers about the velocity vector (stability x-axis), while the roll actuators provide moments about the body axes. At high angles of attack, this tends to create a large angle of sideslip. The Apollo control system translates roll commands directly into roll body axis commands, but it achieves turn coordination by feeding roll rate into the yaw damper through a gain which depends on angle of attack. An alternative method used in this study is to replace the yaw damper turn coordination loop with a cross-coupling transformation on the attitude error signals, as shown in Slide 3. Selected simulation runs are presented in a later section.

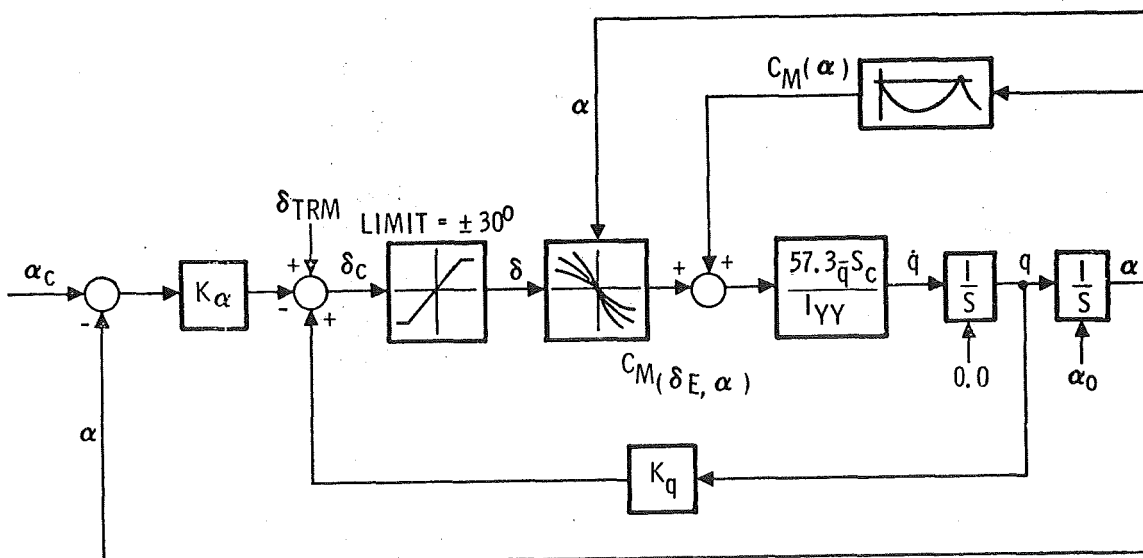
LOW CROSSRANGE ENTRY CONTROL SYSTEM BLOCK DIAGRAM



In this study, the entry angle of attack (60 degrees) is maintained until the orbiter has reached subsonic flight. At approximately 400 fps velocity, a pitchdown maneuver is performed, and the orbiter glides at maximum L/D to the recovery site. Actually, there is a good possibility that pitchdown will be performed at supersonic speeds. The pitchdown maneuver to low angle of attack was performed by the elevator in response to an angle-of-attack command. Stabilization was provided by a pitch rate damper loop. Inasmuch as there were two stable pitch attitudes, control action was required to force the vehicle from one stable state at 60 degrees to the other at a 15-degree angle of attack, while damping the motion to prevent any significant overshoot. In view of the highly nonlinear and unconventional nature of the pitch moment coefficient, there was some question as to what restrictions on vehicle design would be required for this phase of the mission (e.g., tail size). Air-speed variations during the pitchdown maneuver also were studied.

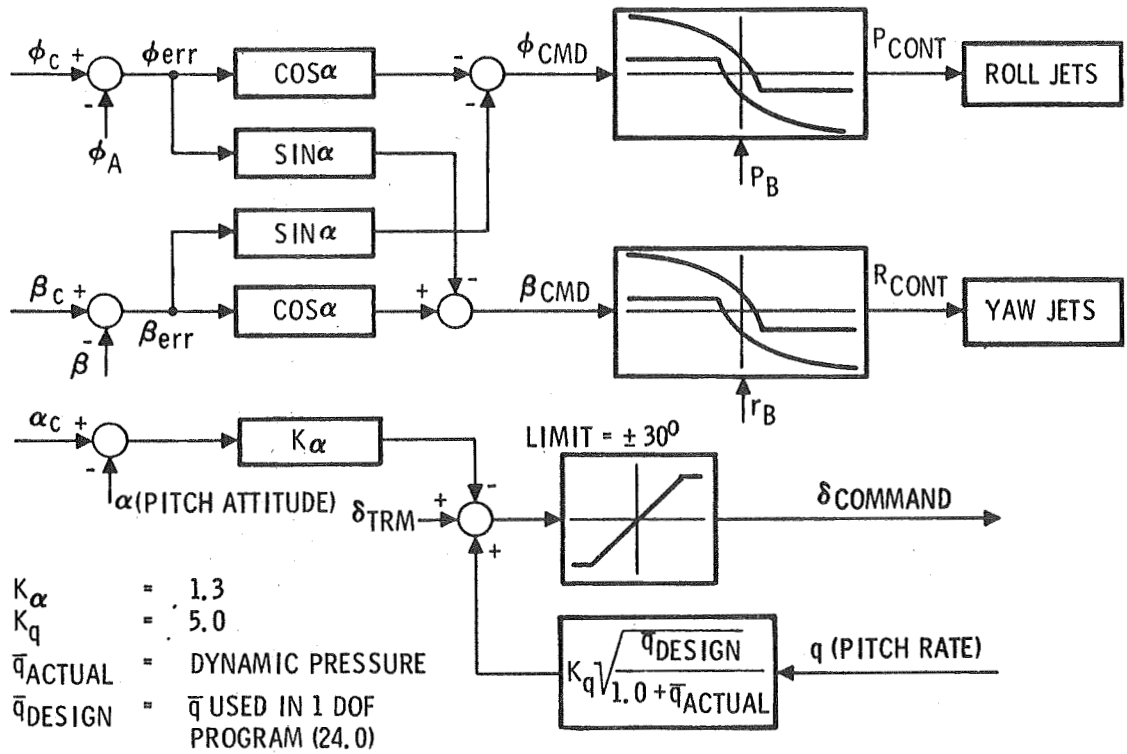
A simplified one degree of freedom version of the pitchdown control system is shown in Slide 4.

PITCHDOWN CONTROL SYSTEM DIAGRAM (ONE DEGREE OF FREEDOM VERSION)



The six degrees of freedom pitchdown control system is shown in Slide 5. Gain scheduling was used to compensate for large variations in airspeed and attitude during and after the maneuver.

PITCHDOWN CONTROL SYSTEM



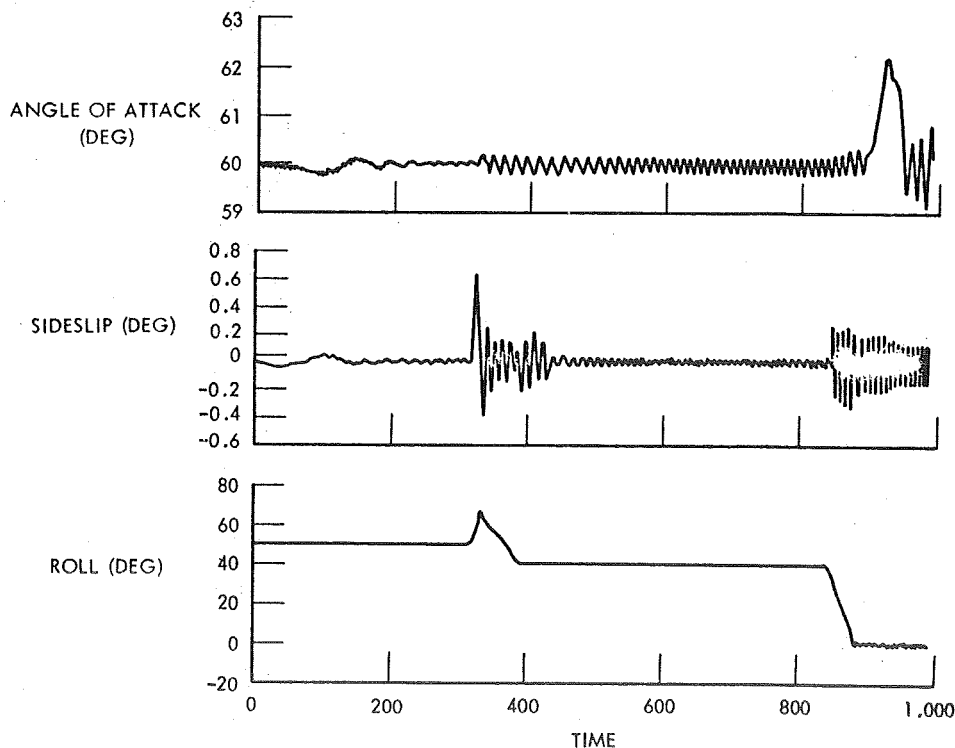
LOW CROSSRANGE ORBITER SIMULATION

Stability and control characteristics of the shuttle orbiter were assessed by performing a 6-degree of-freedom digital simulation. Included were a study of the effects of yaw and roll stability characteristics and a study of response for the pitchdown transition from entry to cruise attitude. All entry simulations started at 400,000 feet altitude and 25,992.5 feet/sec velocity. The vehicle was trimmed aerodynamically to 60 degrees angle of attack, and reaction jet control was used in all three axes. At 400 feet per second, the elevator was deflected to pitchdown the vehicle to a new stable angle of attack of 15 degrees.

The control system studied accepts roll angle commands from the guidance input, which, for these simulations, was programmed as a function of time. The roll command was based on an entry trajectory to provide maximum crossrange. The guidance scheme called for a constant (50 degree) bank angle until the flight path angle reached zero. Altitude was held constant by banking until an equilibrium glide condition was reached at a 40-degree bank angle. Bank angle was then held constant until aerodynamic velocity dropped to 3000 fps, then reduced immediately to zero (wings level) until pitchdown at 400 fps.

Slide 6 shows a nominal trajectory flown from earth-orbital conditions down to 400 feet per second to check out the simulation and generate initial conditions for the pitchdown maneuver.

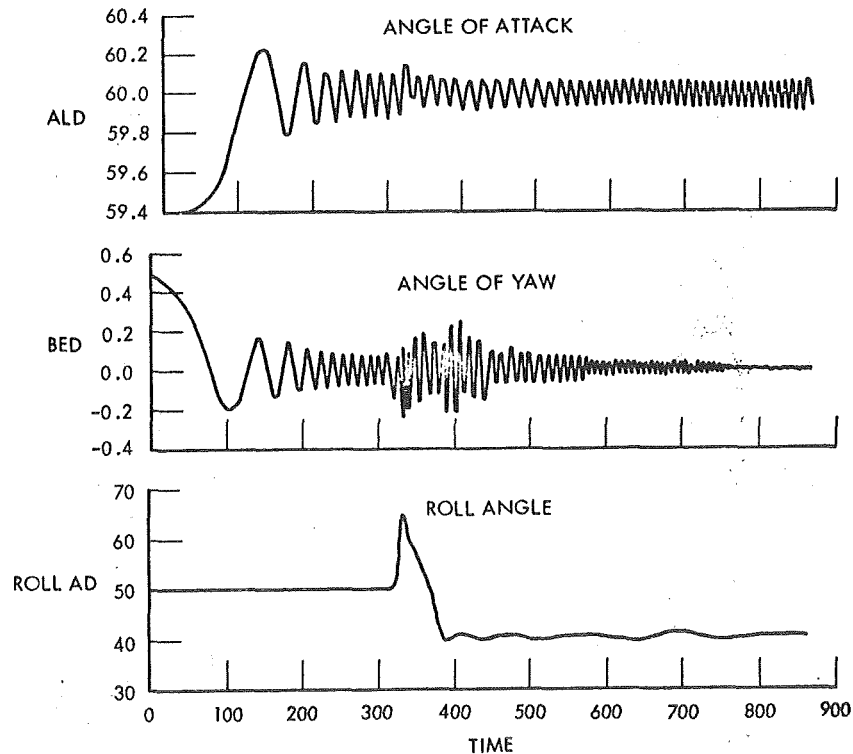
ORBITER ENTRY SIMULATION INCLUDING FINAL ROLL MANEUVER ATTITUDE HISTORIES



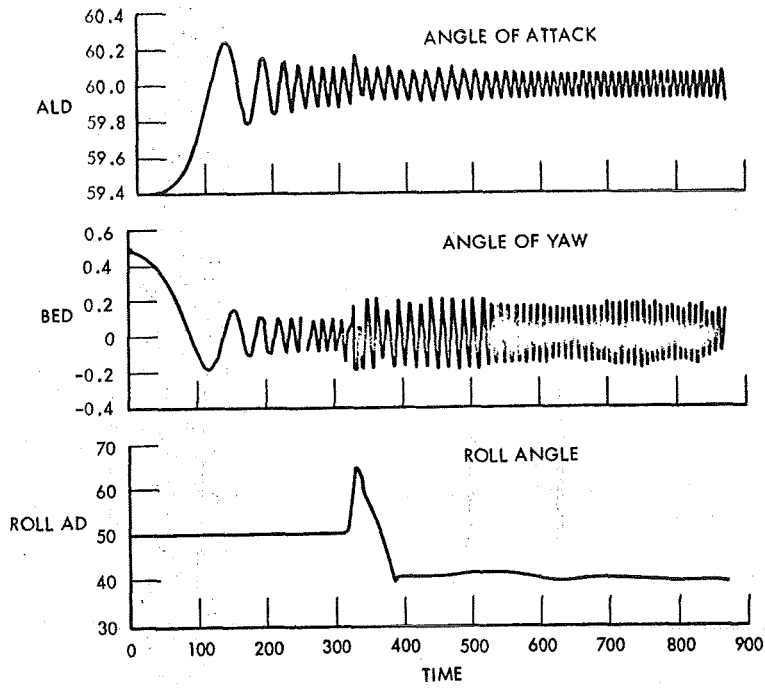
To study the effects of directional stability variation on orbiter entry a standard 95% wind profile was introduced in the lateral plane. Runs were made for the vehicle stable, neutrally stable, and unstable in yaw. Results were compared for stability, control effectiveness, and for ACPS fuel consumption.

Slide 7 is for a vehicle that is statically stable in yaw (positive $C_{n\dot{\beta}}$); Slide 8 for neutral stability; and Slide 9 for unstable $C_{n\dot{\beta}}$. In each case, the trajectory began at 400,000 feet and was terminated at about 130,000 feet. Inertial velocity started at 25,992.5 fps, and the run continued until the total vehicle velocity with respect to the atmosphere was 3000 fps. Vehicle response was stable and well damped in all cases, indicating that the control system functioned well for either stable or unstable directional derivatives.

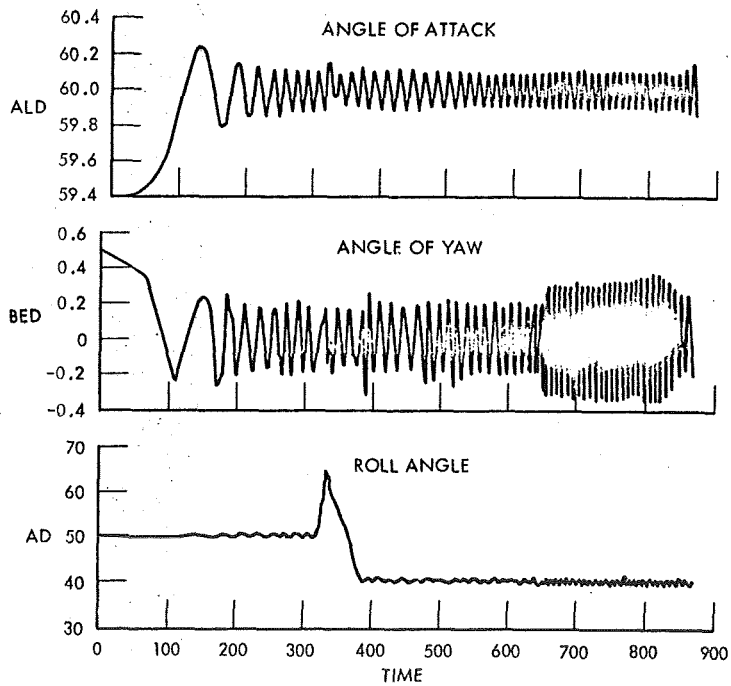
ORBITER ENTRY SIMULATION TIME HISTORY, STABLE $C_{n\dot{\beta}}$



ORBITER ENTRY SIMULATION TIME HISTORY, NEUTRALLY STABLE $C_{\eta\beta}$



ORBITER ENTRY SIMULATION TIME HISTORY, UNSTABLE $C_{\eta\beta}$



Results of the study are summarized in Slide 10. The only serious problem was sharply increased fuel consumption for the unstable $C_{n\beta}$ case. Roll jet on-time increased by a factor of about 15, and yaw jet on-time by a factor of about 10. The pitch damper jets never fired. Aerodynamic forces along the Y-axis remained small in all cases, indicating good turn coordination.

The jet on-time results in Slide 10 do not include the roll maneuver to wings-level attitude. Neither do they involve rate limits in the phase plane logic.

It was noted that a vehicle with stable or neutrally stable directional derivatives is readily controlled. However, fuel consumption increases sharply for unstable $C_{n\beta}$ and the reaction jet engines must be large enough to overcome any of the unstable aerodynamic moments generated. Since these moments increase for larger vehicle oscillations, vehicle attitude must be closely controlled for unstable $C_{n\beta}$ if vehicle stability is to be maintained. If vehicle attitude exceeds a critical value, recovery with reaction jet control is impossible. In the case considered, the jets were sized to provide an angular acceleration of 0.5 deg/sec² in all axes, neglecting aerodynamic moments. This value provided good performance, but any reduction in ACPS thrust would tend to increase the risk of losing control of a vehicle with unstable directional characteristics.

ORBITER ENTRY STABILITY SIMULATION RESULTS

YAW MOMENT COEFFICIENT $C_{n\beta}$ (PER DEGREE AT 60° (ANGLE OF ATTACK))		0.01 (STABLE)	0.0 (NEUTRAL)	-0.01 (UNSTABLE)
JET ON TIME (SEC) (870-SEC RUN)	ROLL	4.0	4.7	60.0
	PITCH	0.0	0.0	0.0
	YAW	10.4	9.0	103
PEAK SIDESLIP β (DEGREES)		0.25	0.22	0.38
Y-AXIS AERODYNAMIC FORCE Y_B (LB)		110	240	470
PEAK AERODYNAMIC MOMENTS (FT-LB)	ROLL	2,800	6,300	12,000
	PITCH	9,300	10,000	17,000
	YAW	1,450	13	60,000
PEAK BODY RATE OSCILLATIONS (DEG/SEC)	ROLL	0.1	0.15	0.5
	PITCH	0.05	0.06	0.1
	YAW	0.13	0.0	0.55

In the previous simulation, a stable $C_{l\beta}$ derivative was used. The value of $C_{l\beta}$ was assumed fixed at -0.002 , and $C_{n\beta}$ was varied from -0.01 to $+0.01$. It was desired to test the effects on vehicle performance and fuel consumption of variations in $C_{l\beta}$. Runs were made with values of 0.0 and $+0.002$. Results are shown in Slide 11 together with those from previous runs.

It is significant that when positive (unstable) values of $C_{l\beta}$ were used, the reaction jets were unable to stop the final roll maneuver at wings-level attitude prior to the pitchdown maneuver. This problem could be resolved. Either the aerodynamic control systems could be used for this maneuver, or the reaction jet control logic could be modified to reduce sideslip by shutting off jets in whichever axis is rolling faster than required for precise turn coordination.

Slide 11 indicates that an unstable value ($+0.002$) of $C_{l\beta}$ increases consumption of ACPS propellant about 60 percent, although not nearly as much as an unstable value of $C_{n\beta}$. It was assumed that three jets, each producing 800 pounds of thrust were used in each axis (one jet failed in each axis). The resulting accelerations were 4.6, 0.5, and 0.5 degrees/second² in the roll, pitch, and yaw axes, respectively. In view of the increased roll acceleration, results were not strictly comparable with earlier runs.

EFFECTS OF $C_{l\beta}$ VARIATIONS ON ORBITER ENTRY

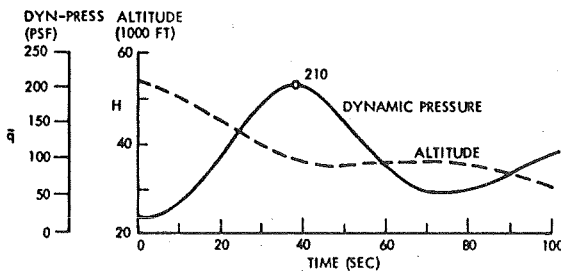
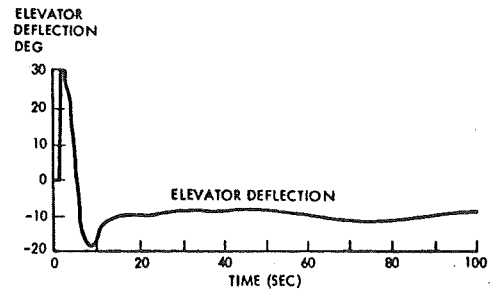
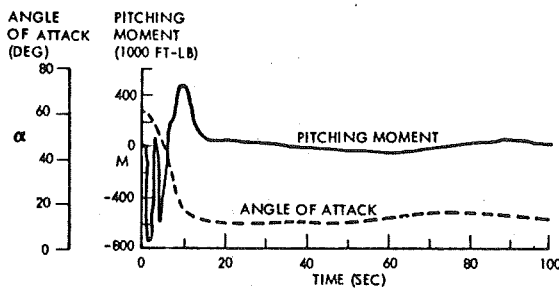
$C_{l\beta}$	$C_{n\beta}$	WIND	ACCELERATION (DEG/SEC ²)			ACPS ON TIME (SECONDS)			PROPELLANT USED (LB)		
			ROLL	PITCH	YAW	ROLL	PITCH	YAW	ROLL	PITCH	YAW
-0.002	0.01	YES	0.5	0.5	0.5	4.0	0.0	10.4	25.3	0.0	65.8
-0.002	0.0	YES	0.5	0.5	0.5	4.7	0.0	9.0	29.7	0.0	56.8
-0.002	-0.01	YES	0.5	0.5	0.5	60.0	0.0	103.0	369.0	0.0	652.0
+0.002	-0.009	NO	4.6	0.5	0.5	19.0	0.0	26.0	.	.	.
0.0	-0.009	NO	4.6	0.5	0.5	4.4	0.0	16.0	27.2	0.0	101.1

*REACTION JETS DID NOT STOP FINAL ROLL MANEUVER TO WINGS LEVEL AT A VELOCITY OF 3,000 FPS

A 6-DOF simulation of the pitchdown maneuver was conducted to verify the capability of the orbiter to perform the transition to horizontal flight. The maneuver was initiated at an altitude of 54,000 feet at a velocity of 400 fps. Dynamic response was smooth and well damped. There was little or no overshoot even though it was necessary to maneuver from one stable equilibrium point to another with nonlinear aerodynamic moments.

Inspection of the pitching moment history shown in Slide 12 indicates that the pitch ACPS system could be used to augment elevator authority, thereby allowing a reduction in size of the elevator surface. A moment of 162,000 foot-pounds is available from the pitch jets of the 50,000 pound-payload-class orbiter. The maximum moment developed by the elevator was about 750,000 foot-pounds, rapidly decaying to zero as the vehicle pitched down. As now sized, the ACPS can provide about 20 percent of the peak aerodynamic moment, and will supply an equivalent integrated moment by maintaining the jet on for five seconds. Additional investigations of combined ACPS plus aerodynamic control should be conducted to minimize orbiter vehicle weight.

ORBITER SUBSONIC PITCH DOWN MANEUVER 50K LB PAYLOAD CLASS

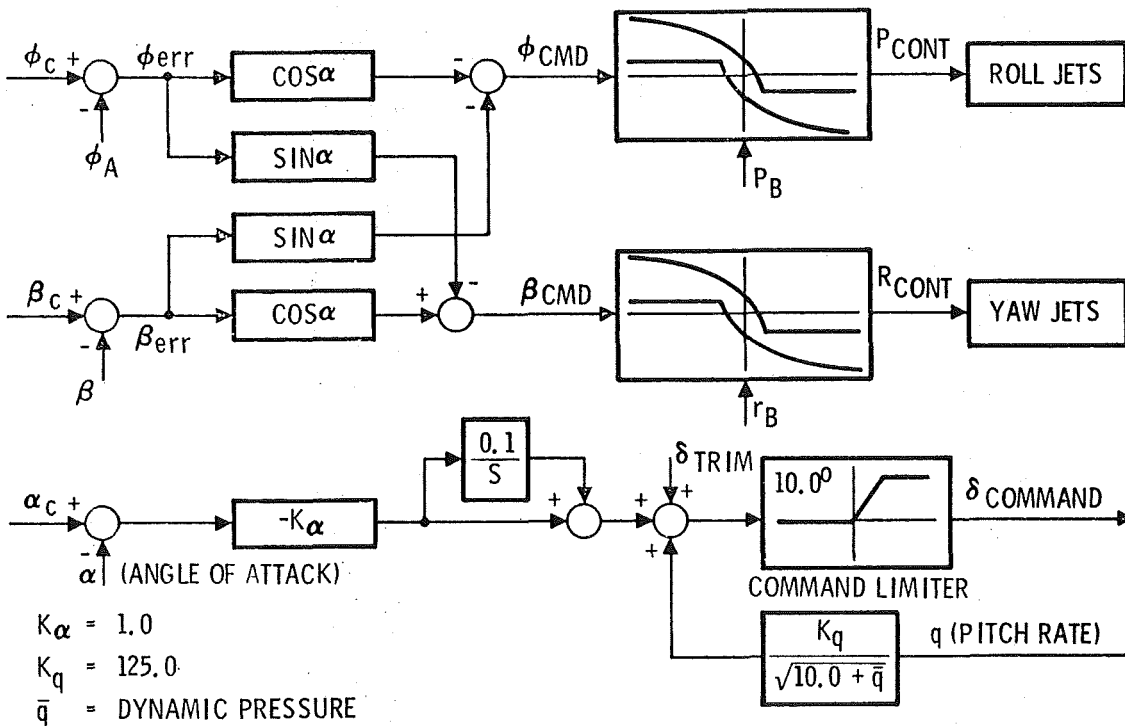


- INITIAL CONDITIONS
 - ALT 54,000 FT
 - DYN PRESS 24.2 PSF
 - MACH NO. 0.41
- SMOOTH & WELL DAMPED
- USE PITCH RCS TO AUGMENT CONTROL AUTHORITY & REDUCE TAIL SIZE

HIGH CROSSRANGE ORBITER CONTROL SYSTEM DESIGN

The roll and yaw control systems are identical for the High and Low crossrange orbiters. Aerodynamic control is used in the pitch axis of the High crossrange orbiter, as shown in Slide 13. An integrator was used in the forward path of the control loop to compensate for unexpected trim variations, and rate gain was scheduled as a function of dynamic pressure to maintain damping ratio constant at a value of 1.0.

HIGH CROSSRANGE ENTRY CONTROL SYSTEM BLOCK DIAGRAM

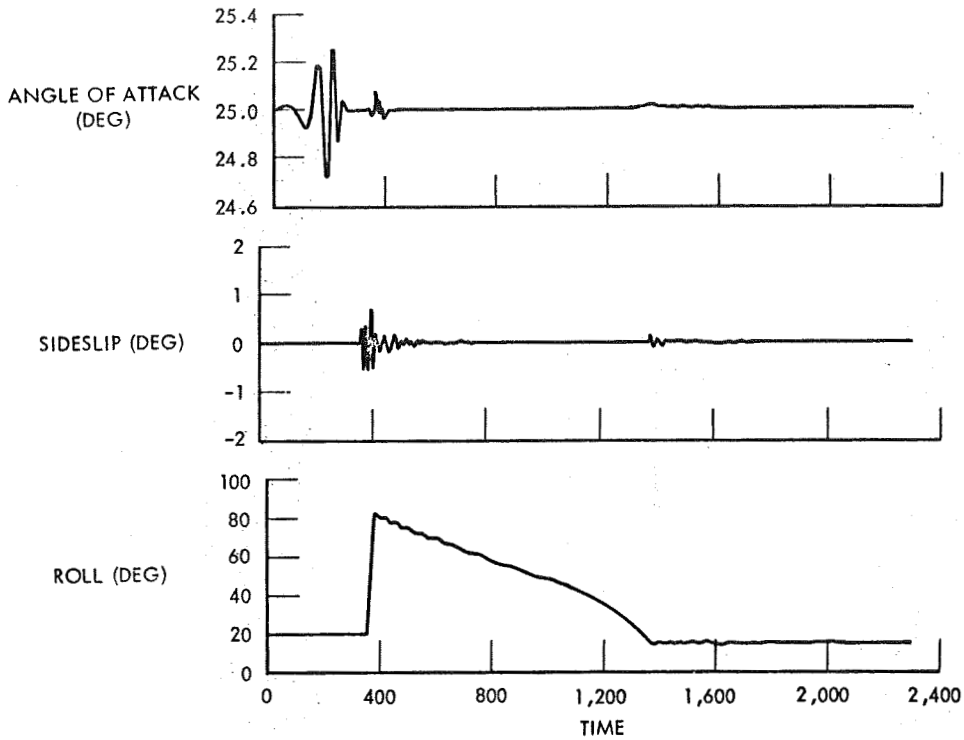


HIGH CROSSRANGE ORBITER SIMULATION

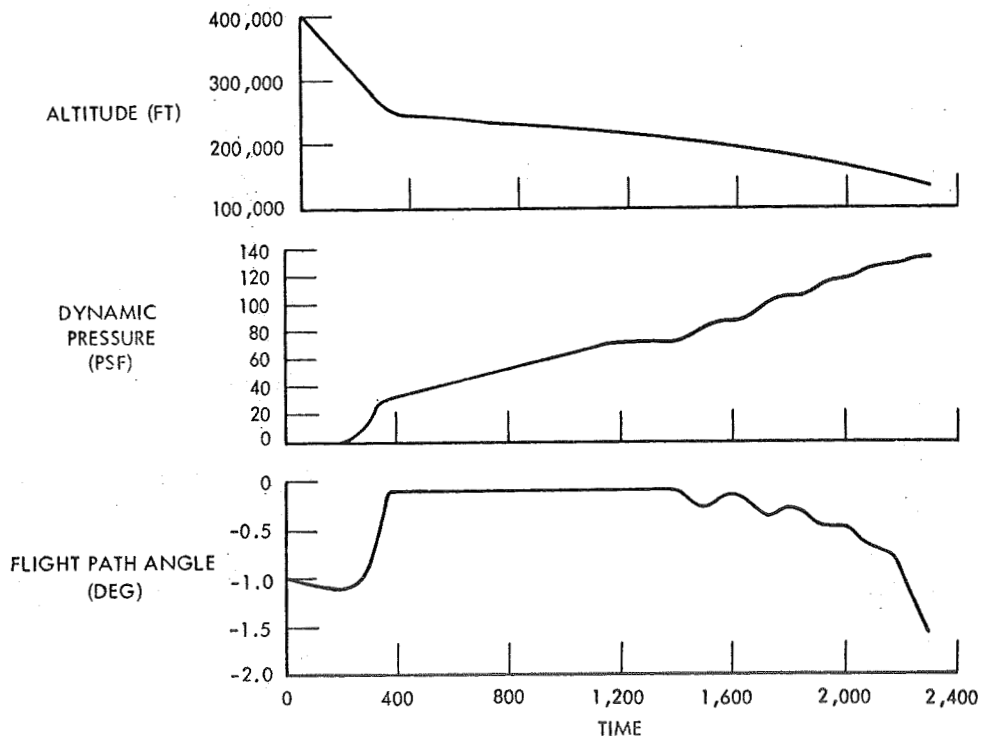
Simulation runs began at 400,000 feet altitude and 25,569.5 feet/second velocity. Angle of attack was held constant at 25 degrees throughout the run. Bank angle was held at 20 degrees until flight-path angle reached -0.3 degrees, at which time guidance was switched to equilibrium glide mode. By the time the initial roll maneuver was completed, the flight-path angle was -0.1 degree, in agreement with the nominal trajectory. Equilibrium glide was flown until bank angle limited at 15 degrees, after which bank angle was held constant until the end of the run.

The High crossrange orbiter simulation results are shown in Slides 14 and 15. The results were quite satisfactory.

HIGH CROSSRANGE ORBITER ENTRY: VEHICLE ATTITUDE TIME HISTORIES



HIGH CROSSRANGE ORBITER ENTRY: TRAJECTORY TIME HISTORIES



CONCLUSIONS

For the low crossrange orbiter, an ACPS capable of providing 0.5 degree/sec² gave adequate control authority for reentry. Vehicle motion was stable and well damped. Unstable directional derivative ($C_{n\dot{\theta}} < 0$) were not significant to vehicle controllability, but can cause high ACPS propellant consumption. Unstable dihedral effect ($C_{l\dot{\theta}} > 0$) could result in loss of control.

Control of the high crossrange orbiter was satisfactory with aerodynamic control in pitch and reaction jets in roll and yaw. For aerodynamic control loops, conventional linear feedback with gain scheduling appears adequate for entry and pitchdown maneuvers.

N70-40964

GUST ALLEVIATION AND MODAL SUPPRESSION CONTROL TECHNOLOGY

Mario H. Rheinfurth

NASA-Marshall Space Flight Center
Huntsville, Alabama

Introduction

A necessary condition for satisfactory flight performance of an aerospace vehicle is to keep its responses due to atmospheric disturbances within the design limits of the control deflections and the structural loads of the vehicle. This task is solved in two ways: One is the proper design of the vehicle configuration such that aerodynamic lift and moment coefficients are minimized. The other is the judicious selection of a controller which provides gust alleviation during those periods of flight when aerodynamic disturbances become severe. The following discussion describes a method of designing a controller which will actively control both rigid body modes and flexure modes. This objective is met by formulating the problem as a stochastic minimization problem. The atmospheric disturbances and the vehicle responses are described as random processes and the probability of mission failure is defined. In order to render the problem mathematically tractable, the stochastic problem was reformulated in a manner that permits application of quadratic optimum control theories. Despite their limitations, these theories have proven themselves the best theories of coping with the dimensionality of the problem.

In an optimal control problem, the objective is to find a set of control functions $u(t)$ which can transfer the vehicle (plant) from its initial state (x_0, t_0) to some final state (x_T, T) such that a given performance criterion is optimized. The most general performance criterion is that of Bolza as given in equation (1), where F_1 and F_2 are nonlinear functions and where the plant is described by a set of nonlinear differential equations of the form $\dot{x} = f(x, u, t)$.

Since the solution of this optimal control problem presents formidable mathematical difficulties for most practical cases, an attempt is often made to cast the problem at hand into a linearized form where the equations describing the plant appear in the form $\dot{x} = A(t)x + B(t)u$ and the performance criterion as given by equation (2). Although the linear optimal control problem yields a direct solution in form of a linear state feedback, the theory still has certain deficiencies. One of the major weaknesses of the theory is the arbitrariness in specifying the weighting matrices Q_0 , Q_1 , and Q_2 of the performance criterion. Another formulation of an optimal control problem is given by the "minimax" performance criterion (equation 3). The problem considered here is that of minimizing the maximum value of some vehicle response of interest no matter when this maximum occurs during flight time. Although quite some research effort has been expended in recent years toward practical solutions of this problem, many obstacles remain to be overcome, before this theory can be readily applied to the controller design of aerospace vehicles. The remaining portion of this paper is concerned with the statistical optimal control problem. The motivation for the stochastic formulation arose from the fact that the wind is not a deterministic quantity but represents a stochastic process. Under the reasonable assumption that the wind is a Gaussian Markov process and a linear description of the vehicle dynamics about a nominal trajectory, a stochastic optimal control theory can be readily formulated. The theory centers around the definition of the probability of mission failure as given by equation (4) where a_i ($i = 1, \dots, m$) represent the events that the m responses $r_i(T)$ fall within specified limits at time T , and b_j ($j = m + 1, \dots, n$) represents the event that the responses $r_i(t)$ exceed their respective limits j times during flight time. Minimization of the probability of mission failure is obviously a logical basis for the stochastic optimal control theory.

PERFORMANCE CRITERIA

● DETERMINISTIC NON-LINEAR OPTIMAL CONTROL

$$(1) J(x_0, t_0; u) = F_1(x_T, T) + \int_{t_0}^T F_2(x, t, u) dt$$

● DETERMINISTIC LINEAR OPTIMAL CONTROL

$$(2) J(x_0, t_0; u) = x(T)Q_0x^T(T) + \int_{t_0}^T [x(t)Q_1x^T(t) + u(t)Q_2u^T(t)] dt$$

● MINIMAX CONTROL

$$(3) J(x_0, t_0; u) = \max_{t_0 \leq t \leq T} C(x, t)$$

● STOCHASTIC OPTIMAL CONTROL

$$(4) J(x_0, t_0; u) = 1 - P[a_1, \dots, b_n(0)]$$

Unfortunately, no analytical expression for the probability of mission failure is known. This holds true even for Gaussian processes. It is, however, possible to establish a useful upper bound for the probability of mission failure J . This upper bound J^* is the sum of the probabilities that the responses $r_i(t)$ exceed their prescribed limits at burnout time T (events \bar{a}_i occur, i.e., a_i does not occur) plus the sum of the average number for which the responses $r_i(t)$ ($i = m + 1 \dots n$) exceed their prescribed limits during flight. The expression for J^* can be reformulated in form of a deterministic performance criterion of the Bolza type involving the mean response matrix $R(t)$ and the covariance matrix $S(t)$. It can be shown that for general random processes $J^* \geq J$. If the optimum controller yields a value for J^* which is sufficiently small, the value for the true probability of mission failure J is even smaller and the controller which minimizes J^* will be acceptable. It was mentioned above that direct minimization of the general performance criterion presents some computational difficulties. These difficulties can be circumvented by an iterative procedure which is based on the principle of quadratic equivalence. This principle states that the linear controller which minimizes J^* also minimizes a quadratic functional J^{**} whose weighting matrices $Q(t)$ and $V(t)$ are the partial derivatives of J^* with respect to the mean response and covariance matrix. The iteration procedure starts by choosing initial weighting matrices $Q(t)$ and $V(t)$ and applying the well known solution of the quadratic problem. The response matrices are then calculated to obtain the partial derivatives of the upper bound J^* . The process is repeated until the initially chosen coefficients and the derived partial derivatives are equal.

STOCHASTIC OPTIMIZATION

- PROBABILITY OF FAILURE

$$J(x_0, t_0; u) = 1 - P[a, \dots, b_n(0)]$$

- SUM OF EXPECTATIONS OF EXCEEDING CONSTRAINTS

$$\begin{aligned} J^*(x_0, t_0; u) &= \sum_{i=1}^m P(\bar{a}_i) + \sum_{i=m+1}^n E\{N_i\} \\ &= f_1[S(T), R(T)] + \int_0^T f_2[S(t), R(t)] dt \end{aligned}$$

$$J^* \geq J$$

- WEIGHTED QUADRATIC FORM

$$J^{**}(x_0, t_0; u) = TR\{Q(T)S(T) + V(T)R(T) + \int_0^T [Q(t)S(t) + V(t)R(t)] dt\}$$

- SOLUTION: 1. FIND WEIGHTS $Q(t)$ AND $V(t)$ SUCH THAT THE FIRST VARIATION OF J^{**} IS THE SAME AS J^* .
- 2. MINIMIZE J^{**} .

The stochastic optimal control theory requires that the wind be represented as a Gaussian Markov process. This means that the stochastic wind process can be generated by a linear differential system (wind filter) which is excited by white noise. By proper choice of the wind filter parameters, its output can be made to approximate the variance and covariance of the wind. For flights at constant altitude, the atmospheric disturbance can be assumed stationary and isotropic. A widely used wind filter for both the lateral and vertical components of the wind is that of H. Press as given in equation (1) where L is the scale length of the wind V the horizontal velocity of the vehicle and σ^T its standard deviation. This wind filter seems to be acceptable for altitudes below 50,000 feet. The scale length L varies from 500-1000 meters depending on altitude and the standard deviation from 1-2 m/sec depending on weather conditions.

For vertical flights through the atmosphere, the wind can no longer be considered a stationary random process and the construction of an appropriate wind filter becomes more difficult. The reason for this is twofold. One is the proper statistical analysis of existing wind measurements, the other the development of a general theory of wind filter synthesis. Wind velocity profiles are usually measured by two methods; the rawinsonde and the FPS-16 radar/Jimsphere. The rawinsonde system provides measurements of horizontal wind velocities at altitude intervals of approximately 600 meters. Because of the inherent smoothing, the rawinsonde cannot measure the small-scale features of the wind profile which can contribute significantly to the aerodynamic loads of an aerospace vehicle. The newer FPS-16 radar/Jimsphere method provides considerable more accurate wind measurements at intervals of 25-50 meters altitude with an RMS error of approximately 0.5 meters per second. At the present time, there exist approximately 2000 wind measurements for the Eastern Test Range, Florida. Some 500 measurements are available for the Pacific Missile Range, California.

There are several approaches presently considered for the wind filter synthesis. The most promising of these methods seem to be the synthesis using analytical curve fits for the covariances or multiple regression analysis to determine the coefficients of the matrices $A(h)$ and $B(h)$ of the altitude-varying equation for the wind filter (equation (2)). In order to use the wind filter for the stochastic optimal control problem, it has to be transformed to the flight-time domain as given in equation (3) where \dot{h} is the vertical velocity of the vehicle. It is important to notice that this transformation makes the wind filter trajectory dependent, such that an optimum controller would have to be designed for each individual trajectory. Fortunately, the controller parameters are not very sensitive to these trajectory variations and one controller is acceptable for quite a number of flight profiles.

WIND MODELS

- HORIZONTAL FLIGHT (Stationary random process)

$$(1) \frac{L^2}{V^2} \frac{d^2 w}{dt^2} + \frac{2L}{V} \frac{dw}{dt} + w = \sigma_T \sqrt{\frac{L}{\pi V}} \left[\sqrt{3} \frac{L}{V} \frac{d\eta}{dt} + \eta \right]$$

- VERTICAL FLIGHT (Nonstationary random process)

- a) ALTITUDE VARYING EQUATION

$$(2) \frac{d}{dh} \underline{w}(h) = A \underline{w}(h) + B \underline{\eta}(h)$$

- b) TIME VARYING EQUATION

$$(3) \frac{d}{dt} \underline{w}(t) = \dot{h} A \underline{w}(t) + \sqrt{\dot{h}} B \underline{\eta}(t)$$

The representation of the wind disturbance as a Gaussian Markov process allows a combination of the wind filter and the linearized vehicle differential equations in form of an "adjoint system" as shown in the adjacent figure. In this model, the wind is assumed to consist of two parts: the mean wind, which is given as a deterministic quantity and the deviations from this mean, which is a random process. The sum of both parts act as the input function of the vehicle dynamics. Sensors and the linear optimal controller are shown in their respective feedback paths. The particular form chosen for the controller accounts for the fact, that in most practical applications some of the vehicle and wind filter states have to be estimated, because no measurements are available for them.

STOCHASTIC MODEL

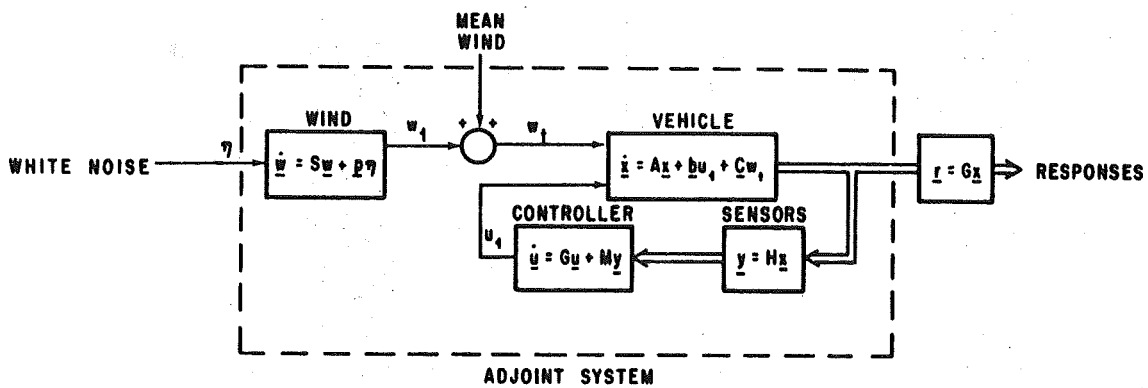
- ASSUMPTIONS

GAUSSIAN WIND

VARIATIONAL EQUATIONS FOR THE VEHICLE

LINEAR CONTROL

- MODEL



Based upon the stochastic optimal control theory, which was developed by Honeywell, Inc. for NASA-MSFC in 1965 and 1967, Honeywell designed and flight tested the B-52 LAMS (Load Alleviation and Mode Stabilization) system. The program was conducted to demonstrate the capabilities of an advanced flight control system to actively control both rigid body and flexure modes on a large flexible aircraft. The system used multiple inputs: elevator plus symmetric ailerons and spoilers for the longitudinal motion, rudder plus differential ailerons and spoilers for the lateral motion. The atmospheric turbulence model used for the LAMS B-52 structural performance studies was the Press power spectrum as discussed in figure 3. In the original analysis, it was assumed that all states of the system were measurable. As expected, this led to an excessive number of feedbacks (81 for the symmetric axis and 90 for the antisymmetric axis) for practical purposes. However, this optimal controller was used as a baseline for determining the relative merits of simplified and more practical controllers. Also, the magnitude of the optimal feedback gains generally indicate the relative importance of the particular feedback loop in terms of structural performance benefits. After simplification, the final operational flight control system contained four rate gyro feedback signals for the longitudinal motion and six rate gyro feedback signals for the lateral motion. Flight control gains were established for three different flight conditions. The mathematical model for longitudinal and lateral motion is shown in figure 5. The performance criterion for the stochastic optimization was a combination of ride qualities and structural integrity. Meansquare linear accelerations experienced by the pilot were used as ride quality measures. Structural integrity was measured by the probability of exceeding static ultimate strength and fatigue life time for several critical airframe members. This measure of structural integrity is a function of stresses and stress rates.

A theoretical evaluation of the structural performance of the B-52 showed, that the LAMS Flight Control System reduced fatigue damage rates at the key wing stress points by more than 30% with respect to the Baseline SAS (Stability Augmentation System). Of importance is the fact that the structural loads were reduced throughout the airframe and not just at the selected stations. The ride qualities at the pilot station were improved slightly, with the remainder of the fuselage showing varying amounts of improvement over its length.

APPLICATION - B-52 (LAMS)

1. MATHEMATICAL MODEL

a. LONGITUDINAL MOTION

TWO RIGID BODY MODES; FIRST, SECOND, AND SIXTH STRUCTURAL MODE; FIRST ORDER ACTUATORS.

b. LATERAL MOTION

THREE RIGID BODY MODES; FIRST, EIGHTH AND NINTH STRUCTURAL MODE; FIRST ORDER ACTUATORS.

2. RESPONSE CONSTRAINTS

a. STRESSES

b. STRESS RATES

c. LONGITUDINAL AND LATERAL ACCELERATIONS EXPERIENCED BY PILOT

In another study, the stochastic optimal control theory was applied to the design of a control system for the Saturn V/Voyager launch vehicle. Although the system was never flight tested, it was demonstrated that a practical control system can be designed using the physical insight provided by the optimal controller which was obtained from the theory assuming complete measurement capability. The analysis was restricted to vehicle motion in the yaw plane. As required by the stochastic optimal theory, the equations of motion were linearized about the nominal (no-wind) trajectory. They included the two rigid body modes, three bending modes and three slosh modes. Actuator dynamics was described by a first order model. Due to the lack of a general theory for wind filter synthesis, the form of the wind filter was selected to conform with a nonstationary exponential-cosine autocorrelation function. The available wind measurements were based on the rawinsonde method and did, therefore, not include the small-scale content of the wind field which affects the elastic body dynamics. Because of this, it was felt that construction of a higher order nonstationary wind filter was not worthwhile. The stochastic performance criterion was based on the probability of mission failure in terms of the response constraints shown in figure 6. As in the case of the B-52 LAMS system, the optimal controller derived from the theory was unduly complicated and required the physical measurements of the wind states. However, the optimal controller provided the smallest theoretical possible probability of mission failure ($J^* = 8 \times 10^{-4}$) and was, therefore, used as a standard for comparison of simplified controller performance. It also served as a starting point for the synthesis of a practical controller. An important result derived from the theory was that the simplified controller obtained by deleting specific feedbacks does not necessarily represent the optimal controller which uses the remaining feedbacks. Other conclusions reached on the basis of the theory were that it is important to estimate the wind states and retain the highest-frequency flexure mode feedback but that feedback of the fuel slosh states was not necessary. After several experiments were performed to determine the degradation in performance caused by deleting the feedbacks of certain states from the optimal controller, a final simplified controller was arrived at which contained a fifth-order estimator and the outputs of five accelerometers and their integrals. This simplified controller gave a fairly good performance with a value for $J^* = 1.73 \times 10^{-2}$. Due to the inherent expenses associated with the digital simulations, the controller simplification studies were not carried out very extensively. It is, therefore, believed that the performance of this simplified controller could be still improved and that the controller could be further simplified by additional simulation studies.

APPLICATION - SATURN V / VOYAGER

1. MATHEMATICAL MODEL

- a. TWO RIGID BODY MODES; THREE BENDING MODES;
THREE SLOSH MODES; FIRST ORDER ACTUATOR.*

2. RESPONSE CONSTRAINTS

- a. MAGNITUDE OF TERMINAL DRIFT.*
- b. MAGNITUDE OF TERMINAL DRIFT RATE.*
- c. MAGNITUDE OF TERMINAL ANGLE OF ATTACK.*
- d. MAGNITUDE OF GIMBAL ANGLE.*
- e. MAGNITUDE OF BENDING MOMENT AT THREE
CRITICAL STATIONS.*

3. PROBABILITY OF MISSION FAILURE

- a. IDEAL CONTROLLER $p = 8 \times 10^{-4}$*
- b. SIMPLIFIED CONTROLLER $p = 1.73 \times 10^{-2}$*

The results obtained from the application of the stochastic optimization theory to the controller design of a large flexible aircraft and launch vehicle are very favorable. They indicate that with some further improvements of the theory, the same design technology can be successfully used to design controllers which actively control rigid body and flexure modes of the Space Shuttle Vehicle. It is expected that a proper choice of the stochastic performance criterion will result not only in a considerable reduction of loads and fatigue damage but also increase the flutter speed and flying qualities for the boost and fly-back portions of the mission. Since bending dynamics effects dominate the loads at certain critical stations of the vehicle, it is important to construct a more accurate nonstationary wind model which includes the high frequency turbulence content of the wind field. This calls for a more sophisticated statistical analysis of the wind data and a corresponding increase in the order of the differential equations defining the wind model. Several research programs within NASA and industry are presently under way to solve this problem. Improvements of the quadratic control theories center around three major problem areas. One is that of computer cost. Since the optimal control theory arrives at an overly complex control system, simplifications have to be introduced in order to make the controller practical. However, present computer iteration methods for the best gains for the candidate simplified controllers are still too expensive as a design tool. Several partially developed improvements of some iteration methods are exceptionally promising showing substantial cost reductions. The other two problem areas--parameter sensitivity and sensor choice--require the development of new mathematical methods. The objective of the parameter sensitivity study is to include parameter variation constraints in the preliminary design studies. Sensor choice and location is presently done by brute-force methods. Developing a mathematical theory for best sensor choice and location is a difficult but decisive step towards practical application of quadratic optimal control theories.

FUTURE RESEARCH PROGRAM

- 1. DEFINE PERFORMANCE CRITERIA FOR SPACE SHUTTLE*
- 2. IMPROVE WIND MODELS*
- 3. DEVELOP ITERATION METHOD FOR SIMPLIFIED CONTROLLER*
- 4. DEVELOP THEORY FOR PARAMETER SENSITIVITY*
- 5. DEVELOP THEORY FOR SENSOR CHOICE AND LOCATION*

REFERENCES

- (1) Edinger, L. D. et al
"Design of a Load-Relief Control System," Final Technical Report
Honeywell Document 12013-FR 1, 1966
- (2) Bender, M. A. (Honeywell), P. M. Burris (Boeing)
"Aircraft Mode Alleviation and Mode Stabilization (LAMS)"
Final Report, AFFDL-TR-68-158, 1969
- (3) Harvey, C. A.
"Application of Optimal Control Theory to Launch Vehicles"
Final Technical Report
Honeywell Document 12073-FR 1 and 2, 1968

N70-40965

ACTIVE FLEXURE CONTROL TODAY

G. B. Skelton

Honeywell Inc.
Minneapolis, Minnesota

SYNOPSIS OF TOPIC

Background

Space Shuttle vehicles may have aeroelasticity problems caused by their large sizes, having to withstand reentry heating, wings, and side-by-side boost geometry. Obtaining needed maneuver capability, ride, low peak-stresses and fatigue may require stiffening or active bending mode control.

Question

Is active bending mode control a viable alternative to adding stiffening weight?

Answer

Active bending mode control is on the edge of out technical capability; it should be a viable alternative.

- The only aircraft systems flown that tried more than rigid body control phase-stabilized at the first bending mode, the B52-LAMS and XB-70-GASDSAS systems, were both flown in technology-oriented studies. There are no fleet-wide practical systems.
- Active mode control pushes physical limits. These include control surface aeroelasticity and inertias, mechanical actuation lags, local deformations and temperature limits at sensor locations, and available force-producer locations.
- Controller design is analytically difficult. Multiloop control of many coupled degrees-of-freedom taxes existing design theories and computer programs.

Continuous research and development since B52-LAMS and XB-70-GASDSAS is reducing these difficulties and limits. NASA is now considering a technology program to test a LAMS system on an SR-71, and North American Rockwell has announced plans to employ active flexure control on the B1.¹ Active flexure control is an arriving technology.

DISCUSSION

Active Flexure Control Today

The topic of this discussion is the state of the art of active flexure control.

The message of the talk is that active control of flexure degrees of freedom is on the edge of our technical capability, and active flexure control should be a viable alternative to adding stiffening weight for the solution of Space Shuttle aeroelasticity problems.

Rigid Body Roll Coupling in Boost

To begin, will Space Shuttle have aeroelasticity problems? Is active flexure control a concern?

It's too early to say. First-cut flexure data are just now being calculated. Certainly there will be some aeroelasticity problems-- there always are. I suspect that some of them will be severe.

The slide shows one of the potential sources of flexure, the roll coupling of rigid orbiter and booster through elastic connecting mechanisms in boost. Other potential sources include

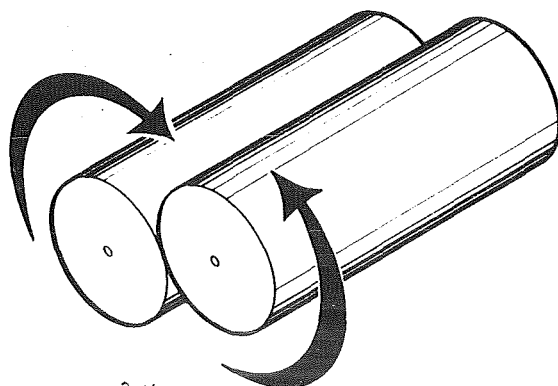
- Having to allow the delta winged orbiter to bend to withstand reentry heating
- The vehicles' large sizes and thin wings
- The opportunities for aerodynamic coupling in boost, and
- The uneven orbiter mass distribution during reentry, where there are engines in back, payload in front, and little between

Quoting some preliminary design numbers, the first (lowest) symmetric mode frequency of

the NAR piggyback launch configuration is	1.85 Hz
the NAR delta winged orbiter is	2.36 Hz
the MSFC belly-to-belly launch configuration is	2.68 Hz

In comparison, the lowest X-20 Dynasoar mode was 1.8 Hz and the lowest B52 mode was 1.07 Hz. Accepting the preliminary design numbers, Space Shuttle is likely to have bending problems in my opinion.

The remainder of this talk will be devoted to sketching a picture of current active flexure control capability. Bandwidth and bandwidth limits will be discussed first, to define notions. The three flexure control methods which have been flight tested will then be described. The talk will be concluded with a discussion of where we stand today.



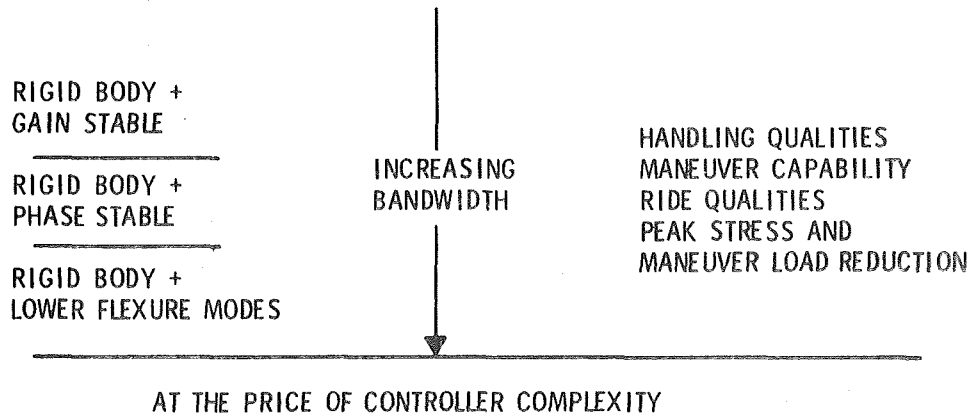
Bandwidth

This slide shows the benefits of increasing control system bandwidth and what has to be done to buy that bandwidth. On the right, the benefits are first handling qualities (largely rate responses), then ride qualities (more accelerations), then maneuver load and peak stress reduction. Increasing bandwidth always improves the lower frequency responses but one must get to fairly high bandwidths to do much for the higher frequency ones.

Increasing bandwidth (or decreasing flexure frequencies) requires successively going from gain stabilizing the lowest mode to phase stabilizing it to actively controlling the lowest few modes. The price of this increase is control system complexity--more notch filters, more sensors, more control forces.

Active flexure control is thus not a black-white thing where flexure is controlled or it isn't. Where flexure frequencies are low, increasing bandwidth requires more and more flexure control. It's a matter of degree.

INCREASING BANDWIDTH BUYS



Bandwidth Limits

Nature won't let us raise control loop bandwidths as high as one would like. The slide lists the three major reasons why--phase lags, parameter variations, and parameter uncertainties.

Phase lags can be overcome to some extent by employing more powerful actuators. Most controllers are designed to live with parameter variations for reasons of controller simplicity, implying keeping bandwidths down because of changing phase relations. Even where gain changing with flight condition is employed, however, the controller must be designed to withstand the phase differences between the mathematical and real vehicles.

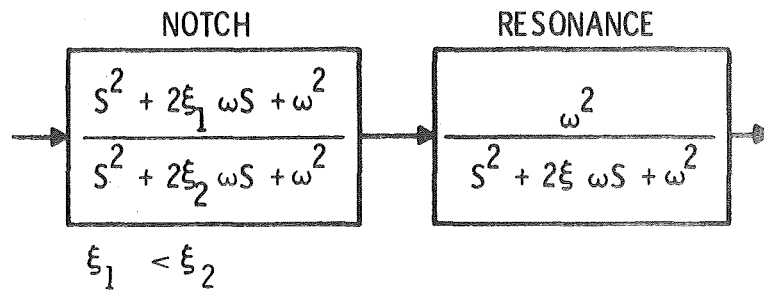
The flexure control problem in one sense is to push further into these phase variation limits.

WHAT LIMITS BANDWIDTH

- PHASE LAGS - ACTUATOR NONLINEARITIES, TAIL-WAG-DOG SURFACE AERODYNAMICS
- FLEXURE FREQUENCY, MODE SHAPE CHANGES WITH Q, M MASS DISTRIBUTION, TEMPERATURE
- UNCERTAINTIES IN FLEXURE FREQUENCIES, MODE SHAPES

Notch Filtering

Three techniques for increasing bandwidth through flexure control have been shown. The first of these, notch filtering, consists of changing the gain and phase near the flexure resonant frequency by cascading a ratio of second-order polynomials or a filter of equivalent effect with the resonance. Note that the resonant frequency and the natural frequencies of the second orders are (nearly) the same.

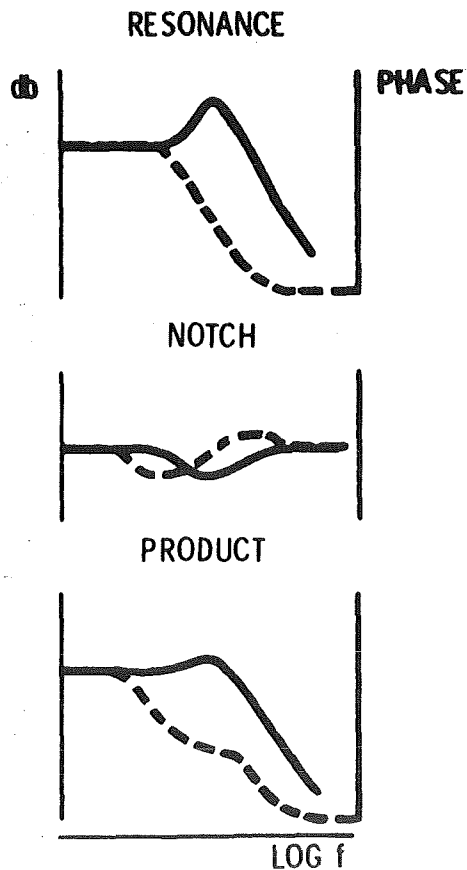


Gain and Phase Addition

This slide shows the resulting cascaded gain and phase responses. By having the numerator of the filter less damped than the denominator, the overall effects are to

- Lower the resonant peak
- Add some phase lag below the peak
- Add phase lead beyond the peak, and
- If near ninety degrees phase lag can be obtained at the peak, to damp the flexure mode in the closed loop system by rate feedback.

If the resonant frequency is far beyond the 180 degree (bandwidth) frequency, lowering the resonant peak is the main effect desired; this is called gain stabilization. Where the phase near resonance is a concern, notch filtering is normally called phase stabilization; the terminology is perhaps a matter of taste in this case as gain must also be taken into account.



Examples of Notch Filtering

Notch filtering is definitely well within control capability. It is (to my knowledge) the only method that has been used in large missiles, where the control systems are single loop and the lowest mode is a simple fuselage mode.² Notch filters are in fact used almost everywhere where single loop control is employed and where controlled plant phases and frequencies don't vary too much.

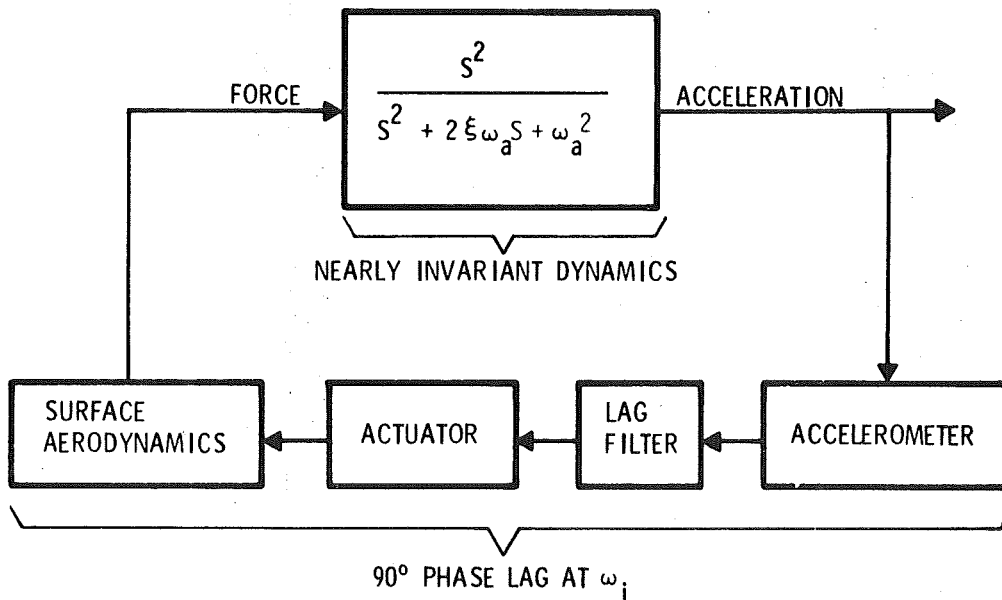
But notch filtering alone won't solve all flexure control problems. Its Achilles' heel is variations in mode shapes and frequencies--it is a tuned filter method and when severely detuned it can produce instability itself.

<u>VEHICLES</u>	<u>MODES</u>	<u>STABILIZATION</u>
ATLAS	} 1st HIGHER	PHASE GAIN
THOR		
SATURN 1B		
TITAN III	1st	PHASE
	2nd	GAIN ON PHASE
	HIGHER	GAIN
SATURN V	1st	PHASE
	2nd	GAIN AND PHASE
	HIGHER	GAIN

ILAF Concept

The ILAF concept is a sensor location concept designed to defeat changes of mode frequency and shape with changing flight condition. ILAF stands for Identically Located Accelerometer and Force Producer. The two ILAF notions are

- By putting the sensor near the force producer, the phase relation between the sensor and force producer will be nearly independent of mode shape, the effect of force on each mode and the acceleration response due to each mode being in nearly constant ratio.
- Using an accelerometer and integrating (90 degrees phase lag at the resonant frequency) rate damps that flexure mode. (A rate measurement with lead to compensate for actuator and aerodynamic lags would in principle serve the second purpose as well, but it would fail the first objective as rate depends upon mode slope and force effect on mode amplitude.)

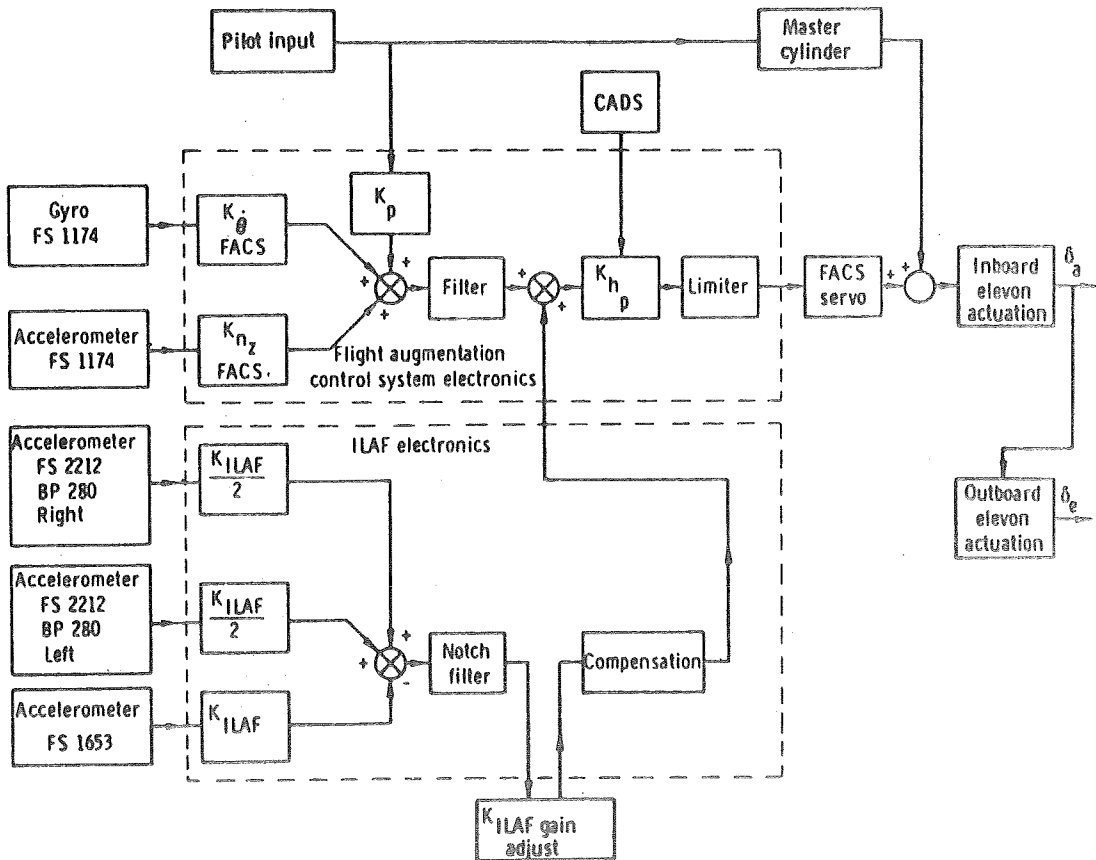


XB-70 ILAF Implementation

This slide shows the ILAF system flight tested on the XB-70 and reported in 1966.³ There are four points to be made regarding this system.

1. ILAF can't be used on a large missile where the control force is gimbaled thrust as the acoustic noise there will saturate any sensor. But ILAF is very well suited for aerodynamic control surfaces on winged vehicles.
2. Winged vehicles in general have more complex mode shapes than missiles and these mode shapes and frequencies vary more with flight condition. In consequence, parameter variations and uncertainties are a very large concern in aircraft.
3. This particular ILAF system was designed to be switched on over an existing rigid body control system, hence its appearance. Whether one regards flexure control as part of a SAS or in addition to a rigid body SAS is a matter of semantic preference; the flexure control problem is the same in either case.
4. Gains were changed manually with flight condition in this system (it was an experimental system); the system was not a fully automatic, scheduled gain, all flight-condition flexure control system.

XB-70 LONGITUDINAL SYSTEM



XB-70 ILAF Performance

There are very little XB-70 flight test performance data in turbulence in the literature. The data shown here were calculated in the course of design.⁴ The basic aircraft data shown are for the XB-70 controlled by a rigid body SAS.

These data show the ILAF system to be beneficial.

CALCULATED $\sigma_{n_z}^2 / \sigma_{\omega_g}^2$ AT PILOT STATION

MACH	WEIGHT	ALTITUDE	BASIC A/C	ILAF
0.4	LIGHT	0	0.0467	0.0405
0.4	LIGHT	15,000'	0.0197	0.0124
0.4	HEAVY	7,000'	0.0389	0.0347
0.9	LIGHT	25,000'	0.0453	0.0405
0.9	HEAVY	25,000'	0.0501	0.0291
3.0	MEDIUM	70,000'	0.0125	0.0091

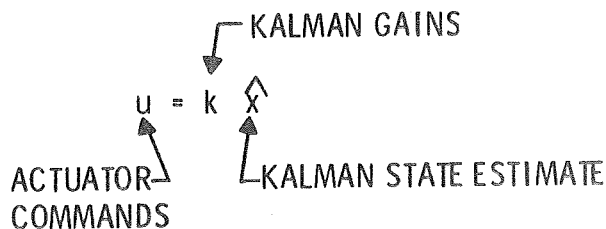
Quadratics

The final flexure control technique that will be described is the quadratic technique employed on the AFFDL sponsored LAMS program.

The basis of this technique is to design a practical flexure control system by simplifying a least-mean-square-response optimal system. The Kalman optimum system is to generate actuator commands by multiplying least-mean-square-error state estimates by control gains. In practice the estimation filters are far too complex to be implemented and the optimum system must be grossly simplified.

The inherent advantage of the quadratic design methods is that they are inherently capable of designing multiloop control systems (systems with multiple control inputs, multiple sensed responses, and multiple controlled responses). Frequency response methods are far less able to cope with this dimensionality.

The advantage of multiloop control is that one can always do a better job forcing and sensing multiple degrees-of-freedom with more control inputs and sensors. For example, it is easier to control a symmetric wing mode with ailerons, leading-edge surfaces, and elevator than with elevator alone; an elevator can only force the wings by bending the fuselage. A second example, it is easier to obtain rigid body pitch performance and first fuselage mode damping with elevator and canard than with elevator alone; with both controls the two degrees of freedom can almost be decoupled from each other. The B52 LAMS pitch control system employed elevator and symmetric ailerons and spoilers and four rate gyros, and it was designed to simultaneously control eight different vehicle responses.

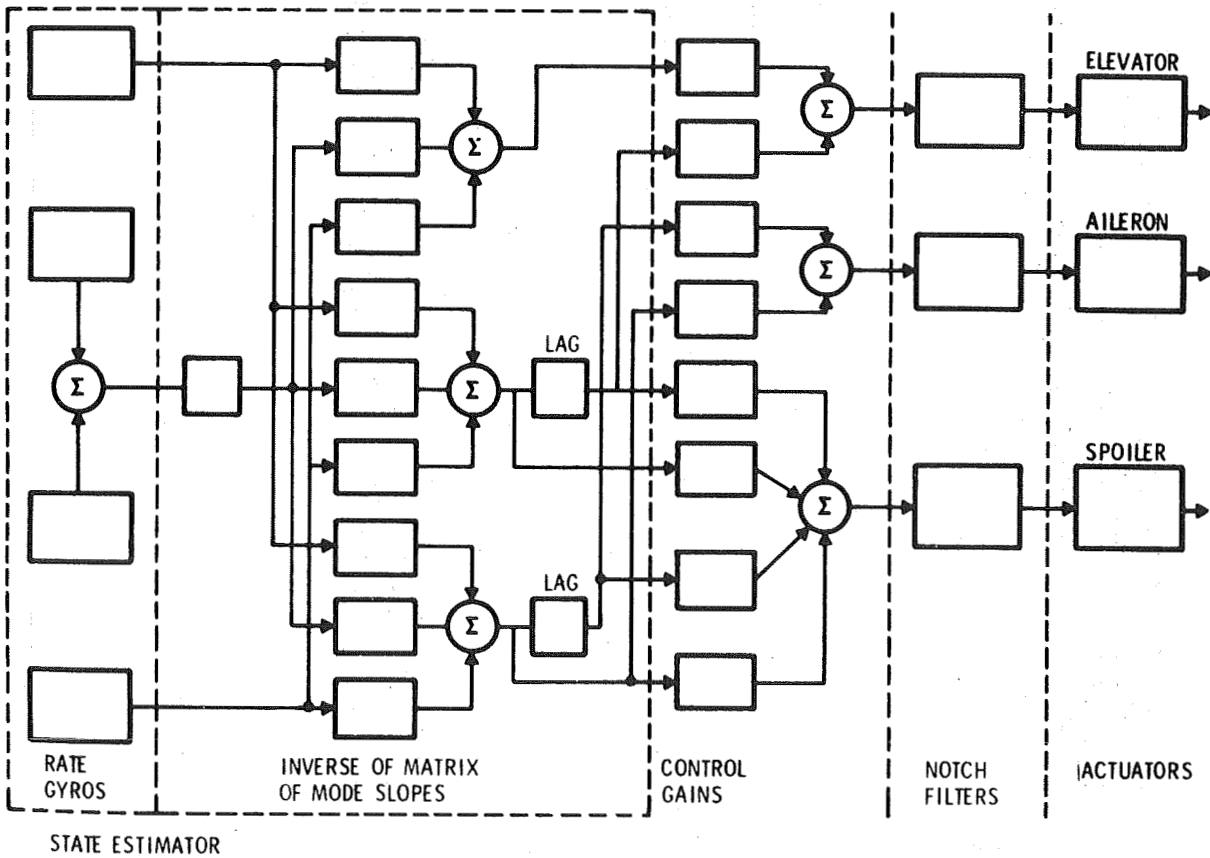


B52 LAMS Pitch Control System

The B52 LAMS pitch control system flown is shown in this slide.⁵ Note the notch filters used to evade surface flutter and actuation problems. The system, left to right, consists of sensors, approximation to a state estimator, control gains, notch and drift "fix" filters, and actuation.

This system was designed to fly any of three specific flight conditions (it too was an experimental system). Gains were changed manually with flight condition.

B-52 LAMS LONGITUDINAL BLOCK DIAGRAM

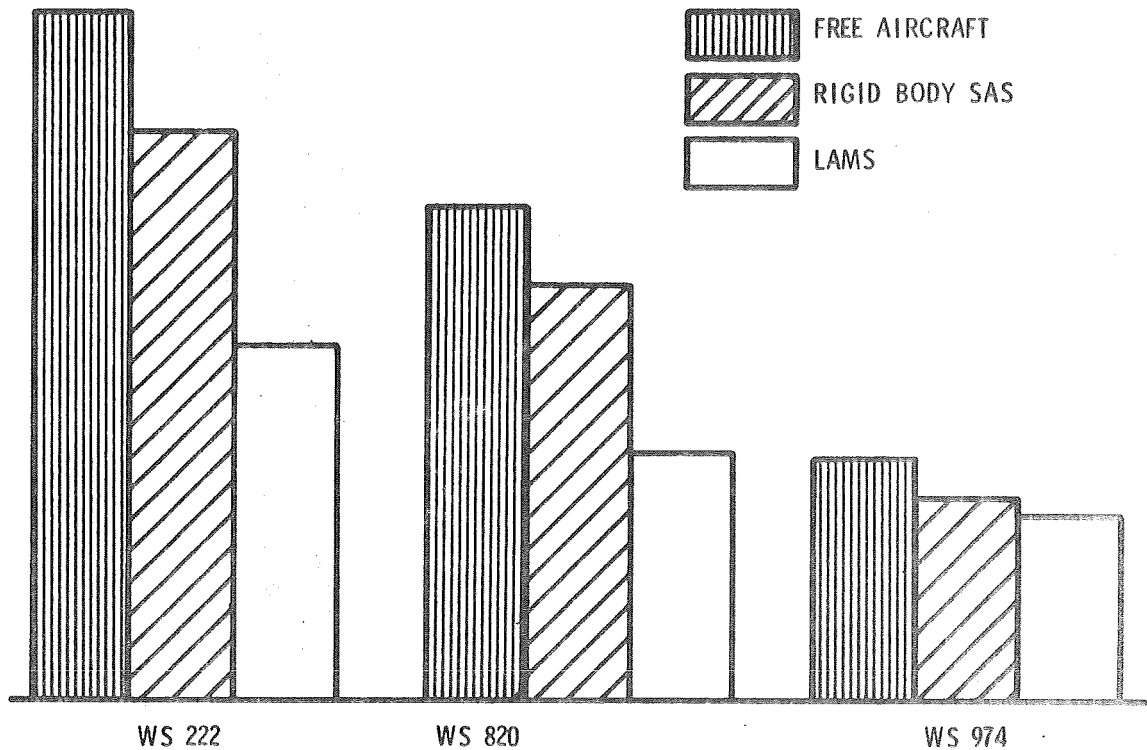


B52 Fatigue Response

This slide shows structural fatigue damage rates due to turbulence calculated from flight test data for the B52 at various vehicle locations. The height of each bar is proportional to the damage done. These results and others show the LAMS system to be beneficial.

This slide tells an incomplete story of structural fatigue lifetime. The slide relates only to fatigue in turbulence, perhaps twenty percent of total aircraft fatigue. Also, the fatigue theory used to generate these results is based upon a chain of weakly supported hypothesis (Palmgren-Miner linear cumulative damage, Gaussian stresses, Rice level crossing method of counting cycles). The results are thought meaningful for comparing systems but not as being good measures of fatigue lifetime.

FATIGUE DAMAGE RATES



Status

The status of flexure control practice is summarized on this slide.

Single loop designs (notch filtering and simple ILAF applications) are well within current design capability. Many such systems have been flown.

Multiloop designs have been flown, but only with manually set gains at selected flight conditions. No fixed gain or adaptive multi-loop system that controlled flexure over an entire flight envelope has been flown. This is the next major milestone for flexure control.

Achieving this milestone will be difficult. I would like to close this talk with comments on why it will be difficult.

SINGLE LOOP - FLIGHT PROVEN, PRACTICAL

**MULTI-LOOP - HAVE YET TO FLY A SYSTEM (FIXED)
GAIN OR ADAPTIVE) OVER AN ENTIRE
FLIGHT ENVELOPE**

B52 Flexure Modes

First, the physics of flexure control are not simple.

This slide shows B52 longitudinal resonant frequencies and damping with and without flexure control. Note that the first and sixth modes were the only ones controlled, that the frequencies of both were increased, and that the damping of one was decreased while the other was increased.

On a YF-12 analysis we are doing at Honeywell, we are achieving best results by lowering the first flexure mode, the opposite of the B52 result.

NAR/LAD damped the lowest three modes on the XB-70 ILAF study.

With this history of conflicting examples, no one can predict a priori which Shuttle modes should be stiffened, which should be damped, which should be slowed down.

Second, current control theory and computer computation methods are not fully up to the job. For example,

- We do not know how to include parameter variations implicitly within a multiloop design method (the equivalent of gain and phase margin for single loop systems).
- We do not have any fundamental mathematical approach to specifying the form of a practical multiloop controller (how many filters, how many sensors, what sensors and where should they be, etc.). We must rely on trial and error and experience.
- We do not have fast enough computation methods. The methods available today are more than 100 times faster than those used in the B52 LAMS design, but we still can't afford computer searches for best gains for a high order, multiple flight condition design.
- We do not have a good theory for designing fail-safe multiloop systems.

The research and development fraternity is working on all of these problems, and the fraternity has a good record of consistent progress. I am personally confident that we will be able to meet the demands of Shuttle.

For these reasons I see active flexure control as being at the edge of our technical capability. It should offer a Shuttle a viable alternative to adding stiffening weight.

FIRST TEN FLEXURE MODES

FREQUENCY		DAMPING	
FREE A/C	LAMS	FREE A/C	LAMS
1.07	1.23	.146	.109
1.91	1.92	.056	.051
2.02	2.02	.035	.035
2.34	2.35	.041	.033
2.37	2.40	.086	.082
2.66	3.10	.095	.164
3.13	3.09	.038	.037
3.42	3.46	.085	.063
5.35	5.32	.072	.074
5.79	5.79	.045	.043

REFERENCES

1. Aviation Week, May 4, 1970, p. 53.
2. "Effects of Structural Flexibility on Launch Vehicle Control Systems," NASA SP 8036, February, 1970.
3. Wykes, J. H., and Kordes, E. E., "Analytical Design and Flight Tests of a Modal Suppression System on the XB-70 Airplane," AGARD 34th Flight Mechanics Panel Meeting, Marsulles, France, April 21, 1969.
4. Wykes, J. H., and Mori, A. S., "An Analysis of Aircraft Structural Mode Control," AFFDL TR 65-190, June, 1960.
5. Burris, P. M., and Bender, M. A., "Aircraft Load Alleviation and Mode Stabilization (LAMS)," AFFDL TR 68-158, April, 1969.

N70-40966

FLY-BY-WIRE

E. Bumby

Grumman
Bethpage, New York

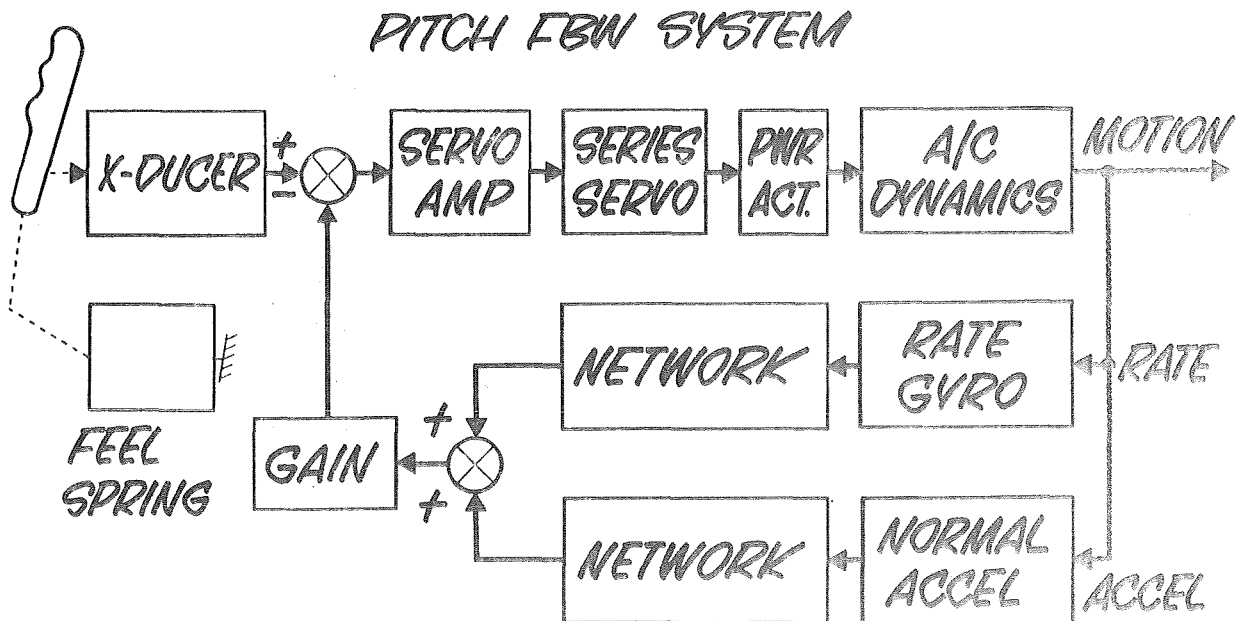
Introduction

Recent mechanizations of flight control systems for high-performance aircraft are trending toward electrical rather than mechanical systems. These electrical flight controls have been given the generic name "Fly-by-Wire." Present studies and projected implementations integrate this function within the automatic flight control system with a view toward greater survivability, reduced weight, and improved performance of military aircraft. The size, flight regime, and projected structural design of the Earth Orbiting Shuttle create a situation where the fly-by-wire implementation of the aerodynamic flight control system is a definite possibility. This paper is an introduction to the fly-by-wire concept and points out some techniques for solving the major problems associated with the development of such a system.

System Description

The Fly-by-Wire (FBW) flight control system has been previously defined as "an electrical primary flight control system employing motion feedbacks so that vehicle motion is the controlled parameter." That is, control stick and rudder pedal positions correspond to vehicle rates and accelerations. These positions are sensed by transducers to generate commands to the control system. These commands are summed with the motion sensor (rate gyro and accelerometer) signals to produce an error signal which drives the control surface actuators. Thus, this closed-loop system positions the control surfaces to meet the particular flight requirements throughout a mission.

The FBW system is more than a means of maneuvering the aircraft in accordance with the pilot's commands. The system also provides the necessary stability augmentation system (SAS) functions since the feedbacks are inherent within the FBW system. Disturbances create vehicle motion which causes the sensors to transmit error signals to the control surfaces. Thus, the effects of the disturbances are damped and the undesirable aircraft rates are returned to zero. The full surface authority of the SAS function, a benefit of the inherent reliability built into the FBW system, provides a degree of stability augmentation heretofore unavailable in any aircraft. However, there are several technical problems which require extensive investigation prior to the installation of an FBW flight control system in the Earth Orbiting Shuttle.

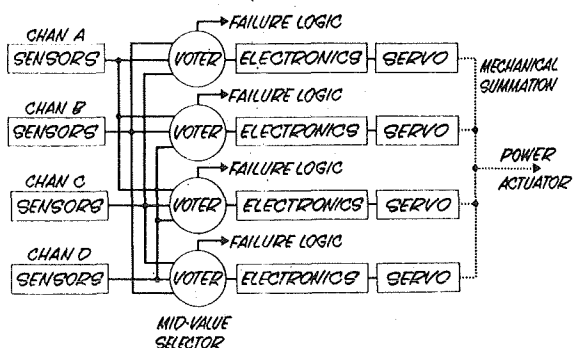


Redundancy Requirement

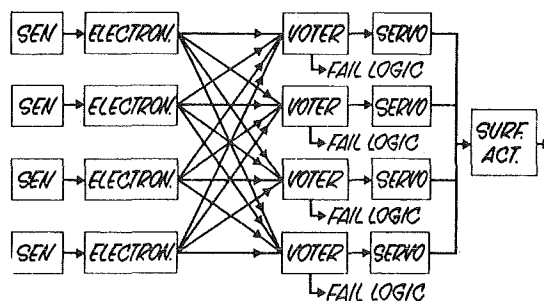
The FBW system must be highly reliable; it must be at least as reliable as the mechanical system it replaces. It has been debated in many forums as to whether the electronics or hydraulics are the weak link in the system, and there is insufficient time here to renew the discussion. Instead, the data available have been used in preliminary computations, resulting in the conclusion that a quadruple-redundant configuration is required. However, it is insufficient to just provide an implementation employing four independent channels. To take full advantage of the quadruple-redundant configuration, additional networks are required in each channel thereby ensuring that the system can sustain two identical failures and remain fully operational.

Voter-monitor networks in each channel select the valid signal, detect failures, and isolate failed signals. The networks must also signal their own failure and prevent the propagation of failures between channels. In implementing a quadruple-redundant system we can use either sensor voting (Fig. 2), electronics voting (Fig. 3), or a combination of both. In each case the voter output is a valid signal until two or three failures occur. In the former case the voter output remains valid until a second failure occurs, and then the voter removes that channel as an active component. In the latter case it requires three failures for a voter to reduce the number of operating channels. The voter is the only functionally non-essential component in the electronics channel, but is the heart of the quadruple-redundant system.

QUADRUPLE FBW-FCS (SENSOR VOTING)



QUADRUPLE FBW-FCS (ELECTRONICS VOTING)

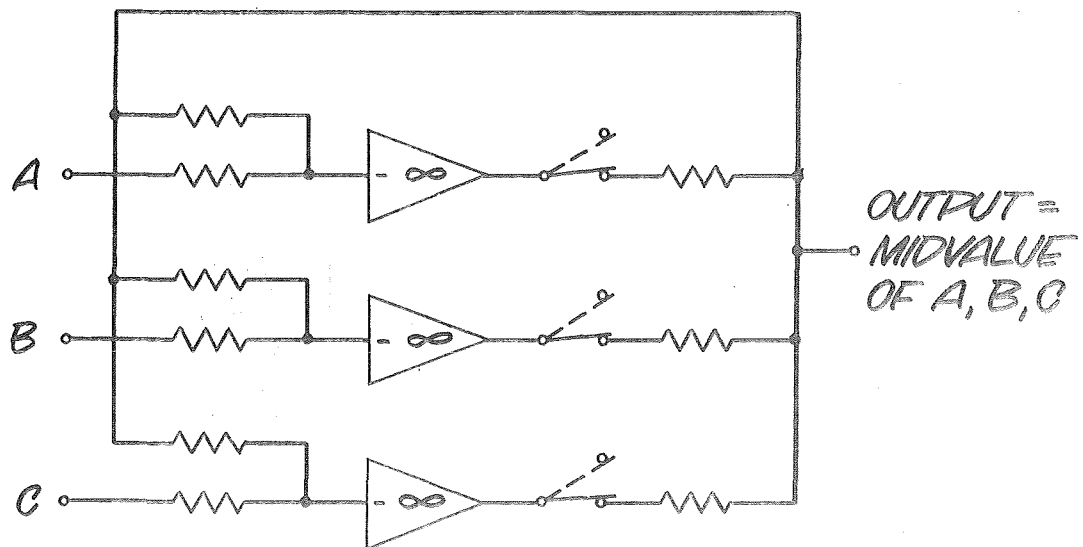


Triple-Signal Voter

This type of voter operates on three signals, of which the mid-value one is selected as the valid signal. The high-gain operational amplifiers will be driven to one of three states as a function of the error voltage present at the input of the amplifier. Ideally, all three input signals are identical, but, due to varying component tolerances of the devices producing the input signals, one signal will be the lowest, one the highest, and one the mid-value. Therefore, the amplifier with the highest input signal will be driven into positive saturation by a positive error signal, and, in a like manner, the amplifier with the lowest input signal will be driven into negative saturation. Thus, the amplifier with the mid-value input signal is in the active region transmitting this signal to the next functional block of the system.

This type of voter then becomes a two-input comparator upon the failure of either one input or a branch in the voter itself. In this case a single input failure appears at the input of three voters (Fig. 2) without affecting system performance. The failure of a second input signal will cause two of the four voters to shutdown the associated channel electronics, leaving two active channels. A third failure then results in the fail-safe condition for that axis.

THREE CHANNEL VOTER-MONITOR

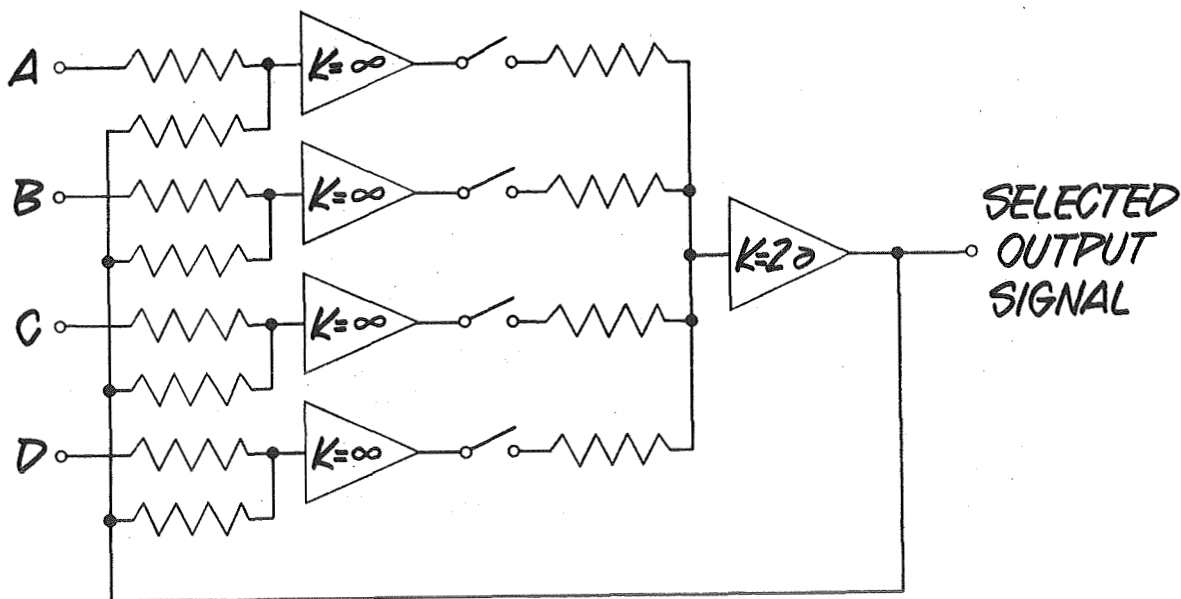


Quadruple-Signal Voter

For quadruple-signal voting, the second-from-lowest value of the four signals is selected as the valid signal. This value was selected as the basis for this configuration to ensure that, if two hardover failures in the same direction occur consecutively, the second of them cannot be selected as the valid signal. The logic is that we can afford a null or zero command as the valid signal in some instances, but in no case can we afford to select a failed hardover as a valid command. In the case of this network, a bias is needed to ensure that when all inputs are functioning properly, the valid signal is indeed the second-from-lowest. This network of amplifiers functions similarly as in the case of the triple voter. The bias must be a negative voltage so that two amplifiers will be driven into positive saturation, one amplifier driven into negative saturation, and the fourth left in the active region.

This network becomes a mid-value selector upon a single failure; at this time the bias must be removed to ensure that the mid-value of the remaining three signals is selected as the valid signal. The voter continues to function in an identical manner upon second and third failures, as does the triple-signal voter for the first and second failures, respectively.

4 CHANNEL VOTER



Voter-Monitor Requirements

If one examines the functions of these two types of voters from a single-point-failure viewpoint, the conclusion is reached that further investigation is required. The following requirements have been set as a goal for the voter-monitor networks to be employed in any FBW control system:

- Select second-from-lowest absolute value
- Select mid-value after first failure
- Select lower value after second failure
- Shutdown axis after third failure
- Fail-safe monitoring; must signal own failures
- Maintain both gain and linearity with failures
- Failed network must latch until manually reset
- Transient-free upon signal failure

At present there is no scheme which meets all of these requirements, but it is hoped that a solution will be found in the near future. It may appear that these networks have been unduly stressed, but, in truth, they are the heart of the quadruple-redundant system. One need only refer to Fig. 1 to see that the voter-monitor network design holds the key to a successful FBW system.

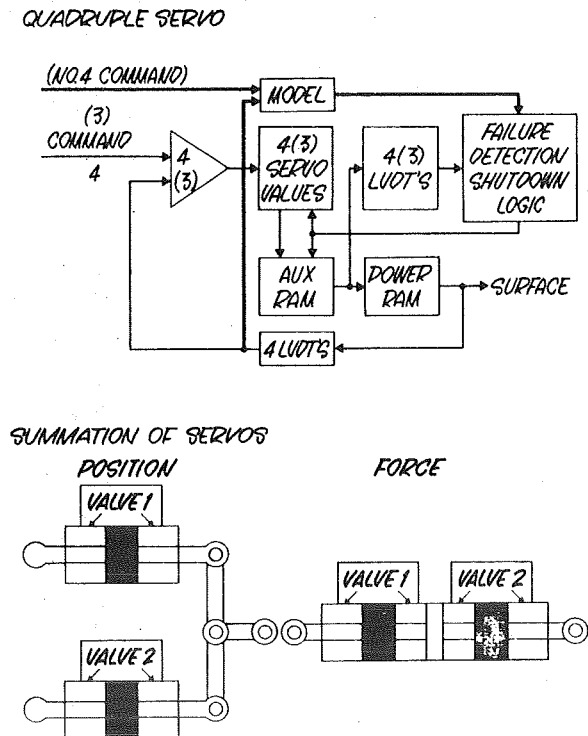
VOTER REQUIREMENTS

- SELECT 2ND FROM LOWEST ABSOLUTE VALUE
- SELECT MID-VALUE AFTER 1ST FAILURE
- SELECT LOWER VALUE AFTER 2ND FAILURE
- SHUTDOWN AXIS UPON 3RD FAILURE
- FAIL-SAFE MONIT'G - MUST SIGNAL OWN FAILURE
- MAINTAIN BOTH GAIN & LINEARITY WITH FAILURES
- FAILED NETWORK MUST LATCH UNTIL MAN. RESET
- TRANSIENT FREE UPON SIGNAL FAILURE

Electronics/Control Surface Interface

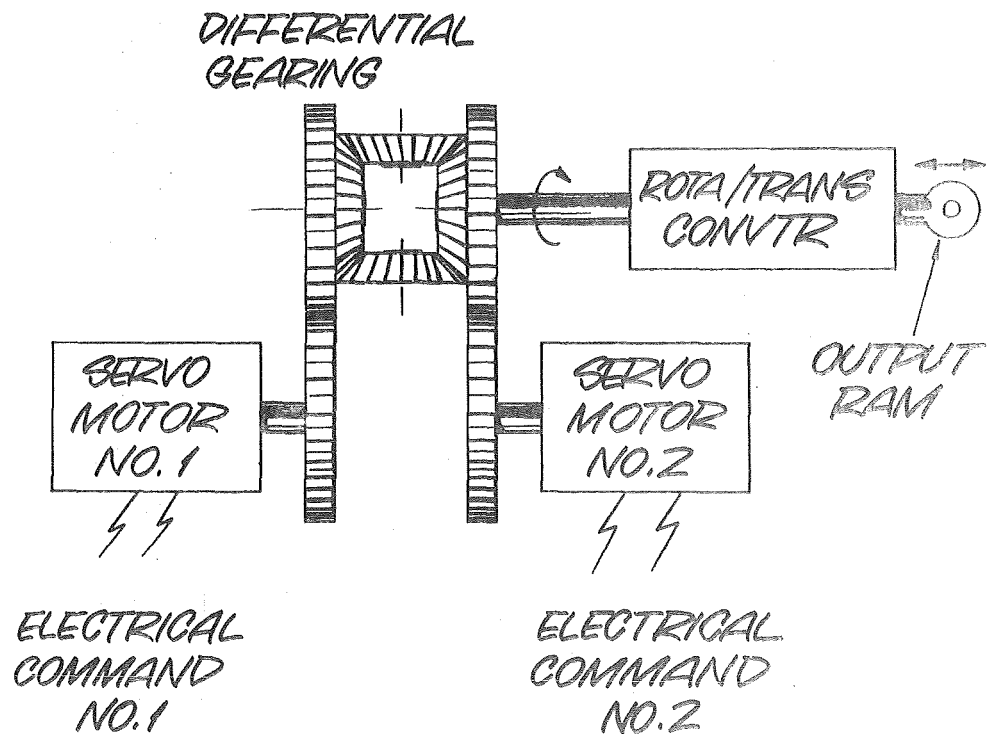
Another area of key importance is the electronics/control surface interface. That is, obtaining a single mechanical position from four electronic signals. Many quadruple-redundant, electrohydraulic servo actuators have been designed recently. Some have four active channels, some have three active channels with a model (Fig. 7). Implementation in each case varies from active-standby configurations to position- or force-summing (Fig. 8) of the active channels. Each configuration has unique features which must be evaluated with respect to the particular airframe design, mission, and performance requirements. In the case of force-summation, degraded performance results from a failure. Degraded performance also results after a failure in position-summing, which can employ switching functions to return the servo to its original authority.

The use of the active-standby configuration, where one channel is selected as the primary channel and the others as backups, is questionable. The addition of special monitoring functions to ensure that no failure is present in the switching function when a primary-channel failure occurs adds to the servo complexity and reduces the overall reliability. This monitoring function is required to ensure that when a switchover is required, control will not be lost due to a faulty switching function.



A new configuration, in the form of an electromechanical servo actuator, has recently been proposed to perform this function. This unit offers several distinct advantages over the electrohydraulic unit. First, the need for a quadruple hydraulic power source is eliminated; second, velocity-summing is used which maintains both position and force, unlike the position- and force-summing methods in which neither is maintained in the event of a failure. The ram velocity is a function of the number of channels operating and, by the addition of some minor switching functions to the failure detection circuits, it is possible to maintain the maximum available ram rate in the presence of failures. This is the most promising design to come along recently and appears to have direct application to the shuttle.

ELECTRO-MECHANICAL SERVO



Electrical Power Redundancy

Another important function which requires a critical review when applying an FBW flight control system to the shuttle is the electrical power distribution system. Extreme care must be exercised to prevent generator, power bus, or any other equipment failure from transmitting the failure to other power busses or generators. The power busses feeding the FBW system must be so arranged that power is available to all four channels of each control axis at all times, regardless of the number of operating generators.

Conclusion

This presentation was intended to indicate some of the major design problems involved in configuring a fly-by-wire flight control system for the shuttle. The techniques to solve these problems are available and need only be applied to the development of hardware. Subsequent to voter-monitor and interface hardware development, reliability can be verified from a single-point-failure analysis. Finally, a complete system should be evaluated on a moving-base simulator to verify the operational characteristics.

N70-40967

SCANNING LASER RADAR FOR RENDEZVOUS AND DOCKING

Terry Flom

ITT Aerospace/Optical Division
San Fernando, California

ABSTRACT

This paper discusses the development of laser radar systems that can be used to aid vehicles to perform automatic rendezvous and docking maneuvers. A description is presented here of a laser radar system under development that has the capability of scanning its narrow laser transmitter beam simultaneously with an equally narrow receiver field-of-view without the use of mechanical gimbals. System performance characteristics (i. e., maximum range, range accuracy, angle coverage, etc.) and the general characteristics of size, weight and power are described for this developmental system. In addition, comments are made on the basic advantages of laser radar over microwave radar for spaceborne applications.

A radar range analysis, for laser systems in general, indicates the basic capabilities of laser radar systems for both the cooperative and non-cooperative (skin) target applications. This paper includes pertinent graphs such as target range versus required laser power for some particular rendezvous and docking problems.

PRECEDING PAGE BLANK NOT FILMED.

INTRODUCTION

Laser systems that can be used to aid vehicles to perform automatic or manual rendezvous and docking maneuvers have and are being developed. The particular hardware system that is described in this paper has been given the name Scanning Laser Radar (SLR) in order to best describe its general function (radar); and also indicate the specific type of radar used. Radar is an electronic device for the detection and location of objects¹ and almost any electromagnetic transmitter-receiver can be used as the electronic device. In the radar system described here, the electromagnetic transmitter emits energy in the optical spectrum using a laser. An optical lens system collects the laser radiation and a photo-sensor converts the optical energy to electrical energy for signal processing. The word scanning is used to indicate that the narrow radar beam, associated with laser systems, is pointed and scanned internally within the radar system in order to cover a wide field-of-view. The scanning technique used by the SLR does not need mechanical gimbals, and it has the capability of scanning the narrow laser transmitter beam simultaneously with an equally narrow receiver field-of-view.

A short section on the general system development follows this introduction. Next is a major section that describes in detail the SLR under present development. Also in another short section a few pertinent comments are made which show the advantages of optical (laser) radar over microwave radar for spaceborne applications. The last section is a laser radar range analysis, and it graphically shows the required laser power versus target range for both the cooperative (corner cube reflector) and non-cooperative (skin) target acquisition cases.

GENERAL SYSTEM DEVELOPMENT

ITT's recent and present involvement in the development of laser radar systems for spaceborne rendezvous and docking applications are summarized below.

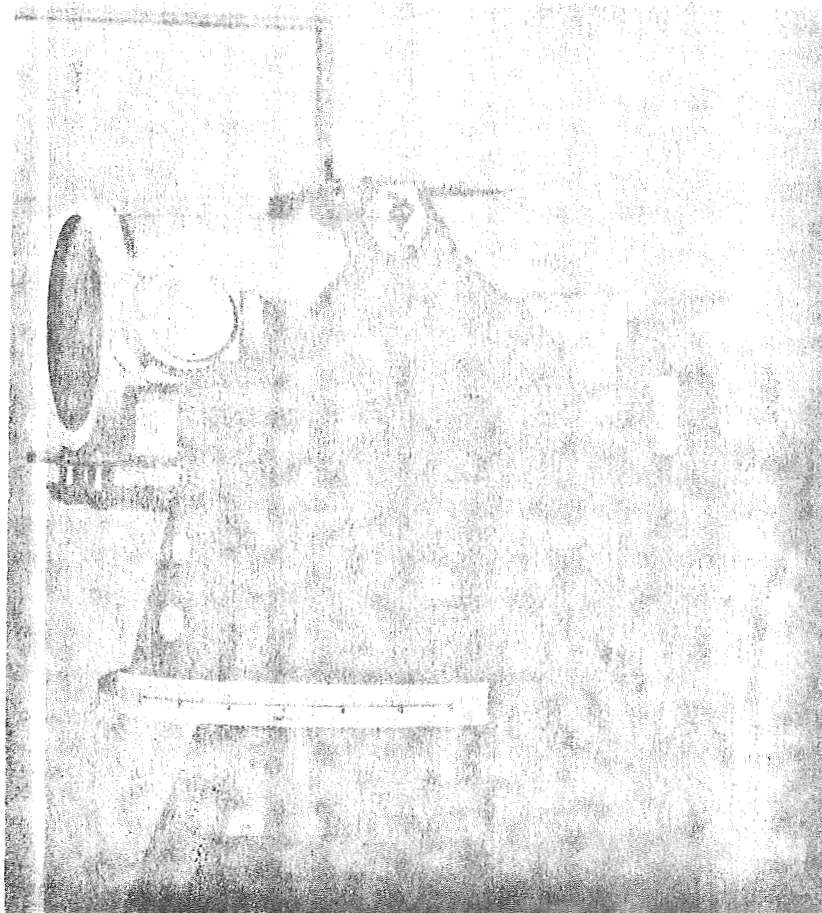
- "LASER GUIDANCE SYSTEM FOR RENDEZVOUS & DOCKING"
Contract NAS8-11673, 1964-67

A laboratory prototype radar system (Generation #1) for rendezvous and docking, was designed, built, and tested. The system used gallium arsenide (GaAs) injection laser arrays and GaAs spontaneous diodes as transmitting sources and a scanning optical detector (image dissector) as the receiver sensor. The prototype system developed during this program was the culmination of more than five years of work performed both in-house at NASA/MSFC and by industry under contract to NASA. The program progressed from a feasibility study, through a breadboard development and evaluation, to the development, test and evaluation of the prototype system.² Short-range testing on a six-degree freedom docking simulator was performed at Martin-Marietta in Denver, Colorado.³ Two hundred consecutive dockings were performed successfully. Long-range tests were performed at California White Mountain Research Station (10,000 feet elevation). The laser system acquired and tracked a supercharged helicopter out to an effective freespace maximum range of 152 km (95 miles).

Figure 1 is a picture of the generation #1 system, and a chart of the test results.

- "OPTICAL GUIDANCE SYSTEM FOR RENDEZVOUS & DOCKING"
Contract NAS8-20717, 1967-69

The design and analysis of an Optical Guidance System that could be used on an Apollo Applications Program flight experiment was accomplished under this effort. General equipment specifications such as size, weight, power and thermal constraints were generated. Analysis of expected system performance (i. e., maximum range, range accuracy, tracking rate errors, etc.) was also accomplished. It should be noted that this interim designed system did not have the newly developed laser beam steerers, and therefore, does not accurately reflect the overall system performance of the lightweight Scanning Laser Radar system that is being developed for space flight using a 1972 technology base.



SHORT RANGE TESTS

• TEST SITE

DOCKING SIMULATOR
MARTIN MARIETTA, DENVER, COLORADO

• SUMMARIZED RESULTS

ALL DOCKING RUNS SUCCESSFUL (IN 200 RUNS)
EXCISE CONDITION AIRS ERRORS

Δ RANGE	< 0.1 METER
Δ RANGE-RATE	1.6 CM/SEC
Δ LATERAL POSITION	0.30 IN
Δ VERTICAL POSITION	0.30 IN
Δ YAW ANGLE	< 0.1 DEG
Δ PITCH ANGLE	< 0.1 DEG

LONG RANGE TESTS

• TEST SITE

MAINTAIN T80-T8 HELICOPTER
U. OF CALIF. WHITE MOUNTAIN RESEARCH STATION

• SUMMARIZED RESULTS

SUCCESSFUL ACQUISITION & TRACKING OF
HELICOPTER AGAINST SUNLIT CLOUD BACKGROUND
EFFECTIVE FREESPACE MAXIMUM RANGE OF
152 KM (95 MILES)

Figure 1. Picture of Generation No. 1 System and Chart of Test Results (1964-67).

- "ADVANCED LASER TRACKING TECHNIQUE"
Contract NAS8-20833, 1967-71

ITT is currently developing a lab prototype radar system (Generation #2) herein referred to as the lightweight Scanning Laser Radar (SLR) system. A piezoelectric beam steerer, a single mode GaAs laser transmitter, and a scanning optical detector (image dissector) will enable the SLR to acquire and track targets anywhere within a 30 degree x 30 degree field-of-view without the use of mechanical gimbals. Folding optics and maximum practical use of integrated circuits will allow the Generation #2 system to be packaged in a possible space flight configuration to demonstrate the size, weight, power and accuracy advantages of optical radar techniques.⁴ The estimated characteristics of the lightweight SLR described later in this paper are derived from the lab prototype being built under this contract. This system will be completed and be ready to start the rendezvous and docking simulator tests in early 1971.

- "AUTOMATIC RENDEZVOUS & DOCKING STUDY"
Contract NAS8-23973 (Phase I) 1969-70

Computer programs to simulate the chaser and target vehicle motions during certain phases of automatic rendezvous and docking of two space vehicles while in earth orbit were developed. The emphasis of the computer simulation was to study the performance of the Scanning Laser Radar system used in a closed loop vehicle control system. Vehicle fuel requirements for some selected automatic station-keeping and docking closure maneuvers was one of the primary data outputs of the study.⁵ The Phase I study used the control parameters of the LM (chaser) and the AAP workshop (target).

- "EXPANDED EVALUATION AND DESIGN OF THE SCANNING LASER RADAR"
Contract NAS8-23973 (Phase II & III) 1970-71

Phase II: Evaluate the SLR performance similar to the phase I effort except use the preliminary characteristics of the space shuttle orbiter (chaser) and the space station (target).

Phase III: Design the SLR to meet the requirements of the space shuttle. For trade-off analysis and flexibility, more than one system configuration will be designed until the shuttle requirements for rendezvous and docking have been finalized. Automatic test and checkout capability is to be designed into the system.

SYSTEM DESCRIPTION - SCANNING LASER RADAR

The lightweight Scanning Laser Radar (SLR) system will accurately determine the relative position and orientation between two vehicles in space flight. The present hardware under development is aimed at meeting rendezvous and docking requirements when the target is considered cooperative (i. e., having a minimum of at least a small optical reflector mounted on the target in order to enhance the radar reflection). The non-cooperative passive case (i. e., bouncing a radar beam off the skin of the target vehicle) requires significantly more laser transmitter power which results in increasing the radar system size, weight, and power because a different laser transmitter and associated components must be incorporated. In the lightweight Scanning Laser Radar system for cooperative targets the laser power is a small percentage (<10%) of the total power required for the entire radar system. For the non-cooperative passive target case the power required for the laser transmitter can become the dominant power consumer depending on the target range and the constraints of the initial target acquisition. A section later in this paper on laser radar range analysis will quantitatively show the significant differences between the two cases. This section will only pertain to the SLR for the cooperative target.

Figure 2 shows the Scanning Laser Radar (SLR) in a Vehicle Guidance and Control block diagram. The radar data from the SLR can be used in a closed loop control system to aid the vehicle to perform automatic rendezvous and docking maneuvers or the radar data could be displayed on an instrumentation panel to aid the astronauts in performing the rendezvous and docking maneuvers manually.

Two basic system configurations of the SLR are presented here. Both systems are identical in that they will provide the Vehicle Guidance and Control system with the eleven (11) basic data inputs shown pictorially in Figure 3. Simplified system

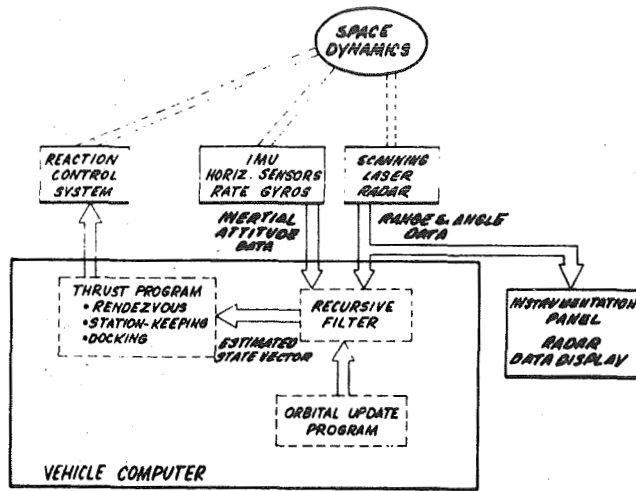


Figure 2. Vehicle Guidance & Control System Block Diagram

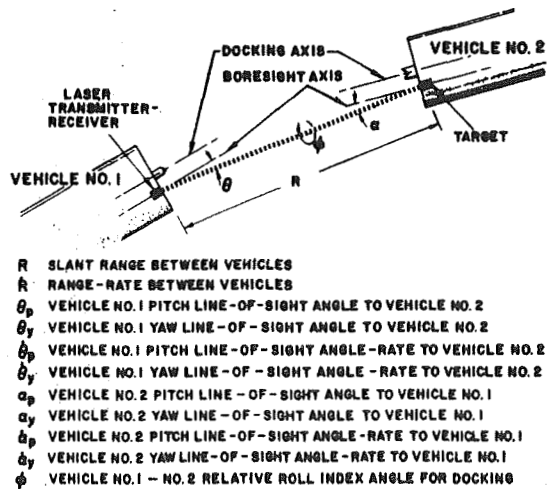


Figure 3. Basic Data Outputs of the Scanning Laser Radar

block diagrams of the two configurations (A1 and A2) are shown in Figures 4 and 5. Configuration A1 has a radar transmitter-receiver on one vehicle and the second vehicle has a target reflector-receiver. At this point we will arbitrarily define the line-of-sight angles from the radar transmitter-receiver to the target as the θ angles and vice versa for the α angles. Each θ and α angle is broken up into pitch and yaw components. Configuration A2 has a radar transmitter-receiver on one vehicle but the second vehicle has only a target reflector (no receiver, meaning no electronics!). In configuration A1 the target has an electronic receiver that measures the incoming angle of the laser radar beam, thus the " α " pitch and yaw angles with respect to the docking axis are measured by a direct measurement technique. This target receiver hardware is also identical to the receiver in the radar transmitter receiver. A communications or telemetry link between the two vehicles is then needed to transmit the data to one vehicle so that one vehicle Guidance and Control system can compute and direct the necessary flight maneuvers.

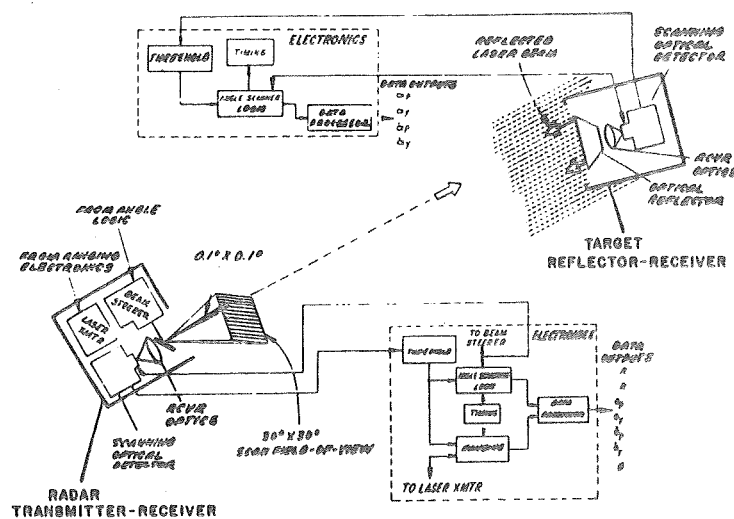


Figure 4. SLR Block Diagram - Configuration A1

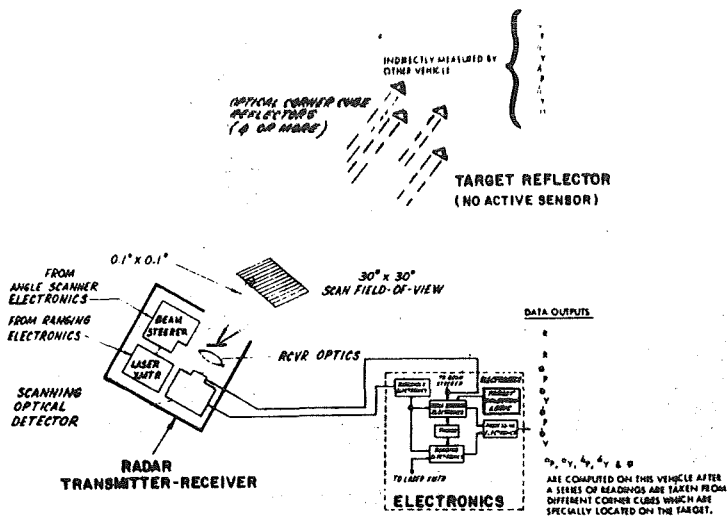


Figure 5. SLR Block Diagram - Configuration A2

As seen in Figure 4 the major subsystems that make up of the heart of the radar transmitter-receiver are the (1) laser transmitter, (2) beamsteerer, (3) receiver optics, and (4) the scanning optical detector. Figure 6 is a picture of the main components for each subsystem. Except for the scan electronics the major subsystems in the scanning laser radar are almost identical for Configuration A1 and A2. The above components will be integrated and assembled together to form the generation #2 system. Figure 7 is an artist conception of the radar transmitter-receiver package and the associated electronics package. The size, weight and power estimates are also shown. These subsystems will be integrated and in-house tested in the latter part of 1970. Rigorous testing is presently being accomplished on each subsystem. The major subsystems on the target reflector-receiver are (1) Optical corner cube reflector, (2) receiver optics, (3) scanning optical detector, and (4) the associated electronics.

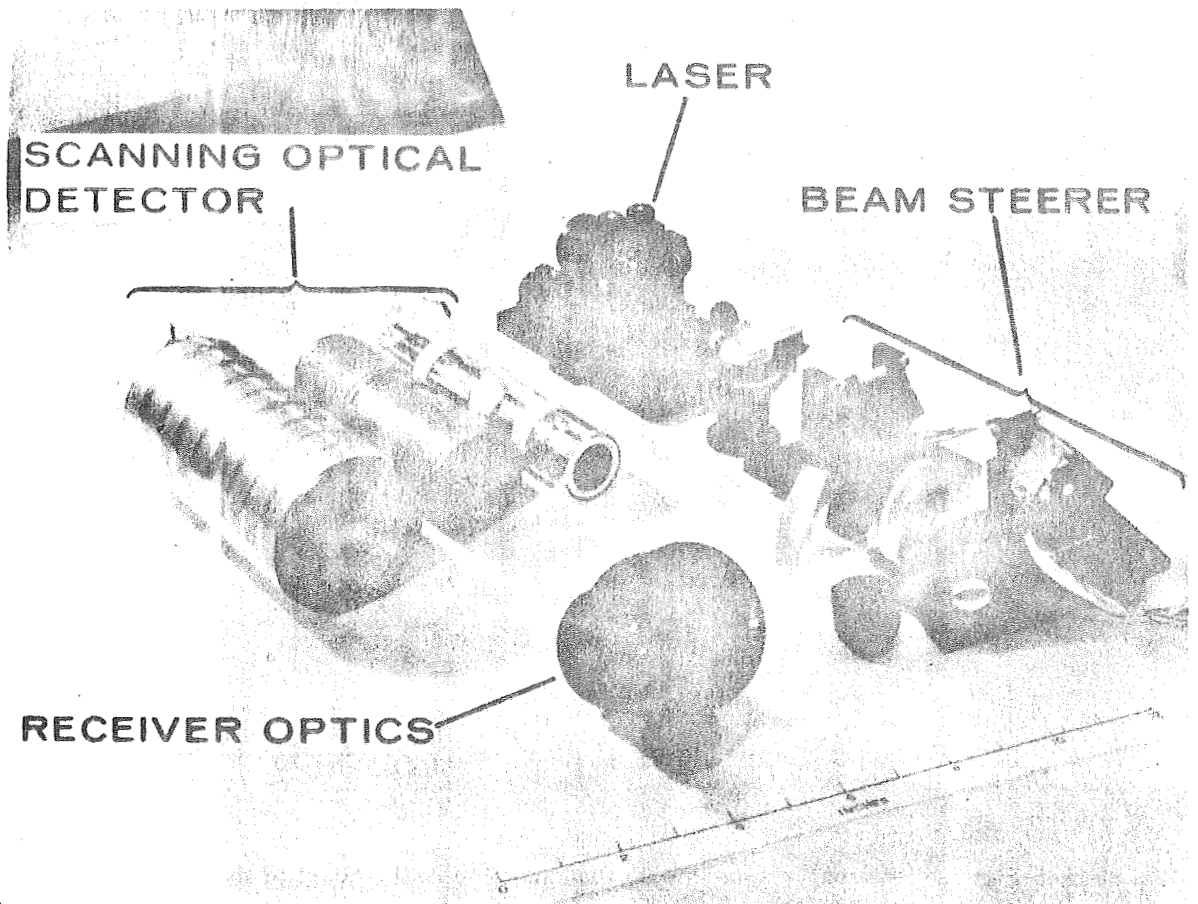


Figure 6. Picture of the Major Subsystem Components in the Radar Transmitter-Receiver

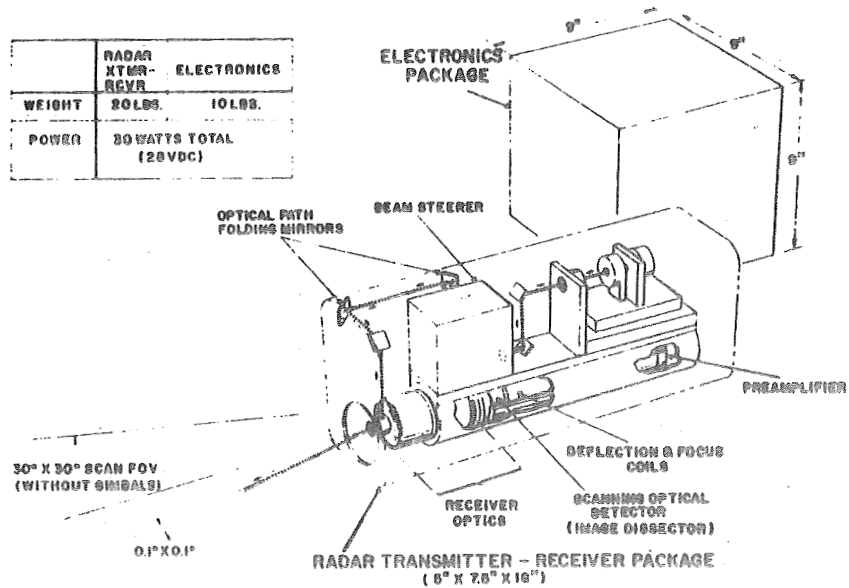


Figure 7. Artist Conception of Radar Transmitter-Receiver and the Associated Electronics Package

The estimated system performance characteristics for SLR configuration A1 are shown in Table 1 below.

TABLE 1. ESTIMATED SYSTEM PERFORMANCE CHARACTERISTICS
SCANNING LASER RADAR - CONFIGURATION A1

RANGE	
RANGE COVERAGE	0-120 km (± 75 MILES)
RANGE ACCURACY (3σ)	± 0.02% OR ± 10 cm (WHICHEVER IS >)
RANGE-RATE COVERAGE	0-1 km/SEC
RANGE-RATE ACCURACY (3σ)	± 1.0% OR ± 0.5 cm/SEC (WHICHEVER IS >)
ANGLE	
ANGLE COVERAGE (WITHOUT GIMBALS)	
PITCH & YAW (θ & α)	± 15°
ROLL (φ)	± 90°
ANGLE RESOLUTION	
PITCH & YAW (θ & α)	± 0.02° (0.35 mRAD)
ROLL (φ)	± 1.0°
ANGLE-RATE COVERAGE	
ACQUISITION MODE	
PITCH & YAW	0-0.4 DEGREE/SECOND
ROLL	TO BE DETERMINED
TRACK MODE	
PITCH & YAW	0-10.0 DEGREE/SECOND
ROLL	TO BE DETERMINED
ANGLE-RATE RESOLUTION	
PITCH & YAW	± 1.0% OR ± 0.01 DEGREE/SECOND (WHICHEVER IS >)
ROLL	TO BE DETERMINED
ACQUISITION TIME	
	0-140 SECONDS
TARGET REFLECTOR	
ACCEPTANCE ANGLE (α) OF THE INCOMING LASER BEAM*	± 30° PER INDIVIDUAL REFLECTOR
* TARGET RECEIVER CAN ONLY MEASURE INCOMING LASER BEAM ANGLE (α) OVER ±15° BUT THE TARGET REFLECTOR CAN ACCEPT AND REFLECT BACK ANY INCOMING BEAM OVER ±30°.	

The basic radar functions of target acquisition and tracking are accomplished by scanning the Scanning Laser Radar transmitter-receiver without the use of mechanical gimbals. In SLR system the transmitter beam is very narrow (0.1°) and the associated scanning optical detector simultaneously looks at only a similar very narrow field-of-view (0.1°) at any one instant of time. The transmitter-receiver are aligned so that the above two 0.1° angles are superimposed thus providing maximum radar transmitter-receiver efficiency with regard to the beam geometry. If the transmitter beam was larger than the receiver instantaneous FOV all the radar energy outside the receiver instantaneous FOV would be lost. If the transmitter beam was smaller than the receiver instantaneous FOV, the sky background noise and receiver dark current noise would be larger, thus reducing the signal-to-noise ratio of the radar system. Also, the angle readouts for the radar are derived from the direction of the received signal, and if the receiver instantaneous field-of-view was larger than needed, the angle accuracy of the radar system could be degraded.

The radar scan patterns for the acquisition mode and track mode are shown in Figure 8. The full square raster acquisition scan pattern covers 30 degree by 30 degree in digital steps of 0.1 degree by 0.1 degree (the instantaneous field-of-view), but can be logically programmed to scan smaller areas. Reduced raster scan could be used for example if the vehicle navigation data indicates that the target is within a smaller than a 30 degree by 30 degree field. Also, if the SLR loses track for any reason, the re-acquisition scan is already internally digitally programmed to scan a smaller angular field (1.0 degree by 1.0 degree) around the last sensed location before returning to the full angular field. The target presence signal is activated only when returns pulses having an amplitude above a preset threshold level appear within a designated timing gate or range interval. When this condition occurs, the SLR angle scanner automatically switches over to the track mode. In the track mode the instantaneous field-of-view (0.1 degree by 0.1 degree) is deflected in a cross-scan pattern, as shown in Figure 8 around the target location. The cross-scan pattern is exaggerated in the figure for better visibility. This pattern is driven to any point in the full 30 degree by 30 degree field-of-view in order to maintain track while the vehicles are in motion.

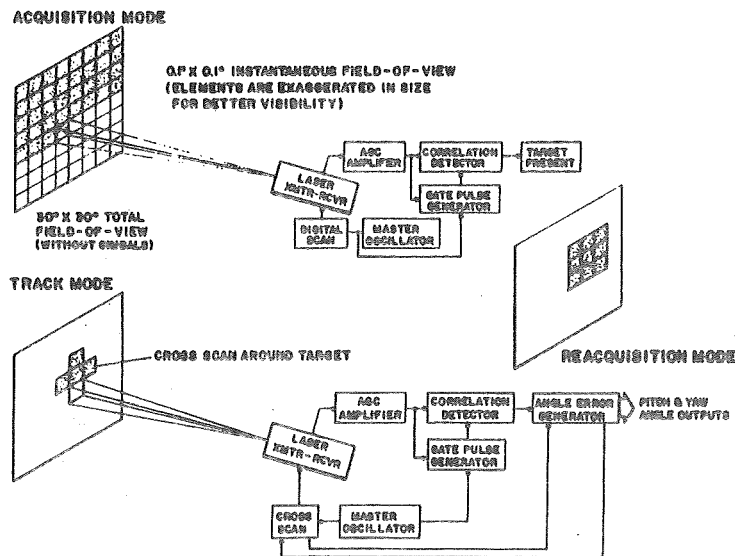
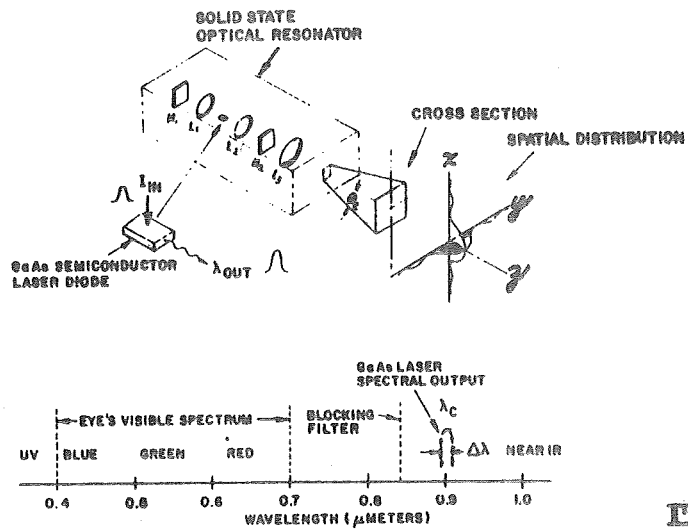


Figure 8. Radar Scan Patterns

There are key components associated with each major subsystem in the laser radar transmitter-receiver. The key component in the laser transmitter is the newly developed "single mode GaAs laser." It is small, lightweight and will operate at room temperature without cooling. The Gallium Arsenide (GaAs) laser is a specially fabricated semiconductor p-n diode. All p-n diodes, when forward biased electrically, emit radiation when the holes and electrons combine. In a laser diode a stimulated emission process occurs that amplifies the radiation on the p-n junction axis that is perpendicular to the parallel sides of the diode. The normal semiconductor laser diode emits its light into about a 15° beam, unlike most all other lasers (i.e., ruby, HeNe, YAG etc.) that emit with beamwidths much less than a degree. A laser diode by itself emits its radiation in many electromagnetic modes that causes the beam in the far-field to be very non-uniform and difficult to define. The new "single mode" GaAs laser places a laser diode in an optical resonator⁶ and this is schematically depicted in Figure 9. The only active component in the optical resonator is the laser diode itself; Figure 10 shows its relative size with respect to a dime. The optical resonator allows only one transverse electromagnetic mode (TEM_{00}) to oscillate with high gain in the resonator, and the resulting "single mode" laser radiation has a gaussian shaped far-field radiation pattern. Figure 11 depicts the difference between the far-field radiation pattern for multi-mode and single mode cases. In the multi-mode case the target can appear in the peaks and valleys of the radiation pattern and thus cause the return signal to vary tremendously, even to the point of preventing acquisition or of losing track of the target. Obviously then, for radar systems it is very beneficial to have the radiation in the far-field in the TEM_{00} single mode.



ITT

Figure 9. Single Mode GaAs Laser

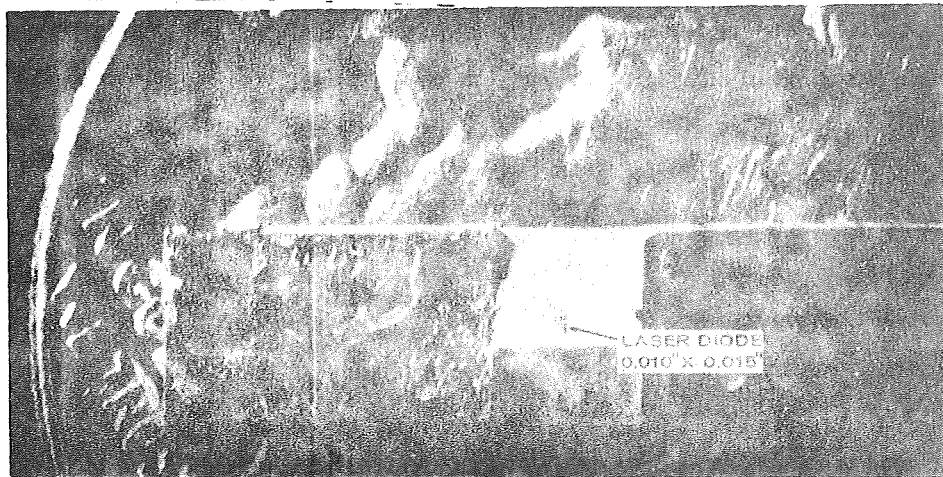


Figure 10. Picture of the Laser Diode

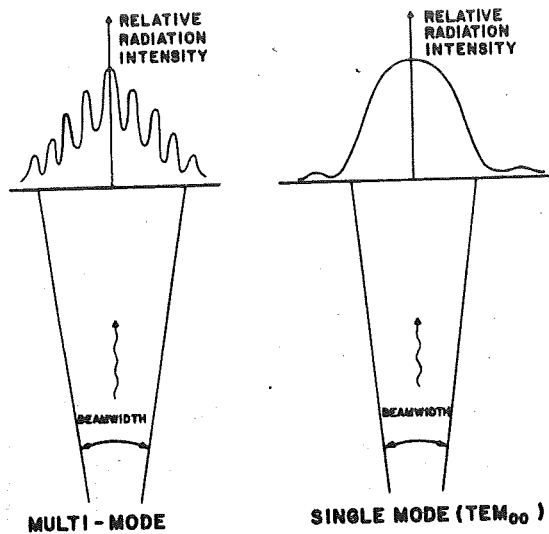


Figure 11. Far-Field Radiation Patterns

The other advantage of having the GaAs laser emit in TEM_{00} single mode (often referred to as the diffraction limited mode) is that with very small collimating optics (<1 inch) the output beam can be reduced to 0.1° degree or less very easily. The wavelength (λ) of the GaAs laser radiation is approximately 0.9μ meters ($9,000$ angstroms). The eye's visible spectrum is $4,000$ to $7,000 \text{ \AA}$, therefore to eliminate any potential hazards of narrow beam laser energy to the retina of the human eye a thin-film interference optical coating can be put on any window, view port, etc., that could possibly get in the line-of-sight of the laser radar beam. The optical coating would block out the laser wavelengths but would allow the light radiation in the eye's visible spectrum to pass. It should be noted that the low powered GaAs laser used in SLR would have no harmful radiation effects on any other part of the human body at any range (the eye has an excellent lens system that focuses the incoming collimated laser energy down to a very small area on the retina of the eye, thus tremendously increasing the energy per unit area). It should be noted that the low powered GaAs would only be potentially harmful to the eye at the shorter ranges (<1 mile for the 0.1° beam).

There are two key components in the beam steering subsystem shown schematically in Figure 12. One is the piezoelectric beam deflector.⁷ It is used to deflect the beam from the laser transmitter so that the narrow laser beam (0.1°) can be pointed or scanned anywhere in the 30° by 30° field without the use of mechanical gimbals. A piezoelectric crystal is mounted along with a small lightweight mirror as shown in Figure 13. When a voltage is applied across the piezoelectric crystal it bends proportional to the applied voltage and deflects the attached mirror. The bending action is essentially frictionless! A precision strain gage is also attached to monitor the actual deflection thus taking care of any off axis hysteresis. A piezoelectric beam deflector is used to deflect the laser beam ± 0.5 degrees in approximately 300 incremental steps in both the pitch and yaw axes. A special passive optical system (no electronics) is used to amplify the $\pm 0.5^\circ$ deflection out to $\pm 15^\circ$, and this is the second key component in the beam steerer. The 0.1° laser beam can thus be pointed or scanned anywhere in the 30 by 30 degree field ($\pm 15^\circ$ yaw by $\pm 15^\circ$ pitch) by applying a known voltage to the piezoelectric deflector.

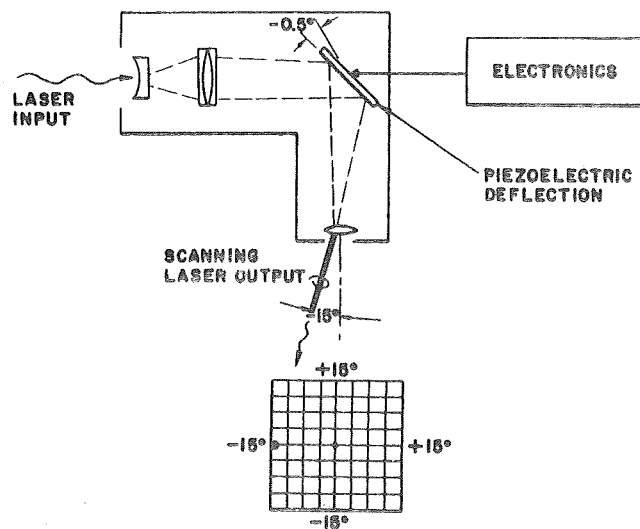


Figure 12. Beam Steerer Schematic

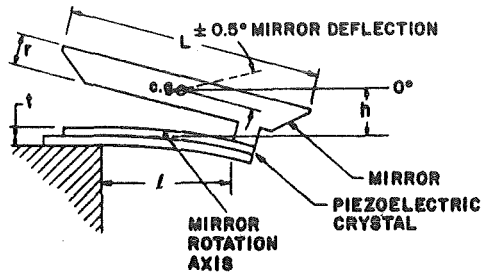


Figure 13. Piezoelectric Beam Deflector Schematic

The key components in the receiver optics are the narrow band optical filter and the multi-element lens assembly. Figure 14 schematically shows the receiver optics and the scanning optical detector. The narrow band optical filter allows only the radiation centered around the laser wavelength to get through to the scanning optical detector. Figure 15 depicts this narrow band filtering graphically.

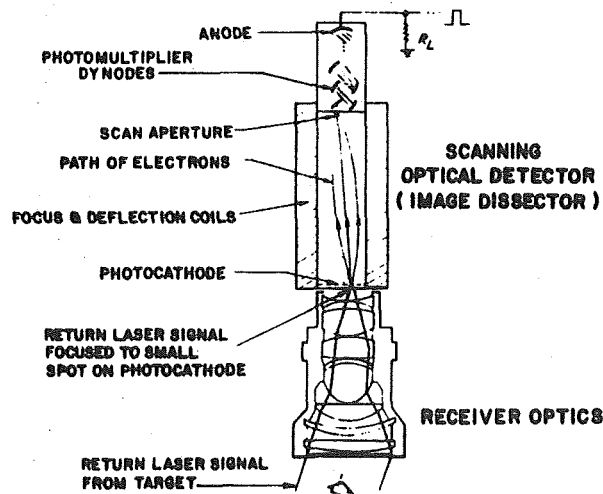


Figure 14. Receiver Optics and Scanning Optical Detector

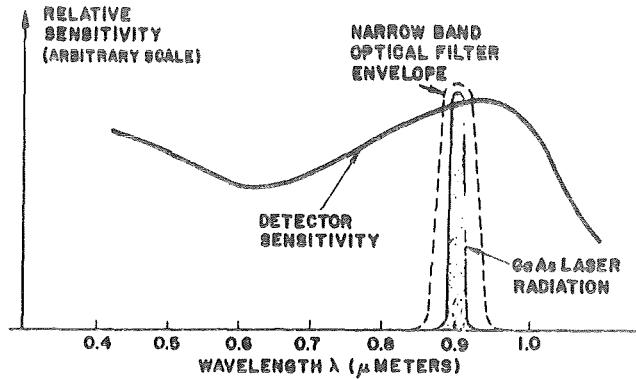


Figure 15. Narrow Band Optical Filter

The multi-element lens assembly collects the energy from the return laser radar signal and focuses it to a small spot at the focal plane. The small spot will be uniquely located at only one place in the focal plane and this location will be directly proportional to the radar transmitter-receiver pitch and yaw angle (θ). Figure 16 pictorially shows this effect by showing two different return beams. A single lens representation is used to simplify the drawing. A multi-element lens assembly is needed to obtain good resolution off-axis, especially for a high speed lens system.

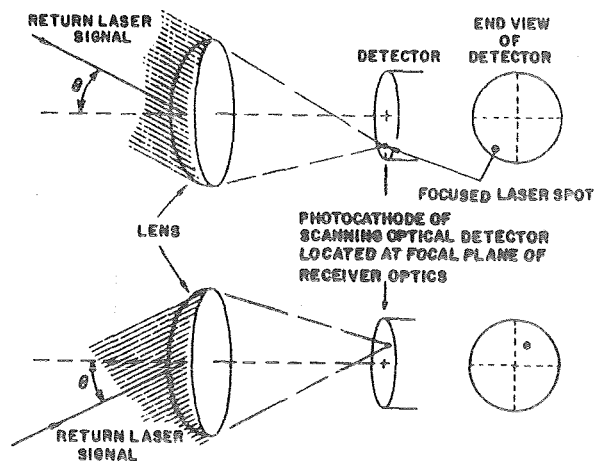


Figure 16. Receiver Lens Schematic - Angle Correlation

The key component in the scanning optical detector is the image dissector photosensor. The image dissector works like a television picture tube in reverse. A TV picture tube has a centrally located aperture that emits electrons and these electrons are directed toward and into one small spot on the TV screen by an electromagnetic field. The small spot on the TV screen is accurately positioned by controlling the electromagnetic field with a known current. When the electrons hit the small spot on the TV screen, the screen emits photons of light which form one small part of the image the viewer will see. The image dissector operates in the reverse process, the photons of laser light strike one small spot on the screen (photocathode of image dissector), and then electrons from the small spot are emitted toward the central aperture. By varying the electromagnetic field the image dissector can effectively scan the surface of the photocathode to determine where the laser spot is located. Figure 17 shows electro-optical sketches of the TV - Image Dissector analogy.

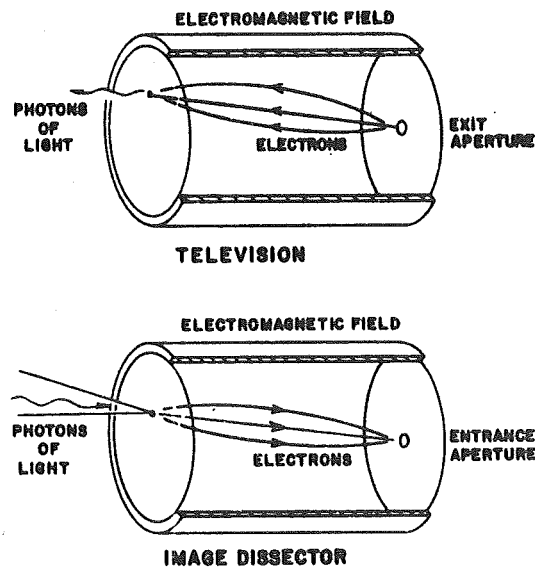


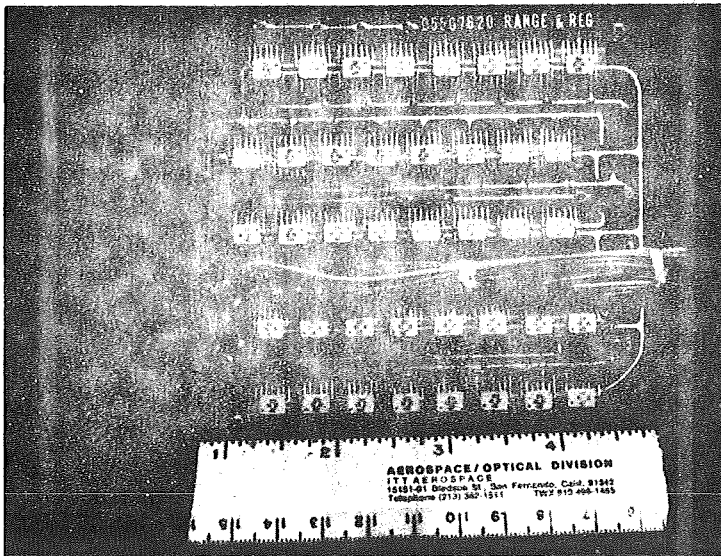
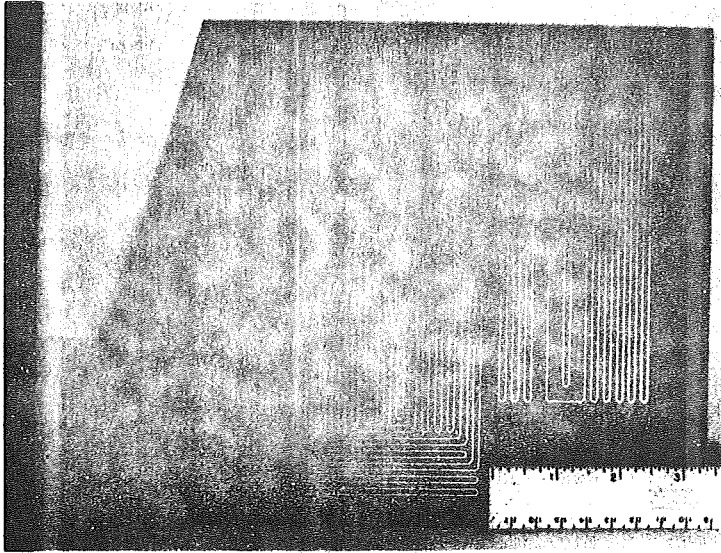
Figure 17. Television - Image Dissector Analogy

The receiver optics focused the return laser signal to a position on the image dissector photocathode that was proportional to the pitch and yaw angle (θ), therefore by reading the current needed to control the electromagnetic field the pitch and yaw angle (θ) can be determined. The diameter of the photocathode used in the SLR is 1.1 inches. The image dissector can resolve 1,000 spots per line or more if needed, and this is how the fine angle resolution is obtained. After the electrons get into the entrance aperture they go into an electronmultiplier section. The electronmultiplier can have and essentially noise-free gain of up to 1×10^6 .

There are many key components in the SLR transmitter-receiver electronics subsystem. In terms of state-of-the-art the most important are the components used in the newly developed pulse ranging section. The pulse ranging system determines range by measuring the GaAs laser pulse propagation time from the transmitter to the target and back to the receiver in increments of 0.67 nanoseconds (1500 MHz). The range pulse propagation time is resolved by using a multiple tap stripline delay line and Motorola MECL III ultra high speed logic modules. The MECL III logic is used to obtain range resolution from 1500 MHz down to 23 MHz. Figure 18 is a picture of the stripline side of the fine range printed circuit board. The logic modules are mounted through the ground plane on the opposite side of the board.

Texas Instrument 54H logic modules are used in the frequency range between 23 MHz and 1.5 MHz. Below 1.5 MHz and in all of the processing and readout circuitry the 54L series low power logic modules are used. Approximately 80% of all the electronic components used in both the range and angle electronics are already listed on the NASA Apollo Applications preferred parts list.

At a maximum range of 150 km a range resolution of 0.67 ns requires 21 binary bits for each range measurement. Since a range measurement is made each millisecond large data capacity storage registers are required to process all of the information. Figure 19 shows a printed circuit board which contains 2 such large data capacity storage registers, one of 24 binary bits and one of 16 binary bits.



In configuration A2 the target does not have any electronics but only passive optical reflectors. The incoming beam angle (α) of the laser radar beam must then be determined with an indirect method by the vehicle with the radar transmitter-receiver. IIT is currently performing error analyses on several techniques to accomplish this task. One candidate technique is to place four (4) optical reflectors on the target with known spacing. Separate range and angle readings to each target reflector are made and the incoming beam angle (α) is calculated by a triangulation method using the on-board vehicle computer. The SLR obviously must scan faster to sequentially acquire and track four targets. At short ranges the transmitter beam is spread out larger than the receiver instantaneous field-of-view, and only the receiver has to scan at the faster rate. It is much easier to increase the scan rate of the radar receiver from a component point-of-view. The four (4) target reflector technique for obtaining the " α " angle is accurate only for short target ranges (less than 1,000 feet) because of the practical limitation on the spacing between each target reflector. The target reflectors would have to be sufficiently separated so that each could be angularly resolved by the radar. A 0.1° radar receiver instantaneous FOV would see a projected area with a diameter of 1.75 feet at a target range of 1,000 feet. Since the knowledge of the incoming beam angle (α) is critical only for docking closure maneuvers this 4 target reflector technique may be adequate. Docking closure is generally considered the final 1,000 foot line-of-sight trajectory prior to docking contact. At target ranges from 1,000 feet out to the maximum range (≈ 75 miles) if the " α " angle was needed a separate technique could be implemented (i. e., using the relative attitude information supposedly known for each vehicle). The 4 target reflector technique would still allow the radar transmitter-receiver to get the range (R) and angle (θ) measurements out to the maximum radar range. Analysis has shown that the 4 target reflector technique will obtain the angle (α) to an accuracy of one degree from 1,000 feet to 15 feet. From 15 feet to 0 feet an autocollimation technique can be implemented to increase the angle accuracy with only minor modifications to the radar transmitter-receiver. All other system performance characteristics for configuration A2 are similar to A1 except the " α " angle resolution.

MICROWAVE VS OPTICAL TRADE-OFF COMMENTS

There are three major reasons why it is advantageous to use optical radar instead of microwave radar for spaceborne applications such as rendezvous and docking. Figure 20 and the following paragraphs will explain these three reasons.

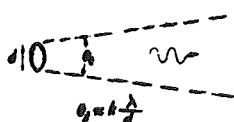
The first and most important reason is related to the directive antenna gain of any electromagnetic radiator or receiver. The purpose of the radar antenna is to act as a transducer between free-space propagation and guided-wave (transmission-line) propagation. A measure of the ability of an antenna to concentrate energy in a particular direction is called the directive gain, and can be examined by looking at the effective beamwidth of the concentrated energy. The smallest beamwidth that any system can obtain is determined by the fundamental equation for the diffraction-limited beamwidth of any electromagnetic transmitter or receiver, and can be approximated by the following equation:

$$\theta \approx 2 \frac{\lambda}{d}$$

where λ is the wavelength of the radiation, d is diameter of the antenna, and θ is the smallest full angle beamwidth that can be obtained.

The wavelength (λ) of microwave systems is typically 1×10^{-2} meters compared to approximately 1×10^{-6} meters for optical systems, thus for the same beamwidth, considerably smaller antenna size is needed for the optical (laser) system.

- **DIRECTIVE ANTENNA GAIN**



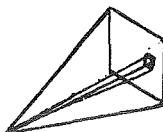
OPTICAL ADVANTAGES
BETTER ANGULAR
RESOLUTION, SMALLER
ANTENNA SIZE

- **SIDE LOBES**



OPTICAL ADVANTAGES
NEGLECTABLE SIDE LOBES

- **BEAM SCANNING**



OPTICAL ADVANTAGE
ANGLE-LESS BEAM STEERING

Figure 20. Optical vs Microwave

The main reasons that narrower beamwidths are desired are (a) the resulting higher power density at the target; (b) the potential increase in angle tracking accuracy.

The minimum antenna size needed for a 0.1 degree beamwidth would typically be the following for microwave and optical systems:

$$d_m \approx \frac{2 \lambda}{\theta} = \frac{2 (1 \times 10^{-2} \text{ meters})}{1.75 \text{ mrad}} = 38 \text{ feet}$$

$$d_o \approx \frac{2 \lambda}{\theta} = \frac{2 (1 \times 10^{-6} \text{ meters})}{1.75 \text{ mrad}} = 0.0038 \text{ feet}$$

The smaller antenna size is a significant factor for spaceborne systems where size, weight, and power are very important considerations. Note that the laser system can obtain 0.1 degree beamwidths with still a negligible antenna size where a microwave antenna would have to be approximately 38 feet in diameter to obtain the same 0.1 degree beamwidth.

The second major reason that makes it advantageous to use optical instead of microwave radar concerns sidelobes in the antenna radiation pattern. For microwave radar systems the sidelobes can typically be reduced to 20-30 db below the mainlobe. In optical systems the receiver sidelobe pattern can be greatly reduced to levels of typically 60-70 db below the mainlobe.

The third major reason making it advantageous to use optical radar instead of microwave radar involves the ability to scan the transmitter and receiver over a field-of-view much larger than its own beamwidth in a relatively simple fashion. The most common way to scan the microwave radar beam is to place the radar antenna on two-axis mechanical gimbals. Except for phased arrays, which are very large and power-consuming, the microwave scanning radar systems have to depend on the mechanical gimbals for scan coverage. Optical radar presently has the capability to scan the transmitter and the receiver over a 30 degree x 30 degree field-of-view without the use of mechanical gimbals. The transmitted laser beam can be deflected and scanned by using piezoelectric beam deflectors (or acoustical-optical beam deflectors) and amplifying optics. The optical receiver can scan its instantaneous field-of-view (which is matched to transmitted laser beamwidth) by using an image dissector.

LASER RADAR RANGE ANALYSIS

Since one of the primary functions of a radar system is to acquire or find a given target (or targets) this section will present an analysis to determine the basic capabilities of using laser type radar systems to search and acquire spaceborne targets. One of the most important tradeoffs to be made when considering the practicality of using any radar system is the "required transmitter power vs. target range" for the particular application. A typical earth orbit rendezvous acquisition problem will be presented here and then the required transmitter power vs. target range tradeoff will be examined for both the non-cooperative (skin) target and the cooperative (optical corner cube reflector) target cases.

A typical earth orbit rendezvous "acquisition" problem might have the following requirements imposed upon the radar system used in the vehicle guidance and control system:

- a. No continuous ground tracking data available.
- b. Navigation data available on the vehicle with the radar transmitter-receiver will allow this vehicle to know the relative angular direction of the target vehicle to within a $15^\circ \times 15^\circ$ field-of-view or smaller.
- c. The maximum time to acquire the target shall be 120 seconds. The probability of target detection should be large (>0.99) for high confidence of acquisition. The probability of false alarm (noise) should be sufficiently small so that the maximum acquisition scan time is not significantly increased due to stopping the scan numerous times to evaluate the false signals.
- d. For the non-cooperative case, the projected area of the target shall be 10 square meters. The target surface can be assumed to be lambertian,

thus providing a diffuse reflection. For the cooperative case the target can have one or more optical corner cube reflectors, but no electronics. Any one corner cube shall be no larger than 10 cm (4") in diameter.

- e. The relative range shall be measured to an accuracy of $\pm 1.0\%$ at the nominal acquisition range or less. The range-rate accuracy shall be $\pm 2.0\%$ of the average range over a one second time period.
- f. Immediately after tracking has begun, the angle tracking rate capability shall be compatible with the rendezvous catch-up flight maneuvers and the angle tracking accuracy shall be 1.0 mrad or less.
- g. The maximum radar aperture diameter shall be as small as practically possible ($\approx 3''$) because it will probably have to be mounted behind a window inside the vehicle.
- h. The target background can be considered to be a dark sky (i.e., not a sunlit cloud background) for the acquisition mode. However, the sun's illumination off the target shall be considered.

Problem: Determine the required radar transmitter power needed to acquire the target for target ranges from 10 to 120 miles using the above constraints or requirements.

The analysis for the solution of the acquisition problem just described shall use the following assumptions or guidelines:

- a. No mechanical gimbals will be used to point or scan the transmitter-receiver.

- b. The transmitter beamwidth and the receiver instantaneous field-of-view shall be the ideally matched (same size) throughout the entire acquisition scan field.
- c. In order to take advantage of the image dissector and its salient characteristics (high resolution, rapid scan rate, gimballess, high noiseless gain, scanning optical detector) only laser transmitters that emit radiation with wavelengths in the image dissector spectrum (0.4 to 1.1 μ meters or visible to near IR) shall be considered. Since the CO₂ laser emits at 10 μ meters this is one of the reasons it is not considered in this analysis. The CO₂ laser radar system also uses different range equations when using coherent detection techniques. The CO₂ laser system vs. the visible-near IR system can only fairly be compared when all aspects of the radar system are taken into account (i. e., size, weight, power, radar acquisition and tracking performances, gimbal requirements, cooling requirements, detector detectivity, system complexity, stability, and reliability, etc.).
- d. A pulsed laser transmitter shall be used and a corresponding "photon bucket", or incoherent detection technique shall be used to in the optical receiver.

Figure 21 shows the 15° x 15° search field-of-view (FOV) that is to be scanned in the maximum acquisition time of 120 seconds. A 0.5 mrad transmitter and receiver instantaneous FOV were chosen as the smallest scan element, thus for a square raster type scan there are 524 scan elements per line and 274,476 scan elements

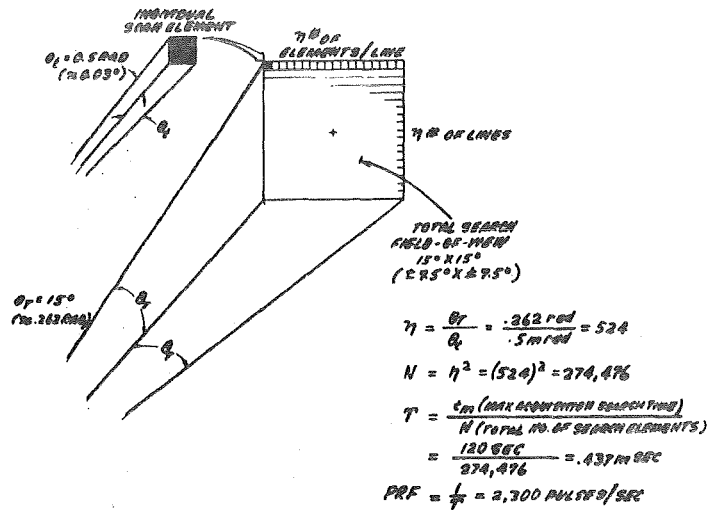


Figure 21. Typical Radar Acquisition Problem
 (120 Second Acquisition Time for 15° x 15° Search FOV)

for the entire 15° x 15° FOV. To complete the entire scan in 120 seconds the dwell time per element would be 0.437 msec and for a pulsed system the corresponding pulse repetition frequency (PRF) and scan rate would be 2,300 pulses per second (pps).

Equations for the average input power ($P_{\text{avg in}}$) into the laser transmitter as a function of the target range (R) for both the cooperative (optical corner cube reflector) and non-cooperative (skin) target cases can be derived in a straight forward manner. The equation for each case are shown in Figures 22 and 23 and the parameters are listed in Table 2. The equations have been broken down into five (5) major parts so that one gets a better understanding of the rather long equation. Note that the only difference between the cooperative and non-cooperative case is the first part of the equation that is related to the Radar Geometry. Both are a function of target range to the fourth power (R^4), however there is a significant difference between the

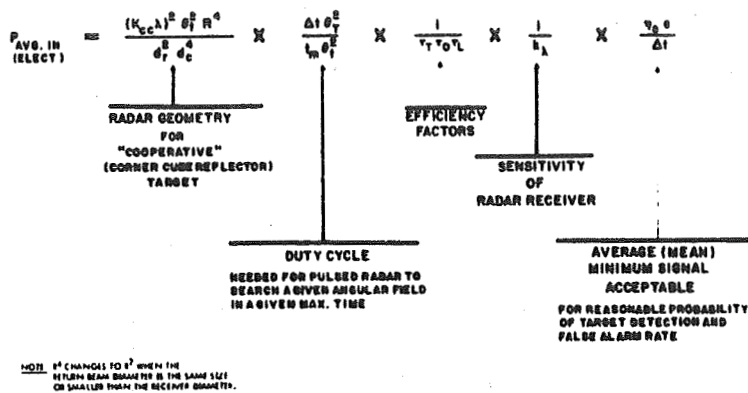


Figure 22. Equation for Average Input Power into Laser (Cooperative Target Case)

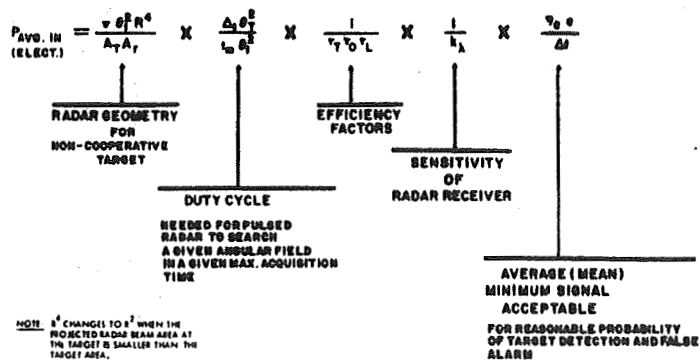


Figure 23. Equation for Average Input Power into Laser (Non-cooperative Target Case)

θ_1 = LASER TRANSMITTER BEAMWIDTH (FULL ANGLE) (RAD.)
 R = SLANT RANGE TO TARGET (METERS)
 π = 3.14 STERADIANS (FACTOR INTRODUCED BY DIFFUSE RETURN FROM LAMBERTIAN SURFACE OF TARGET)
 A_T = PROJECTED AREA OF TARGET [M²]
 A_r = AREA OF RADAR RECEIVER COLLECTOR APERTURE [M²]
 Δt = LASER PULSEWIDTH (SECONDS)
 θ_1^2 = TOTAL ACQUISITION SEARCH FIELD-OF-VIEW [RAD² OR STER.]
 t_m = MAXIMUM ACQUISITION SEARCH TIME
 τ_T = REFLECTIVITY OF TARGET (FRACTION)
 τ_o = TRANSMITTANCE OF LASER ENTR-RCVR OPTICS (FRACTION)
 τ_L = ELECTRICAL-TO-OPTICAL EFFICIENCY OF LASER (FRACTION)
 k_λ = SENSITIVITY OF LASER RECEIVER DETECTOR (AMPS/WATT)
 η_e = AVERAGE (MEAN) MINIMUM NUMBER OF SIGNAL ELECTRONS
 e = 1.6×10^{-19} COULOMBS (CHARGE PER ELECTRON)
 λ = WAVELENGTH OF TRANSMITTED LASER RADIATION (METERS)
 d_c = DIAMETER OF THE OPTICAL CORNER CUBE REFLECTOR ON THE TARGET (METERS)
 K_{cc} = 1.22 (FACTOR INTRODUCED BY EXAMINING THE CENTRAL MAXIMUM TO THE FIRST NULL OF THE DIFFRACTION PATTERN FROM THE OPTICAL CORNER CUBE REFLECTOR).

magnitude of these two when the rest of the parameters are evaluated. For a cooperative target with a corner cube reflector having a diameter (d_c) of 10 cm (4"), a non-cooperative target with a projected area (A_T) of $10m^2$, and a laser wavelength (λ) of 1 μ meter the ratio between the Radar Geometry for the two cases is 1.7×10^7 for any given target range. This means that for all other four parts of the equation being equal for a given system, than the non-cooperative laser transmitter would require 1.7×10^7 more average input power than the cooperative target for any given range. This can be dramatically seen in the semi-log graphs that are presented later.

The fifth part of the equation, the AVERAGE (MEAN) MINIMUM SIGNAL ACCEPTABLE is determined after evaluating the probability of signal detection. The laser radar noise equation is shown in Table 3 along with a listing

Table 3. Laser Radar Noise Equation and Parameters

$$i_N^2 = \left(k\sqrt{2e(I_S + I_B + I_{DC})\Delta F} \right)^2 + \left(\frac{i_T}{G} \right)^2$$

i_N = RMS NOISE CURRENT AT RECEIVER PHOTOCATHODE [AMPS]

k = 1.25 (NOISE FACTOR DUE TO AMPLIFIER GAIN IN PHOTOMULTIPLIER)

e = 1.6×10^{-19} COULOMBS (CHARGE PER ELECTRON)

I_S = AVERAGE (MEAN) SIGNAL CURRENT AT P. C. [AMPS]

I_B = AVERAGE (MEAN) CURRENT AT PHOTOCATHODE DUE TO THE BACKGROUND RADIATION [AMPS]

I_{DC} = AVERAGE (MEAN) PHOTOCATHODE DARK CURRENT [AMPS]

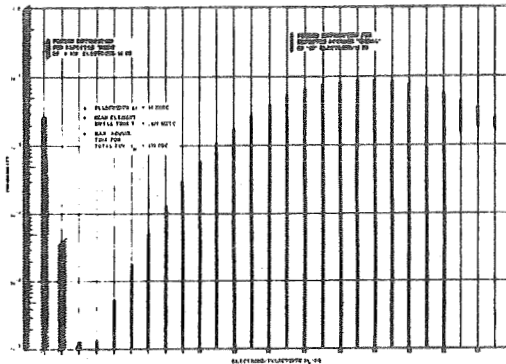
ΔF = ELECTRICAL BANDWIDTH OF RECEIVER ELECTRONICS (HZ)

i_T = THERMAL NOISE CURRENT AT "ANODE" [AMPS]
(JOHNSON NOISE)

G = GAIN OF PHOTOMULTIPLIER

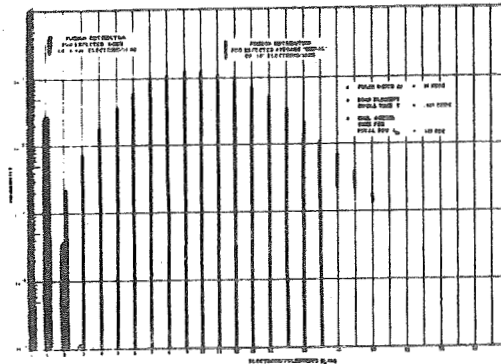
of each parameter. An average (mean) minimum number of "20" signal electrons (n_e) per a 10 nanosecond laser pulse width (Δt) was chosen for this analysis as a reasonable return signal level at the detector photocathode. The noise level came out to be "0.028" electrons per 10 ns pulse width and was due primarily to the thermal noise for the relatively high bandwidth needed in the receiver.

The rationale behind choosing an average (mean) Minimum of signal electrons per laser pulse width can be shown graphically. Graphs of the poisson distribution of the expected average signal (20) and expected noise (0.028) are shown in Figure 24. Figure 25 shows a similar graph except the expected average signal was chosen to be 10 instead of 20. In both figures there are corresponding tables that show the probability of "signal" detection (P_d), probability of false alarms, and the search time lost due to the false alarms for different receiver threshold levels.



THRESHOLD LEVEL (σ^2/AS)	PROBABILITY OF "NORMAL" DETECTION P_D (Per Total FFA)	PROBABILITY OF "NOISE" (FALSE ALARM) DETECTION P_{FA} (Per AS)	AVERAGE NUMBER OF FALSE ALARMS (Per Total FFA)	AVERAGE NUMBER OF FALSE ALARMS (Per Total FFA)	GRABER TIME LOGS DUE TO F.A.'s (Per Total FFA)
0	.0000	1×10^{-10}	1.0×10^{-11}	1.0×10^{-6}	0
1	.0000	1×10^{-10}	1.0×10^{-9}	1.0×10^{-4}	0
2	.0000	1×10^{-10}	1.0×10^{-7}	1.0×10^{-2}	0
3	.0000	1×10^{-10}	1×10^{-5}	10	10000
4	.0000	1×10^{-10}	1×10^{-3}	100	100000

Figure 24. Probability of Signal Detection and False Alarm (Expected Signal "20" Electrons/10 ns)



THRESHOLD LEVEL (σ^2/AS)	PROBABILITY OF "NORMAL" DETECTION P_D (Per Total FFA)	PROBABILITY OF "NOISE" (FALSE ALARM) DETECTION P_{FA} (Per AS)	AVERAGE NUMBER OF FALSE ALARMS (Per Total FFA)	AVERAGE NUMBER OF FALSE ALARMS (Per Total FFA)	GRABER TIME LOGS DUE TO F.A.'s (Per Total FFA)
0	.0000	1×10^{-10}	1.0×10^{-11}	1.0×10^{-6}	0
1	.0000	1×10^{-10}	1.0×10^{-9}	10	100000
2	.0000	1×10^{-10}	1×10^{-7}	100	10000
3	.0000	1×10^{-10}	10	1000	100000
4	.0000	1×10^{-10}	100	10000	1000000

Figure 25. Probability of Signal Detection and False Alarm (Expected Signal "10" Electrons/10 ns)

A very high probability of signal detection ($P_d > .999$) and a negligible search time lost due to false alarms is easily obtained for the "20" expected signal level case. For the "10" expected signal level case a high probability of signal detection ($P_d > .99$) and a negligible search time lost due to false alarms cannot be obtained for a given threshold. An expected signal level slightly lower than "20" could probably be used successfully, but no attempt was made here to optimize the selection of the expected signal level.

For evaluating the cooperative and non-cooperative cases graphs of laser average input power versus target range are plotted assuming that the third and fourth part of the power equations are idealized (i. e., no losses, 100% power efficiency and sensitivity). Graphs are also made for the situation where a state-of-the-art laser transmitter and receiver detector are used in the radar system. An Ytterium-Aluminum-Garnet (YAG) laser was chosen for the laser transmitter in the non-cooperative case and a Gallium Arsenide (GaAs) laser was chosen in the cooperative case. The receiver detector in both systems is an image dissector with the new Spaced Reflective Photo - Cathode (SRPC) S-1 photoemissive surface. Tables 4 and 5 list all the system parameters for the Cooperative (idealized and state-of-the-art) and Non-cooperative (idealized and state-of-the-art) cases, Figure 26 graphically shows laser average input power versus target range for all four situations. The curves dramatically show the significance of using optical corner cube reflectors on the target whenever possible.

TABLE 4
LIST OF PERTINENT CHARACTERISTICS FOR
A TYPICAL LASER RADAR ACQUISITION PROBLEM
(COOPERATIVE TARGET CASE)

<u>TARGET</u>	IDEALIZED	STATE-OF-THE-ART
Projected Area A_T (Corner cube reflector)	79 cm ² (10" dia.)	79 cm ² (10" dia.)
Reflectivity (diffuse return) τ_T	1.0	.9
Max. Acquisition Time t_m	120 Sec.	120 Sec.
Range	See Fig. 26	See Fig. 26
<u>RADAR TRANSMITTER</u>		
Wavelength λ	.9 μ m	.9 μ m
Optical Transmittance τ_{ot}	1.0	.7
Pulse Width Δt	10 ns	10 ns
Beamwidth θ_t	.5 mrad.	.5 mrad.
Ω_t	.25 x 10 ⁻⁶ ster.	.25 x 10 ⁻⁶ ster.
* Total Search FOV $(\theta_T)^2$	15° x 15°	15° x 15°
Total Scan Elements N	(524) ² =274,476	(524) ² =274,476
Pulse Rep. Freq. (1/T)	2,300 pps	2,300 pps
Electro-Optical Laser Eff. ($\tau_L \times 100$)	100%	1.0%
Avg. Input Power (Elect.)	See Fig. 26	See Fig. 26
<u>RADAR RECEIVER</u>		
Optical Collector Aperture d_r	3", ($A_r=45 \text{ cm}^2$)	3", ($A_r = 45 \text{ cm}^2$)
Effective Detector Dia.	2.0"	2.0"
Detector Inst. Aper. Dia.	.004"	.004"
Instantaneous FOV θ_r	.5 mrad	.5 mrad
Ω_r	.25 x 10 ⁻⁶ ster.	.25 x 10 ⁻⁶ ster.
* Total Search FOV $(\theta_T)^2$	15° x 15°	15° x 15°
Total # Scan Elements N	(524) ² =274,476	(524) ² =274,476
Photo-Sensitivity k_λ	.7 a/w (100%QE)	.0064 a/w (SRPC S-1)
Elect. Bandwidth ΔF	50 MHz	50 MHz
Optical Bandwidth $\Delta \lambda$.01 μ m	.01 μ m
Optical Transmitter τ_{or}	1.0	.7
Avg. Minimum Signal $\eta_e/\Delta t$	20 elect/10ns	20 electrons/10ns
Avg. Input Power	≈10 watts	≈10 watts
* Electro-Optical Scan, no mech. gimbals!		

TABLE 5
LIST OF PERTINENT CHARACTERISTICS FOR
A TYPICAL LASER RADAR ACQUISITION PROBLEM
(NON-COOPERATIVE TARGET CASE)

	IDEALIZED	STATE-OF-THE-ART
TARGET		
Projected Area A_T (skin)	10 m ²	10 m ²
Reflectivity (diffuse return) τ_T	1.0	.9
Max. Acquisition time t_m	120 Sec.	120 Sec.
Range R	See Fig. 26	See Fig. 26
RADAR TRANSMITTER		
Wavelength λ	1 μ m	1.06 μ m (YAG)
Optical Transmittance τ_{ot}	1.0	1.0
Pulse width Δt	10 ns	10 ns
Beamwidth θ_t	.5 mrad.	.5 mrad
Ω_t	.25 x 10 ⁻⁶ ster.	.25 x 10 ⁻⁶ ster.
* Total Search FOV (θ_T) ²	15° x 15°	15° x 15°
Total # Scan Elements N	(524) ² =274,476	(524) ² = 274,476
Pulse Rep. Freq. (1/T)	2,300 pps	2,300 pps
Electro-Optical Laser Eff. (τ_L x100)	100%	5%
Avg. Input Power (Elect.)	See Fig. 26	See Fig. 26
RADAR RECEIVER		
Optical Collector Aperture d_r	3", ($A_r=45$ cm ²)	3", ($A_r = 45$ cm ²)
Effective Detector Dia.	2.0"	2.0"
Detector Inst. Aper. Dia.	.004"	.004"
Instantaneous FOV θ_r	.5 mrad	.5 mrad
Ω_r	.25 x 10 ⁻⁶ ster.	.25 x 10 ⁻⁶ ster.
* Total Search FOV (θ_T)	15° x 15°	15° x 15°
Total # Scan Elements N	(524) ² =274,476	(524) ² = 274,476
Photo-Sensitivity k_λ	.8 a/w(100%QE)	.0027 a/w (SRPC S-1)
Elect. Bandwidth ΔF	50 MHz	50 MHz
Optical Bandwidth $\Delta \lambda$.01 μ m	.01 μ m
Optical Transmittance τ_{or}	1.0	.7
Avg. Minimum Signal $\eta_e/\Delta t$	20 elec./10 ns	20 electrons/10 ns
Avg. Input Power	~ 10 watts	~ 10 watts
*Electro-Optical Scan, no mech. gimbals!		

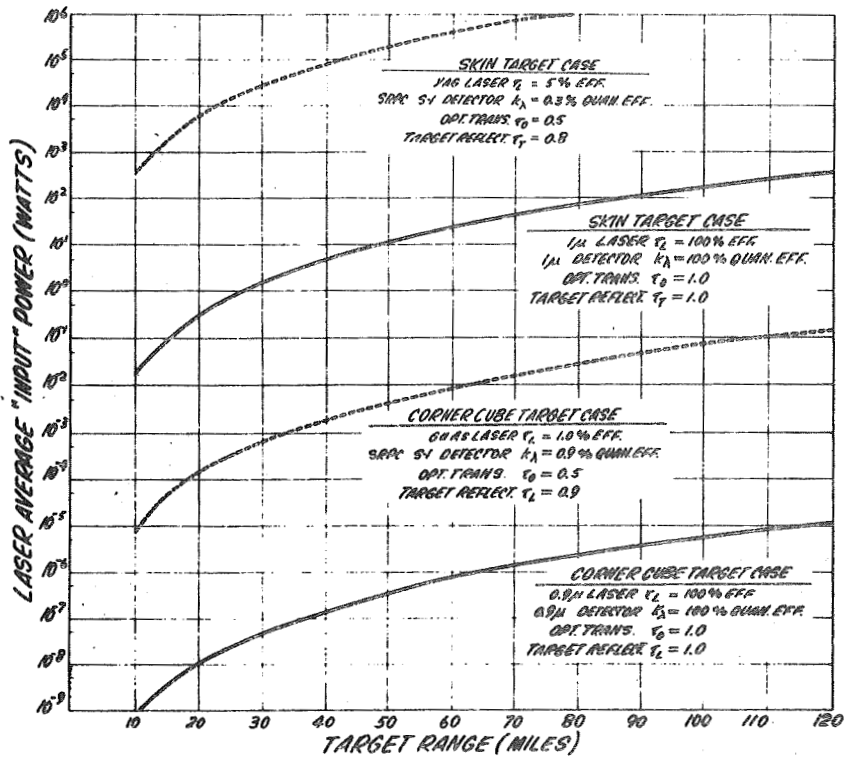


Figure 26. Laser Avg. Input Power vs Target Range
 (Non-cooperative & Cooperative Target Case,
 15° x 15° Search FOV & 120 Sec. Acquisition Time)

The total search FOV (θ_T^2) to be scanned in 120 seconds effects the laser power required by the square of the FOV. Reduced FOV's are examined here for the non-cooperative case using the state-of-the-art parameters. Figure 27 graphically shows the laser average "input and output" power versus target range for the $15^\circ \times 15^\circ$ Search FOV. Curves with three different electrical-to-optical efficiencies ($\tau_L \times 100$) for the YAG laser transmitter are shown. Figure 28 graphically shows the average laser "output" versus target range for seven (7) different search FOV's varying from $15^\circ \times 15^\circ$ down to $0.232^\circ \times 0.232^\circ$. The individual scan element size was kept the same ($0.5 \text{ mrad} \times 0.5 \text{ mrad}$). The number of pulses per second (pps) and the scan rate was reduced so the entire 120 seconds could be used and thus reduce the required laser power. The tremendous reduction in the required power for smaller search FOV's sharply point out an advantage of good navigation data prior to starting the rendezvous acquisition.

The required laser power for the non-cooperative target case may be more power than the vehicle can practically allot for the radar system.

There are alternate methods for the rendezvous acquisition with slight modifications to the above laser radar systems. One attractive method is to use the sun's illumination off the target vehicle to acquire the target. Only the angular direction can be directly obtained with this method, however if the initial angular direction is determined the total search FOV for the active laser radar system could be reduced down to one degree or less very easily.

The laser radar system would use the receiver's scanning optical detector (image dissector plus optics) to search for the sun's illumination off the target. The narrow band optical filter that selected only the laser light could be taken out if necessary for

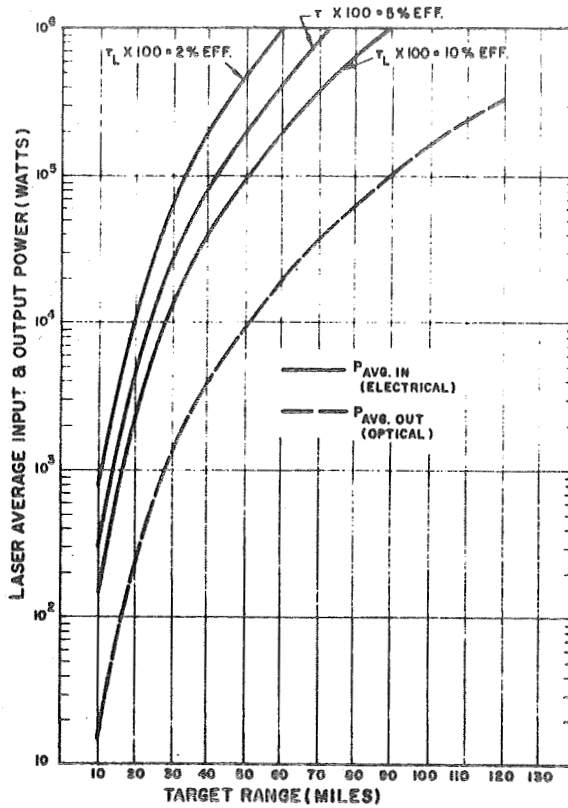


Figure 27. Laser Avg. Input & Output Power vs Target Range (Non-cooperative Target Case 120 Second Acquisition Time And 15° x 15° Search FOV)

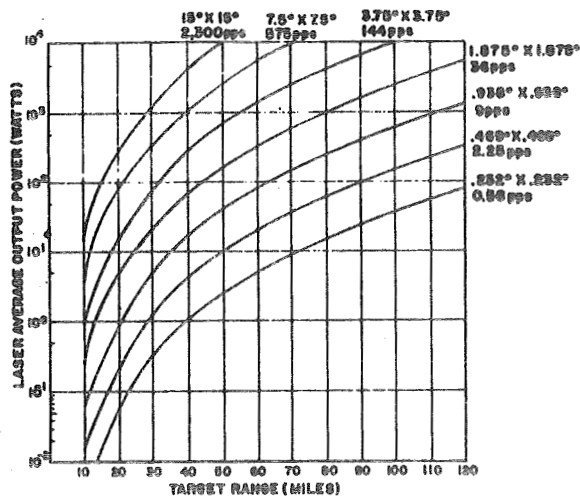


Figure 28. Laser Avg. Output Power vs Target Range (Various Search FOV's for Non-coop. Target Case)

the initial angle acquisition. For the receiver-only type of target acquisition, the image dissector can increase its scan rate to at least 30 KHz and could scan the entire $15^\circ \times 15^\circ$ FOV in about ten (10) seconds. After angle acquisition with the receiver the radar's laser transmitter could be turned on and pointed to where the receiver located the target. A laser transmitter-receiver acquisition could then be accomplished in 110 seconds very easily over smaller search FOV's with a significant reduction in laser power. Table 6 lists the system parameters for the sun illumination case, and Figure 29 is a graph showing the irradiance received versus target range. The primary source of noise in this situation would be any bright star that appeared in the $15^\circ \times 15^\circ$ FOV. From Figure 29 it can be seen that the irradiance received from the sun illuminated target is equal to the irradiance of a "0" magnitude star when the target range is 90 miles. There are only two (2) stars in the entire sky that are brighter than "0" visual magnitude and only nine (9) between "0" and "+1".

The sun illumination method would put an obvious constraint on the rendezvous acquisition; the initial angle acquisition would have to occur when the target was illuminated by the sun, and thus initial acquisition could not occur on the dark side of the earth.

TABLE 6. LIST OF PERTINENT CHARACTERISTICS FOR TARGET ACQUISITION USING THE SUN'S ILLUMINATION

TARGET

Projected Area A_T	10 m^2
Reflectivity (diffuse return) τ_T	0.8
Geometric dilution τ_G	0.1
Max. Acquisition time t_m	120 sec
Range	see Figure 29

RADAR RECEIVER

Optical Collector Aperture d_r	3" ($A_r = 45 \text{ cm}^2$)
Effective Detector Dia.	2.0"
Detector Inst. Aper. Dia.	0.004"
Instantaneous FOV θ_r	0.5 mrad
Ω_r	0.25×15^{-6} ster.
Total Search FOV $(\theta_T)^2$	$15^\circ \times 15^\circ$ (without gimbals)
Total #Scan Elements N	$(524)^2 = 274,476$
Photo-Sensitivity k_λ (avg.)	0.3 a/w
Elect. Bandwidth ΔF	50 MHz
Optical Bandwidth $\Delta \lambda$	0.4 μm
Optical Transmitter τ	0.7
Irradiance at Receiver (H_r)	See Figure 29
Average Input Power	≈ 10 watts

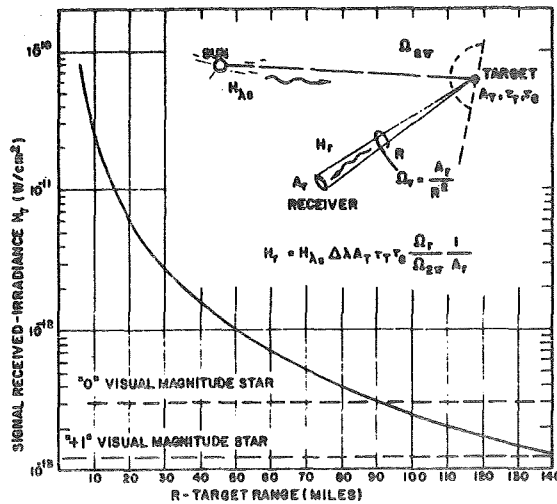


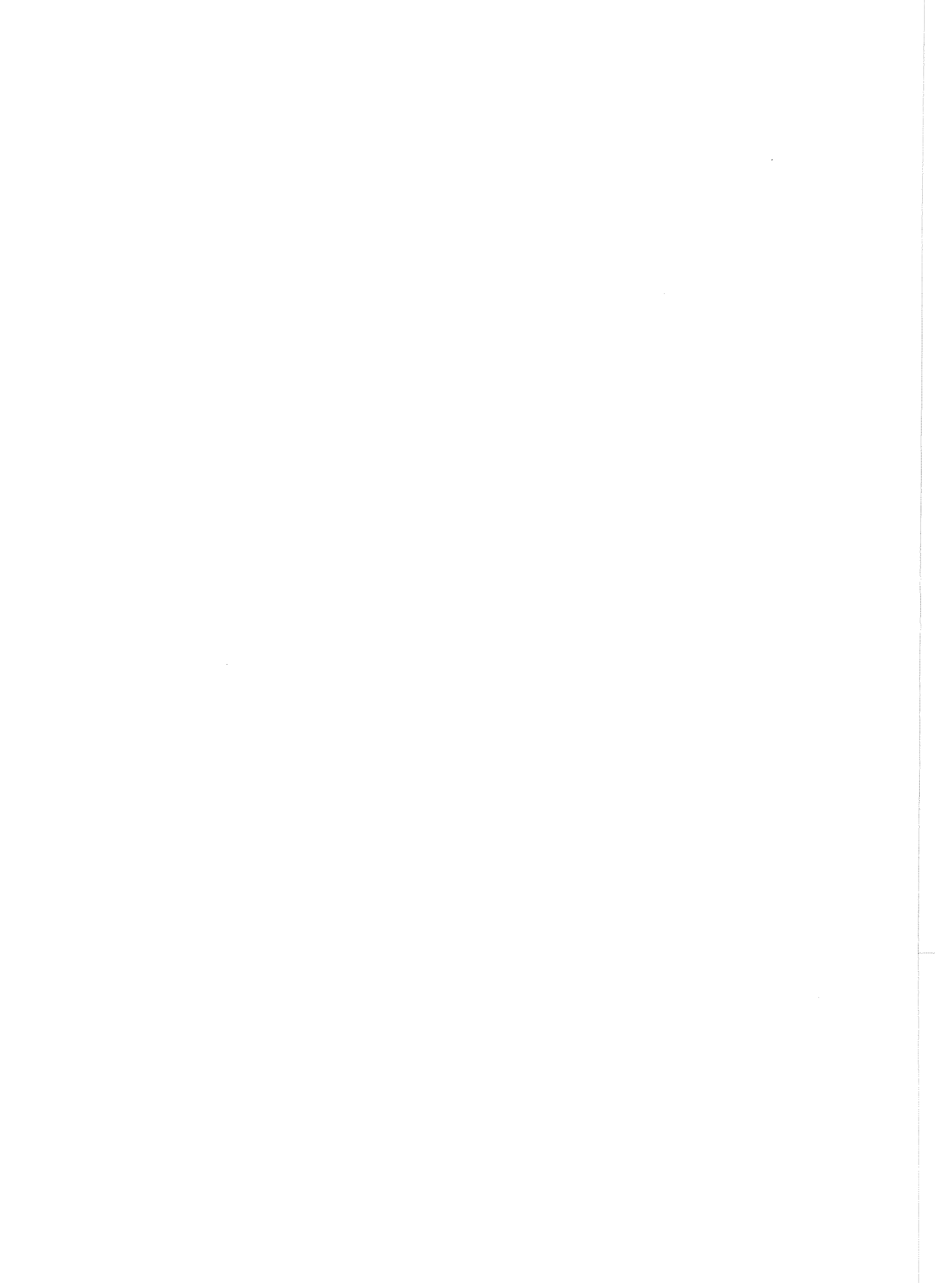
Figure 29. Irradiance Received from Sun Illuminated Target vs Target Range

ACKNOWLEDGMENTS

The author wishes to especially acknowledge the work of L. Cardone, D. Coombes, T. Dixon, and R. Schmidt as they have been the key personnel at ITT who have designed and developed the scanning laser radar over the last several years. Acknowledgment also to R. Ayyar, R. Deters, G. Horn, J. Priebe, L. Rosenberg, H. Sarrafian, S. Valdes, J. Ward, D. Weaver, and R. Yancey of ITT for their various technical contributions during the long term hardware development. The author wishes to recognize the outstanding technical guidance and leadership of C. L. Wyman (NASA) who has been responsible for most of the contract work since the inception of the space-borne laser radar programs at ITT.

REFERENCES

1. M. I. Skolnik, "Introduction to Radar Systems," McGraw-Hill, 1962.
2. T. P. Dixon, C. L. Wyman, H. D. Coombes, "A Laser Guidance System for Rendezvous & Docking," *Journal of the Institute of Navigation* Vol 13, No. 3, Autumn 1966.
3. W. H. Tobey, L. M. Hunt, "ITT Optical Rendezvous Radar Evaluation," Contract report MCR-67-220, Martin-Marietta, Denver, Colorado, June 1967.
4. C. L. Wyman, "An Advanced Laser Tracking Technique for Future Space Guidance Systems," AIAA Guidance, Control and Flight Mechanics Conference, August 1969.
5. S. A. R. Ayyar, T. E. Flom, "Automatic Rendezvous and Docking," Final Report Contract NAS8-23973 (Phase I), ITT San Fernando, California, April 1970.
6. E. M. Phillip-Rutz, H. D. Edmonds, "Diffraction-Limited GaAs Laser with External Resonator," *Applied Optics*, Vol. 8, September 1969.
7. J. Schalafer, S. Reich, V. J. Fowler, "Investigation of Electro-Optical Techniques for Controlling the Direction of a Laser Beam," Interim Report TR69-722.57, GT&E, Bayside, N. Y., February 1969.



N70-40968

A LASER SYSTEM SUITABLE FOR SPACE APPLICATIONS

P. Schuddeboom, M. Teare, and D. Bennett

RCA Research Laboratories
Montreal, Canada

INTRODUCTION

While a number of experimental laser communications links have been established on the ground^{1,2}, space communications using a laser is still very much in its infancy. The first space laser communications system will be the Laser Communications Experiment to be flown on the ATS-F satellite. This experiment is expected to provide two-way video transmission between the ground and the synchronous satellite using a FM CO₂ laser transceiver. Although careful trade-off studies will have to be conducted, a laser communications link may well be the best means of communicating between the Shuttle Orbiter and a Synchronous Data Relay Satellite, due to the large antenna required for RF communications. This may be very difficult to incorporate into the Orbiter design.

In considering lasers for space applications it is necessary to evaluate the ground based systems to ensure that their components are suitable for space use. At the present time our work in this area is divided into three sections.

- 1) The development of a small long life sealed-off ceramic CO₂ laser tube.
- 2) The development of a simple laser frequency stabilizing control system which will operate over large excursions in cavity length in order to compensate for the effects of the change in refractive index with temperature of a GaAs modulator internal to the laser cavity.
- 3) The development of a highly efficient laser power supply which does not require a ballast resistor.

LASER TUBE

Conventional CO₂ lasers have been glass with water cooling. For a space system we must use a sealed off laser tube which is rugged, can be passively cooled, and has both a long shelf lifetime as well as well as a long operative lifetime. Figure 1 shows a ceramic laser tube made of high purity alumina which meets these requirements. With GaAs Brewster windows this 15 cm tube is capable of 1 watt of single mode CW power output. Over 2000 hrs lifetime has been achieved with the first two of these tubes. Longer lifetimes are anticipated with subsequent tubes.

FREQUENCY CONTROL SYSTEM

The frequency stability of the laser is directly related to the stability of the laser cavity by:

$$\frac{\Delta f}{f} = \frac{\Delta L}{L}$$

where, for a CO₂ laser $f \approx 3 \times 10^{13}$ Hz.

If we have a 50 cm cavity length we must be able to control this length to within 5A to obtain a laser frequency stability of 1 part in 10⁹.

PRECEDING PAGE BLANK NOT FILMED.

One fairly standard way of obtaining this type of stability is through the "center dither" method. This method makes use of the fact that the laser power output versus frequency characteristic has a smooth approximately parabolic shape with a unique maximum. It has been established by Mocker³ that the peak of the power profile of any particular line is an absolute frequency reference. This allows us to tune two lasers, independently, to the same frequency.

By applying a small sine wave perturbation to the laser cavity we can make use of the power profile to form a discriminator characteristic when the AC component of the signal detected on the power meter is passed through a phase sensitive detector. The discriminator formed in this manner, which is really the average value of the fundamental component of the dither detected on the power meter versus frequency, has a null which corresponds to the peak of the power profile. The null is only dependent on the position of the peak of the power profile and is independent of phase errors between the detected signal and the reference signal due to component changes with time and temperature. This means that the stabilization scheme is entirely dependent on the laser and is independent of any external reference. The output of the phase sensitive detector can therefore be used as an error voltage which can be fed back to the laser cavity transducer to maintain the laser at the peak of its power profile. Long term frequency stabilities in the order of one part in 10^8 have been achieved by this method.

Figure 2 shows the basic stabilization scheme. The proper vibrational rotational line is selected by means of an external diffraction grating. The dither frequency has been selected at 50 Hz with an amplitude equivalent to ± 1 MHz change in laser frequency. Due to the responsivity and break point of the thermistor bolometer power meter, a much higher dither frequency would require a larger amplitude dither in order to obtain a reasonable signal to noise ratio at the output of the power meter. Figure 3 shows a typical laser signature over three half wavelengths. For this laser the P18 line would be suitable for the operation of a communications system. Since we have established the center of the line as the carrier frequency, by increasing the dither amplitude the available bandwidth for communications is decreased since we must remain within the confines of the P18 line. The control system bandwidth is therefore limited to somewhat less than 5Hz as we have to be well down in gain at 50Hz to avoid responding to the dither signal. FM modulation can be achieved by means of an in-cavity GaAs modulator. If we use the modulator outside the cavity we can obtain equivalent modulation performance at the expense of a significant increase in power consumption in the modulator driver.

The control system block diagram is shown in figure 4. As a performance index we have attempted to maximize the open loop gain while still being well down in gain at the dither frequency. This has led to the inclusion of a lead lag compensation network to obtain system stability. It can be seen that this is a type 1 system, thus the system is not limited by a steady state error. From the Bode diagram, figure 5, we can see that the system is stable and has adequate gain and phase margins.

By inserting an offset in the phase sensitive detector we can change the position of the null of the discriminator. We can thus stabilize the laser at

any point on the power profile and take maximum advantage of the bandwidth available for communications. This will also allow us to perform the initial tuning of a local oscillator laser using the peak of the power profile as a frequency reference.

ELECTRO-MECHANICAL LASER CAVITY TRANSDUCER

When evaluating the ground based laser stabilization system it soon became evident that a major obstacle would be the laser cavity transducer. Traditionally the laser cavity transducers have been piezo-electric devices. These devices can be broken up into three classes; tubular, stacked and bimorph benders. While different trade-offs can be made among these devices they are all basically governed by the following restrictions.

(a) The PZt has a limited translation of less than 15μ for most devices of suitable size.

(b) The PZt requires a high voltage driver of up to 2000 volts for 5μ translation with a 2 inch long tubular device. High voltage amplifiers for space applications are difficult and complex designs.

(c) The PZt is easily depoled by exceeding its voltage stress limits. This depoling causes the device to lose its sensitivity. For space applications these voltage limits will have to be reduced in order to provide adequate reliability. This will then compound the difficulties of (a) and (b)

(d) The piezo-electric material is very brittle and the transducer will therefore be difficult to mount in order to survive launch vibrations while still being free to move properly during its normal operations.

To circumvent these problems an electro-mechanical transducer was investigated; several have been fabricated and tested with satisfactory results. This transducer operates on the principal of a plunger magnet whose armature is restrained by a thin diaphragm. Figure 6 shows the cross section of the electro-mechanical transducer. The armature has been made as light as possible in order to raise the mechanical resonant frequency to well over 300 Hz. Two diaphragms support the armature to ensure linear operation without skewing. The main advantages of the electro-mechanical transducer are listed below.

(a) The transducer operates on a current drive. This means that the device can operate from a low voltage driver, such as a normal IC operational amplifier.

(b) Displacements of over 100μ can be easily achieved at very low current levels.

(c) The device is very rugged and is easy to mount. Figure 7 shows the typical performance of the electro-mechanical transducer. The operation of the laser stabilizing system with the electro-mechanical transducer has been very satisfactory.

LASER POWER SUPPLY

For ground systems the laser power supply usually consists of a high

voltage power supply with a ballast resistor in series with the laser tube to overcome the negative dynamic impedance of the tube. This system requires a large high voltage transformer and is very inefficient due to the power wasted in the ballast resistor.

The laser power supply that we are presently developing is shown in figure 8. Since we are looking for a highly regulated current through the laser we have placed a current source in series with the laser tube. We now make use of the high positive dynamic impedance of the current source to overcome the negative impedance of the laser tube. This gives us stable operation without wasting power in a ballast resistor.

In order to overcome the need for a high voltage transformer and to eliminate all the problems of voltage stresses related to it, we have made use of a converter with a relatively low output voltage followed by a voltage multiplier. At no load the voltage multiplier provides the extra high voltage required to start the laser discharge. Once the laser starts the voltage drops as the current is regulated by the current source. The performance characteristics are shown in Table 1.

POWER SUPPLY PERFORMANCE FIGURES

Input Voltage	+28v \pm 1%
Output Operating Voltage Range	2500 - 4500 volts
Output Power	20 - 30 watts
Starting Voltage Supplied to Laser Tube	up to 10 Kv
Efficiency - present	70%
- expected	80%
Current Stability - expected	better than .1% ripple

TABLE 1

CONCLUSIONS

The relatively simple systems discussed above have performed very well in initial testing. The laser stabilizing system has been able to maintain frequency stability during a complete day without losing lock. The control system, which has been constructed with six operational amplifiers and two FET's, consumes less than 500 mw., which includes the electro-mechanical transducer.

With the aid of a very stable, yet flexible, laser heterodyne test facility that we have just completed, which is shown in figure 9, we plan to conduct extensive measurements on both the long term and short term stability of the laser control system. This facility will also enable us to perform detailed measurements on the effect of the laser power supply on the stability of the laser control system.

This work was supported in part by the Canadian Directorate of Industrial Research and NASA GSFC.

REFERENCES

1. F.E. Goodwin, "Optical Heterodyne Communications Experiments at 10.6μ "
IEEE Journal of Quantum Electronics, October 1968, pp 612-617.
2. Mocker H.W., "A 10.6μ Heterodyne Communications System",
App. Optics, Vol. 8, No 677 (1969).
3. Mocker H.W., "Pressure and Current Dependent Shifts in the Frequency
of Oscillation of the CO_2 Laser", Applied Physics Letters, Vol. 12, No. 1,
pp 20-23, Jan. 1968.

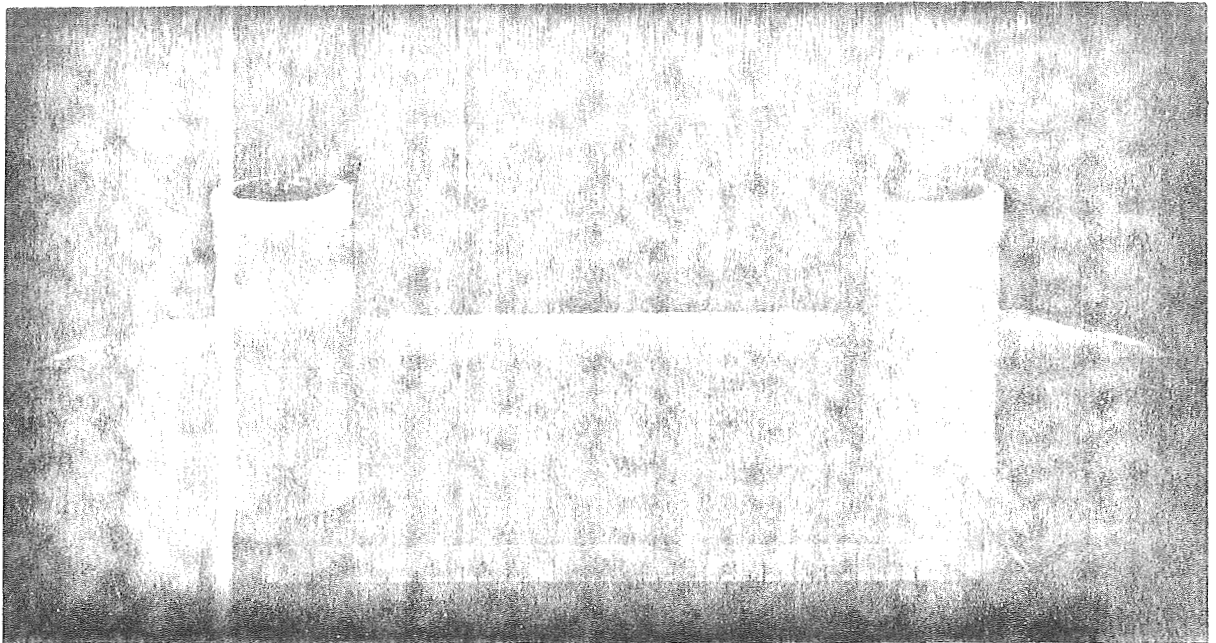


Figure 1.....Ceramic CO₂ Laser Tube

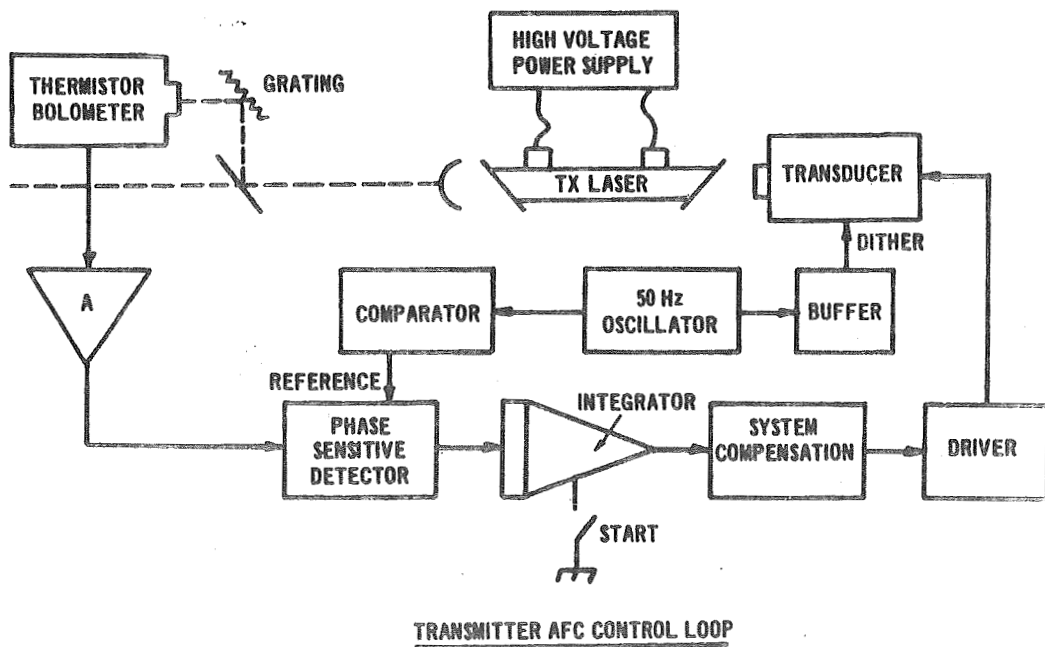


Figure 2.....Block Diagram of Basic Laser Stabilizing Scheme

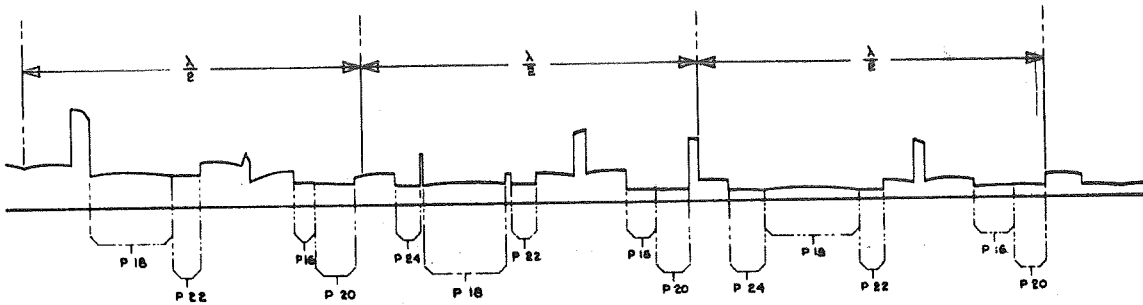
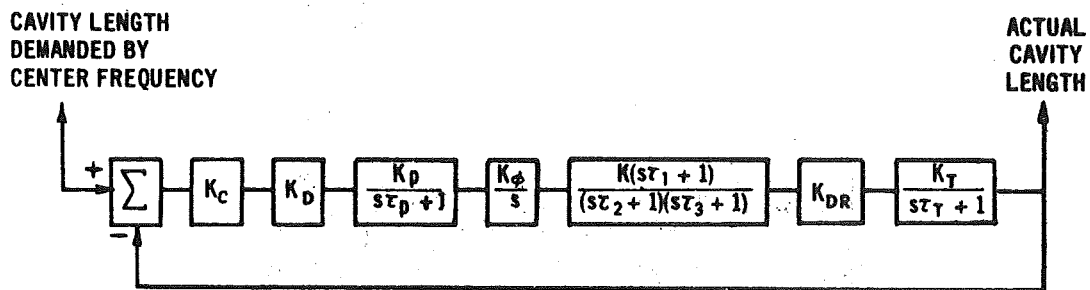


Figure 3.....Laser Signature Over Three Half Wavelengths



TX AFC SYSTEM BLOCK DIAGRAM

- | | |
|--|--|
| $K_C = \text{Cavity Gain} = 60 \text{ MHz}/\mu$ | $\tau_1 = \text{Phase Advance Time Constant} = 265 \text{ mS}$ |
| $K_D = \text{Discriminator Gain} = 0.89 \text{ mW/MHz}$ | $\tau_2 = \text{Lag Time Constant} = 3.18 \text{ sec}$ |
| $K_p = \text{Power Meter Gain} = 0.00811 \text{ V/mW}$ | $\tau_3 = \text{Lag Time Constant} = 10.6 \text{ sec}$ |
| $\tau_p = \text{Power Meter Time Constant} = 1.2 \text{ mS}$ | $K_{DR} = \text{Driver Gain} = 0.91 \text{ mA/V}$ |
| $K_\phi = \text{Phase Detector Gain} = 50 \text{ V/V}$ | $K_\tau = \text{Transducer Gain} = 10 \mu\text{mA}$ |
| $K = \text{System Additional Gain} = 2.3 \text{ V/V}$ | $\tau_\tau = \text{Transducer Time Constant} = 1 \text{ mS}$ |

$$OLTF = \frac{K_C K_D K_p K_\phi K K_{DR} K_\tau (s\tau_1 + 1)}{s(s\tau_p + 1)(s\tau_2 + 1)(s\tau_3 + 1)(s\tau_\tau + 1)}$$

Figure 4.....Control System Block Diagram

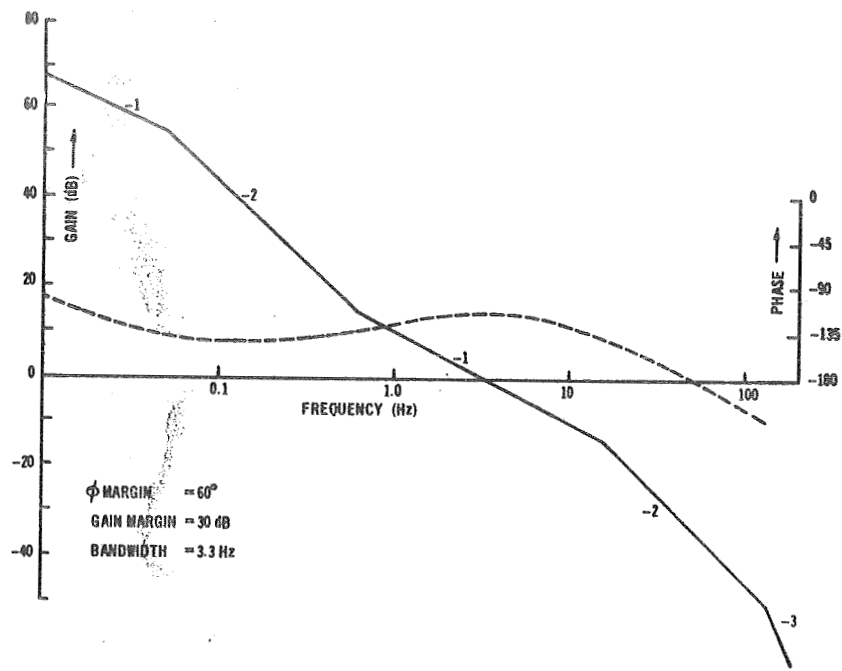


Figure 5.....Bode Diagram Showing Control System Stability

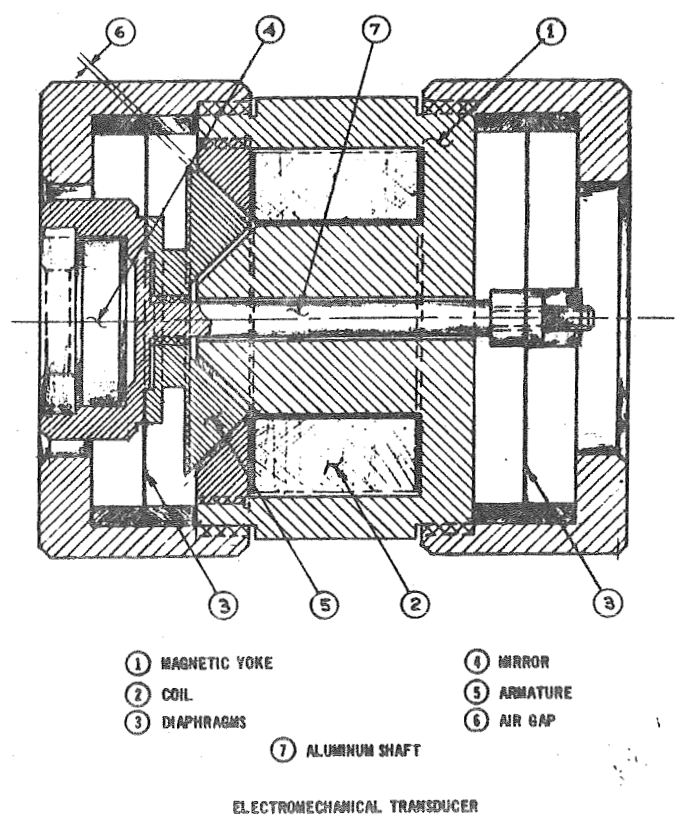
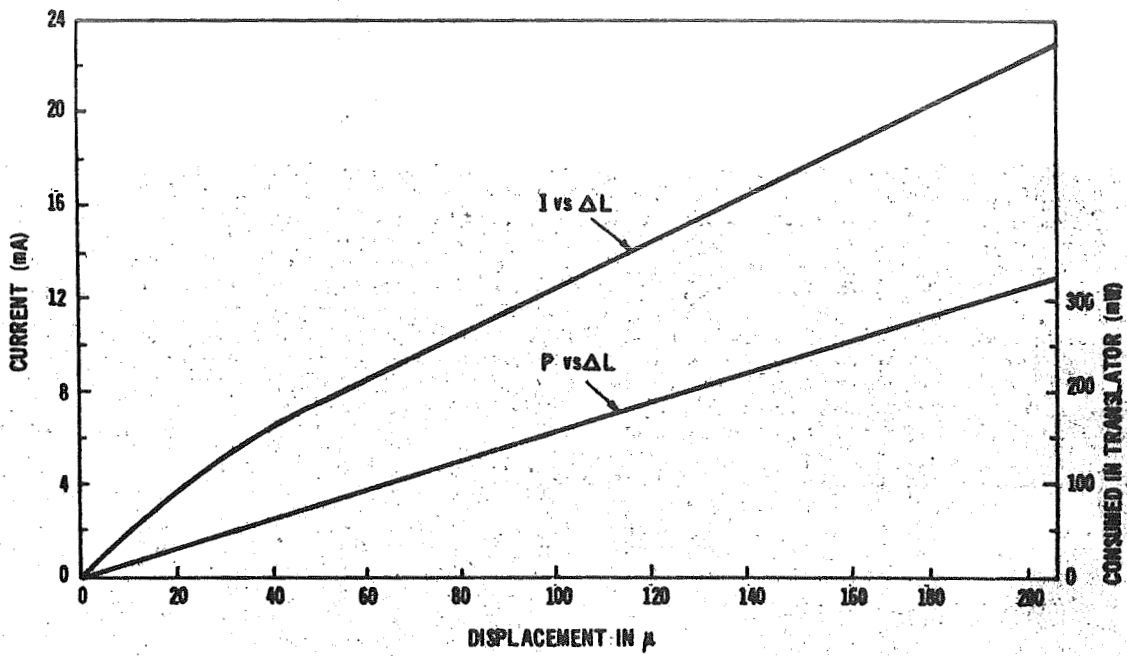
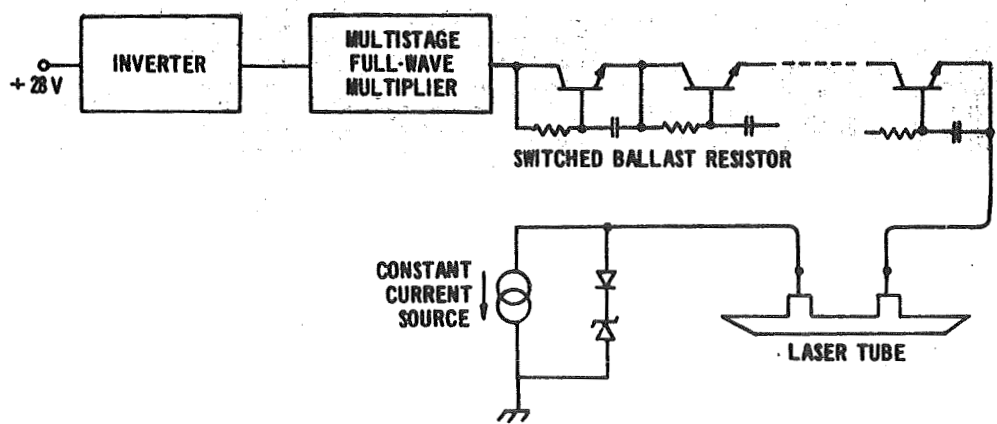


Figure 6.....Cross Section of Electro-Mechanical Transducer



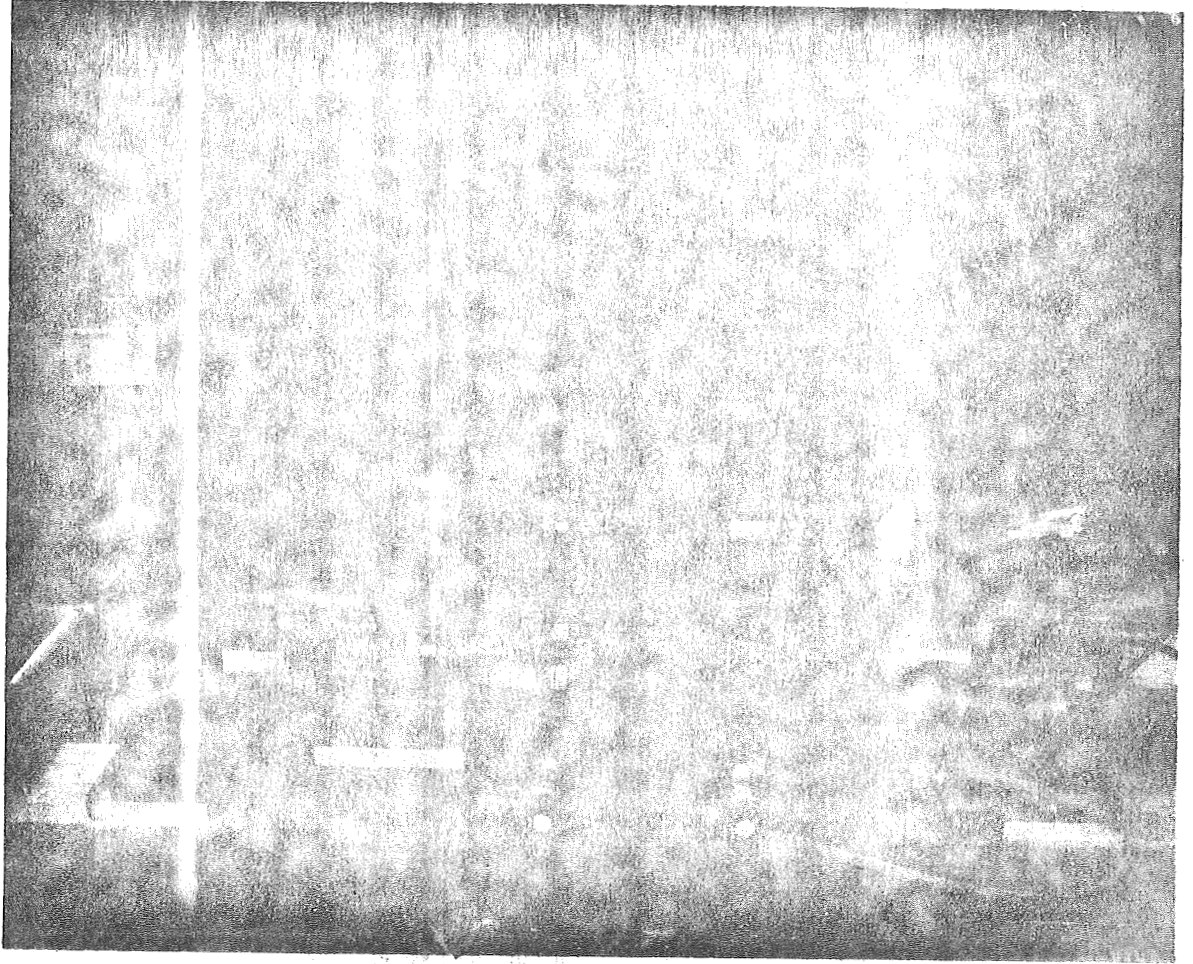
ELECTROMECHANICAL TRANSDUCER PERFORMANCE

Figure 7.....Electro-Mechanical Transducer Performance



HIGH VOLTAGE LASER POWER SUPPLY

Figure 8.....Block Diagram of High Voltage Laser Power Supply



N70-40969

AN ALL-SOLID-STATE, S-BAND PARAMP UTILIZING
MICROWAVE INTEGRATED CIRCUITS

P. H. Dalle Mura

NASA-Goddard Space Flight Center
Greenbelt, Maryland

SUMMARY

An all solid state paramp developed for use aboard a Data Relay Satellite in synchronous orbit is described. The paramp is a wide instantaneous bandwidth, low noise unit which utilizes a Gunn Device Oscillator as a pump source and a hybrid microwave integrated circuit in the circulator-paramp section. Some of the difficulties encountered in the application of microstrip circuitry to the paramp components are described. Selection of the type of solid state pump oscillator based on paramp noise performance is discussed. Test results which were measured on the paramp are presented.

INTRODUCTION

Until recently, the application of low noise parametric amplifiers to spacecraft systems was unrealistic for two reasons. First, the size and weight of conventional paramps were prohibitively large to be considered for inclusion in a spacecraft where weight and size are always at a premium. Second, klystron tubes required for pump sources are limited lifetime devices unsuited for satellite applications.

Two areas of development during the past few years have removed the barriers impeding the application of paramps to spacecraft systems. These are the developments in microwave integrated circuits, and the development of various solid state oscillators suitable for paramp pump sources. The microwave integrated circuits have allowed a tremendous reduction in the size and weight of paramps by the use of high dielectric substrate microstrip circuits using hybrid techniques. The solid state pump sources have also contributed to the size and weight reduction by allowing smaller oscillator structures and smaller, low voltage power supplies. They also eliminate the second barrier by providing a long life, highly reliable pump oscillator to replace the klystron tube.

Utilizing these developments in microwave integrated circuits and solid state oscillators, a prototype paramp was developed* to fulfill the requirements of the Data Relay Satellite for a low noise preamplifier operating in a synchronously orbiting spacecraft.

*This work was performed under contract NAS5-10657 by Airborne Instruments Laboratory, Melville, L. I., N. Y.

DESCRIPTION

A decision was made early in the program to employ thin film microstrip utilizing a twenty mil thick glazed alumina substrate. The choice of a ferrimagnetic substrate was ruled out because of the loss factor, although this choice would have accommodated the circulator development more easily. Figure 1 is a photograph of the completed paramp depicting the circulator-paramp portion in microstrip and the solid state pump source in Ku-Band waveguide.

The circulator consists of a one inch diameter ferrite "puck" cemented into a one inch diameter hole in the alumina substrate with the "Wye" junction and matching transformers deposited on top of the ferrite-alumina combination. The ferrite is lapped flat with the surface of the alumina before the top conductor pattern is deposited. A one and one-quarter inch diameter permanent magnet having a field strength of 400 Gauss is cemented to the ground plane side of the circulator as shown in Figure 2. Also shown are paramp bias circuit components including a miniature bias control potentiometer.

The microstrip circuit is fabricated as follows: A copper-over-chromium film is first deposited over the entire top and bottom surface of the substrate. Then the top conductor pattern is outlined with etch resist by means of a suitable mask. The excess copper is then etched away leaving the desired conductor configuration. Critical electrical connection points such as the circulator-transformer junction, circulator-paramp junction, and the OSM coax-to-microstrip junctions are reinforced by small sections of gold ribbon parallel-gap welded across the junction.

The varactor employed is a Sylvania Type 5147E utilizing a pin cap package. Figure 3 depicts the method of mounting the varactor through the microstrip substrate and shows how contacting to the varactor is effected. Low temperature, pure indium solder is used to secure the varactor to the substrate ground plane before the substrate is positioned into the aluminum frame. The frame is machined out to allow entrance of the varactor cap and pin. The contact to the top of the varactor is by means of a gold ribbon which is indium soldered to the varactor and gap welded to the microstrip conductor.

Early in the development program, an attempt was made to realize the solid state pump oscillator completely in microstrip circuitry. Both Avalanche and Gunn Effect Oscillators were explored. This effort was abandoned in favor of an approach in which the active oscillator device is embedded in a waveguide cavity, lightly coupled to the microstrip paramp circuit, and which is integral with the overall amplifier enclosure. The advantages of this approach, as compared to the microstrip oscillator are: (1) significantly higher oscillator resonator selectivity resulting in better pump spectral purity, (2) better oscillator device heat sinking

and (3) lower pump circuit losses. The pump oscillator waveguide cavity was designed to accommodate either an Avalanche Diode or a Gunn Effect Device so that a direct comparison could be made of their respective influence on the paramp noise performance. Each type of oscillator was capable of producing 100 mW of cw power at 14 GHz. This amount of power is more than adequate to fully pump the varactor under broadband conditions. The loaded Q of the cavity is the same ($Q_L = 400$) for both devices.

Noise figure measurements showed that the Avalanche Oscillator pump caused the paramp noise figure to increase by about 3 db over that obtained with the Gunn Oscillator pump. Also, improving the Q_L of the Avalanche Oscillator cavity still did not bring its performance up to that of the Gunn Oscillator, although it did improve the noise figure of the paramp somewhat. Although these experiments did not divulge the mechanism of noise degradation due to the Avalanche Oscillator, the Gunn Oscillator was selected as the pump source in order to expedite the paramp development. It appears that further investigation is required into the exact nature of the Avalanche Oscillator noise contribution before making a final determination as to its applicability as a paramp pump source.

TEST RESULTS

Complete test results for the paramp are presented in Table 1, while Figure 4 shows a swept frequency response of the paramp bandpass. The 1 db bandwidth of the amplifier comes close to covering the entire 2.2 to 2.3 GHz Telemetry Band which was the program objective. The noise temperature was measured by means of an accurate hot and cold input termination setup and compares favorably with the best standard wideband paramps operating in this frequency band, the latter showing a noise temperature of about 100°K., against 139°K. for the integrated paramp. The gain stability was measured only over standard laboratory temperatures, since a complete environmental operating specification was not deemed necessary for a first developmental model.

Table 1

Integrated Paramp Test Results

Gain	15 db
Bandpass (3 db)	120 MHz
(1 db)	94 MHz
Center Frequency	2250 MHz
Noise Temperature	139°K
	(N.F. = 1.7 db)
Gain Stability (24 Hr.)	±0.2 db
Input VSWR	4 to 1
Weight	9 oz.
Volume	6 cubic inches

The input VSWR is seen to be excessively high and was a major cause of concern. Investigations into the problem have shown that the layout of the microstrip circuit itself is the chief offender. Referring back to Figure 1, it can be seen that the paramp broadbanding stubs are located tangentially to the circulator disc. Magnetic coupling between the ferrite disc and the stubs causes a distortion in the circulator symmetry and thereby adversely affects the reverse isolation of the circulator. This in turn results in a high input VSWR when the amplifier is operating at 15 db gain. The obvious solution to the problem is to relocate the broadbanding stubs so that their effect on the circulator is negligible. In order to verify this, the broadbanding stubs were relocated so that they angled away from the circulator junction rather than being tangential to it. This did indeed improve the circulator isolation to the extent that the input VSWR was reduced to under 1.6 to 1. Angling of the stubs, however, does not represent the optimum solution to the problem, which is a relayout of the microstrip circuit with at least a quarter wavelength spacing between the circulator and the stubs.

CONCLUSIONS

It is felt that this integrated paramp development represents a significant first step in providing low noise paramps for use in a variety of space applications. No fundamental limitation appears to exist which would prevent the use in space of a component employed successfully for many years in sensitive ground receiving systems. For this signal frequency range, microstrip circuitry seems well suited for use in the signal and idler circuits; however, the use of waveguide components in the pump circuit seems a better choice for the reasons pointed out earlier.

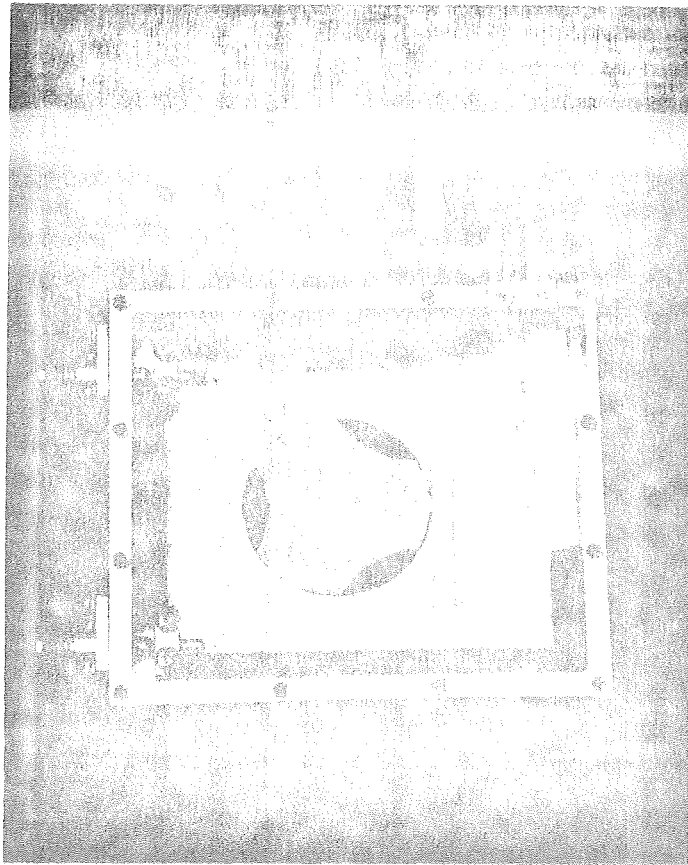


Figure 1

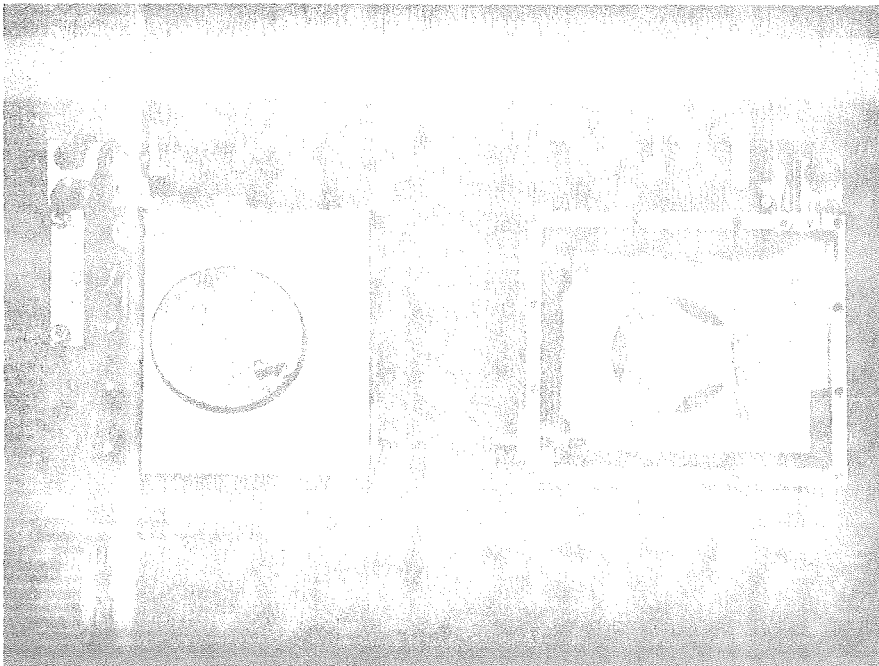
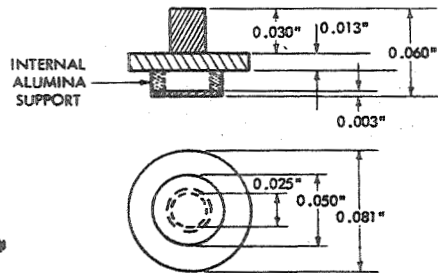
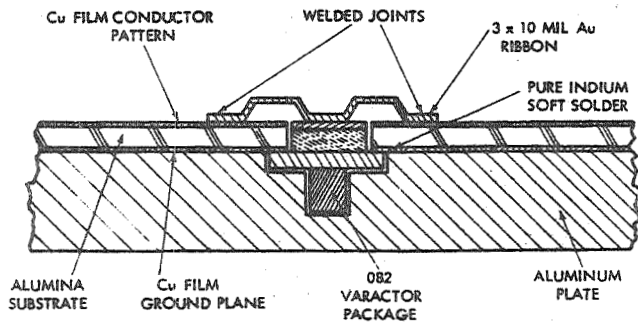


Figure 2



A - MICRO PILL (082) VARACTOR PACKAGE OUTLINE



B - SHUNT MOUNTING CONFIGURATION IN MICROSTRIP

Figure 3

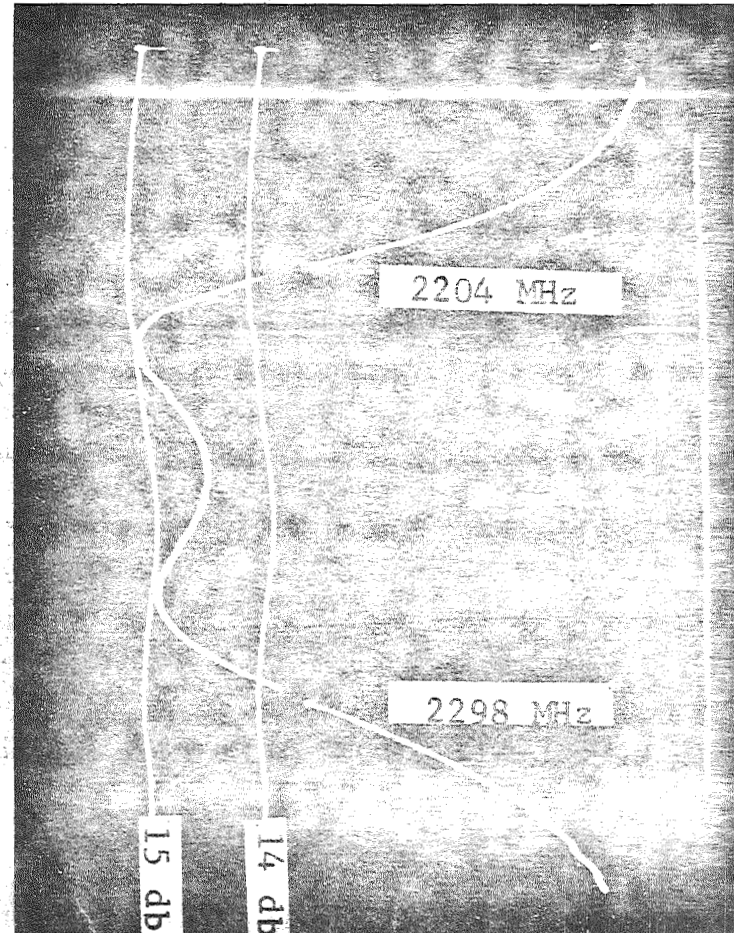


Figure 4

N70-40970

INSTRUMENT LANDING SYSTEMS FOR THE SPACE SHUTTLE

Herbert P. Raabe

IBM Corporation
Gathersburg, Maryland

Abstract

The terminal flight characteristics of the returning space shuttle are described and the requirements for an instrument landing system (ILS) derived. The presently available systems are reviewed and their deficiencies to serve the shuttle are pointed out. The effort of the special committee SC-117 of the Radio Technical Commission for Aeronautics (RTCA) is reported. This effort consists of defining future requirements for aircraft ILS's, screening proposed techniques for their potential in meeting these requirements and establishing a common waveform. The requirements for space shuttle and aircraft landing operations are compared. An ILS concept potentially capable of meeting shuttle and aircraft requirements is described.

Terminal Flight Characteristics and Requirements for a Shuttle ILS (Figure 1)

The terminal flight characteristics of the space shuttle have not been definitized yet. Since the shuttle may have to land safely in various configurations as dictated by emergency conditions, various terminal flight paths will have to be accommodated. From preliminary studies two configurations have been selected which place extreme demands on an instrument landing system:

1. Space Shuttle unpowered with wings.
2. Space Shuttle powered without wings.

These two configurations operate on glide angles of 20 degrees and 3 degrees, respectively. Both flight paths flare out into a final glide angle of 0.75 degrees to touchdown. The horizontal speed will be 300 ft/s with a corresponding sink rate of 4 ft/s. Except for the steep glide angle the approach of the shuttle is like that of a jet plane. The required range of the landing guidance system should be 20 nmi where the altitudes are 40,000 feet and 6,000 feet, respectively, for the two configurations.

Angular guidance and distance data must be available from a 20 nmi range all the way to roll out. The sampling rate of these data should be at least 5Hz at long ranges and at least 15Hz before the shuttle enters the flare-out maneuver until it reaches the end of the roll out. Various glide angles up to 20 degrees must be provided. Hence manual as well as automatic landing capability must be provided.

Fly-out guidance for a missed approach and repeated landing support must be provided.

The allowable error at touchdown shall be +15 feet lateral, +800 feet longitudinal on a runway of 150 ft. x 10,000 ft.

The Present FAA ILS and its Suitability to Serve the Space Shuttle and to meet future Requirements of Aircraft Operations (Figure 2)

The present ILS is shown schematically. It consists of a localizer, glide slope facility and distance measurement equipment. The localizer defines the vertical plane over the center of the runway by radiating two overlapping beams from the end of the runway. The carrier of both beams is the same ≈ 110 MHz but the two beams are modulated by different audio frequencies, 90 Hz and 150 Hz, respectively. Balance of the modulation intensity identifies the localizer plane.

The glide slope equipment operates on the same principle as the localizer. The radiating array is vertical and positioned off the forward end of the runway. Again two overlapping beams are formed. Radiation of the carrier of ≈ 330 MHz is restricted to the forward sector. The two beams are also modulated by 90 Hz and 150 Hz, respectively. The glide slope angle is ~ 3 degrees. The intersection of the glide slope cone with the localizer plane defines the single available approach path. However, guidance to touchdown is not provided so that landing requires pilot control and visibility of the runway on the final approach.

The distance measurement equipment (DME) requires the initial pulse transmission from the spacecraft to which the ground transponder responds. Thus range measurement requires a wide band signal.

The present ILS can serve the space shuttle only when approaching as configuration 2, with manual landing control with visibility assured before the flare-out maneuver starts. Even in this case the present ILS must perform nearly ideally.

The major deficiencies of the present ILS to serve the space shuttle and aircraft operations are:

1. Limitation to one approach path of low glide angle. The space shuttle requires guidance along a variety of glide angles up to 20 degrees. Many types of aircraft will require steeper glide paths and curved approaches in the horizontal plane.
2. The glide path does not terminate on the ground. Flare-out to touchdown and roll out maneuvers must be made manually and visibility of the runway is required.
3. The wide VHF beams of the localizer lead to RF scattering from buildings and terrain features resulting in errors of the flight path.
4. No guidance in elevation is provided by the present system for the fly-out in the case of a missed approach.

In January 1969 SC 117 published the "Tentative Operational Requirements for a New Guidance System for Approach and Landing" and invited submission of proposals to meet these requirements. In response to this invitation twenty-three specific proposals were received. From the SC 117 membership the Techniques Assessment Team (TAT) of experts was chosen which divided the proposals into three categories. The first category comprised seven microwave Scanning Beam Systems, the second category included Multilateration Systems, while the remainder of proposals based on various techniques was placed into the third category of Miscellaneous Systems.

Although no single proposal met all requirements, TAT decided in October 1969 that the scanning beam techniques held the greatest promise and that the signal structure should be based on the capabilities of these techniques. Therefore the proposers of the seven scanning beam techniques were invited to participate in the Signal Format Development Team and to establish final specifications for the signal structure.

So far the effort of SC 117 has been highly successful considering the complexity of the task. The working group of Signal Format Development Team will present their recommendations to SC 117 in August 1970. If these recommendations are supported by the full committee, then it is up to the Federal Aviation Administration (FAA), the military, foreign governments and other interests if they are willing to accept the recommendations of SC 117.

In the case of acceptance by these interests, verification hardware should be built and tested at selected locations. Thus a number of years will pass before the new system will begin to replace the existing installations. This may occur by 1980.

The Effort of Special Committee SC-117 of RTCA to Promote the Evolution of an Advanced ILS (Figure 3)

In 1967 the airlines agreed that it was about time to start work on the evolution of an advanced ILS to overcome the deficiencies of the present system. These deficiencies were not and still are not severe enough as to require a pursuit of this effort with great urgency. On the contrary, the system is still doing such a good service that more installations are recommended which will be quite useful for years to come. However, in anticipation of increased traffic density and a greater variety of aircraft with different flight characteristics and in order to overcome certain restrictions due to inclement weather, an advanced ILS was eventually needed, and an early coordinated effort was necessary to avoid wasteful proliferation of new techniques.

The task was not merely a technical one, economic and political consideration played a major part. The military had already adopted advanced systems, meeting very specific requirements and the future system should serve the military as well.

Furthermore, international acceptance was required to make the effort a success. Last but not least the cost should be low, especially for smaller aircraft, although they may not get the full service of the system.

To maximize the chance of success for the evolution of a new ILS, it was mandatory that a committee was organized in which all interests were represented. Thus, the Executive Committee of the Radio Technical Commission of Aeronautics (RTCA) established in 1967 the Special Committee 117 under the able leadership of S. Poritzky of the Air Transport Association (ATA).

The task of SC 117 was two-fold. First they had to establish specifications or requirements for the future ILS, second a standard signal structure had to be agreed upon so that any airborne equipment could communicate with any ground installation. Specifications of techniques and hardware were to be limited to the absolute minimum to allow full participation and competition between manufacturers. However, techniques and hardware considerations were initially important so that the final specifications and signal structure would be realistic and economical. Thus an Operational Working Group developed a Statement of Operational Requirements during 1968.

Principles of Angle and Distance Measurement Techniques (Figure 7)

To generate the two angular inputs for the guidance function on-board of an aircraft or the space shuttle a receiver records the time t when the scanner illumination takes place. If the angular positions of the scanners with respect to time are known, azimuth and elevation angles can be derived. To avoid the requirement of a clock which is accurate in absolute time, a timing signal is transmitted from the ground. Two principles are illustrated, the time reference and the code reference technique.

To provide the time reference signal an omnidirectional transmitter generates a pulse at the periodicity of the scanner transmission. For example in the case of an azimuth scanner the omnidirectional pulse may be transmitted whenever the fan beam is parallel to the center line of the runway which happens at time t . In the case of code reference, the timing information is modulated on the scanner signal.

To obtain distance information, an on-board transmitter generates a wideband signal, e.g. a short pulse. The pulse is received by a ground transponder which generates a pulse to be received by the on-board receiver. From the time delay the distance is derived.

Integrated Precision Angle and Distance Measurement Technique (Figure 8)

The precision of time measurement when the peak illumination of the scan beam function occurs is inadequate. A split beam technique offers much greater precision. To generate this beam system, a phased array with two RF inputs may be used. Perfect symmetry of the split beam system is assured if the same frequency is applied to these inputs. To enable the receiver of the scanner signal to keep the two beam signals apart, pulse transmission and time multiplexing is suggested.

The receiver demultiplexes the received pulse series and derives the beam envelope-time function of the two beams in two low-pass filters. A subtractor generates the difference function of the two beam envelopes. This function shows a zero crossing which triggers a pulse. The timing of this pulse indicates the time t_0 when the fan beam plane scans the on-board receiver, except for a fixed time delay due to the low-pass filters.

The precision of the zero crossing time is also assured by the fact that no electronic components are used in the separate paths between the demultiplexer and the subtractor.

To automatically generate distance measurement signals at the rate of the angular signals, the on-board pulse transmission is triggered by the pulse at time t_0 which propagates to the ground and releases a pulse in the ground transponder. This pulse is received by the on-board receiver at time t_D .

The ILS V-Beam Concept by IBM (Figures 9, 10)

An ILS concept which shows promise of meeting all requirements for the service of the space shuttle as well as the great variety of aircraft is based on the V-Beam scanning technique. The scanner which rotates continuously in azimuth generates a left beam system B_l and a right beam system B_r . Each beam system consists of split beam pair, a leading and a tracking beam, B_{ll} with B_l and B_{lr} with B_r , respectively. These beam systems define precise beam planes I_l and I_r which are inclined 45 degrees to form a "V". As the scanner rotates, two scanner pulses f_l and f_r are triggered in the airborne receiver during each revolution. The receiver also receives a pulse 0 from the omnidirectional transmitter 0 every time when the scanning beam plane intersection is parallel to the runway center. From the timing of the three pulses the azimuth angle α and the elevation angle ϵ can be derived. While aircraft A is still waiting outside of the main approach path of the runway, shuttle S is descending over the runway center line. Thus the fan beam pulses are symmetrically disposed to either side of the omnidirectional pulse. The distance measurement may be triggered by the leading fan beam signal and is not shown. The scanner may be located beyond the runway on the center line or off the side of the runway. Its location determines the variation of α and ϵ with distance D for a given approach pattern. The space shuttle computer will derive these angles.

The range and angular accuracy requirements necessitate the use of two frequencies: C-band offers adequate penetration of dense rain over a distance of at least 20 nmi, K-band enables the construction of narrow-beam antennas of reasonable dimensions. Furthermore, the sampling rate of guidance information should be at least 15 Hz during the final phase of the landing while a sampling rate of 5 Hz is adequate for the long range guidance.

These requirements are met by a spinning antenna system consisting of a pair of coarse-beam arrays on one face of a cube and 4 pairs of fine-beam arrays covering 4 faces of a cube. Each array has two RF inputs to generate a split-beam fan pattern as previously described. While the coarse-beam arrays are energized over the full azimuth of 300 degrees, the fine-beam arrays are energized only over the quadrant pointing in the direction of the approaching space shuttle. The signal structure due to the two systems is the same, except that the repetition rate of the fine-beam system is 4 times that of the coarse-beam system and the precision of the former is 2.5 times greater. Thus the computation of the guidance data does not require any change in the computer.

By switching the receiver from the coarse-beam to the fine-beam scanner, the distance measurements also repeat at the higher rate.

FIG. 1.

TERMINAL FLIGHT CHARACTERISTICS OF THE SPACE SHUTTLE

CONFIGURATION 1: SPACE SHUTTLE UNPOWERED WITH WINGS.
CONFIGURATION 2: SPACE SHUTTLE POWERED WITHOUT WINGS.

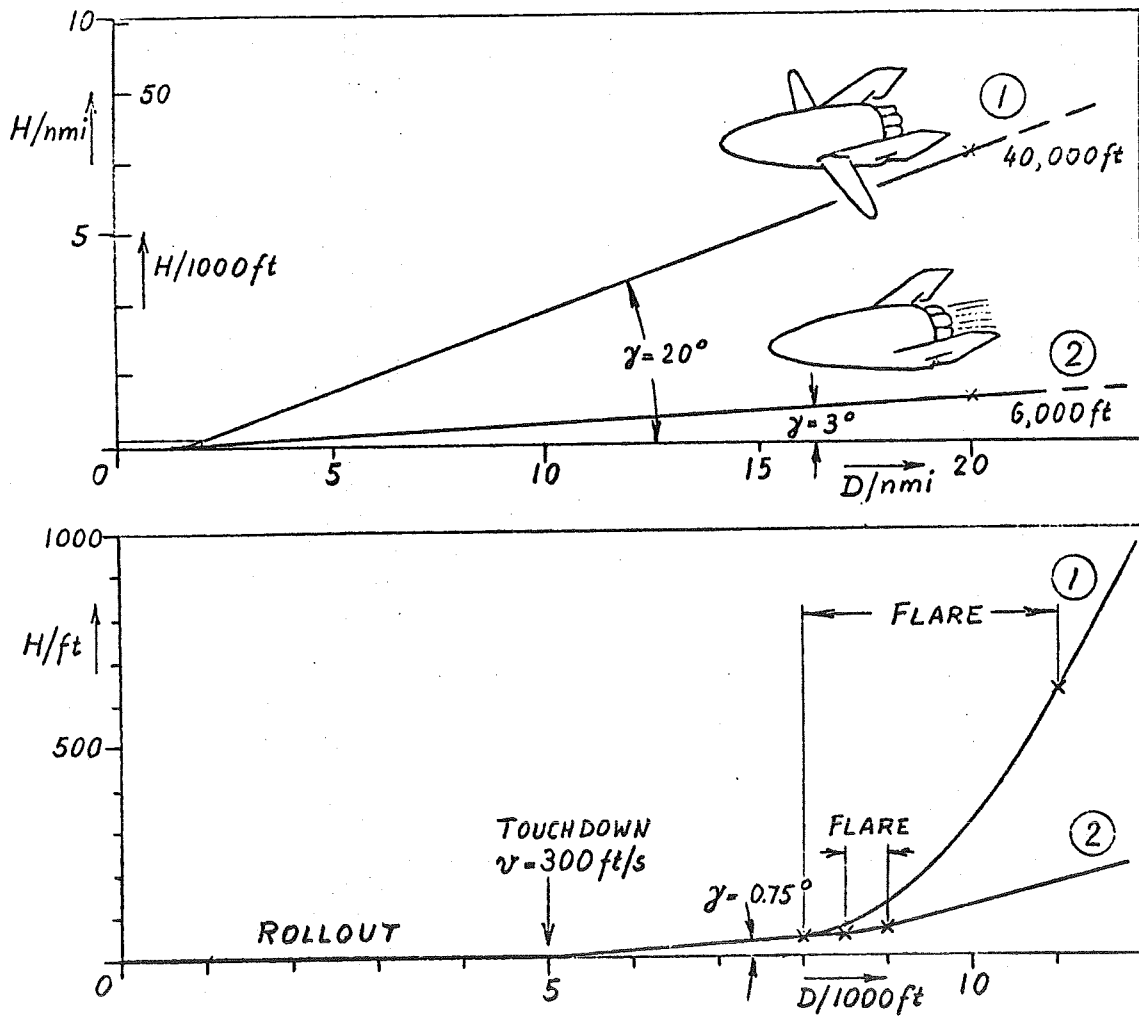


FIG. 2

THE PRESENT FAA ILS AZIMUTH AND ELEVATION GUIDANCE

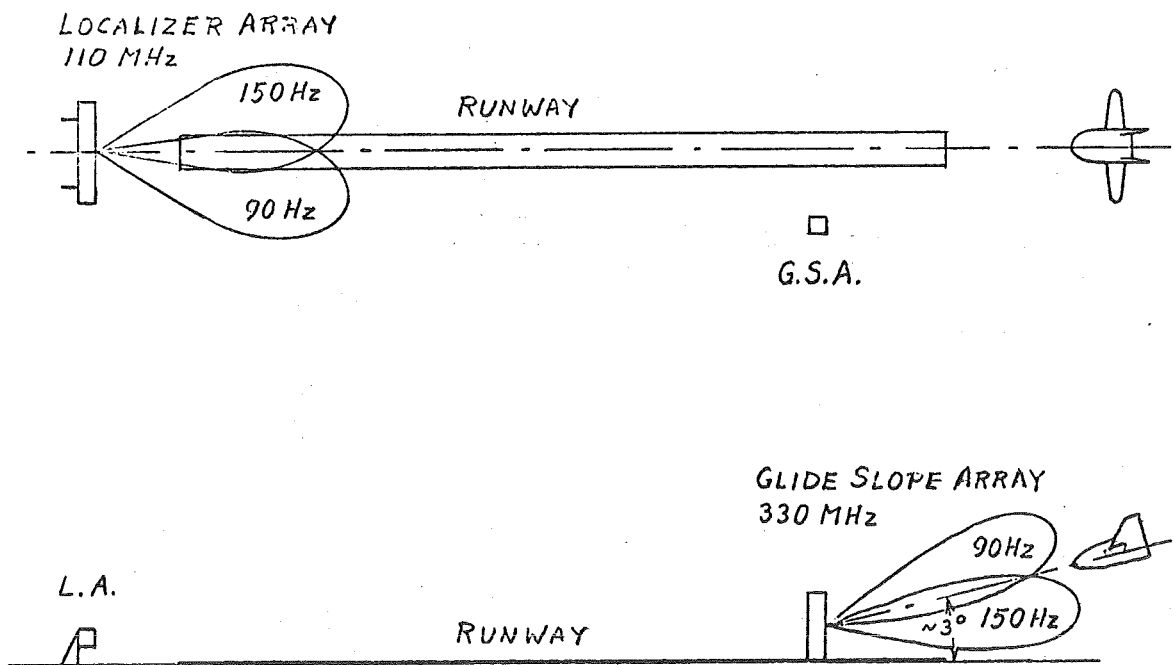


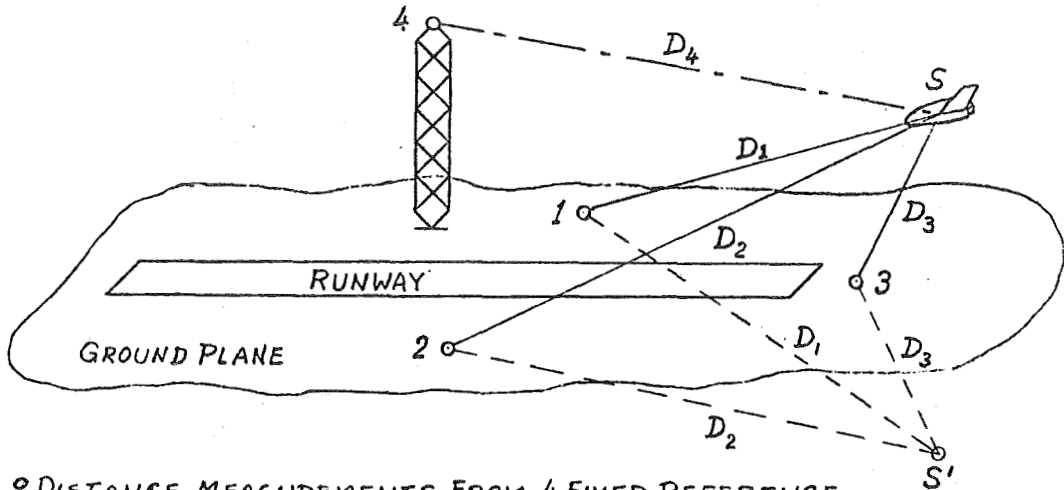
FIG. 3

THE EFFORTS OF SPECIAL COMMITTEE SC 117
OF RTCA TO PROMOTE THE EVOLUTION OF
AN ADVANCED ILS

- (1) IN ANTICIPATION OF THE NEED OF AN ADVANCED ILS, THE SC 117 WAS ESTABLISHED BY THE EXECUTIVE COMMITTEE OF THE RADIO TECHNICAL COMMISSION OF AERONAUTICS IN 1967.
- (2) AN OPERATIONAL WORKING GROUP DEVELOPED A STATEMENT OF OPERATIONAL REQUIREMENTS DURING 1968.
- (3) TENTATIVE OPERATIONAL REQUIREMENTS FOR A NEW GUIDANCE SYSTEM FOR APPROACH AND LANDING PUBLISHED JANUARY 1969.
- (4) CALL FOR PROPOSALS OF NEW GUIDANCE SYSTEM FOR APPROACH AND LANDING ISSUED FEBRUARY 1969.
- (5) EVALUATION OF PROPOSALS BY THE TECHNIQUES ASSESSMENT TEAM DURING APRIL THROUGH SEPTEMBER 1969.
- (6) RECOMMENDATIONS MADE BY THE TECHNIQUES ASSESSMENT TEAM AND ESTABLISHMENT OF THE SIGNAL FORMAT DEVELOPMENT TEAM OCTOBER 1969.
- (7) RECOMMENDATION OF A SIGNAL FORMAT BY THE SIGNAL FORMAT DEVELOPMENT TEAM TO SC 117 AUGUST 1970.

FIG. 4

GUIDANCE BY MULTILATERATION



- DISTANCE MEASUREMENTS FROM 4 FIXED REFERENCE POINTS REQUIRED TO DEFINE LOCATION IN SPACE.
- 3 REFERENCE POINTS DEFINE PAIR OF LOCATIONS IN SYMMETRIC POSITIONS WITH RESPECT TO PLANE OF REFERENCE POINTS.
- AMBIGUITY RESOLVED WHEN REFERENCE POINTS ON GROUND PLANE, BUT LOW ELEVATION ANGLES ARE POORLY DEFINED.
- LOW ELEVATION ANGLES REQUIRE 4th ELEVATED REFERENCE POINT.
- RADIATION OMNIDIRECTIONAL, WIDE BANDWIDTH (MICROWAVE), HIGH POWER.

ADVANTAGES:

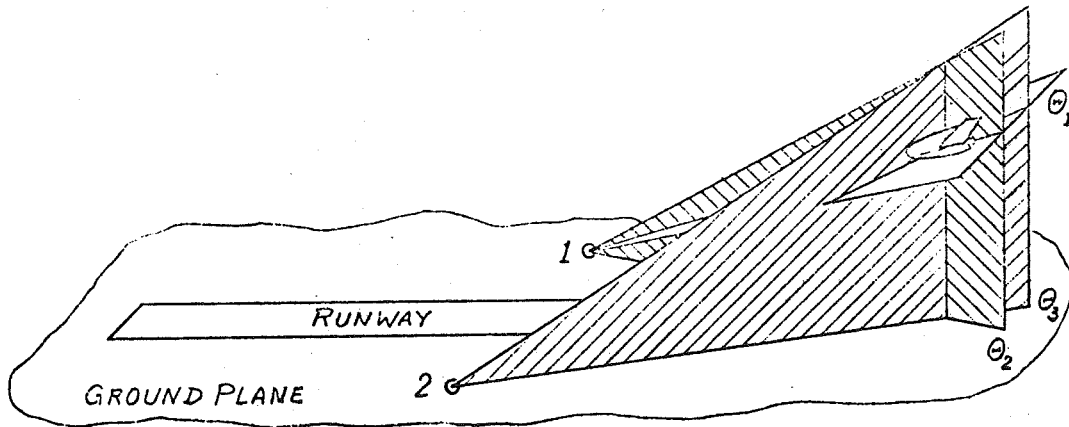
- SMALL ANTENNAS
- REJECTION OF MULTIPATH PROPAGATION
- SMALL RADIAL POSITION ERROR

DISADVANTAGES:

- 4 DISPERSED RADIATORS (ONE ELEVATED)
- HIGH POWER
- WIDE BANDWIDTH
- TANGENTIAL POSITION ERROR INCREASES WITH DISTANCE
- COMPLEXITY OF COMPUTATION

FIG. 5

GUIDANCE BY TRIANGULATION



- ANGLE MEASUREMENTS FROM AT LEAST 2 GROUND BASED REFERENCE POINTS REQUIRED (E.G. ONE ELEVATION ANGLE θ_1 , AND TWO AZIMUTH ANGLES θ_2 AND θ_3).
- PLANAR OR CONICAL FAN BEAMS.
- SCANNING REQUIRED TO COVER SPACE.
- RADIATION DIRECTION (MICROWAVE), NARROW BANDWIDTH (CW), LOW POWER.

ADVANTAGES:

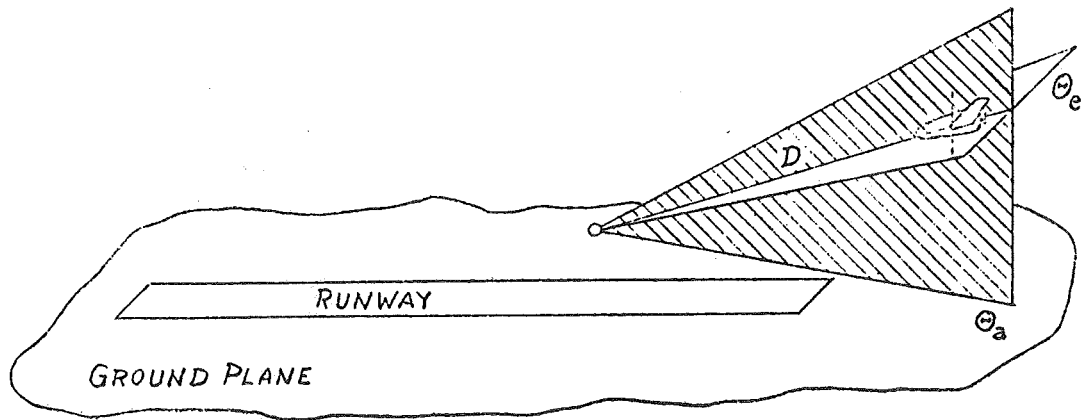
- RADIATORS ON GROUND PLANE
- NARROW BANDWIDTH
- LOW POWER

DISADVANTAGES:

- TWO DISPERSED RADIATORS
- SCANNING WIDE-APERTURE ANTENNAS
- MULTIPATH CAN BE A PROBLEM
- RADIAL AND TANGENTIAL POSITION ERRORS INCREASE WITH DISTANCE

FIG. 6

GUIDANCE BY COMBINATION OF TECHNIQUES



COMBINATION OF ANGLE AND DISTANCE MEASUREMENTS
RESULT IN SUPERIOR SYSTEMS.

EXAMPLE:

TWO SCANNING FAN BEAMS SERVE TO DETERMINE
AZIMUTH AND ELEVATION ANGLES, WHILE
DISTANCE IS DERIVED FROM THE TWO-WAY
PROPAGATION TIME OF A WIDE-BAND WAVEFORM.

ADVANTAGES:

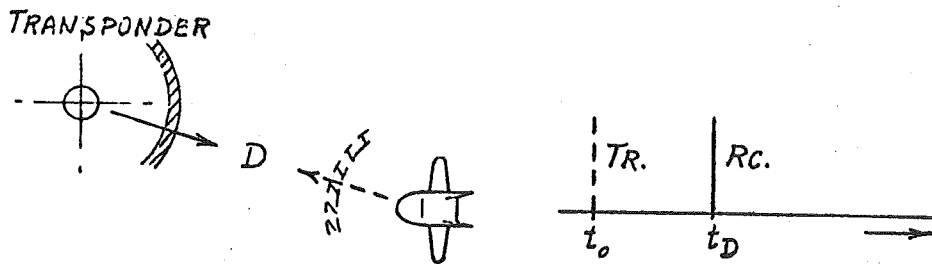
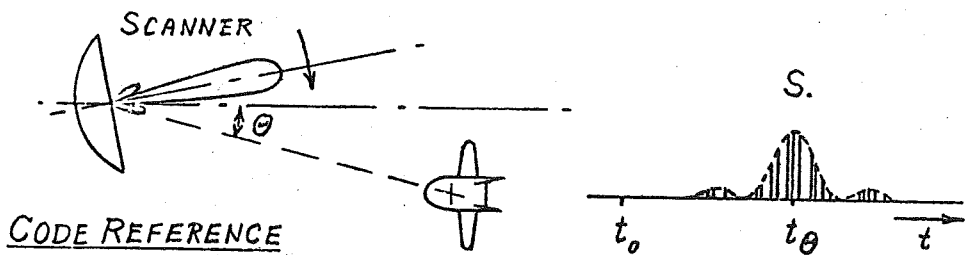
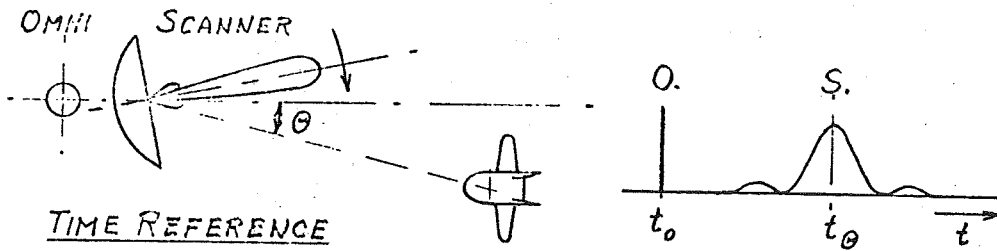
- ALL RADIATORS IN ONE LOCATION ON GROUND PLANE
- SMALL RADIAL POSITION ERROR INDEPENDENT OF DISTANCE
- SIMPLICITY OF COMPUTATION

DISADVANTAGES:

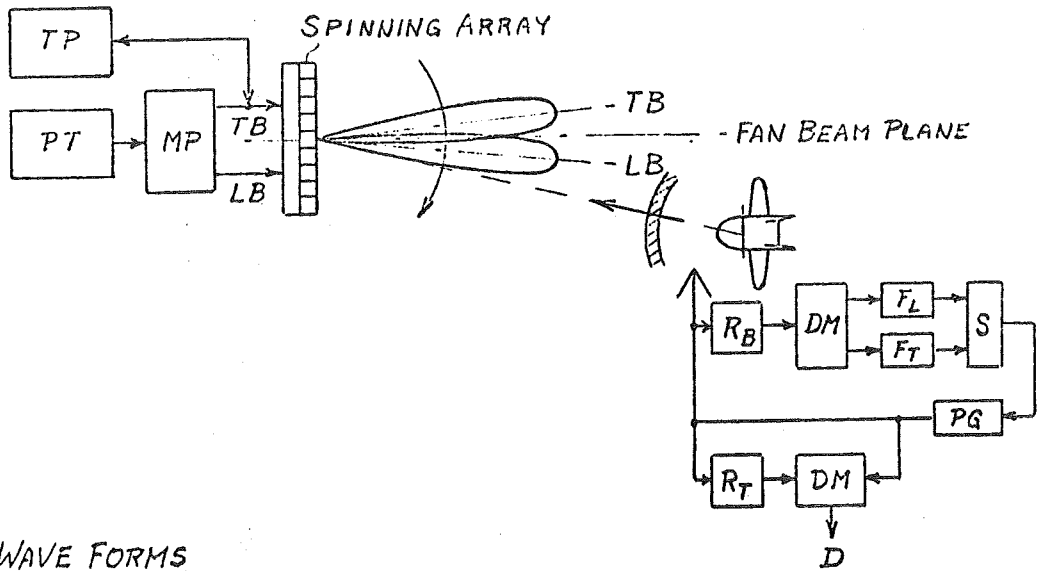
- SCANNING WIDE APERTURE ANTENNAS
- WIDE BANDWIDTH
- TANGENTIAL POSITION ERROR INCREASES WITH DISTANCE

FIG. 7

PRINCIPLES OF ANGLE AND DISTANCE
MEASUREMENT TECHNIQUES



INTEGRATED PRECISION ANGLE AND DISTANCE MEASUREMENT TECHNIQUE



WAVE FORMS

PULSE TRANSMITTER PT

MULTIPLEXER {
LEADING BEAM
TRAILING BEAM

RECEIVER R_B

SUBTRACTOR S

PULSE GENERATOR PG AND
RECEIVER R_T

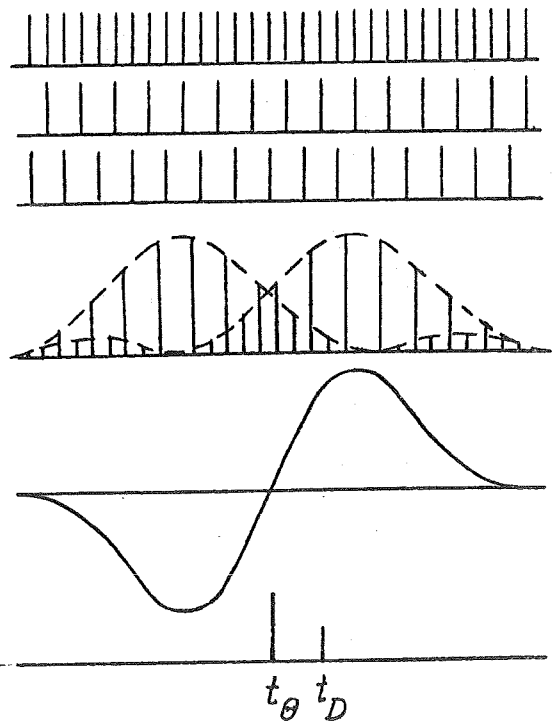
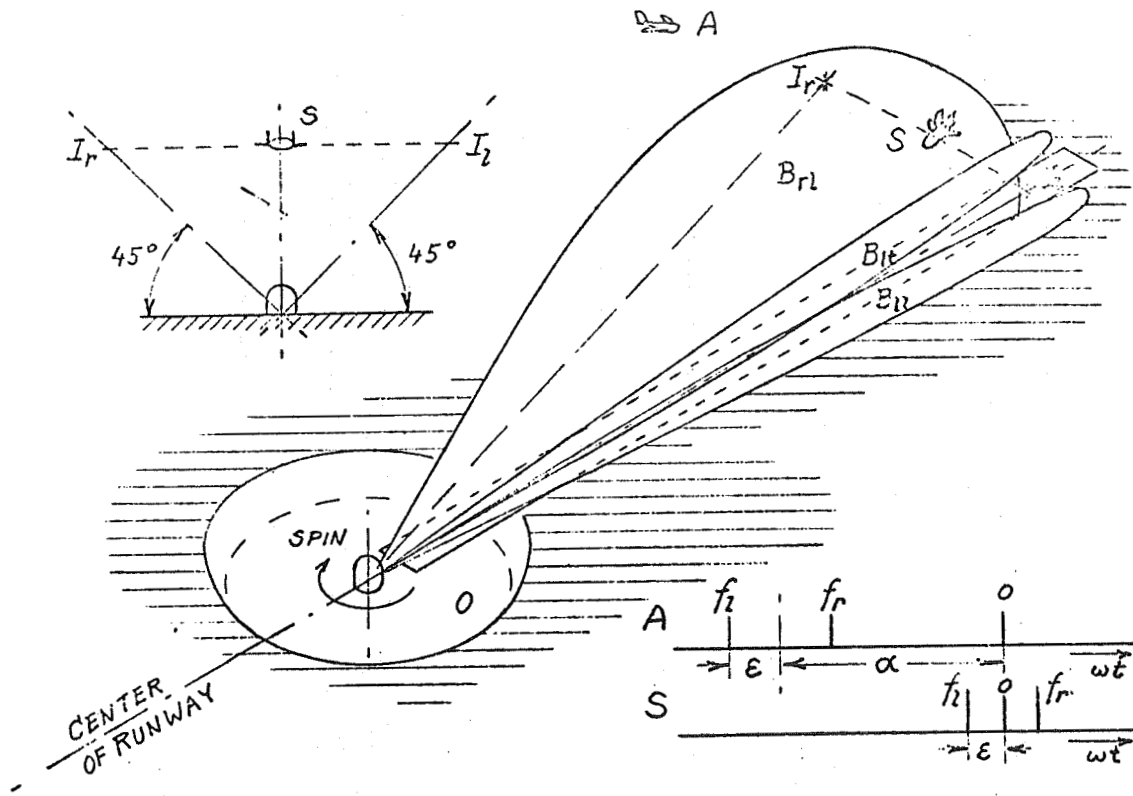
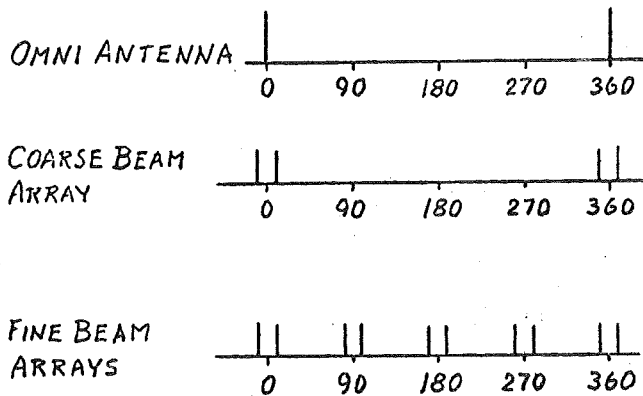
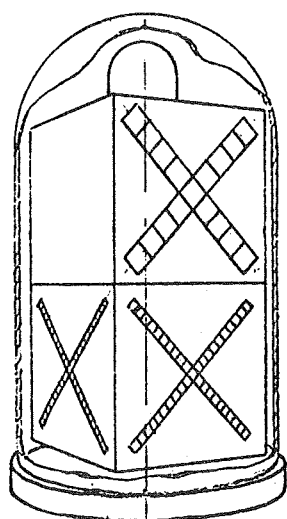
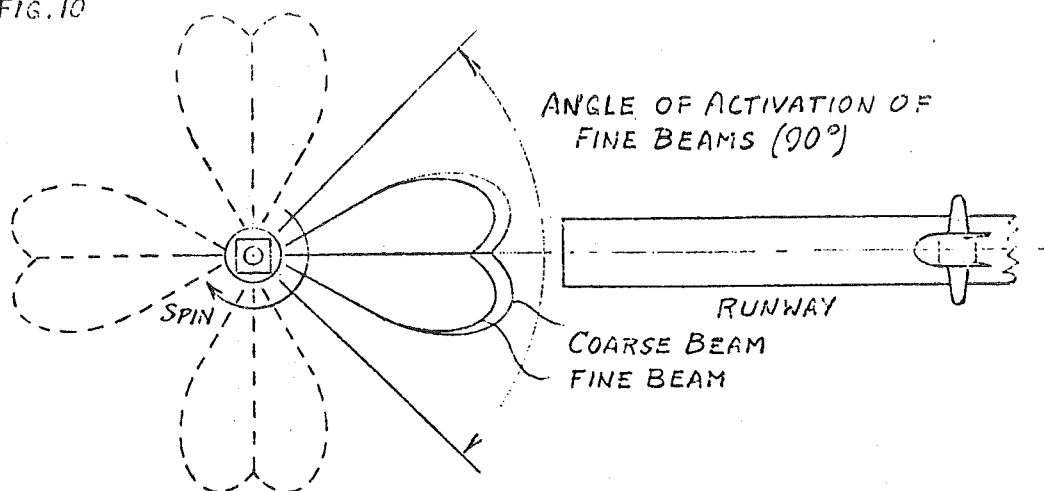


FIG. 9



THE ILS V-BEAM CONCEPT BY IBM

FIG. 10



	COARSE BEAM	FINE BEAM
RADIO FREQUENCY	5 GHz	15 GHz
PULSE REPETITION RATE	12,800/2 Hz	32,000/2 Hz
POLARIZATION	VERTICAL	VERTICAL
BEAM WIDTH, SLANTED	3.54°	1.414°
BEAM WIDTH, HORIZONTAL	5°	2°
PULSES PER BEAM WIDTH	18	18
ARRAY LENGTH	46 in.	39 in.
SIGNAL DWELL TIME	2.78 ms	1.11 ms

COMPUTER GENERATED IMAGERY AS APPLIED TO SPACE SHUTTLE
DESIGN EVALUATION AND SYSTEM SIMULATION

W. Marvin Bunker
General Electric Co.
Daytona Beach, Florida

INTRODUCTION

The term, Computer Generated Imagery, covers a broad field. It can include plotter drawn logic diagrams, CRT alphanumeric displays, "wire figure" drawings, and simulated radar displays, among others. It also should include simulated out-the-window visual scenes showing solid objects in true perspective and in color. This last category of image generation — Visual Scene Simulation — is the subject of this paper.

Visual scene simulation is, of course, also accomplished by other techniques, such as movable TV cameras working in conjunction with three-dimensional models, and projection of moving pictures of actual scenes. Because these techniques have limitations in flexibility, dynamic realism, extent of gaming area, depth of field, difficulty of environment preparation and modification, provision for special effects such as weather variation, and reliability, effort has been directed toward improved techniques. It has long been evident that an all-electronic system, in which the environment definition is stored as numbers in a computer memory and the scene is formed via mathematical operations on these numbers, could either eliminate or greatly relax these limitations. Effort applied to improve efficiency of the computational algorithms required to generate a scene has been paralleled by advancements in circuit element speed and functional complexity per chip. These improvements have simplified the equipment to implement such computer generated image systems to the point where they are now feasible for a variety of applications.

Image Generation System

Figure 1 shows in simplified form the principles of scene formation. The objects comprising a scene are formed of faces with specified color. The faces, in turn, are formed by straight line segments referred to as edges. The computational task consists of determining the images of those portions of edges falling within the current view window, resolving priority conflicts where one object is wholly or partially obscured by another, and arranging this information in scan-element order to form the image.

VIEW PLANE CONCEPT

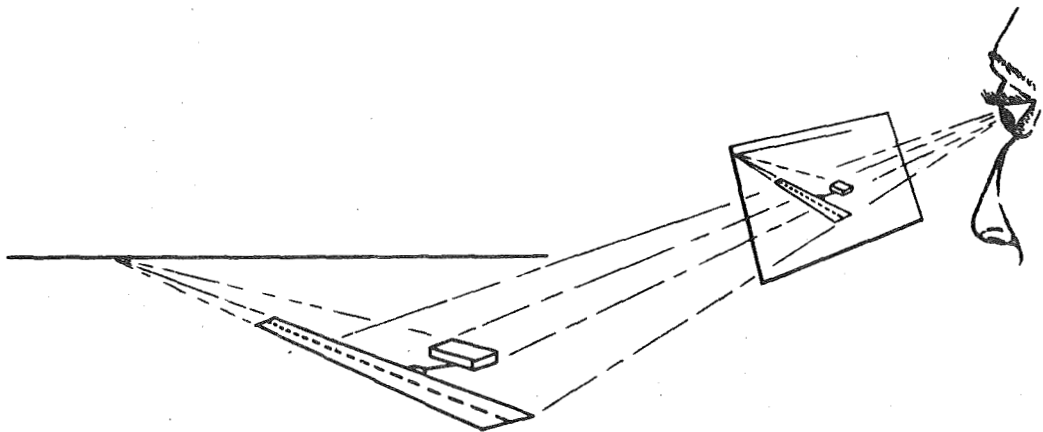
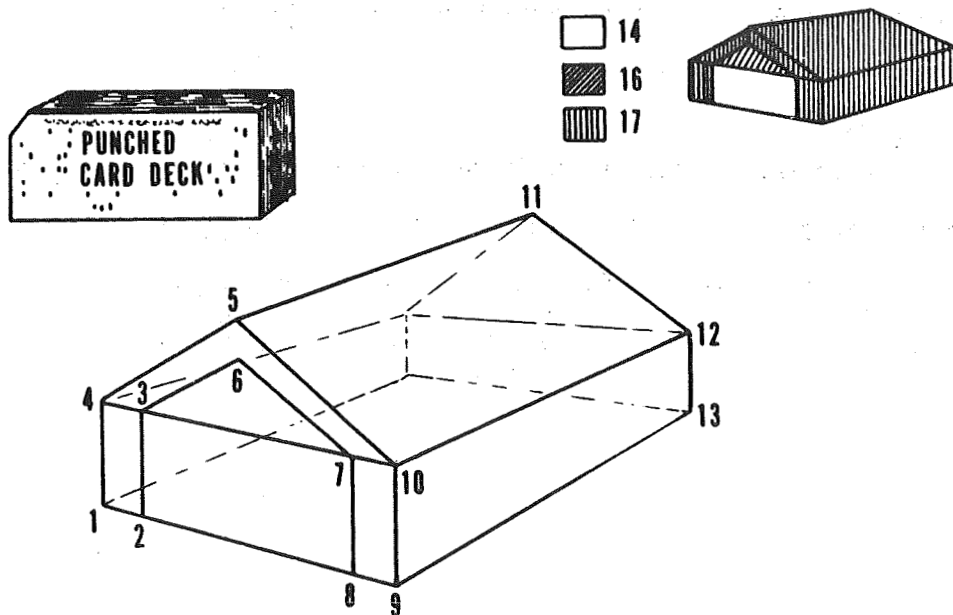


Figure 2 shows the way in which the objects forming the environment are modeled by specifying the three-dimensional coordinates of the vertices of the edges. The hangar shown is formed by 26 edges. The number of edges required to adequately portray the visual cues in a given application is a significant factor in determining the total equipment needed.

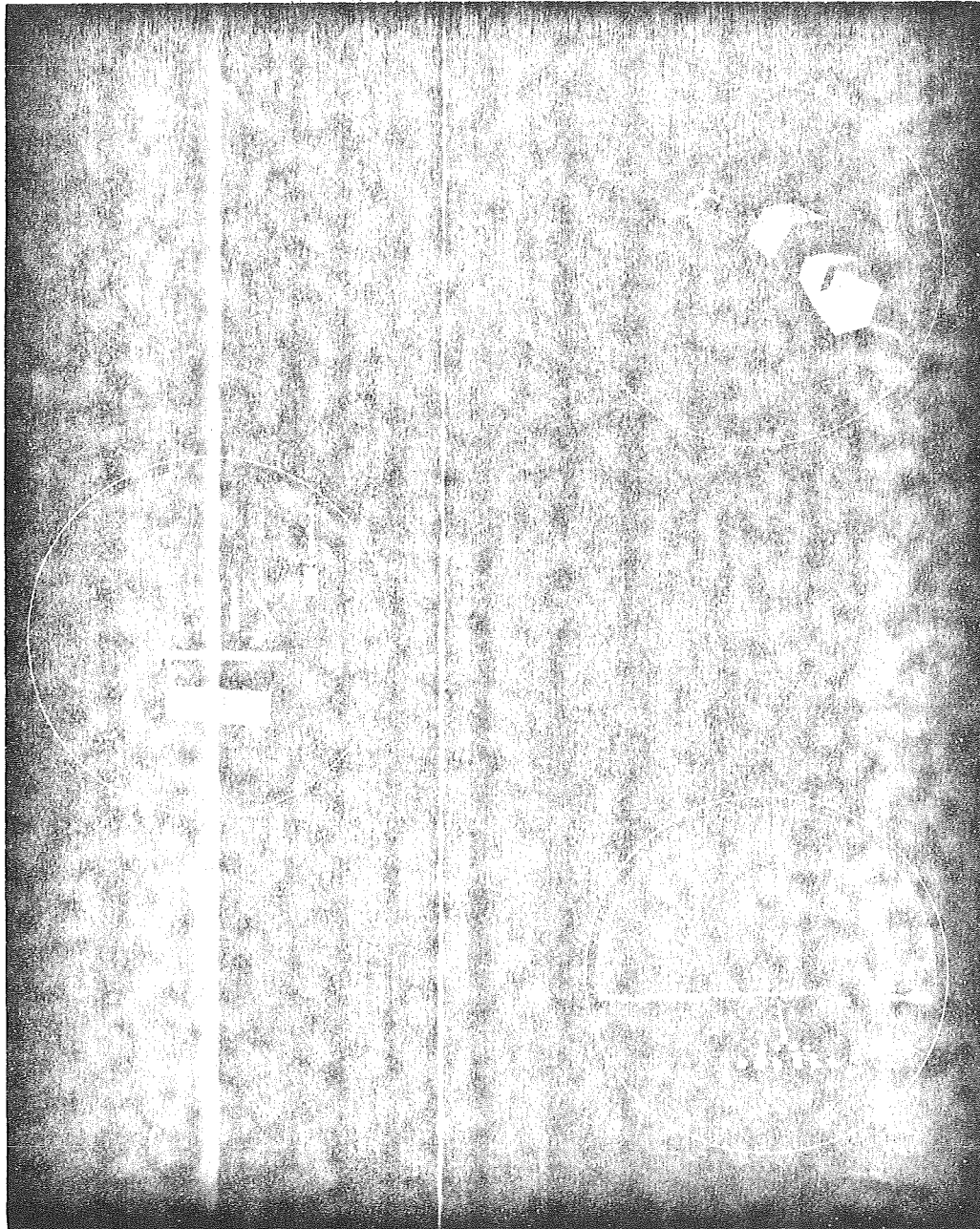
OBJECT DESCRIPTION



System Features and Capabilities

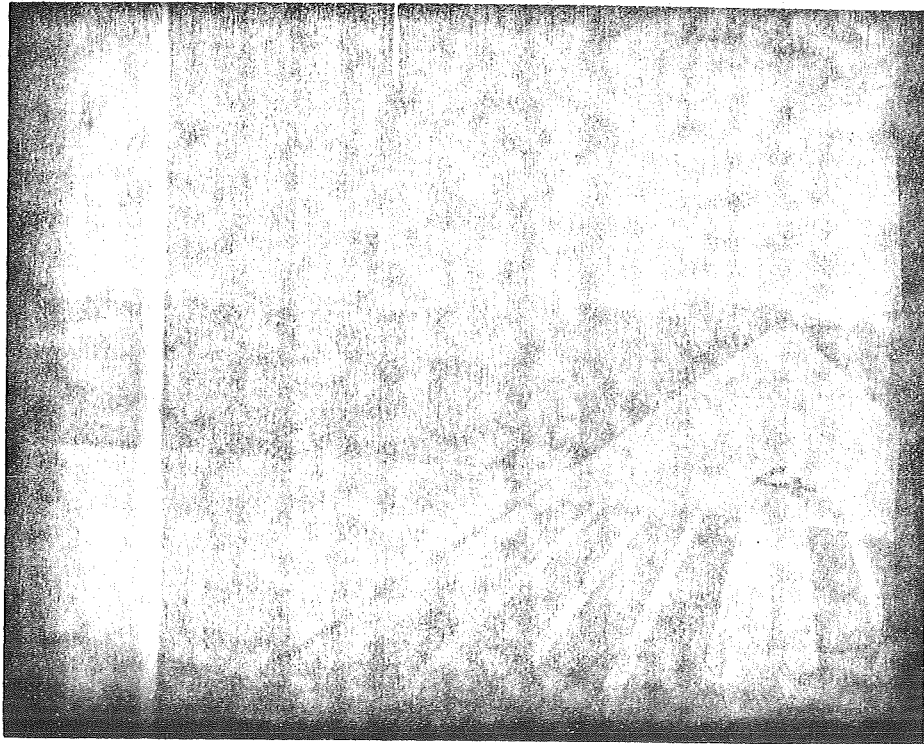
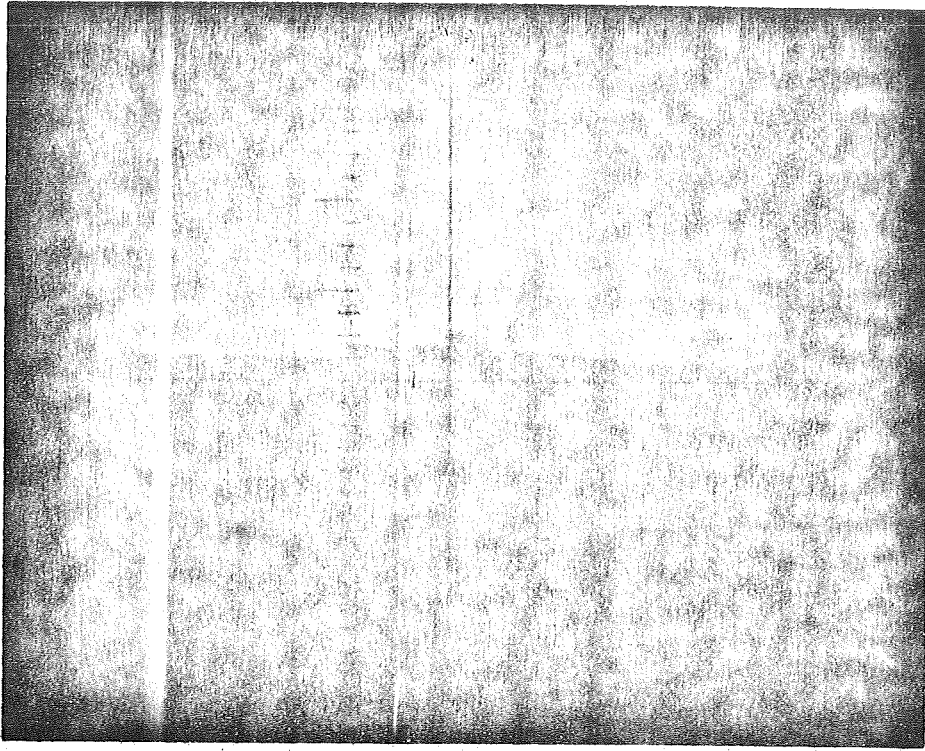
Figure 3 shows three scenes from a system delivered to NASA about three years ago. The illustration shows the type of scenes that can be achieved within the 240-edge capability of that system. To change from the airport runway to the docking simulation and then to the carrier scene involves only changing contents of a core memory. Further, the edge limitation applies to the portion of environment in effect at any one time, not to the total involved in the exercise. This capability could be readily applied to a Space Shuttle simulation. Separate environments applicable to various phases of the mission could be transferred from a mass store to the core at appropriate times without interrupting the exercise itself.

Since that system was delivered, designs have been blocked out for systems with 6 to 12 times the edge capability and with juxtaposed multiple displays for wider fields of view. Moreover, the total racks of equipment will be less than the earlier system.



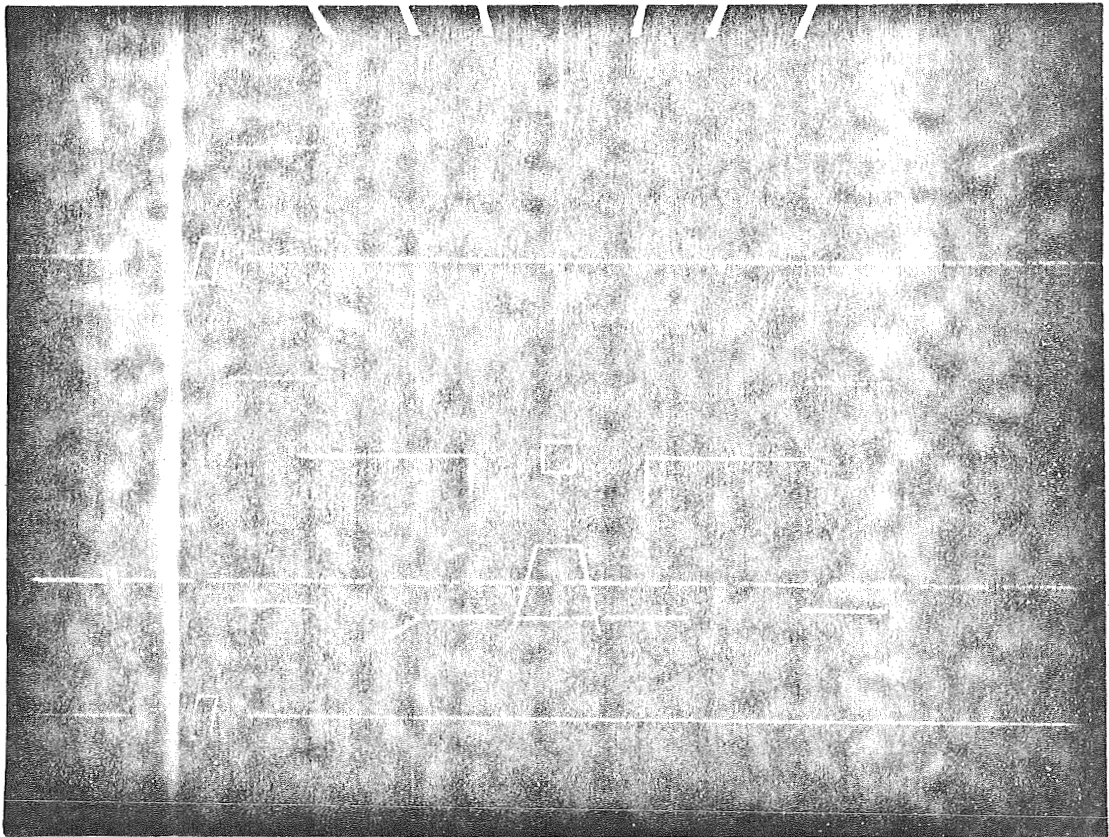
Figures 4 and 5, taken from a static scene generator, show the type of scenes achievable with increased edge count.

The lack of limitation on the dynamic capabilities of this technique may be indicated by considering that the system is generating an entirely new picture each 1/30 second from the environment definition and view window definition applicable at that time. There are no limitations on the magnitude by which either or both of these may change during each such interval. Further, when multiple view windows are defined, they may be associated with different viewpoints. This makes possible such exercises as "dogfight" simulations, a Space Shuttle launch and separation exercise with valid visual scenes for both the launcher and the shuttle, or similar simulation of rendezvous and docking with the Space Station.



The all-electronic nature of the process lends itself readily to adding such features as simulation of an Electronic Attitude Director Indicator, as shown in Figure 6.

These features and capabilities suggest several ways in which Computer Generated Imagery might be applied effectively to the Space Shuttle program.



Space Shuttle Applications

System dynamics at the pilot-controls interface are a function of vehicle dynamics and control system characteristics. Determining actual pilot performance under various conditions with different system dynamics simulated should provide significant inputs to the decision-making process. The validity of these results is a function of the realism of the simulation and of its flexibility in simulating a variety of conditions both normal and abnormal. Computer Generated Imagery could provide the required characteristics.

Visibility from the Space Shuttle will be a function of window area and landing attitude, among other factors. Structural integrity is, in turn, a function of window area and configuration. Window area required for given pilot effectiveness can be reduced by equipment such as the Electronic Attitude Director Indicator mentioned earlier. Here, again, as with vehicle dynamics, a high degree of realism and flexibility is required to assure high-confidence-level results from evaluating various combinations of those factors.

Similarly, design evaluation to determine the effect of critical factors on performance during launch, separation, docking, orbital transfer, reentry, and landing can be effectively accomplished. Later, after vehicle design is complete, a comparable evaluation may be made in simulations of proposed new missions. Certainly, application of the system to training is virtually unlimited.

Availability

To repeat, equipment performing the described functions has been delivered to NASA and is in use. Subsequent design effort has been directed toward improving efficiency and removing limitations associated with that system. This recent effort is reaching maturity. A laboratory version of equipment incorporating current CGI concepts is being fabricated. This includes the design and procurement of several special MOSFET LSI chips which are essential in achieving the most effective ratio of system capability to equipment complexity. The laboratory version is a prototype of the advanced image system which, in a production model, can perform the Space Shuttle program functions discussed here.

N70-40972

SOLID-STATE POWER MANAGEMENT

I. Rakofsky

Grumman
Bethpage, New York

Introduction

Grumman has engaged in extensive analytic and design studies of contactless solid-state electric power management systems for advanced aerospace vehicles. A contactless electric power management system will:

- Replace all conventional electromechanical switching devices (switches, relays, circuit breakers) with functionally equivalent static devices and/or circuitry
- Use low-level, digital, solid-state concepts to implement control logic
- Incorporate multiplex data transmission for transmission of signals
- Include fault detection/isolation test capability
- Use digital data processing techniques for power control, power management, system test, and data transmission integration

The anticipated benefits of the system are:

- Wire Weight Reduction - resulting from shorter wire runs, smaller wire sizes, and multiplexing
- Flexibility - facilitates reconfiguration without extensive rewiring
- Space Conservation - a consequence of reduction in wire bulk, elimination of electromechanical components, use of microelectronics
- Enhanced Performance - improved circuit protection leading to increased safety; optimum power utilization
- Reliability - electromechanical devices, with moving contacts, are inherently less reliable and have shorter lifetimes than static devices; redundancy
- Maintainability - is enhanced by self-test capabilities and greater reliability
- Producibility - installation is simplified through reduction of wiring bulk and improved routing, which require less hardware and structural modification
- Cost-Effectiveness - lower total lifetime costs

Conventional Electromechanical Power Distribution & Control

Conventional power distribution, control, and circuit protection are accomplished by devices with moving, separable mechanical contacts. Contact actuation may be initiated manually, mechanically, electrically, thermally, pneumatically, etc. Control logic is accomplished, at the power level, by physically wiring between the contacts to form the appropriate logic equation.

Electromechanical switching devices have a relatively short operational life expectancy (when compared to static devices), which is a function of mechanical wear, contact erosion, and degrading effects of the operational environment. Thermal circuit breakers, which are the most commonly used protective devices, are generally unpredictable and unreliable.

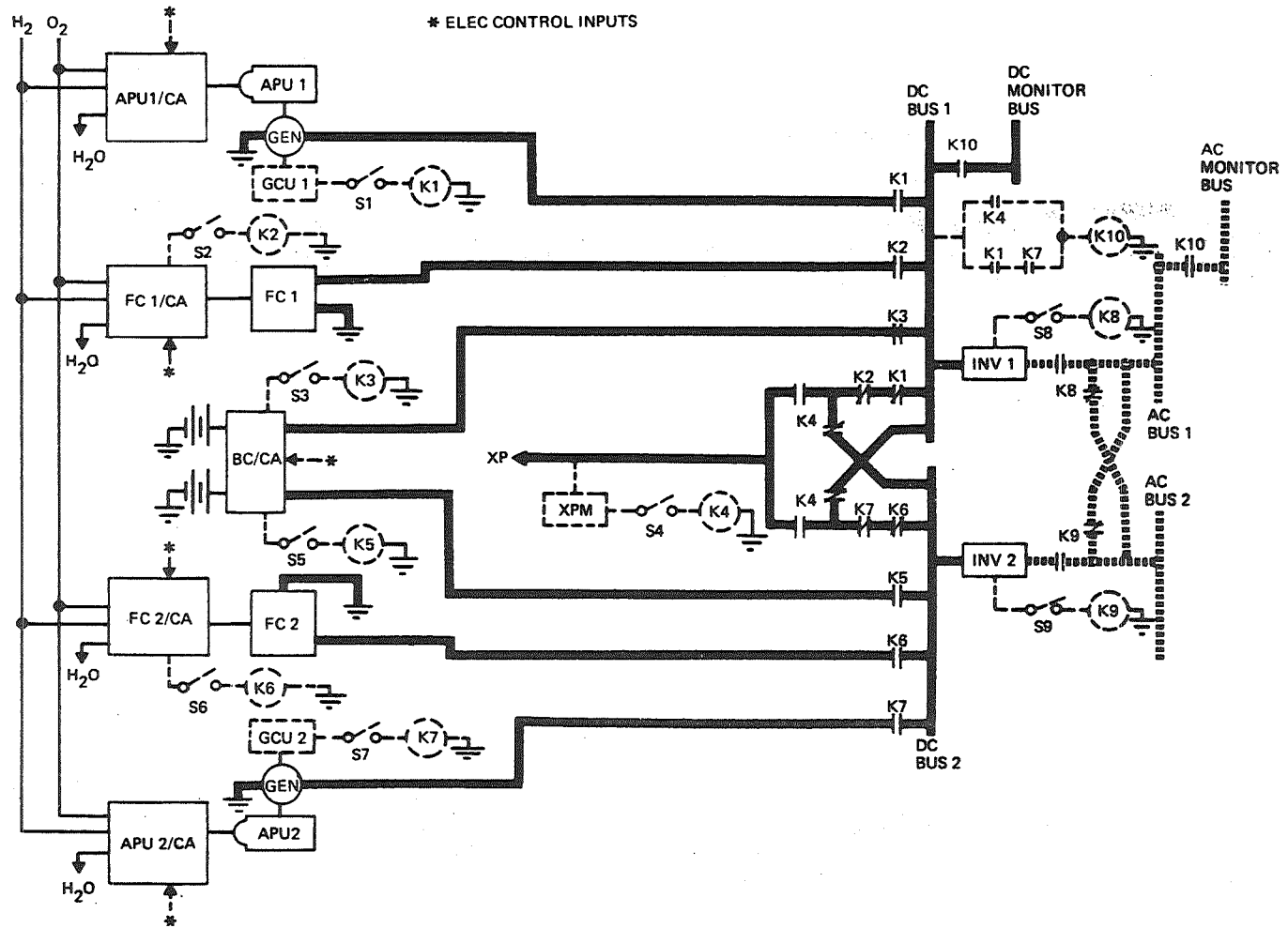
The nature of contact operation, abrupt turn-on/turn-off and contact bounce, produces large transient voltages and problems of electromagnetic interference.

Fig. 1 is a schematic of a typical power distribution/control system for an SSV "Orbiter," utilizing "state-of-the-art" in power source, control, and utilization equipment technology.

Basic power is 28 Vdc supplied by fuel cells during orbital flight, cryogenic-fueled turbine-driven brushless dc generators during aerodynamic flight, or external power during ground operations. Batteries provide for transient power demands and start-up power. Required ac power is supplied thru inverters from the dc busses.

Essentially, the power systems are redundant since each power source is capable of supplying the entire electrical demand for its intended mission usage. Under normal conditions, the active power sources are isolated from one another and each supplies approximately half the demand. Upon loss of one power source, all loads are transferred to the remaining active power source. Experience has shown that normal development and growth will eventually result in a power demand exceeding the capabilities of a single power source. Therefore, monitor busses are shown. Low priority loads are connected to these busses, which are deactivated when only a single power source is available. Basic bus control is by means of solid-state electromagnetic contactors and relays.

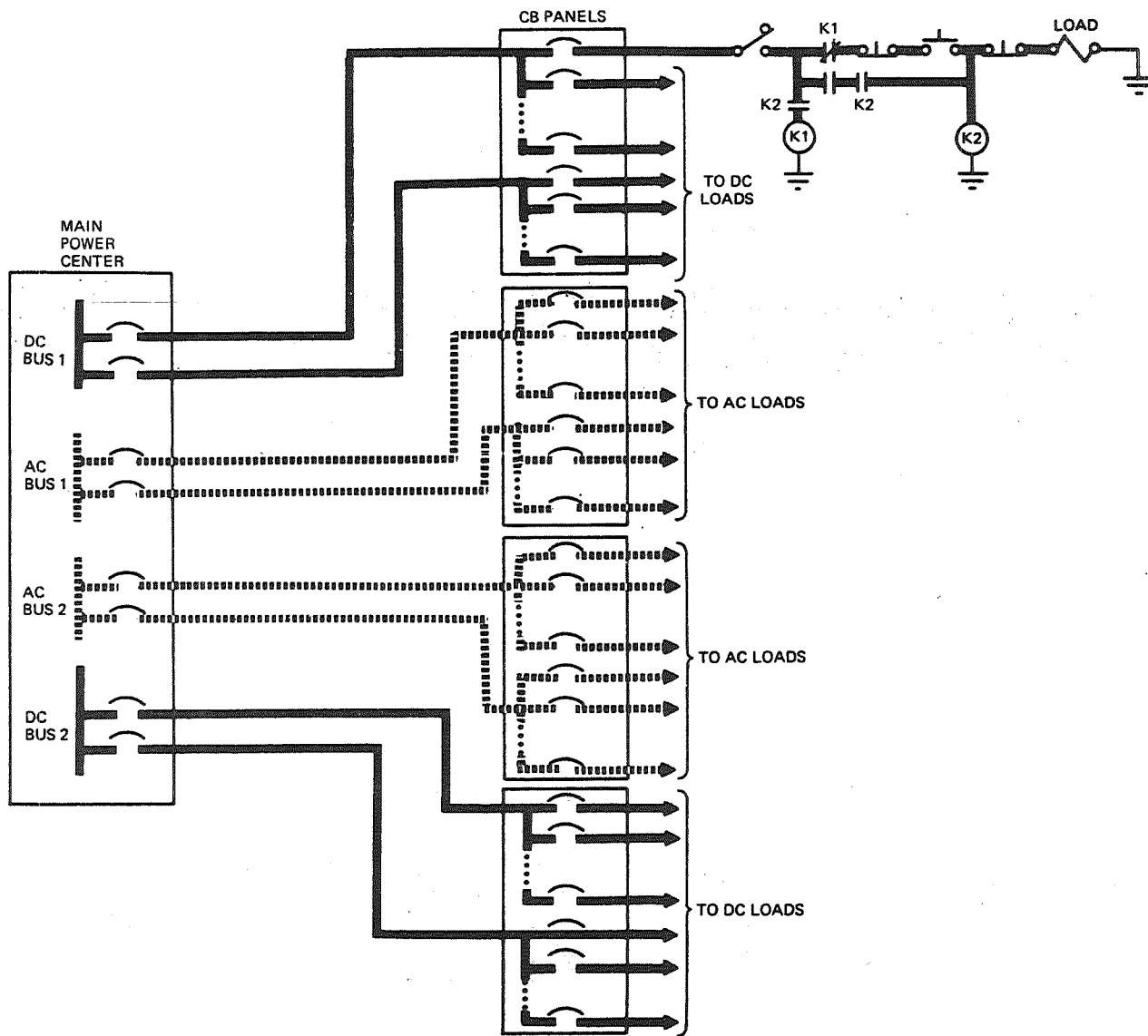
SSV ELECTRIC POWER SYSTEM - ELECTROMECHANICAL SWITCHING



325

Fig. 2 schematically typifies the distribution and control of power to the utilization equipment. As shown, all switching and control functions are accomplished with contact-type devices. Control and distribution of power to the utilization equipment is by means of (and through the contacts of) manual switches, mechanically activated switches, relays, etc. The necessity for specific functional location, crew access and supervision, maintenance, and the requirement that wire must be sized to the load requirements and circuit protector capabilities results in wiring systems that are heavy and bulky.

ELECTRIC POWER DISTRIBUTION & CONTROL - ELECTROMECHANICAL



Solid-State Power Management

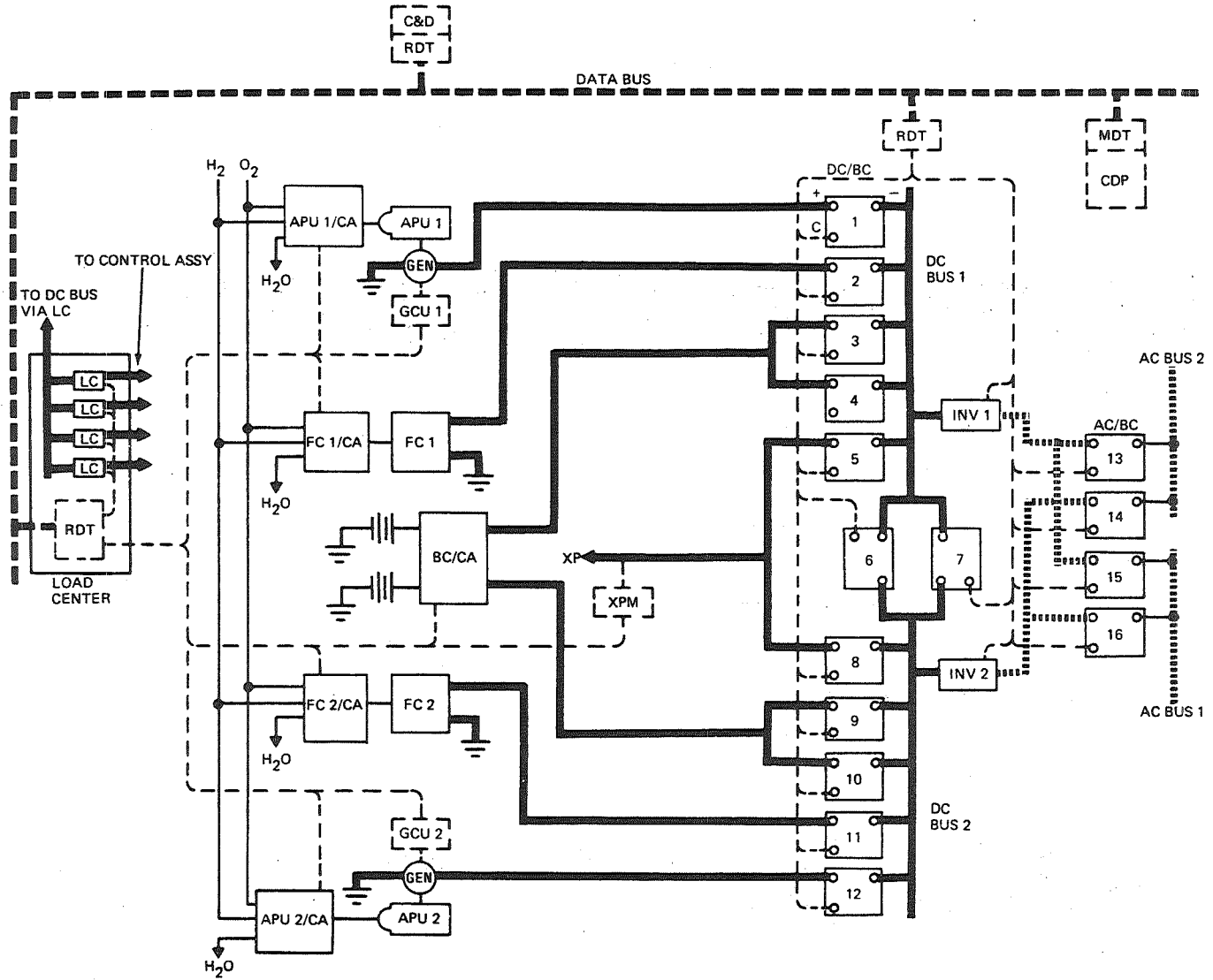
A solid-state power management system replaces all moving contacts with static, solid-state devices. All control logic and circuit protection functions will use solid-state concepts, thus eliminating electromechanical relays and circuit breakers. Since digital solid-state concepts are used for logic and control, data multiplexing techniques are used for the transmission of stimulus and control signals to minimize signal and control wiring.

Digital data processing techniques are used to perform logic, control, multiplex, and test functions. Power management is provided by a programmed load priority assignment.

Fig. 3 is a schematic of a solid-state functional equivalent of the electromechanical system shown in Fig. 1. New device terminology is introduced: bus controller, load controller, signal source, data processor, data terminal, load center, signal center, etc. Each will be more fully discussed.

Note that the bus switching circuitry differs from the electromechanical system. This is a consequence of the characteristics of solid-state switches: there is no equivalent of the normally closed contact of a side-stable relay, and solid-state devices conduct in one direction only. The control logic equations for the bus controllers are stored in the central data processor and are implemented on the basis of input signals from the controls and display panel and the power source control units (via remote data terminals, data bus, and master data terminal).

SSV ELECTRIC POWER SYSTEM - SOLID STATE SWITCHING



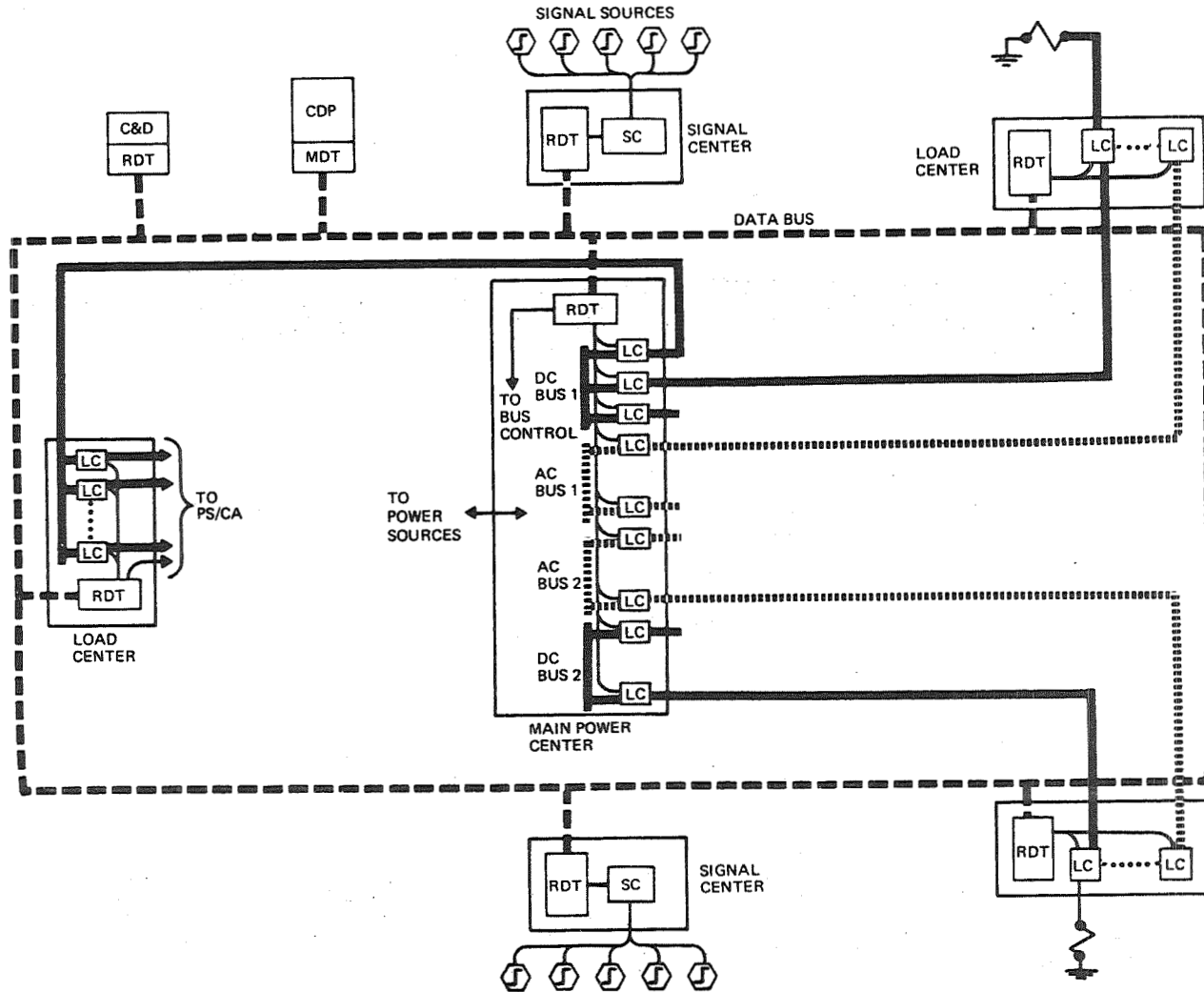
329

Fig. 4 is a schematic of a solid-state functional equivalent of the electromechanical system shown in Fig. 2. Power to the utilization loads is controlled by load controllers acting on commands received (via the data bus and remote data terminal) from the central data processor, which stores the load control logic equations and implements them on the basis of input signals from signal sources and/or controls and display panel. The load controllers are also circuit protectors and will transmit a signal to the panel when a fault occurs.

Note that the monitor busses are eliminated because the program management logic stored in the central data processor will act to inhibit individual load controllers when available power is less than demand.

Wiring from source to load is by the shortest practical route, thus minimizing wire length and, consequently, weight. In addition, solid-state circuit protection is more precise, permitting reduction in wire size and weight.

ELECTRIC POWER DISTRIBUTION & CONTROL - SOLID STATE



Electromechanical Power System Elements

APU 1, APU 2	Auxiliary Power Units. Cryogenic-fueled turbine
APU 1/CA, APU 2/CA	Auxiliary Power Unit Control Assemblies. Monitor and control operation of APU
Gen 1, Gen 2	Brushless dc generators driven by APUs
GCU 1, GCU 2	Generator Control Units. Monitor and control generator output. +28 Vdc to S1/S7 when operational parameters and power quality of associated generator are correct.
FC 1, FC 2	Fuel Cells
FC 1/CA, FC 2/CA	Fuel Cell Control Assemblies. Monitor and control fuel cell operation and output. +28 vdc to S2/S6 when operational parameters and power quality of associated fuel cell are correct.
Batt 1, Batt 2	Batteries, nickel-cadmium
BC/CA	Battery Charger Control Assembly. Monitors battery parameters and controls charge/discharge. +28 Vdc to S3/S5.
XP	External Power
XPM	External Power Monitor. +28 Vdc to S4 when external power quality is correct
Inv 1, Inv 2	DC-to-AC Inverters. +28 Vdc to S8/S9 when power quality of associated inverter is correct.
K1 thru K7	DC bus contactors
K8, K9	AC bus contactors
K10	Monitor bus relay

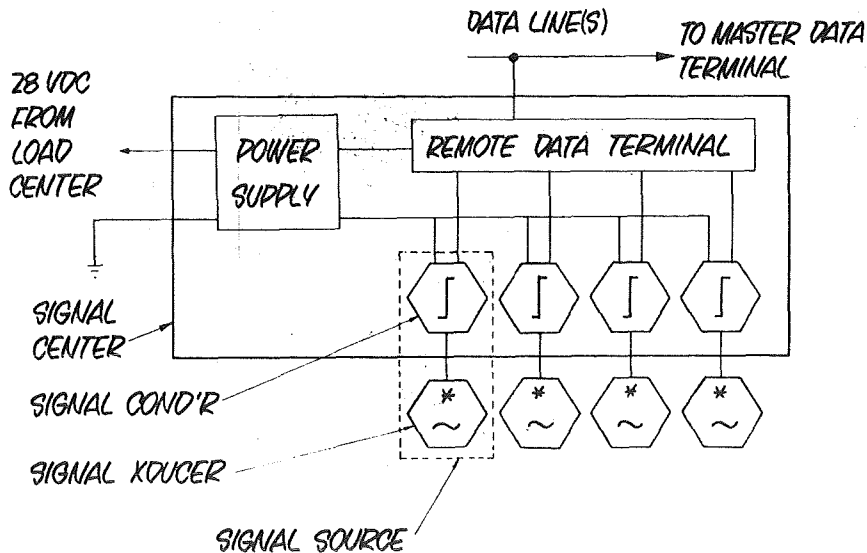
Signal Center With Signal Sources

Signal sources are contactless counterparts of electromechanical switches which produce a digital output (logic "1" or "0") as a result of an input stimulus. A signal source consists of a transducer (which converts the input stimulus to an appropriate electrical signal) and a signal conditioner (which converts the electrical signal to a digital format). The transducer and signal conditioner may form a singular entity or may be housed separately.

Input stimuli may result from: manual actuation (toggle, pushbutton, etc), the relative proximity of moving elements, an electrical quantity, temperature, pressure, etc. In all cases, inputs which affect power switching functions are conditioned to the go/no-go digital format. The specific form or configuration that a signal source will take is dependent on: the action or quantity to be sensed, the ambient environment, reliability, maintainability, total cost, etc.

Signal sources are wired directly to signal centers which are strategically located to service many signal sources in groups of 32, 64, 96, etc. The signal center will contain signal conditioners, as required, and means for interfacing with the data transmission system.

Remote data terminals located at signal centers arrange the inputs from signal sources into correct format for transmission to the central data processor.



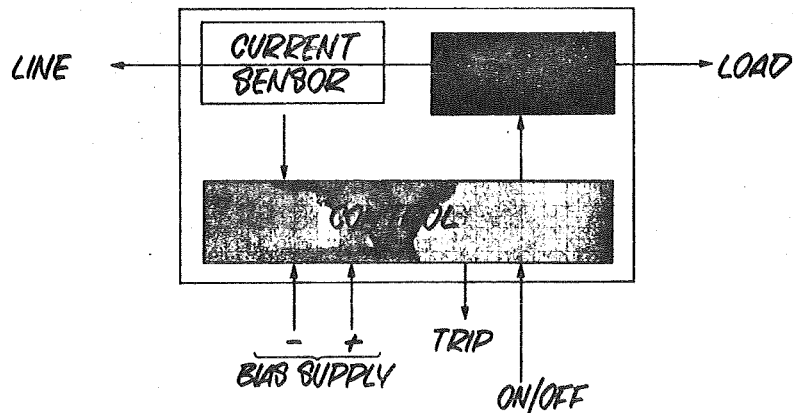
Load Controller (Solid-State)

Load controllers are single-pole single-throw solid-state switches which combine the functions of electromechanical relays and circuit breakers. They act on low-level command signals from the central data processor to energize or de-energize their associated electrical loads. Overload current protection is achieved by solid-state techniques.

The essentials of a load controller are:

- A solid-state load switch
- A current sensor
- Control circuitry

Preliminary analysis of a typical spacecraft electrical system shows that 85% of all loads are less than 10 amp (ac or dc) and 65% are less than 5 amp. Because the size and weight of a solid-state load controller are largely a function of the load current rating, reduction in size and weight per load function can be achieved by an integrated packaging approach. This will permit maximum use of MSI, LSI, sharing of common functions, and redundant techniques for increased reliability.

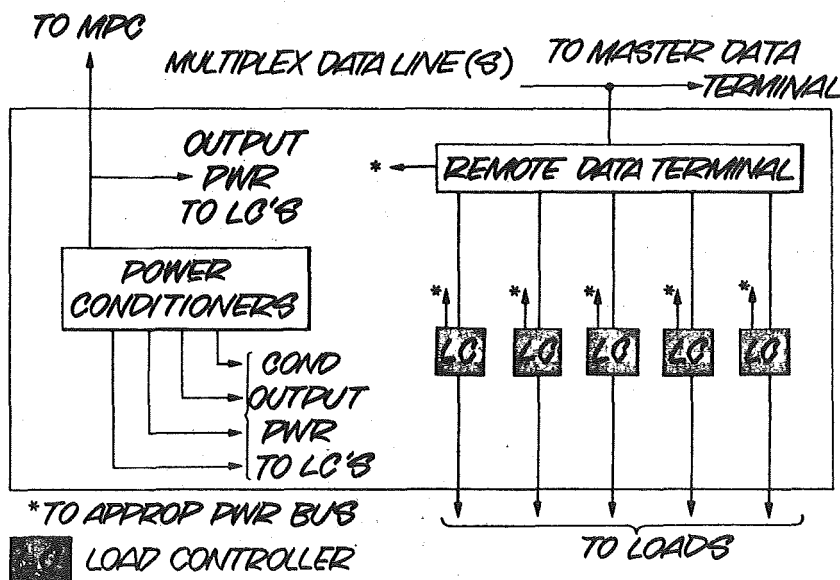


Load Center (With Power Conditioning)

Load controllers are located at load centers, strategically placed to service groups of loads with a minimum of power wiring. A load center contains: load controllers with current ratings appropriate to the associated loads, local power conditioning, and means for interfacing with the data transmission system.

The remote data terminal receives, decodes, and routes command (on/off) signals for the load controllers. It also formats and transmits "overload/trip" signals to the system control center. (Note that the load switch status - conducting or non-conducting - can also be sensed and transmitted, if desired.)

Power conditioners convert standard source power to the specialized requirements of loads, remote data terminal, and load controllers.

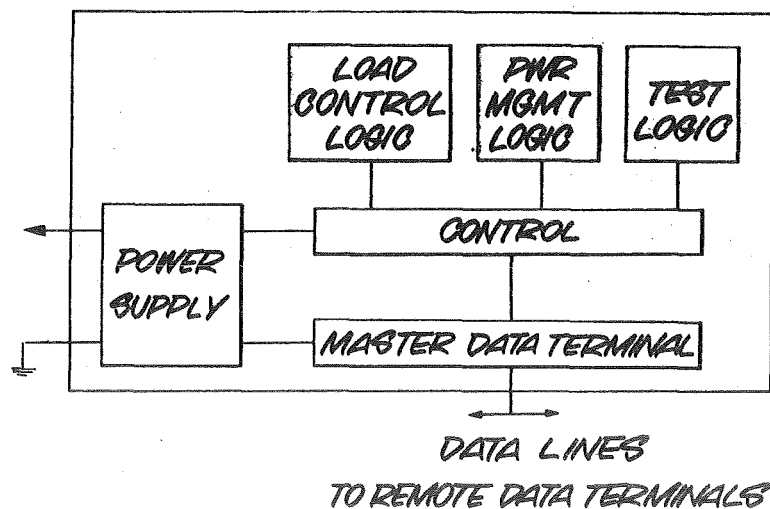


Central Data Processor

The processor is the heart of the contactless power management system. It contains: the load control logic equations, the power management monitoring functions and load priority program, the BITE program and data storage, the data transmission system master control, and the necessary interface control circuitry.

The load control logic is a non-destructive read-only memory containing the individual load control logic equations. It may be electrically alterable from external GSE. Input signals from the signal sources are processed by the load control logic to generate command signals for transmission to the load controllers. The extent and level to which built-in-test are implemented is largely a function of system reliability, maintenance concepts, and total cost. It is technically feasible to test all electrical functions of the power management system, continuously or on command, but it may be uneconomical to do so. Regardless of the ultimate form, it is anticipated the BITE will be used for preflight go/no-go check of the electrical system.

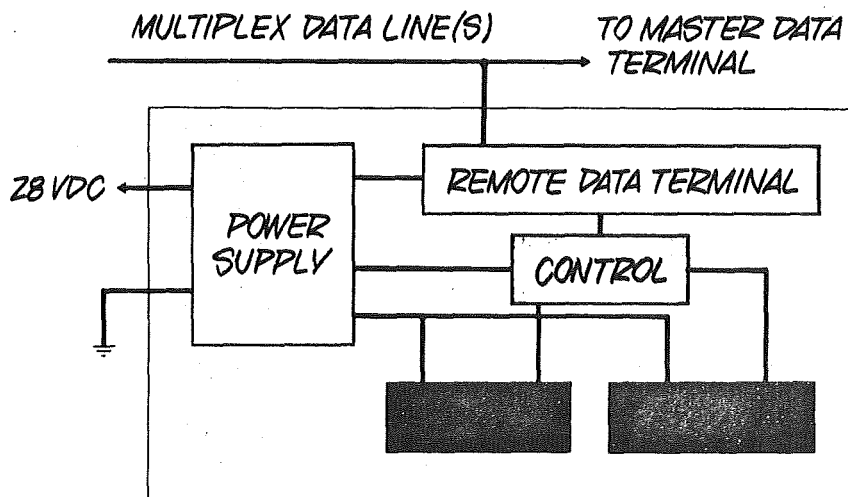
The master data terminal controls the operation of the data transmission system and is the primary interface between the system logic and the signal sources and load controllers. It interrogates and receives data from remote input data terminals at signal centers, load centers, and the control display panel. These data are appropriately processed by the system logic which generates output command signals for coding and transmission to the load centers and control/display panel, under control of the master data terminal.



Control/Display Panel

The panel is somewhat analogous to the electromechanical circuit breaker panel. As presently conceived, it consists of a visual readout and a keyboard to minimize space requirements, improve cognizance, and simplify manual control. The readout may be video or alphanumeric which will continuously monitor system status (on, off, fault detection) and provide test parameter display for any selected test area. The keyboard provides the man/machine interface which allows initiation of system operation (on/off or reset) and the capability of testing a selected test area. A remote data terminal, for interface with the data transmission system, is an integral part of the control/display panel.

Load controller status (on/off or tripped) signals are received for display, while manually initiated control signals (on/off) or reset are transmitted to the central data processor.



N70-40978

POWER PROCESSING AND DISTRIBUTION FOR THE SPACE SHUTTLE CRAFT

Francisc C. Schwarz

NASA-Lewis Research Center
Cleveland, Ohio

INTRODUCTION

The space shuttle craft relies on the electric power processing and distribution system to transform the power from one form - as produced by the generator - to other forms - as required by the individual load systems - and transfer this power from the generator to the corresponding load centers. Uninterrupted and unfailing availability of electric power to, essentially, all systems of the craft such as life support services, guidance, control, communications, and telemetry - to name a few - is mandatory for the safety of personnel on board and success of the mission. This source of electric energy, the power processing equipment and its distribution network, and the internal power supplies of the significant loads form the system of electric power supply. A disturbance in this supply process originating anywhere within that system has the same effect on a specific or on all load systems. It appears, therefore, fair to say that all elements of the power supply systems - as previously defined - are of critical importance for this program.

PRECEDING PAGE BLANK NOT FILMED

SYSTEM ASPECTS AND ITS TECHNOLOGY

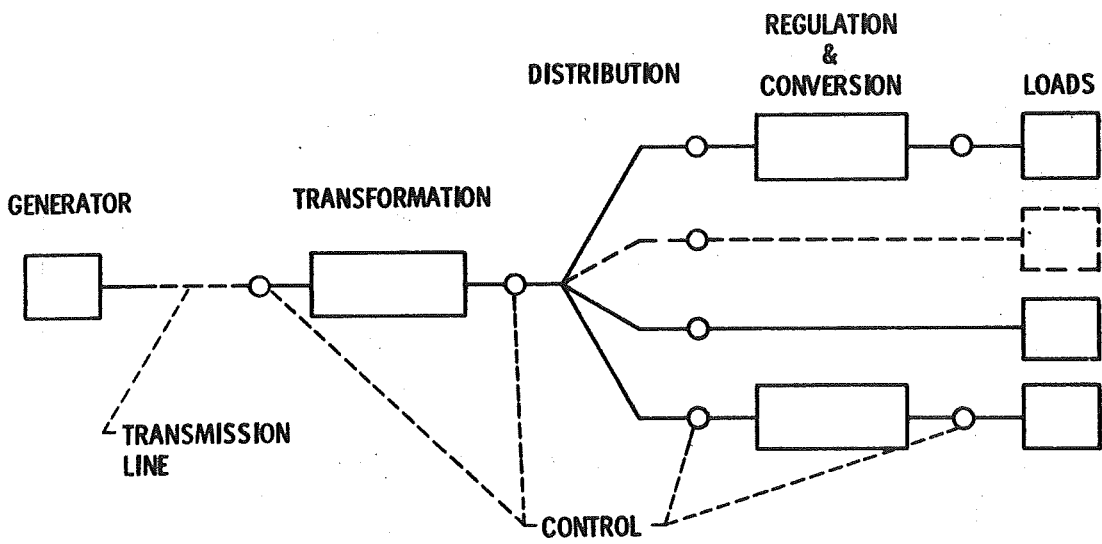
The power processing and distribution systems performs a number of tasks which are discussed with reference to Figure 1, in deriving electric power from the generator which is to be utilized in the individual loads.

1. The character of the voltage waveform at the generator terminals - dc or ac at various frequencies - the magnitude of its voltage, and its static stability rarely match the requirements of any of the loads, not to speak of their composite needs. This waveform is then electronically processed to fit the requirements of the actual load mechanism.
2. The power is transferred through the distribution network consisting of transmission lines of any length, connectors, power transfer switches, breakers and similar gear.
3. The power processing and distribution system holds the responsibility for the static and dynamic stability of the electric power system as a whole, including generator and load, at any time.

One of the significant implementary aspects of this responsibility is that of detection of impending or occurring faults anywhere in the system and remedial energy management.

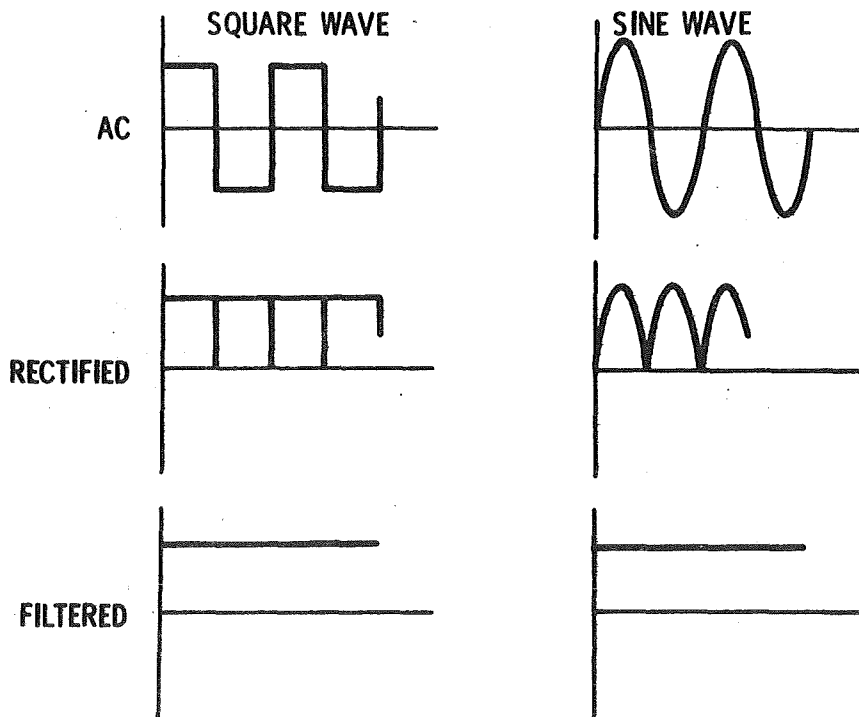
The physical configuration of the system with a given source of electric energy and established characterization of loads is dominated by the choice of the type of distributed power, namely ac or dc power. This choice has profound effects of the quality of supplied power and on the reliability and maintainability of the system. Once chosen it may become almost impossible to alter for decades to come because it affects the technology of every subsystem and even that of component parts in these subsystems. Moreover, it affects the vested interests of industry and the skills of their concerned personnel.

Many of the load mechanisms utilize dc power, although certain pieces of equipment may be envisioned with an ac "front end" that would accept 400 Hz ac power and transform this to dc power. This technical custom is rooted in a traditional application of ac distribution systems on air and spacecraft of long standing.



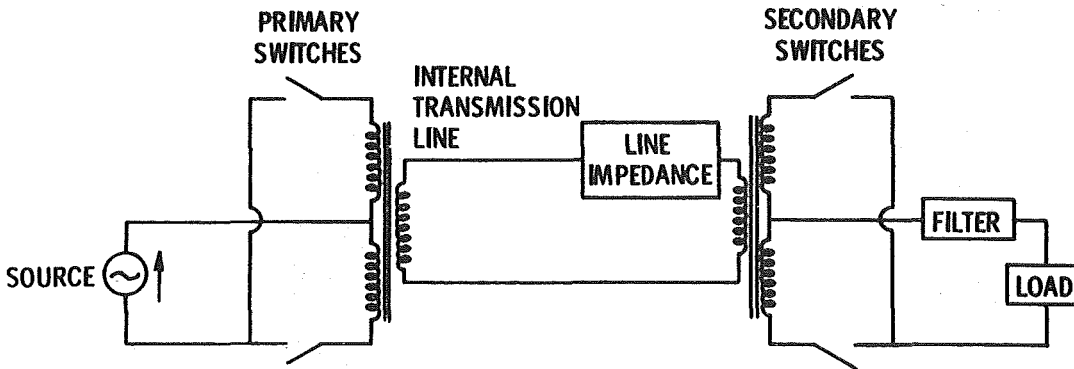
The physical effort required to invert the dc voltage waveform emanating from a bank of fuel cells to ac is illustrated in Figure 2. To the left one recognizes in succession the results of processes of square wave inversion, rectification, and filtering. This type of ac power distribution requires a minimum of modification of the character of the waveform and is therefore economical in that sense. It imposes, however, severe constraints on the bandwidth of impedances in wiring and in associated system elements. The analogous sequence of waveforms resulting in a sinusoidal ac distribution system is depicted to the right of Figure 2. This type of inversion is substantially more complex than the secondary generation of square waves. It usually involves application of complicated pulse modulation or stair case waveform generation techniques. This leads to cumbersome electronic control systems and to undue stresses on the power semiconductor switching components. The net effect is a decreased reliability of power electronics apparatus. Finally, the precariously "cleaned" sinusoid - with a specified minimal maximum distortion - is being rectified and, finally, filtered. Needless to say, that a very substantial effort is generated for the sole purpose of putting a sinusoidal voltage waveform through a distribution network which, in fact, works best under these conditions, provided one has to use an ac distribution system.

AC VOLTAGE WAVESHAPING



A striking aspect of comparing ac with dc power distribution systems is illustrated in Figure 3. An inverter with a set of primary switches is powered from a generator. A transmission line transfers the power to a transformer-rectifier-filter system. Let us assume that one were to stretch the dc feeder cable which powers the inverter and move this inverter to the right while reducing the length of the transmission line. In the limit, one would eventually eliminate the ac transmission line with its transformer windings, and the two transformers blend into one. The former ac transmission system has thus been transformer into a dc transmission system with use of exactly the same type of building blocks. However, the need for generation of a sinusoidal voltage waveform that could negotiate the channel of transmission has been eliminated, and with it the need for a waveshaping process which involves substantial complexity in power electronics technology. It is added that a dc distribution system of that kind utilizes a dc to ac to dc transformation process, which provides inherently, ohmic isolation.

POWER INVERSION TRANSMISSION AND CONVERSION



Certain of these facts are summarized in Table 1.

CERTAIN ASPECTS OF ELECTRIC POWER DISTRIBUTION SYSTEMS

	AC	DC
PROVIDES OHMIC ISOLATION	YES	YES
LOAD MECHANISMS (MAJORITY)	DC	DC
CONCENTRATION OF CONVERSION	HIGH	HIGH OR LOW
NEED FOR		
VOLTAGE STABILIZATION	YES	YES
SCALING	PARTIAL	PARTIAL
INVERSION	YES	NO
CONVERSION	YES	NO
DYNAMIC ISOLATION	YES	YES

Further information on certain characteristics of ac and dc distribution systems are summarized in Table II.

**COMPARISON OF AC AND DC DISTRIBUTION SYSTEMS
ADVANTAGES & DISADVANTAGES**

AC ADVANTAGES	DC DISADVANTAGES
SIMPLE VOLTAGE SCALING TECHNOLOGY (TRANSFORMER) WHERE NO REGULATING FUNCTIONS REQUIRED	VOLTAGE SCALING REQUIRES MORE COMPLEX ELECTRONICS
AC DISADVANTAGES	DC ADVANTAGES
IMPAIRED RELIABILITY DYNAMIC ISOLATION REQUIRES BULKY (400 Hz) BAND PASS FILTERS CONCENTRATION OF POWER CONVERSION PROCESS COMPLEX VOLTAGE WAVESHAPING PROCESSES FOR ALL LOADS NEED FOR SINUSOIDAL VOLTAGE WAVE FORMS TO ACCOMMODATE LINE IMPEDANCES	IMPROVED RELIABILITY DYNAMIC ISOLATION PROVIDED BY LOW PASS FILTERS NO CONCENTRATION OF POWER CONVERSION PROCESS ELIMINATION OF VOLTAGE WAVESHAPING (INVERSION & CONVERSION) PROCESSES FOR DC LOADS IMPROVED UTILIZATION OF POWER DISTRIBUTION LINES (WIRE INSULATION & CROSS SECTION)

The availability of technology is briefly summarized in Table III. It is first recalled that the existing and flight proven technology has not been established for construction of reusable equipment. In that sense everyone of the system components will have to be reexamined and requalified down to procedures on how to harness cables. The capacity of the power system may increase to a level of 3 to 5 times that of Apollo when spaceborne and to a yet significantly higher level during reentry and when airborne. These power levels would require the development of equipment with larger power capacities, if one were to desire to duplicate Apollo's technology which dates back a decade.

AVAILABILITY OF TECHNOLOGY *

	AC	DC
MULTIKILOWATT CONVERTERS	2 KW F**	1 KW F
MOTORS	ALL (400 Hz) F	1 KW SCC***
SWITCH GEAR	ALL (400 Hz) F	k KW F
CONNECTORS & JOINTS	NEED IMPROVEMENT	NEED IMPROVEMENT
ENERGY MANAGEMENT		
IMPENDING FAILURE	NO	NO
ANNOUNCEMENT		
FAULT ANNOUNCEMENT	YES	YES
ACTION CAPABILITY	NO	NO

- *FOR SINGLE SHORT MISSIONS.
- **FLIGHT HARDWARE.
- ***SOLID-STATE COMMUTATOR

CONCLUSIONS

Considerations of advancement of technology, but even more so, feasibility of the mission within the constraints of reliability, physical weight and size of the complete power system, its reusability, maintainability and certainly its cost may turn out to be the dominant consideration which may determine the decisions of its designers. Another area that could gain significance is that of compatibility with the space station technology. The motivating force would be the cost of development of building blocks, their qualification, the simplification of logistics and the reduced training requirements of personnel. But, first of all, a power system that satisfies the requirements of the craft and the associated constraints will have to be devised. The needed technology needs realistic examination at this time to avoid costly and time consuming delays during the hardware phase.

N70-40974

FUEL CELL TECHNOLOGY PROGRAM

David Bell

NASA-Manned Spacecraft Center
Houston, Texas

The advanced fuel cell program at the Manned Spacecraft Center in Houston, Texas is designed to support the primary electrical power requirements of the space shuttle vehicle in the mid-1970's. The objective is to advance the technology of hydrogen-oxygen fuel cells through a rigorous and comprehensive program commencing at the lowest component and material level and progressing through the fabrication and test of an engineering model fuel cell and related components and assemblies.

Two contracts were negotiated by the MSC; one with Pratt and Whitney Aircraft, South Windsor Engineering Facility (SWEF) of East Hartford, Connecticut, and one with the General Electric Company of Boston, Massachusetts. Task I utilizes existing concepts with which the contractor has significant experience to build an engineering model (EM-1) fuel cell as a baseline design. This design will be used to identify open engineering problems related to the baseline and to perform the effort required for resolution of these problems using low-risk approaches. Parallel with this effort is a Task II which is focused on the identification of concepts which would represent a significant extension of present capability in terms of life, power, specific weight and volume, versatility of operation, field maintenance capability and thermal control, but which avoids high technical risk approaches. Those concepts which offer significant improvements will be exploited in EM-1 where possible, or demonstrated at the component or subsystem level where such time phasing precludes their incorporation in the engineering model. Task III is a continuous effort between the fuel cell contractors, the shuttle Phase B contractors, and NASA shuttle organizations. This effort will be used to establish a two-way information exchange for the purpose of early identification and assessment of fuel cell/vehicle interface, integration and safety requirements. Concurrent with the above tasks will be the normal complementary engineering tasks such as Reliability, Quality assurance, Safety and Cost Effectiveness. The overall program requires complete

formal documentation of design and test results for use in future programmatic decisions.

PRATT AND WHITNEY TECHNOLOGY

The Pratt and Whitney Program approach is based on combining technological advancements with the present PC8B-4 technology. The PC8B fuel cell is a low temperature, hydrogen-oxygen fuel cell which utilized potassium hydroxide electrolyte. The electrolyte is maintained in a saturated asbestos matrix supported between two catalyzed electrodes. The electrolyte matrix and electrodes are formed into a unitized structure with a plastic supporting frame. The cells have an active area of .5 square feet each and operate at a current density of approximately 150 amperes per square foot. The cells are integrally cooled by circulating water glycol through the cell stack and a liquid-to-liquid heat exchanger which interfaces with the spacecraft radiator. The nominal operating temperature of the fuel cell is 200°F to 240°F. Proper electrolyte concentration is maintained by removal of the excess moisture from the recirculating hydrogen stream. Excess moisture is condensed and then separated by a centrifugal separator.

Fuel cells of this type have been manufactured in 2.5 KW and 4.5 KW sizes weighing from 100 to 125 pounds. MSC presently has a 4.5 KW system scheduled to go on test August 3, 1970, in the Thermochemical Test Area of the Propulsion and Power Division.

The EM-1 fuel cell will contain all the basic features of the aforementioned PC8B plus the following:

Open-cycle cooling: Evaporative cooling plates are located in the cell stack to facilitate integral cooling by evaporation (boiling) to space. Water is supplied to the evaporator plates from external storage tanks.

Operation on Propulsion Grade Reactants: Operation on low purity, low pressure gases will be considered for the shuttle fuel cell as a possible means of reduction in the areas of weight and system complexity. Operation from low pressure, low purity sources does result in some performance penalties to the fuel cell and further system trade-offs are required in this area.

Elimination of rotating electrical components: In order to improve life and reliability, an effort will be made to eliminate the present coolant pump and hydrogen recirculation pump. Prototype models of an oxygen-driven coolant pump and hydrogen jet pump are presently in test. The preliminary results appear promising. The oxygen driven coolant pump offers a distinct advantage in that the coolant flow rate is directly proportional to the O_2 consumption (and power output), thereby eliminating the need for optimizing at a fixed flow rate as is presently done with the electrically-driven pumps.

Redundant Heat and Water Removal: As previously stated, waste heat is removed by either the closed loop, recirculating coolant, radiator system or by the intercell evaporators. This provides redundant heat removal capability in the fuel cell. Redundant waste water removal is achieved through utilization of the normal method of condensation and removal previously discussed or through controlled venting of the hydrogen stream. In the venting mode the cell concentration is maintained by sensing the moisture content of the venting hydrogen. This is accomplished through wet bulb/dry bulb temperature measurements in the vent stream. Control logic from these measurements determines and controls the venting requirements.

GENERAL ELECTRIC TECHNOLOGY

The General Electric program proposes to advance the technology of the Gemini and Biosatellite programs through use of the new stabilized

"R" membrane, a light back-to-back cell arrangement, improved water removal techniques and other minor changes and improvements in the ancillary components.

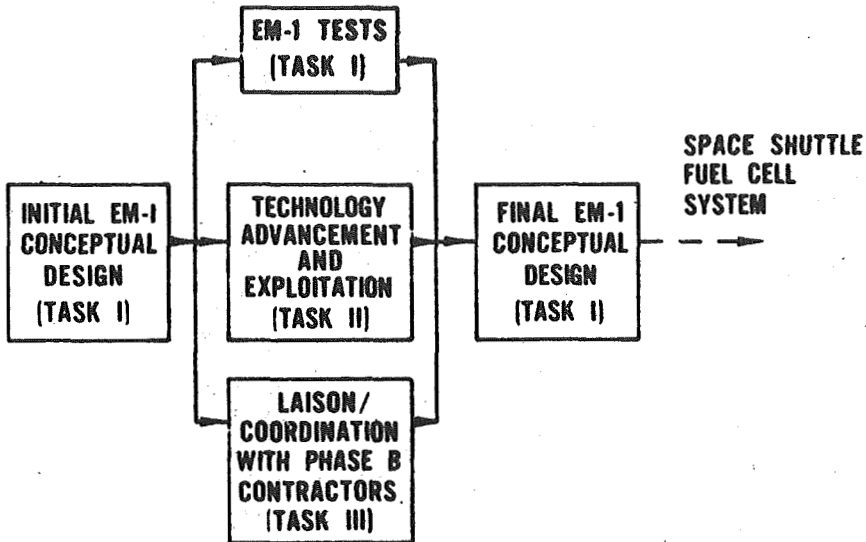
The General Electric fuel cell is a low temperature, hydrogen-oxygen fuel cell which uses a solid polymer electrolyte. The electrolyte is a perfluorinated sulfonic acid solid polymer developed by Dupont. The electrolyte membrane, identified as the "R" membrane, appears to be very stable and does not exhibit the excessive degradation rates experienced with earlier (Gemini) membranes.

Laboratory testing of the stabilized "R" membrane has resulted in potential life predictions of 5000 to 10,000 hours with negligible degradation. This membrane technology coupled with the back-to-back (common H₂ cavity) cell configuration results in a very lightweight fuel cell stack. Continued efforts in water removal indicate that water wicking from one side of the cells is adequate and results in improved cell stacking and purging capability.

A major problem in the Gemini fuel cell, namely electrode bonding failures which permitted cross leakage of the reactants, appears to have been solved with the development by the Air Force of a new high-temperature, stable adhesive, AF-45.

These cell improvements, in conjunction with incorporation of an integral cooling loop interfacing with the S/C radiator, voltage regulation and the design and development of a monitoring and control unit to facilitate ease of operation and checkout, have the potential of producing a fuel cell which meets the shuttle requirements previously specified.

SUMMARY OF PROPOSED PROGRAM

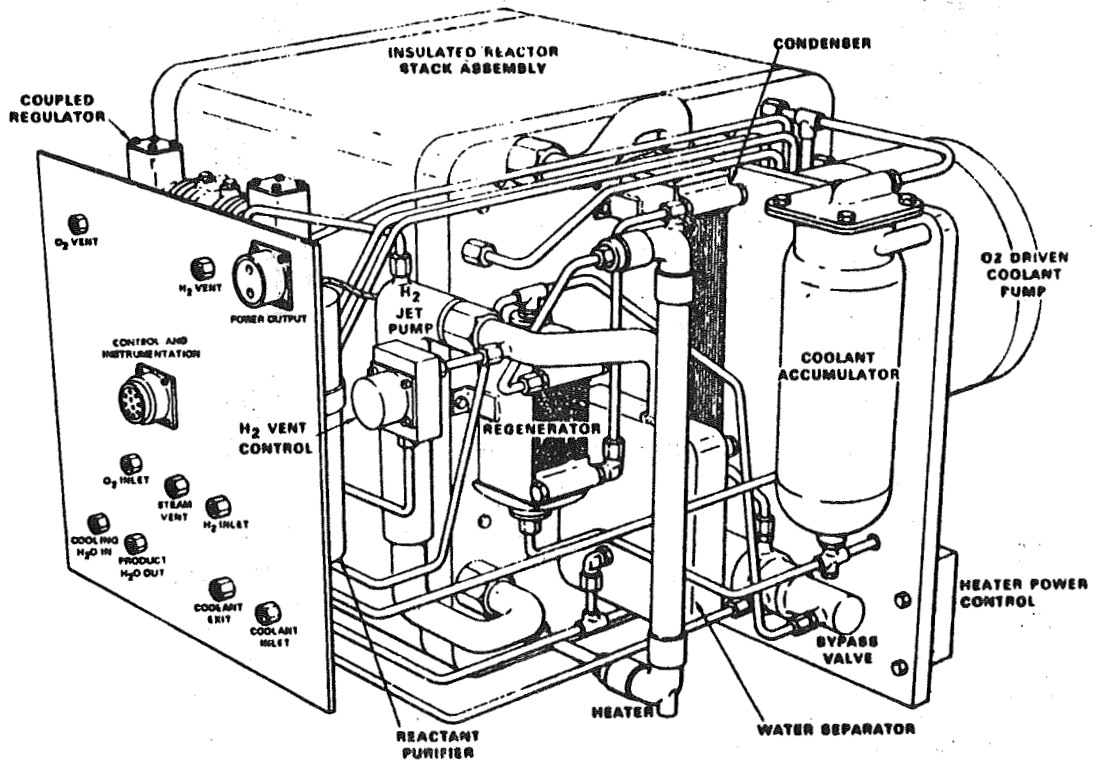


FUEL CELL TECHNOLOGY OBJECTIVES

LIFE	5000 HOURS
POWER	0-5 KW, RATED -2.5 KW, AVERAGE
VOLTAGE	28 VOLT \pm 5%
SP. WEIGHT	40-60 LBS. PER. KW.
REPAIR/MAINTENANCE	FIELD CAPABILITY
START/STOP	AUTOMATED, NO PRIOR CONDITIONING
REACTANTS	PROPULSION GRADE H ₂ -O ₂
HEAT REJECTION	MINIMUM IMPACT TO S/C

PRATT AND WHITNEY AIRCRAFT

FUEL CELL PROGRAM



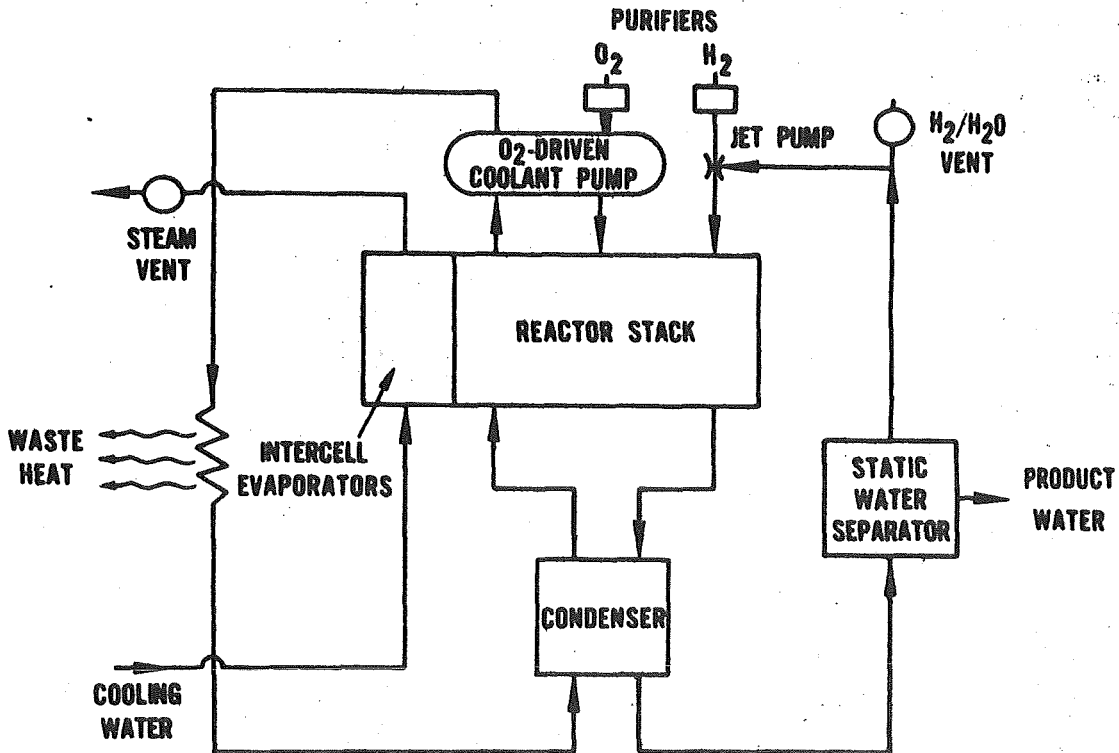
PWA ENGR. MODEL 1

FEATURES OF THE EM-1

ALL FEATURES OF THE PC8B

- o INTEGRAL OPEN CYCLE COOLING AT ALL ALTITUDES
- o OPERATION ON PROPULSION GRADE REACTANTS
- o NO ELECTRIC MOTORS OR ROTATING COMPONENTS
- o REDUNDANT HEAT AND WATER REMOVAL SUBSYSTEMS

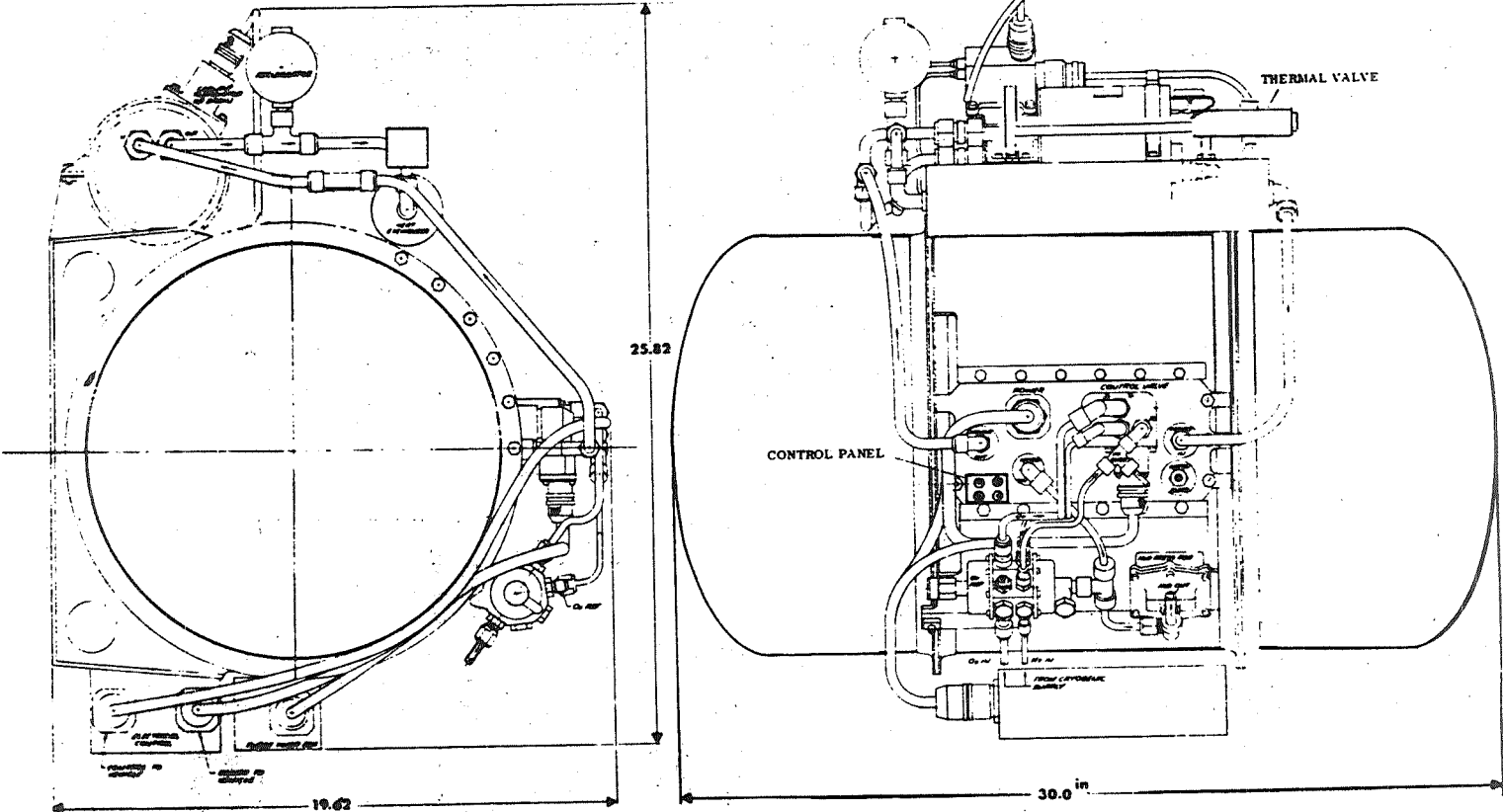
ENGINEERING MODEL FLOW SCHEMATIC



GENERAL ELECTRIC COMPANY

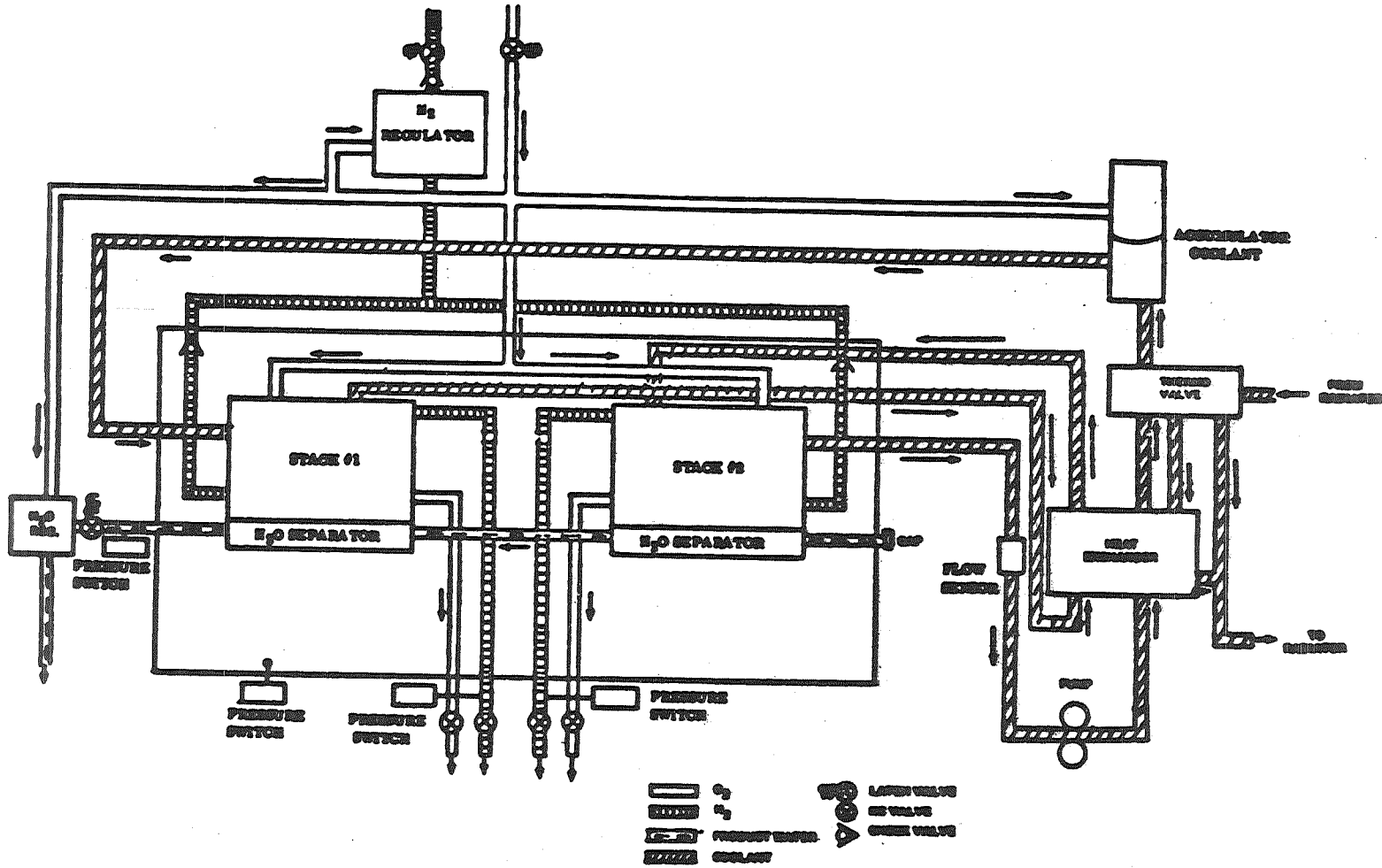
FUEL CELL PROGRAM

356



Fuel Cell Module

357



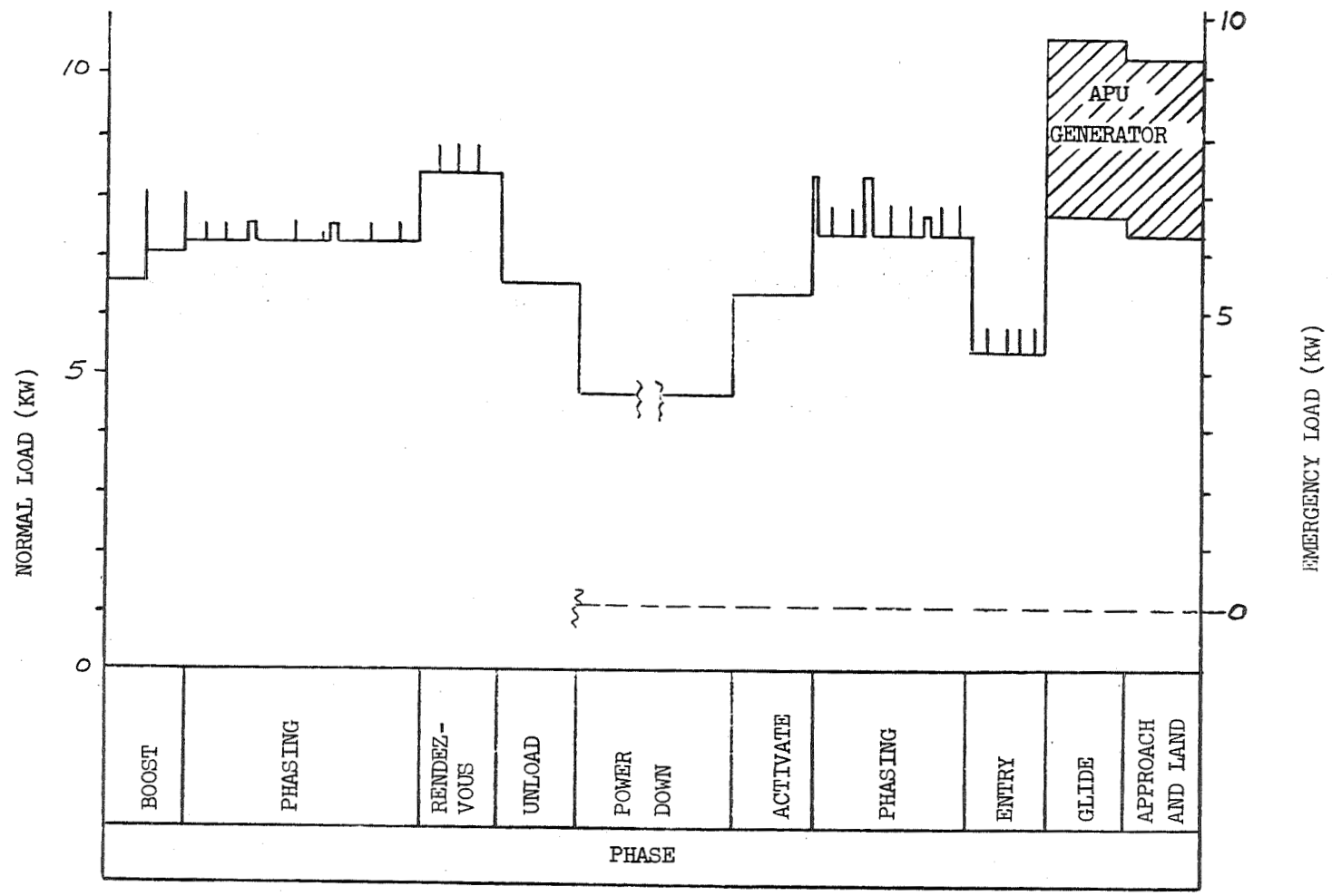
Fuel Cell Module Schematic

FEATURES OF THE EM-1

BASIC ACID CELL DESIGN PLUS

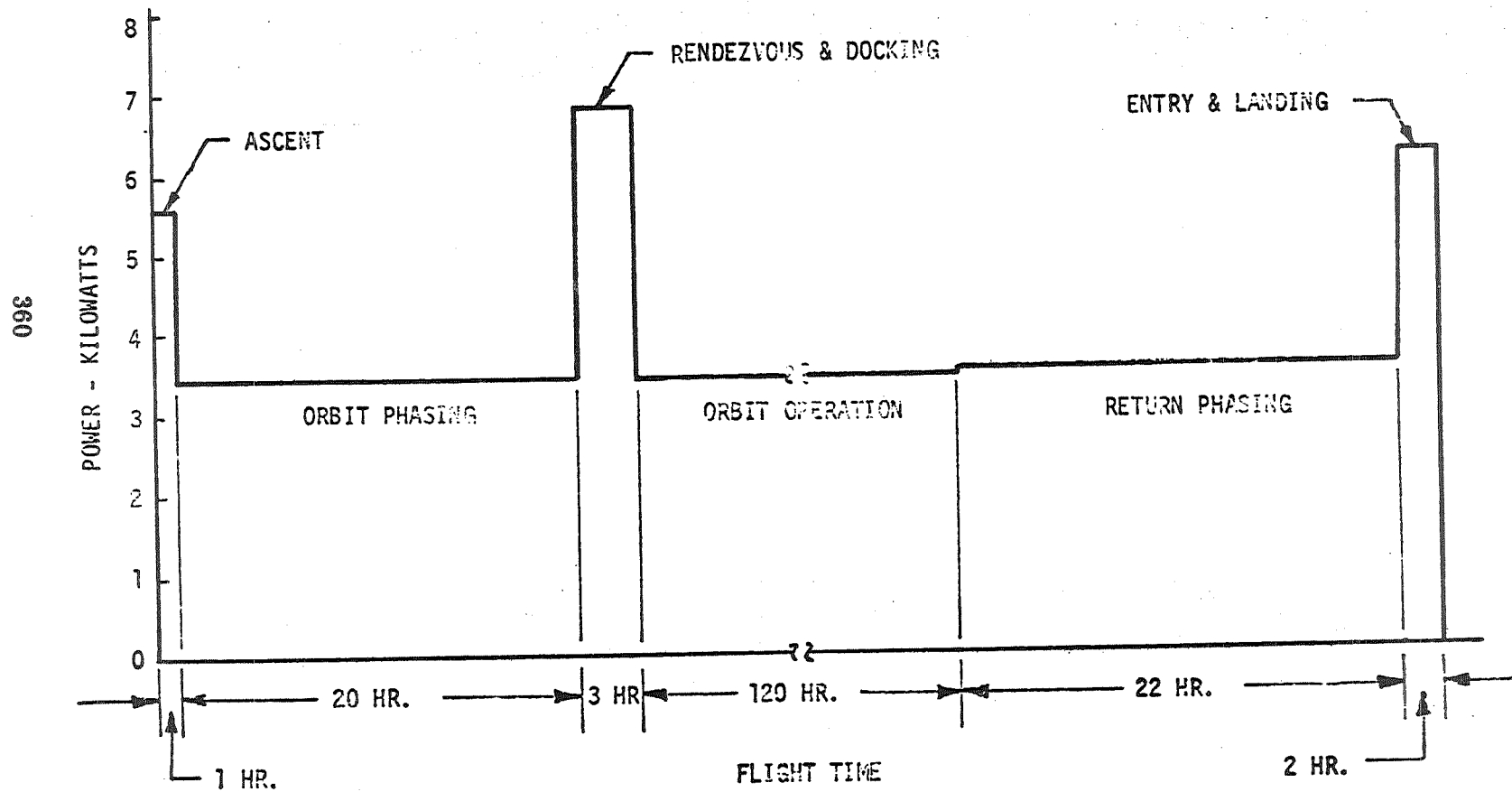
- STABILIZED 'R' MEMBRANE
- LOW WEIGHT SPE CELLS
- BACK TO BACK CELL DESIGN
- ONE SIDE WATER REMOVAL
- IMPROVED BONDING TECHNIQUES
- VOLTAGE REGULATOR
- INTEGRAL COOLING SYSTEM
- MONITORING AND CONTROL UNIT

698



NAR ORBITER ELECTRICAL LOAD PROFILE

ORBITER ELECTRICAL POWER PROFILE



N70-40975

SPACE SHUTTLE AUXILIARY POWER UNIT (APU)

Donald G. Beremand and Harry M. Cameron

NASA-Lewis Research Center
Cleveland, Ohio

INTRODUCTION

The Lewis Research Center is presently engaged in a program to develop the technology that will be required to furnish a hydrogen-oxygen fueled Auxiliary Power Unit (APU) for the Space Shuttle. The requirements for such an APU vary somewhat from one vehicle concept to another and between the Booster and Orbiter vehicles. However, all of the Space Shuttle studies have indicated a requirement for APUs on both vehicles. A review of the project requirements from the various studies has led to the selection of a representative set of APU requirements for initial use in the APU program.

The APU requirements are summarized briefly in figure 1. These requirements have been established to be compatible with basic Space Shuttle requirements (100 missions), and to reflect a common APU for both Orbiter and Booster vehicles.

H₂-O₂ APU REQUIREMENTS

POWER

PEAK, HP 200
NORMAL, HP 45

HYDRAULIC 4000 PSI, 70 GPM

ELECTRIC 15 kW, 400 Hz, 120/208 V, 3 PHASE

LIFE, HR 1000

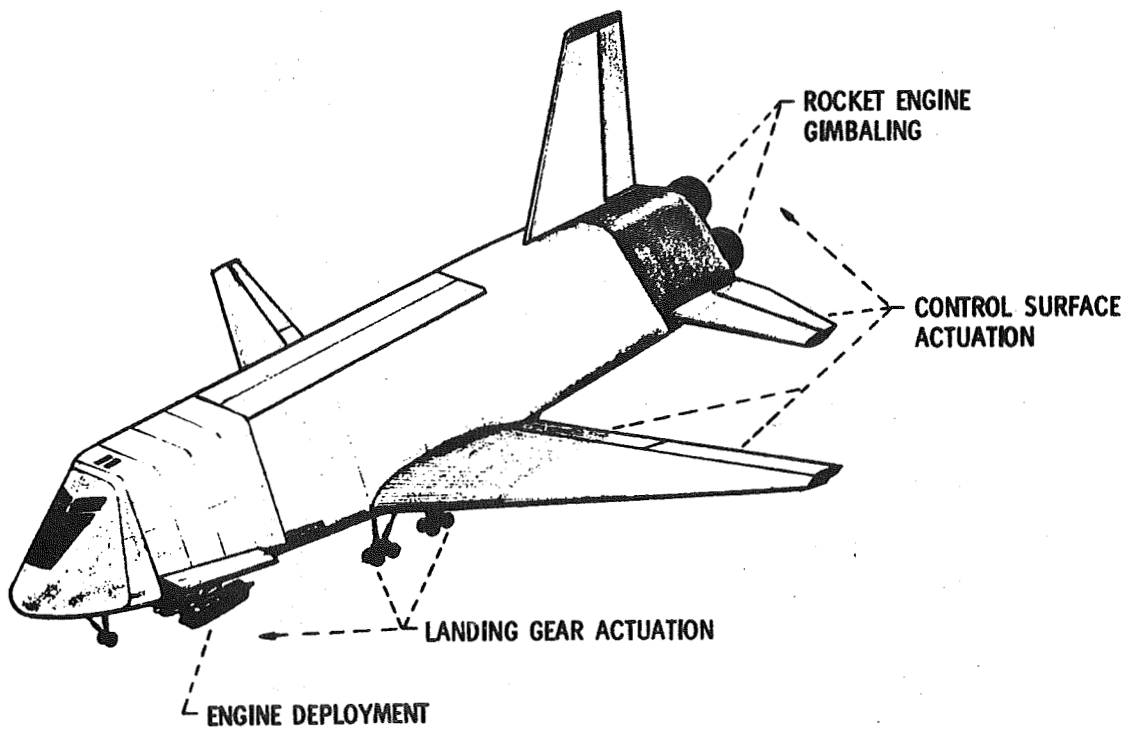
ACTIVE MISSION TIME, HR UP TO 3

NO. OF MISSIONS 100

Requirement for H₂-O₂ APU

Auxiliary Power Units are required on the Shuttle vehicles to provide both hydraulic and electrical power. Some of the typical hydraulic power requirements are shown on the sketch in figure 2. Many of these are typical of standard aircraft hydraulic systems. Other functions such as engine deployment and possibly rocket engine gimbaling are peculiar to the Space Shuttle vehicles.

HYDRAULIC POWER FUNCTIONS



In addition to the hydraulic functions, numerous requirements for electrical power exist, though the total electrical power requirement is small compared to the hydraulic power requirements. Those functions requiring electrical power include avionics, lighting, valve actuation, windshield deicing and fuel boost pumps. While some of these functions could be supplied by auxiliary drives off the air breathing engines, many of the critical high power requirements during the mission occur prior to deployment of those engines. Thus the choice for sources to furnish these auxiliary power requirements are essentially limited to APUs or APUs in combination with engine-driven auxiliary systems.

The selection of hydrogen-oxygen as fuel for the APU is based on two key considerations. First, hydrogen-oxygen offers much lower fuel consumptions than typical monopropellant or hypergolic APU fuels and thus a substantial potential savings in weight, a critical consideration for all Shuttle equipment. Second, it results in commonality of fuel with all other engines on board, resulting in minimization of ground logistics and offering the potential for integration of the APU fuel system with other fuel systems on board, such as those for the Orbital maneuvering system and the attitude control system. While selection of a hydrogen-oxygen fuel system for the APU is being reviewed in the Phase B studies, the choice presently appears to be correct and is not expected to change unless the APU requirements themselves should change significantly.

Detail Requirements

As stated initially, the requirements for the APU vary from one vehicle concept to another and between Orbiter and Booster. Since Booster power levels and operating times generally are greater than for the Orbiter they will probably control the APU design.

A typical mission power profile for the Booster APU is shown in figure 3. While these power levels are somewhat higher than shown in the previous summary both are in the range of typical power levels. The steady load component results from the hydraulic loads required to maintain actuator positions and electrical loads as required for service power. The spike loads occur as follows: (a) during ascent for gimbaling rocket engines for thrust vector control; (b) during reentry for setting and maintaining the elevators for the desired high angle of attack and deployment and startup of jet engines; (c) during flyback for normal aerosurface flight control; (d) during landing for flight control, landing gear deployment, and steering.

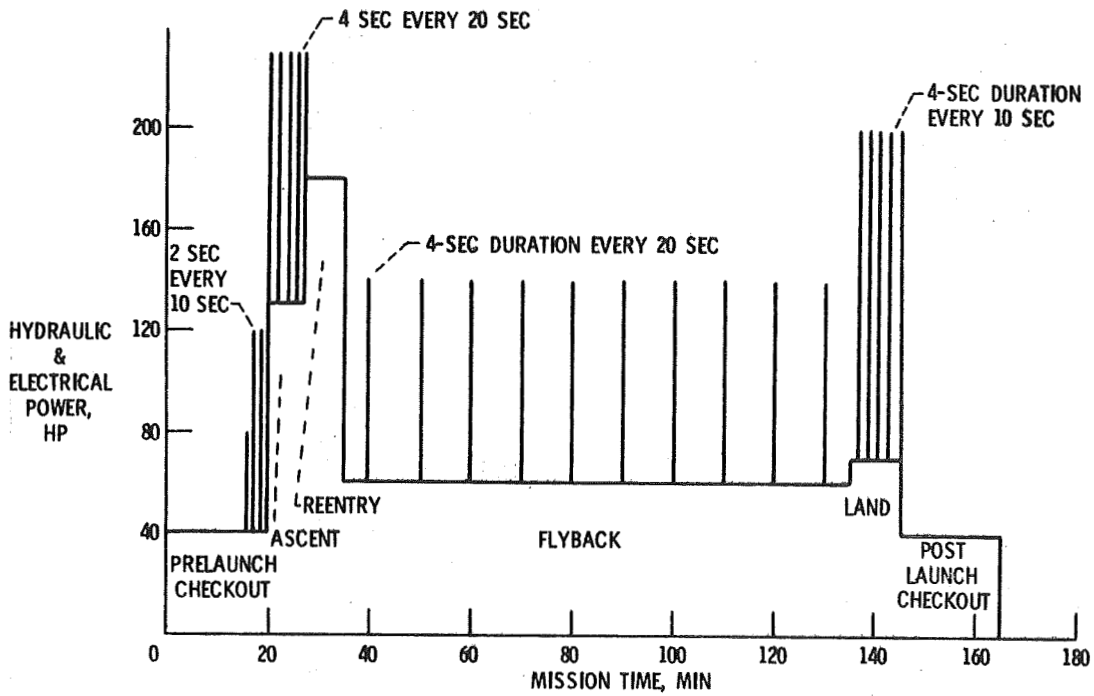
As can be seen from the power profile the APU will have to be capable of peak or near peak power operation from sea level to orbital altitudes. It must, of course, accept whatever conditions of shock, vibration, and acceleration the vehicle may subject it to over the full flight. Acceleration levels will tentatively be limited to 3 gs for passenger comfort but could be somewhat higher for Booster reentry since no passenger would be on board. The thermal environment of the APU will probably vary substantially during the flight and could range from -60° F to several hundred $^{\circ}$ F depending on its location in the vehicle.

The typical Booster power profile of figure 3 represents the power per APU in an installation of four redundant systems. The Orbiter power requirements are expected to be somewhat smaller and could probably be satisfied with an installation of three redundant systems. In general, the redundancy requirement for the systems supplied by the APUs on both vehicles is one unit out-fail operational (continue mission), two units out-fail safe (abort mission). While we have made no attempt to assign reliability numbers to the APU, it obviously must be an extremely reliable unit.

Other key design objectives are those of service life and weight. The vehicle life requirement is for 100 missions and the mission APU operational time can be up to three hours. The design life objective has thus been set at 1000 hours, more than three times the maximum life presently required. System weight and fuel consumption are obviously important and must be kept to a minimum. With a payload for the Shuttle in the order of 20-40,000 pounds it is obvious that an extra 1000 pounds chargeable to the APUs (as could result from excess fuel consumption) would be a significant penalty.

BOOSTER HYDRAULIC AND ELECTRICAL POWER

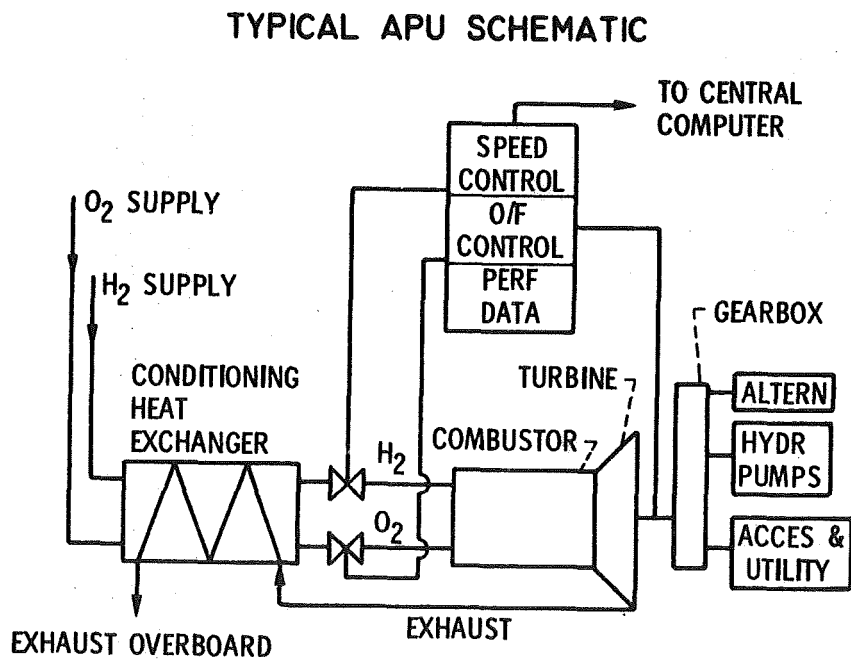
TVC, AEROSURFACES, AVIONICS, & UTILITY



Among the more critical requirements for the APU design are the combination of (a) large power range; (b) peak power operation from sea level to orbital altitudes; and (c) the limited (about 10 percent) operation at peak power.

Typical H-O APU

Figure 4 shows a typical schematic representation of a hydrogen-oxygen turbine APU. The major components are the turbine, the combustor, the fuel and oxidizer valves, the heat exchanger for pre-heating the cryogenic gases with turbine exhaust products and the control system. The high speed turbine output drives through a gearbox to an alternator and one or more hydraulic pumps, as well as parasitic service loads.



Combustor: The combustor burns gaseous hydrogen and oxygen at off-stoichiometric ratios, since stoichiometry (8/1 oxygen/hydrogen) would result in temperatures near 6000° F. For long life reliable turbines temperatures should be limited to 1800° F. This requires an O/F ratio in the neighborhood of 1/1 with the excess hydrogen serving as the diluent to soak up heat and reduce temperature. The product of combustion of an O/F ratio of 1/1 are 55 percent hydrogen and 45 percent steam. The source of ignition might be a spark plug, glow plug, or a catalyst such as platinum deposited on an aluminum oxide substrate. The latter requires no external energy source but is subject to poisoning. Therefore, spark or glow plugs are favored.

In the selection of the combustor and turbine designs the choice of pressure or pulse modulation to control power could significantly impact the combustor design.

Turbine: The basic turbine will likely be an axial flow impulse machine with the number of stages depending on the decreased pressure ratio and the complexity one is willing to accept. A full admission continuous flow turbine with a 300 psi gas inlet pressure would have a mean diameter of 2.5 inches, a blade height of 0.1 inch, and a rotative speed of 170,000 rpm for the required power output. Such a machine would be difficult to build and power extraction would be inefficient. Alternatives are partial admission turbines in which the gas is admitted through a limited number of nozzles into a limited blade section. Such a turbine would be about six inches in diameter, have a blade height of 0.250 inch, and a rotative speed of 64,000 rpm. It would have two stages, and the angle (sector) of admission would be about 60 degrees. Instead of axial staging the same turbine wheel could be reentered by the first stage exit flow through appropriate ducting. Such turbines have been built and give a reasonable efficiency after ducting and interstage leakage losses are accepted.

Another alternative is the pulse turbine which operates with full admission, but not continuous flow. Instead, the propellant flow is cyclically interrupted with on-off pulse durations regulated in accordance with power requirements. This allows the turbine to be optimized at one design flow rate and thus favors minimal fuel consumption. One such machine was built by TRW under contract to NASA to operate with hydrazine and nitrogen tetroxide. This machine was tested and demonstrated the basic feasibility of the pulse turbine.

Control System: The APU control system must maintain the design of O/F ratio, and fuel and oxidizer mass flow at values required to match demand power regardless of density changes which occur as a result of varying inlet temperatures and pressures. The APU control system must also respond to large, rapid power changes and could be tied in with the flight control system in order to anticipate turbine load changes with minimum delay.

Vehicle Interface

Several major interfaces exist between the APU and the vehicle. The first, and perhaps most obvious, are the load interfaces. A typical redundant hydraulic system supplied by four APUs is shown in figure 5. As shown, each control surface or other hydraulically actuated device is driven by three or four independent actuators from separate APUs as required to satisfy the fail operational-fail safe criteria. Obviously, many combinations and variations of this basic approach are possible including the use of accumulators to smooth out load pulses and possibly power transfer units (reversible hydraulic pump-motors) to allow power transmission from one system to another without mixing fluids in the independent systems. The electrical load interface could impose severe problems depending on the frequency control and the degree of paralleling operation that might be required, particularly since the major loads and load fluctuations will come from the hydraulic loads.

Another major interface is with the propellant feed system. There are two extremes of feed systems and many intermediate arrangements that could be used. First all hydrogen and oxygen could be taken from other on board systems already gasified and requiring only minor, if any, temperature conditioning before use in the APU. At the other extreme, both the hydrogen and oxygen could be self-contained in APU tankage alone.

TYPICAL REDUNDANT HYDRAULIC SYSTEM

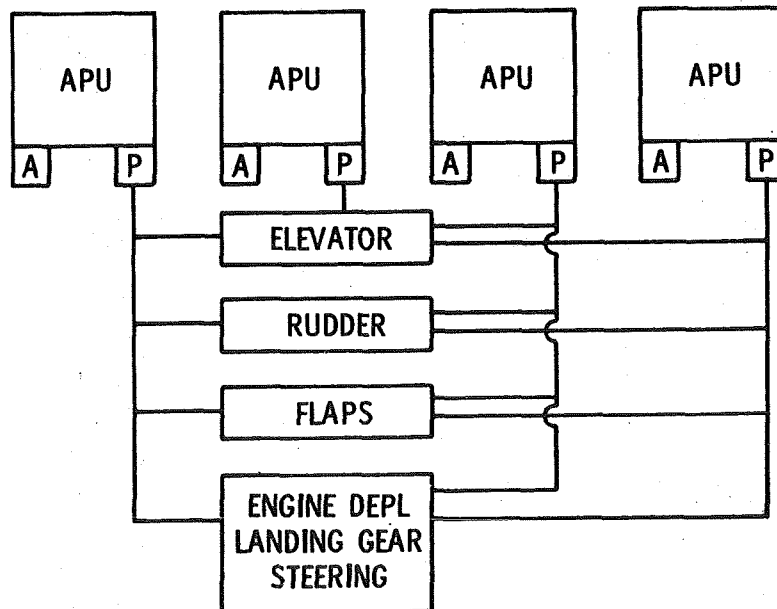


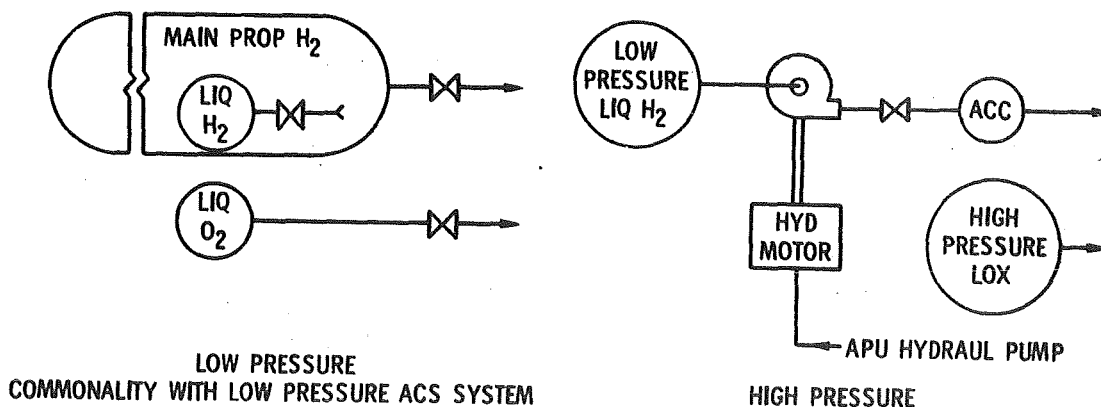
Figure 6 shows two possible propellant supply systems. Sketch (a) shows a supply which is common with a low pressure ACS supply located within the main engine tank. Since the main engine propellants are expended in the first few minutes of flight the ACS propellants can be expanded and gasified, eliminating the need for separate APU storage tank and gasifiers. The simplicity of the system is achieved at the cost of limiting the available expansion ratio through the turbine thus increasing specific fuel consumption.

Sketch (b) shows low pressure liquid storage either separate for the APU or common with other systems with a hydraulic motor-driven pump to pump liquid H_2 to high pressure (300-500 psi). Pumping power would be about 10 horsepower, well worth the gain in fuel economy. The low flowrates, .05 - .2 pounds per second, would however put us into a pump range for which there is little H_2 experience. The low volume of oxygen would make high pressure liquid storage practical, and again could be either separate or common with other systems.

Of considerable importance is the thermal integration with the vehicle. Use of cryogenic fuels, discharge of high temperature exhaust gases and potential heat loads to or from the APU make this an important consideration.

All the above design problems must, of course, be resolved with designs resulting in an optimum integrated APU system. Not only must the resultant overall APU be a well integrated unit but it must also integrate readily and without undue problems into the vehicle.

PROPELLANT SUPPLY SYSTEMS



Planned Program

In order to provide the required hydrogen-oxygen APU technology, the Lewis Research Center has initiated a combined in-house and contractual effort. The in-house efforts are presently directed at establishing and maintaining current the APU requirements based on the Space Shuttle studies, and performing preliminary component and system analyses and evaluation.

At present, contractor proposals are due about July 20 for a two-phase study of a hydrogen-oxygen APU. Phase I of this effort will be a four-month screening analysis. In this phase parametric analysis of the major system components would be performed and components and system design concepts screened. At the conclusion of this phase NASA will select the system concept which will be pursued in more detail in Phase II.

The Phase II effort would include detail system and component analyses and engineering and the generation of detail system and component layout drawings. Phase II is planned as a six-month effort. Dependent on the results of Phase I, it might be desirable to perform some experimental evaluations or verifications of component concepts in parallel with, or as a part of, the Phase II effort.

It is anticipated that the results of the early Phase B trade-off studies can be fed directly into the start of the APU Phase I effort. From that point on, frequent crossfeed of information and coordination between the APU study and the Phase B Shuttle studies is planned.

It is expected that the APU study effort will indicate the component and system technology areas which will require major emphasis in a continuing APU program.

(See figure 7)

SHUTTLE-APU SCHEDULING

